

Toward the Safe Use of Cannabis and Cannabis-Derived Products Si Huang

Toward the Safe Use of Cannabis and Cannabis-Derived Products

*High-Resolution Analytical Methods
based on Selective Molecular Interactions*

Si Huang | 黃思

Propositions

1. Increased molecular understanding of Cannabis is equally effective for facilitating and constraining its globalization.
(this thesis)
2. The incorrect labeling of Cannabis products is more harmful than no labeling at all.
(this thesis)
3. Publishing analytical methods without validation is publishing without evidence.
4. The use of article numbers instead of page numbers denies readers essential information for a quick evaluation of references.
5. Scientific research is like an unending Olympic competition.
6. A power nap is more effective than a coffee break for enhancing productivity during scientific work.
7. Supervising PhD candidates is more challenging than parenting children.
8. A 40-hour work week ends on Thursday morning.

Propositions belonging to the thesis, entitled

Toward the Safe Use of Cannabis and Cannabis-Derived Products:
High-Resolution Analytical Methods based on Selective Molecular
Interactions

Si Huang
Wageningen, 11 December 2024

**Toward the Safe Use of Cannabis and Cannabis-
Derived Products: High-Resolution Analytical
Methods based on Selective Molecular Interactions**

Si Huang

Thesis committee

Promotors

Prof. Dr J. T. Zuilhof

Professor of Organic Chemistry

Wageningen University & Research

Prof. Dr B. Chen

Director of the Laboratory of Phytochemical R&D of Hunan Province

Hunan Normal University, Changsha, China

Co-promotor

Dr G. IJ. Salentijn

Associate professor, Laboratory of Organic Chemistry

Wageningen University & Research

Other members

Prof. Dr H. A. Schols, Wageningen University & Research

Prof. Dr R. Zenobi, ETH Zurich, Switzerland

Prof. Dr M. Honing, Maastricht University

Dr Y. H. Choi, Leiden University

This research was conducted under the auspices of the VLAG Graduate School (Biobased, Biomolecular, Chemical, Food and Nutrition Science).

**Toward the Safe Use of Cannabis and Cannabis-
Derived Products: High-Resolution Analytical
Methods based on Selective Molecular Interactions**

Si Huang

Thesis

submitted in fulfilment of the requirements for the degree of doctor

at Wageningen University

by the authority of the Rector Magnificus,

Prof. Dr C. Kroeze,

in the presence of the

Thesis Committee appointed by the Academic Board

to be defended in public

on Wednesday 11 December 2024

at 3:30 p.m. in the Omnia Auditorium.

Si Huang

Toward the Safe Use of Cannabis and Cannabis-Derived Products: High-Resolution Analytical Methods based on Selective Molecular Interactions, 317 pages.

PhD Thesis, Wageningen University, Wageningen, the Netherlands (2024)

With References, with summary in English

DOI: <https://doi.org/10.18174/676277>

To my son Huaixu He

Our greatest weakness lies in giving up.

The most certain way to succeed is always to try just one more time.

Thomas Edison

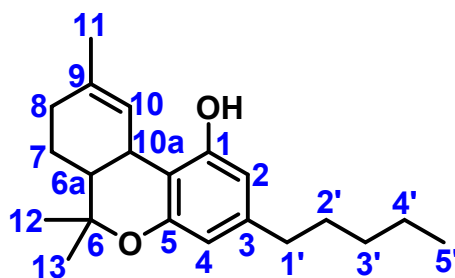
Table of Contents

Chapter 1	General introduction	11
Chapter 2	Advances in the fast analysis of Cannabis and Cannabis products	37
Chapter 3	Rapid distinction and semiquantitative analysis of THC and CBD by silver-impregnated paper spray mass spectrometry	91
Chapter 4	Semiquantitative screening of THC analogues by silica gel TLC with an Ag(I) retention zone and chromogenic smartphone detection	117
Chapter 5	Comprehensive cannabinoid profiling of acid-treated CBD samples and Δ^8 -THC-infused edibles	143
Chapter 6	Ultrafast, selective, and highly sensitive non-chromatographic analysis of fourteen cannabinoids in Cannabis extracts, Δ^8 -tetrahydrocannabinol synthetic mixtures, and edibles by cyclic ion mobility spectrometry-mass spectrometry	179
Chapter 7	Rapid analysis of Δ^8 -tetrahydrocannabinol, Δ^9 -tetrahydrocannabinol, and cannabidiol in Δ^8 -tetrahydrocannabinol edibles by Ag(I) paper spray mass spectrometry after simple extraction	211
Chapter 8	Rim-based binding of perfluorinated acids to pillararenes purifies water	245
Chapter 9	General discussion	263
Summary		287
Acknowledgments		293
Curriculum Vitae		305
Overview of Completed Training Activities		311

List of Cannabinoid Abbreviations

Full name	Abbreviation
Δ 6a,10a-tetrahydrocannabinol	Δ 6a,10a-THC
Δ 7-tetrahydrocannabinol	Δ 7-THC
Δ 8-tetrahydrocannabinol	Δ 8-THC
Δ 9-tetrahydrocannabinol	Δ 9-THC
Δ 10-tetrahydrocannabinol	Δ 10-THC
Δ 9,11-tetrahydrocannabinol	Δ 9,11-THC
Δ (4)8-iso-tetrahydrocannabinol	Δ (4)8-iso-THC
Δ 8-iso-tetrahydrocannabinol	Δ 8-iso-THC
cannabidiol	CBD
Δ 9-tetrahydrocannabinolic acid	THCA
cannabidiolic acid	CBDA
Δ 8-tetrahydrocannabivarin	Δ 8-THCV
Δ 9-tetrahydrocannabivarin	Δ 9-THCV
Δ 9-tetrahydrocannabivarinic acid	THCVA
cannabidivarin	CBDV
cannabidivarinic acid	CBDVA
cannabicyclol	CBL
cannabicyclolic acid	CBLA
cannabigerol	CBG
cannabigerolic acid	CBGA
cannabinol	CBN
cannabinolic acid	CBNA
cannabivarin	CBV
cannabichromene	CBC
11-nor-9-carboxy- Δ 9-tetrahydrocannabinol	Δ 9-THC-COOH
11-nor-9-carboxy- Δ 8-tetrahydrocannabinol	Δ 8-THC-COOH
11-hydroxy- Δ 9-tetrahydrocannabinol	Δ 9-THC-OH
cannabichromenic acid	CBCA
cannabielsoin	CBE
cannabigerovarin	CBGV
cannabicitran	CBT
hexahydrocannabinol	HHC
9 α -hydroxy-hexahydrocannabinol	9 α -OH-HHC

9 β -hydroxy-hexahydrocannabinol	9 β -OH-HHC
10 α -hydroxy-hexahydrocannabinol	10 α -OH-HHC
10 $\alpha\alpha$ -hydroxy-hexahydrocannabinol	10 $\alpha\alpha$ -OH-HHC
7-oxo-9 α -hydroxy-hexahydrocannabinol	7-oxo-9 α -OH-HHC
8-oxo- Δ 9-tetrahydrocannabinol	8-oxo- Δ 9-THC
10 $\alpha\alpha$ -hydroxy-10-oxo- Δ 8-THC	10 $\alpha\alpha$ -OH-10-oxo- Δ 8-THC
9 α -hydroxy-10-oxo- Δ 6a,10a-THC	9 α -OH-10-oxo- Δ 6a,10a-THC
1'S-hydroxy-cannabinol	1'S-OH-CBN
11-hydroxy-cannabinol	11-OH-CBN
8 α -hydroxy- Δ 9-tetrahydrocannabinol	8 α -OH- Δ 9-THC
8 β -hydroxy- Δ 9-tetrahydrocannabinol	8 β -OH- Δ 9-THC
10 α -hydroxy- Δ 8-tetrahydrocannabinol	10 α -OH- Δ 8-THC
10 β -hydroxy- Δ 8-tetrahydrocannabinol	10 β -OH- Δ 8-THC
10 α -hydroxy- Δ 9,11-hexahydrocannabinol	10 α -OH- Δ 9,11-HHC
9 β ,10 β -epoxy-hexahydrocannabinol	9 β ,10 β -epoxy-HHC
11-acetoxy- Δ 9-tetrahydrocannabinolic acid A	11-acetoxy- Δ 9-THCA
iso-tetrahydrocannabifuran	iso-THCBF
Δ 4-iso-tetrahydrocannabinol	Δ 4-iso-THC
Δ 8-cis-iso-tetrahydrocannabinol	Δ 8-cis-iso-THC
4,8-epoxy-iso-tetrahydrocannabinol	4,8-epoxy-iso-THC
8-hydroxy-iso-tetrahydrocannabinol	8-OH-iso-THC



Δ 9-THC

Structure of Δ 9-THC.

General Introduction



1.1 Preface

Even though Cannabis has been used since the Stone Age, a significant surge in popularity started when the US Agriculture Improvement Act of 2018 (2018 Farm Bill) legalized hemp, a category of Cannabis containing less than 0.3% Δ^9 -tetrahydrocannabinol (THC) based on dry weight.¹ Since then, there have been remarkable expansions in the research (**Figure 1.1**), cultivation, distribution, and consumption of Cannabis-related products.² As the Cannabis industry continues to evolve, the legality, safety, and quality of Cannabis (products) have become critical concerns for regulators, consumers, and industry stakeholders alike.³ Therefore, analytical chemistry is indispensable to obtain qualitative and quantitative information about the composition and content of Cannabis (products). In this Chapter, first, the Cannabis plant, its active compounds, cannabinoids, and derived Cannabis products will be discussed (1.2). Then, an overview will be provided regarding the state-of-the-art in the analysis of cannabinoids (1.3 and 1.4). Finally, an outline of the thesis about the scope and aims of the research is given (1.5).

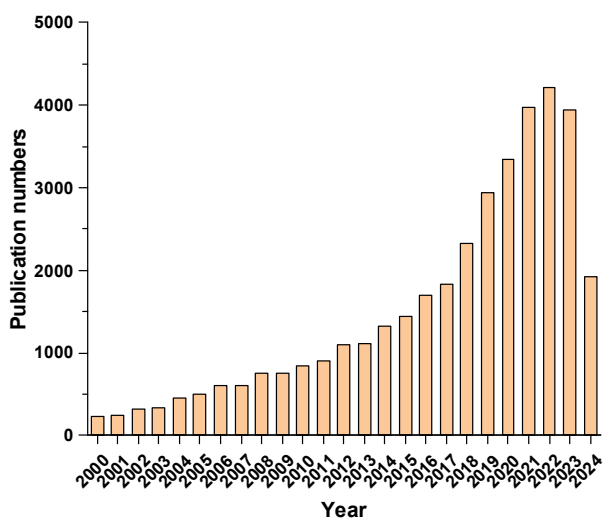


Figure 1.1. Number of publications on the topic of Cannabis in the last 25 years (from Web of Science 24th July 2024).

1.2 Cannabis

Cannabis sativa L., (**Figure 1.2A**) or Cannabis in short, belongs to the Cannabaceae family.⁴ According to archaeological evidence, it has a cultivation history of more than 10000 years for food, fiber, and medicinal purposes and remains a widely cultivated and used plant nowadays.⁵ By 2022, approximately 4% of the global adult population (> 200 million people) has at least once used Cannabis.⁶

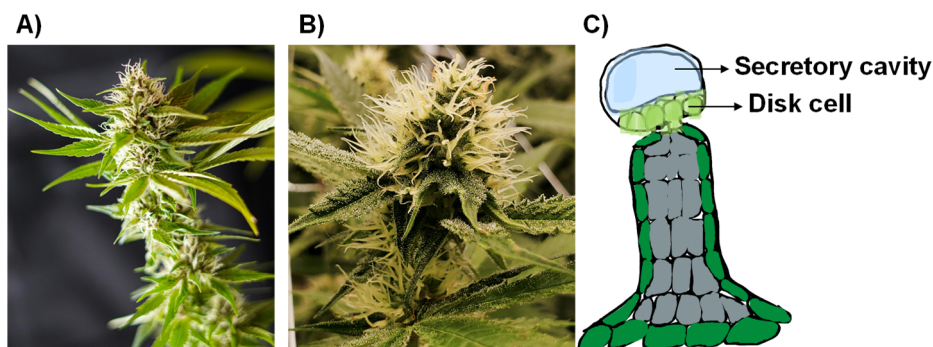


Figure 1.2. A) Cannabis, B) Cannabis inflorescence, and C) graphical illustration of the glandular trichome structure.⁷

1.2.1 Cannabinoids

There are three types of cannabinoids: (i) phytocannabinoids, which are natural compounds found in Cannabis; (ii) endogenous cannabinoids, which are produced in the human body; (iii) synthetic cannabinoids, which are synthesized in laboratories.⁸ Structurally, the three types of cannabinoids are based on different templates (**Figure 1.3**). The main cannabinoids discussed in this thesis are phytocannabinoids and their derivatives.

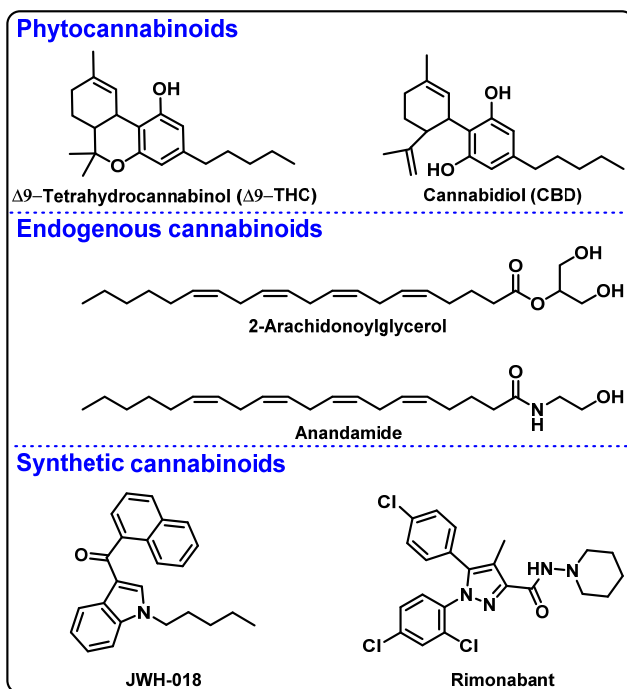


Figure 1.3. Representative phytocannabinoids, endogenous cannabinoids, and synthetic cannabinoids.

Even though more than 500 compounds have been identified in Cannabis, (phyto)cannabinoids are considered the main biologically active ingredient and of most interest to people.⁹ Cannabinoids encompass a diverse group of terpenophenols, mostly consisting of 21 carbon atoms, but also include their corresponding carboxylic acids, analogues, and transformation products. The female flowers (**Figure 1.2B**) of the Cannabis plant contain the highest concentration of cannabinoids. Additionally, cannabinoids are found in different quantities in various plant parts, except for the seeds, from which they are absent.¹⁰

1.2.2.1 Biosynthesis of Cannabinoids

Cannabinoids are biosynthesized and stored in glandular trichomes (formed in the disk cells and stored in the secretory cavity, **Figure 1.2C**).⁷ These glandular trichomes are mainly concentrated in the female inflorescence. The olivetolate geranyltransferase (GOT) enzyme catalyzes geranyl diphosphate (GPP) prenylation

of olivetolic acid (OA) to form the precursor of phytocannabinoids, cannabigerolic acid (CBGA). Subsequently, the formed CBGA is converted to tetrahydrocannabinolic acid (THCA), cannabidiolic acid (CBDA), and cannabichromenic acid (CBCA) by specific enzymes, namely THCA synthase, CBDA synthase, and CBCA synthase, respectively.^{11,12} These acidic cannabinoids are unstable and may lose CO₂ upon exposure to light, air, or heat to produce their neutral counterparts: Δ⁹-THC, CBD and cannabichromene (CBC). Further degradation can occur during storage or consumption to produce cannabicyclol (CBL), cannabinol (CBN), and cannabielsoin (CBE), respectively (Figure 1.4).^{13,14}

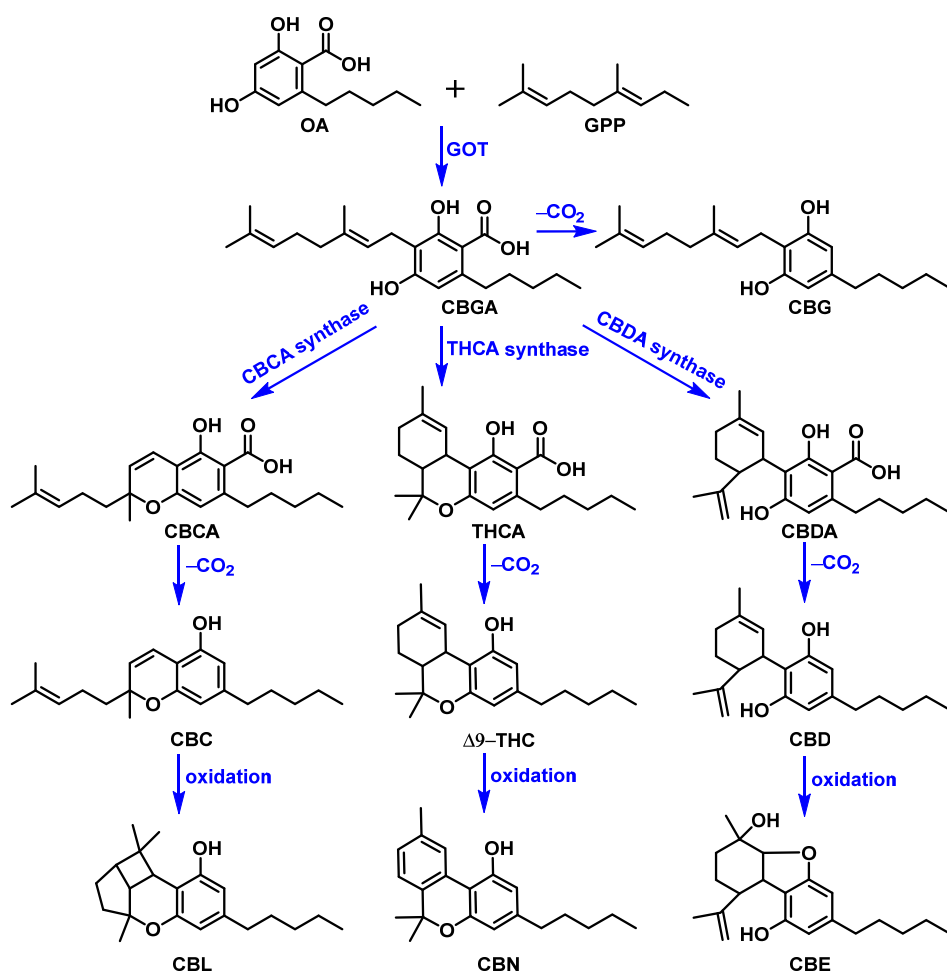


Figure 1.4. Formation of major phytocannabinoids.

1.2.2.2 Δ 9-THC, CBD and Their Isomerization

Of the more than 140 cannabinoids that have been identified, Δ 9-THC and CBD are the most well-known. Δ 9-THC, already identified as the principal psychoactive compound by Mechoulam et al. in the 1960s,¹⁵ is responsible for various pharmacological effects of Cannabis, including psychoactive, analgesic, anti-inflammatory, anti-oxidant, anti-itching, bronchodilatory, anti-spasmodic, and muscle-relaxant activities.¹⁶ Δ 9-THC acts as a partial agonist at cannabinoid receptors (CB₁ and CB₂, primarily located in neurons and immune cells, respectively).¹⁷ The strong binding of Δ 9-THC to the CB₁ receptor is associated with its psychoactive properties, such as mood and consciousness changes, memory processing, and motor control.¹⁸ Some side effects of Δ 9-THC, like anxiety, impaired memory, and immunosuppression can be counteracted by other components of the Cannabis plant (cannabinoids, terpenoids, and flavonoids).^{19,20}

CBD, chemically isolated and identified in 1940 and 1963, respectively,^{21,22} is believed to have significant analgesic, anti-inflammatory, anti-convulsant, and anxiolytic properties without the psychoactive effects of Δ 9-THC.²³ It has a low binding affinity for CB₁ and CB₂ receptors, but can antagonize them in the presence of Δ 9-THC.^{17,24} Studies have shown that CBD can work synergistically with Δ 9-THC, modulating the overall effects of the plant and improving the tolerability and potentially the safety of Δ 9-THC by reducing the likelihood of psychoactive effects and countering various adverse effects (sedation, tachycardia, and anxiety).²⁵⁻²⁷ The varying absolute and relative concentrations of Δ 9-THC and CBD in different Cannabis strains contribute to their distinct effects.

Due to the therapeutic effects of non-psychoactive CBD and its legalization in the 2018 Farm Bill, the CBD market has surged in past years. This has resulted in easy access and lower prices of CBD²⁸ and led to a legal loophole, by means of which non-psychoactive and legal CBD is isomerized into psychoactive and legally controversial THC products (**Figure 1.5**) through easy treatments with acids.^{29,30} Among the many THC isomers, Δ 8-THC — with its mild psychoactivity yet unclear

legal status — gains the most interest. $\Delta 8$ -THC, easily produced from CBD by various methods, is incorporated in different types of commercial products and fervently pursued by consumers as a substitute for $\Delta 9$ -THC.³¹

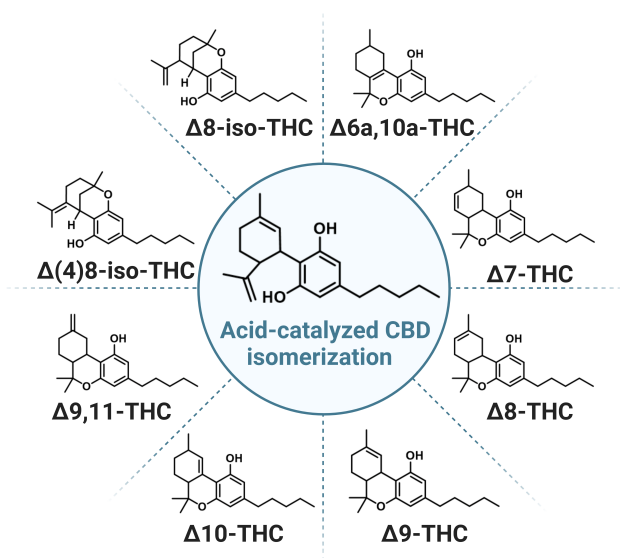


Figure 1.5. Common THC isomers produced by the acid-catalyzed CBD isomerization process.

1.2.2 Cannabis Plant Classification and Regulations

When it comes to forensic and legislative considerations, the drug type (marijuana) and fiber type (hemp) are the two most significant classifications of Cannabis, even though there are several other classification systems based on the content of psychotropic components.³² Marijuana is characterized by a high concentration of $\Delta 9$ -THC, typically ranging from 0.3% to as high as 20% of its dry weight.³³ On the other hand, hemp contains less $\Delta 9$ -THC (< 0.3% of dry weight).³⁴ According to these definitions, Cannabis used in medicinal settings belongs to the drug type due to the high content of $\Delta 9$ -THC.³⁵

For thousands of years, hemp has been used to produce ropes, fabrics, papers, construction materials, and more.³⁶ In the 20th century, many countries banned its cultivation due to its resemblance to marijuana.³⁷ At the same time, a deeper

understanding and accurate quantification of the chemical composition (e.g., Δ^9 -THC) of hemp has become a reality due to advances in analytical chemistry. Thus, the distinction between hemp and marijuana can now be easily achieved. Apart from that, scientific research has demonstrated that the THC levels in industrial hemp are not sufficient to cause intoxication.³⁸ These new scientific findings have led to a shift in global trends and perceptions toward hemp cultivation in recent years, resulting in the enactment of pro-hemp legislation that aims to regulate rather than prohibit hemp.³⁹ As a result, the cultivation of hemp has been reintroduced in many geographical areas, including Canada, the US, Europe, and parts of Asia, such as Yunnan and Heilongjiang in China.⁴⁰

On the other hand, the regulation of marijuana is relatively strict. Many countries, including China, consider marijuana illegal.⁴¹ However, the support for its legalization is growing. In the United States, 37 out of 50 states allow recreational or medical use.⁴² Several other countries (have also revised their laws to) allow recreational or medical Cannabis use, including Canada, Uruguay, Malta, and the Netherlands.⁴³

In summary, Cannabis regulations have rapidly evolved worldwide (and will likely continue to do so) in recent years due to various factors such as policy, economy, and science. The expanding Cannabis industry has brought numerous economic benefits, but it has also presented certain hidden challenges and risks. One of the issues lies in the wide array of Cannabis products, which potentially pose threats to consumer health and require proper legal oversight.

1.2.3 Cannabis Products

The ever-evolving Cannabis regulations create significant opportunities and loopholes for Cannabis cultivators and product manufacturers, which greatly influences the diversity of Cannabis products. Cannabis products are typically based on the main cannabinoids, e.g., CBD, Δ^8 -THC, or Δ^9 -THC type products. Among various Cannabis products, Cannabis edibles and consumables are becoming more popular, pursued by consumers for recreational or therapeutical purposes.⁴⁴⁻⁴⁶

1.2.3.1 Cannabis Product Regulations

In general, regulations of Cannabis products are heterogeneous. Currently, the greatest concern from a regulatory perspective in most jurisdictions is the employment of strict $\Delta 9$ -THC limits to determine whether products are legal or not. Many nations stipulate a zero-tolerance policy or a maximum $\Delta 9$ -THC level (0.05%–1%) for Cannabis products.^{47,48}

1.2.3.2 Safety Concerns with Cannabis Products

Beyond legal issues, there are more concerns for Cannabis products relating to their safety (**Figure 1.6**), especially for edibles, which call for urgent action or regulation. There have been many reports describing Cannabis edibles-induced poisonings and even fatalities, especially among children and young people who may mistake them for regular food items. This poses a significant public health risk.⁴⁹ The reported issues in Cannabis edibles include the following:

- (i) incorrect labels,^{50,51} including claims of therapeutic effects, which is forbidden by the Food and Drug Administration (FDA), incorrect indications of cannabinoid content, and lack of health/age warning messages;
- (ii) illegal levels of $\Delta 9$ -THC,⁵² even though labeled as containing legal content;
- (iii) various solvent residues, remaining mainly from extraction and production processes;⁵³
- (iv) heavy metals, typically from plant bioaccumulation, cross-contamination during processing, or post-process adulteration that have high toxicity even at low concentrations;⁵⁴
- (v) mycotoxins, originating from fungal infection of the Cannabis plant, during growth, processing, and storage that can elicit various forms of toxicity depending on the fungal strain and mycotoxin produced;^{55,56}
- (vi) pesticides, including insecticides, herbicides, fungicides, rodenticides, acaricides, molluscicides, and nematocides, introduced during

- Cannabis cultivation, which are categorized by the World Health Organization (WHO) as moderately hazardous;⁵⁷
- (vii) unknowns, which logically cannot be listed on product labels or the certificate of analysis, e.g., synthetic cannabinoid side products formed during the production of Δ^8 -THC. These are particularly concerning due to their structural analogy with hazardous and/or psychoactive compounds in combination with limited to near-absent toxicological information;⁵⁸
 - (viii) per- and polyfluoroalkyl substances (PFAS): while not studied yet from a safety perspective in Cannabis,⁵⁹ PFAS occur widely, e.g., in water and soil.^{60,61} It has been demonstrated that hemp protein powder is effective at removing PFAS from ground water,⁶² and hemp plants have been found to accumulate PFAS from soil.⁶³ While promising from the perspective of PFAS reduction, impact on Cannabis (product) safety remains unknown. PFAS contamination in Cannabis products might occur at multiple stages including cultivation (through soil and irrigation), processing (via equipment and water), and packaging (through packaging materials).⁶⁴

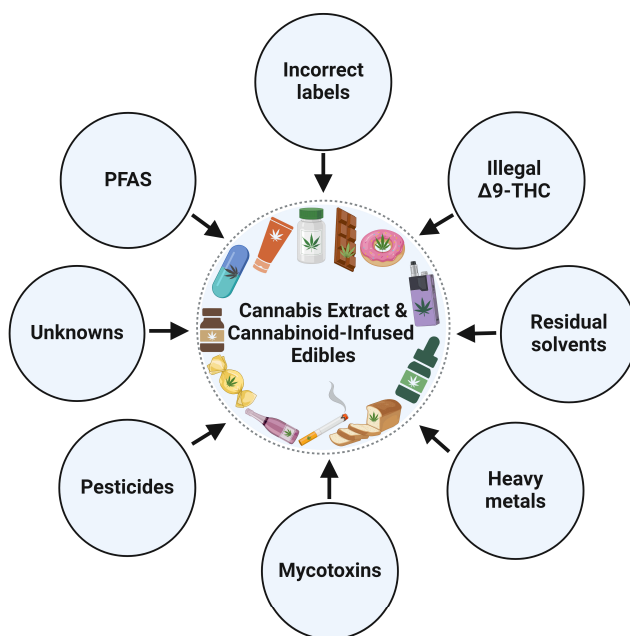


Figure 1.6. Common issues in Cannabis products leading to safety concerns.

1.3 Cannabis and Cannabinoids Analyzed by Official Methods

The expanding Cannabis market and evolving legalization frameworks have sped up the development of various analytical methods to address regulatory and health concerns surrounding Cannabis and cannabinoids. Among these, GC and HPLC are widely adopted by different authorities for analysis.^{65,66} Historically, GC-based techniques have been favored for their simplicity and cost-effectiveness. For instance, the German Federal Institute for Risk Assessment (BfR) employs GC-MS without derivatization to analyze 'total THC' in tea products,⁶⁷ while the European Union (EU) utilizes GC-FID for quantifying Δ^9 -THC in hemp varieties.⁶⁵ Similarly, the United Nations Office on Drugs and Crime (UNODC) recommends GC-FID or GC-MS for Cannabis product analysis.⁶⁸

However, GC has limitations, such as the potential for decarboxylation and other chemical reactions at high temperatures, necessitating derivatization to mitigate these issues.⁶⁹ In contrast, HPLC offers a more mild and versatile approach, allowing simultaneous analysis of acidic and neutral cannabinoids. Recently, the

Association of Official Analytical Collaboration (AOAC) International established Standard Method Performance Requirements (SMPR) for cannabinoid quantification using HPLC-DAD methods, covering a broad range of Cannabis materials, including concentrates, oils, edibles, and different Cannabis plant types. This approach includes a mandated list of cannabinoids (CBD, CBDA, CBN, Δ^9 -THC, Δ^9 -THCA) and a desired list (cannabigerol (CBG), cannabigerolic acid (CBGA), CBC, CBCA, cannabidivarin (CBDV), (cannabidivarinic acid) CBDVA, Δ^8 -THC, tetrahydrocannabivarin (THCV), tetrahydrocannabivarinic acid (THCVA)).⁷⁰ While typically coupled with UV or DAD detectors, HPLC systems increasingly integrate MS detection to enhance resolution and provide structural insights into analytes. MS detection, preferred by Recommendation 2016/2115/EU, is particularly noted for cannabinoid determination in hemp-containing food products.^{71,72}

The scientific literature on GC and HPLC-based methods for the analysis of Cannabis and cannabinoids differs only mildly in the operational parameters over the past decade, meaning that such methods are relatively mature and well-accepted.⁷³ Although low-resolution MS (LRMS) remains widely used in this field, there has been a notable increase in the use of high-resolution MS (HRMS), despite HRMS not yet being incorporated into official guidelines.⁷⁴ While these established methods have their merits, there remains active interest in the development of rapid screening methods for the analysis of Cannabis and cannabinoids, driven by the expanding Cannabis market.

1.4 Cannabis and Cannabinoids Analyzed by Fast Screening Methods

The growing Cannabis market has led to an urgent need for the development of fast screening methods for Cannabis and cannabinoids. While there are many approaches, specifically relevant to the work in this thesis, there are mainly three categories of techniques applied in this field, each with its own advantages and limitations: colorimetric spot tests, ambient ionization mass spectrometry (AIMS) methods, and ion mobility spectrometry (IMS) methods.

1.4.1 Colorimetric Spot Tests

Colorimetric spot tests, with merits of speed, low cost, and ease of use, offer alternatives to instrument-dependent analysis and are widely used as in-field screening methods. Commercial colorimetric test kits, such as fast blue BB salt or Duquenois-Levine reagents, are commonly used by forensic laboratories for screening suspect samples containing high amounts of psychoactive cannabinoids. However, false-positive results from non-cannabinoids or non-psychoactive cannabinoids are easily obtained due to non-specific colorimetric reactions.^{75,76} Therefore, the separation of psychoactive cannabinoids from such interferences before color development would be beneficial in decreasing the fraction of false-positive results. Thin-layer chromatography (TLC) is a fast, easy, and cost-effective candidate to combine with chromogenic reagents for qualitative or quantitative Cannabis analysis. Ongoing efforts are focused on improving the resolution of cannabinoids by optimizing stationary phases and solvent systems.^{30,77,78} For quantitative image analysis of colored spots, compared with currently used photoelectric densitometry devices,⁷⁹⁻⁸¹ smartphones, with their dedicated apps, portability, low cost, and widespread availability, offer the potential for instrument-free TLC plate analysis.^{82,83}

1.4.2 AIMS Methods

The advent of AIMS has revolutionized MS analysis by reducing complexity, time, and cost, thereby making MS more accessible and efficient for various applications. AIMS allows fast, direct, *in situ*, and high-throughput analysis of samples without tedious sample preparation. Since the first AIMS method, desorption electrospray ionization (DESI), was introduced in 2004,⁸⁴ the field of AIMS has expanded rapidly, with various AIMS methods emerging.⁸⁵ Generally, AIMS methods can be classified into APCI-like (plasma-based) methods and ESI-like (spray-based) methods, which are distinguished by their respective ionization mechanisms.⁸⁶

One of the most typical APCI-like AIMS method is the Direct Analysis in Real Time (DART) technique.⁸⁷ Gas, solid, or liquid samples can be directly exposed to a stream of excited gas, where small polar or non-polar analytes are ionized through reactions with electronically or vibrationally excited-state species. With its minimal matrix effects, DART-MS has been widely used in the analysis of cannabinoids in various matrixes such as hair,⁸⁸ vape liquids,⁸⁹ cannabinoid-infused edibles, personal-care products, and hemp materials,⁹⁰ requiring no sample pretreatment.

One representative ESI-like AIMS method is paper spray (PS) ionization.⁹¹ In PS-MS, a triangular piece of paper is positioned in front of the MS inlet. Analytes undergo ionization when a solvent and high voltage are applied to the paper, generating an electric field that forms a Taylor cone at the paper tip.⁹² This cone emits a fine stream of charged droplets directed toward the MS inlet. Upon reaching the inlet, solvent evaporation and Coulombic fission reduce these droplets into smaller charged particles. During this process, charges transfer from solvent to analytes, eventually forming gas-phase ions.⁹³ Importantly, papers are cheap consumables and can be readily modified to enhance PS-MS selectivity and sensitivity through surface modification or coating.⁹⁴⁻⁹⁷ PS-MS methods have been applied to rapidly analyze cannabinoids in urine and oral fluid. Despite all the advantages of AIMS mentioned above, challenges remain in the distinction of cannabinoid isomers and improvement of sensitivity, which is increasingly important with evolving cannabinoid products.

1.4.3 IMS Methods

IMS-mass spectrometry (IMS-MS) enables the separation of ions by their mobility through inert gases under an electric field. This mobility is influenced by the molecular sizes, charges, and shapes. From these mobility measurements, the collision cross section (CCS) can be determined, providing insight into the 3D conformations of gaseous ions.⁹⁸⁻¹⁰⁰ The extra-dimensional separation capability based on mobility enables IMS-MS to analyze compounds in complex matrixes without chromatographic separations and allows for resolution of isomers.

However, current research on IMS-based separation for cannabinoids still faces several limitations on specifically three aspects: (i) inadequate resolution, particularly for THC isomers; (ii) a narrow scope of investigated cannabinoid isomers; (iii) indistinctive or absent reporting of CCS values.¹⁰¹⁻¹⁰³ Clearly, separating such isomeric cannabinoids using IMS has proven challenging. A significant enhancement in separation performance of cannabinoids was achieved by their characteristic behavior in forming adducts with silver ions, which strongly amplifies structural differences and improves isomer separation in the gas phase. This approach was first reported in 2018, although that paper only reported partially separated Δ^9 -THC-Ag(I) and CBD-Ag(I) adducts.¹⁰⁴

1.5 Outline of the Thesis

In response to the challenges of Cannabis and Cannabis product analysis, the aim of this thesis is to enhance the performance of existing analytical methods toward this goal. Efforts will focus on developing techniques that can meet diverse application needs for the analysis of Cannabis and Cannabis products in three distinct scenarios: on-site screening, (potentially) mobile lab testing, and laboratory confirmatory analysis (**Figure 1.7**). The specific aims and hypotheses of each chapter are presented below.

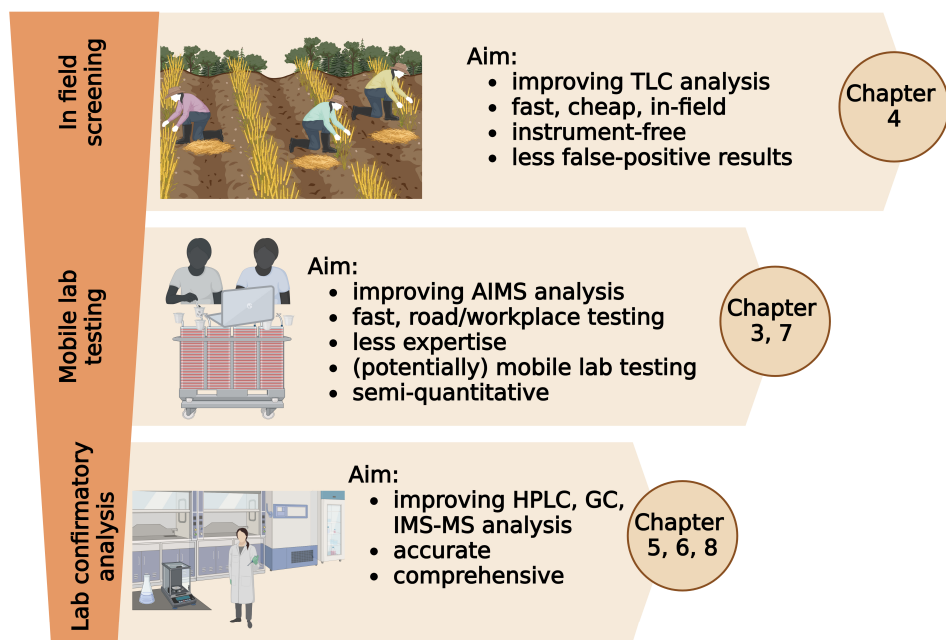


Figure 1.7. Current analytical challenges in Cannabis and Cannabis products and corresponding aims of thesis.

The expanding Cannabis market has created an urgent demand for the development of quick and efficient analytical methods for Cannabis and cannabinoids. A review of the scientific literature from the past decade about the use of fast analytical techniques in the analysis of Cannabis and cannabinoids is presented in **Chapter 2**.

A growing CBD product market requires fast and high-throughput screening of trace amounts of Δ^9 -THC for compliance with the law. However, the current state-of-the-art does not allow one to distinguish Δ^9 -THC and CBD without chromatography. Based on previous research¹⁰⁵⁻¹⁰⁷ in which it was established that Ag(I) has varying affinities for compounds with different numbers and positions of C=C bonds, in **Chapter 3**, studies are described to investigate the hypothesis that the use of Ag(I) adducts would allow the distinction between Δ^9 -THC (one C=C bond, weak) and CBD (two C=C bonds, strong) by MS/MS. When achieved, this

would allow the use of an AIMS technique, such as PS-MS, rather than lengthy chromatography-based methods.

Apart from the need for quality control of CBD products, there is also an urgency for Cannabis plant classification. Ideally, low-cost and high-throughput analytical methods such as colorimetric spot tests for on-site Cannabis classification are available. However, frequent false-positive results are encountered in Cannabis analysis by conventional colorimetric spot tests. To achieve more accurate on-site testability, separation by TLC can be applied before colorimetric analysis. However, commonly used silica TLC plates are unable to separate THC analogues (psychoactive) and CBD analogues (non-psychoactive), which is necessary for Cannabis classification. In **Chapter 4**, studies are reported to answer the question whether an Ag(I)-modified TLC would allow the separation of THC analogues (one or no C=C bond) and CBD analogues (two C=C bonds). Moreover, a smartphone-based analysis of colored THC spots instead of naked eye observation would enable semiquantification of THC analogues. When achieved, more accurate in-field screening of Cannabis varieties should be feasible.

The easy access to ever-cheaper CBD and strict control of $\Delta 9$ -THC catalyzed the popularity of converting CBD to $\Delta 8$ -THC. $\Delta 8$ -THC differs from $\Delta 9$ -THC in the C=C position and has mild psychoactive, yet unclear legal status. With the expansion of $\Delta 8$ -THC-infused products, concerns about whether other THC isomers would be produced in the CBD conversion process and end up in $\Delta 8$ -THC-infused products arise. Therefore, analytical methods that are capable of distinguishing $\Delta 8$ -THC, $\Delta 9$ -THC, and many other isomers are needed. However, commonly used reversed-phase (RP) HPLC methods have insufficient resolution toward multiple THC isomers. Moreover, these isomers produce identical mass spectra and MS/MS spectra from their protonated species when using MS and HRMS. It is hypothesized that the varying Ag(I) affinities could also be used to differentiate $\Delta 8$ -THC, $\Delta 9$ -THC, and other THC isomers (**Chapters 5, 6, and 7**). Therefore, in **Chapter 5**, studies are reported on assessing a combined argentation and normal-phase separation mechanism for enhanced HPLC separation of such THC isomers, and MS distinction

in the presence of Ag(I). When achieved, a more comprehensive cannabinoid profile in Δ^8 -THC products would be feasible. Besides, GC-FID/MS with higher chromatographic resolution should, in principle, result in pronounced separation of these THC isomers and thus could then potentially be cross-validated with the HPLC method. In **Chapter 6**, studies are presented on the hypothesis that differential Ag(I) affinities would result in varying 3D gas-phase conformations of Ag(I) adducts and thus different ion mobilities of cannabinoids. If this happens, the application of advanced cyclic IMS-MS would contribute to non-chromatographic separation before MS differentiation of cannabinoid isomers. When achieved, a fast method allowing for both acidic and neutral cannabinoid isomer analysis would be feasible. In **Chapter 7**, studies are described on the hypothesis that the affinities of Δ^8 -THC and Δ^9 -THC for Ag(I) will be more similar to each other than the affinities of Δ^9 -THC and CBD for Ag(I), due to differences in the position and number of C=C bonds, respectively. This similarity suggests that multi-stage MS fragmentation may be necessary to produce more selective fragments in the presence of Ag(I). Moreover, considering the wide variety of Δ^8 -THC products, a generic yet simple extraction method suitable for different types of matrixes would be preferable when combined with fast PS-MS. Lastly, 3D-printed accessories could simplify paper spray mass spectrometric operations, thereby enabling broader applicability in forensic and food safety screening.

Cannabis products can become contaminated with PFAS when the plants have high PFAS levels, which is an emerging concern for ensuring the safety of Cannabis and its related products. To address this issue, effectively removing PFAS from the growing environment (water) of Cannabis and developing highly sensitive analytical methods to monitor the removal process are crucial yet challenging tasks. As reported in **Chapter 8**, materials with high selectivity and affinity for PFAS based on fluorophilic and generic electrostatic attractions are expected to efficiently achieve reversible binding of PFAS. Additionally, utilizing UHPLC-HRMS would be preferable for achieving trace-level detection of PFAS, thereby effectively

monitoring PFAS removal and potentially for future detection of PFAS contamination in Cannabis and Cannabis products.

In **Chapter 9**, the key work and main achievements in this thesis are summarized, and future perspectives on Cannabis and cannabinoid analysis are provided.

References

- (1) Congress. *Agricultural improvement act of 2018*; **2018**. Retrieved from United States Government. <https://www.congress.gov/115/plaws/publ334/PLAW-115publ334.pdf> (accessed 2024 July 24).
- (2) Salehi, A.; Puchalski, K.; Shokoohinia, Y.; Zolfaghari, B.; Asgary, S. Differentiating Cannabis products: drugs, food, and supplements. *Frontiers in Pharmacology* **2022**, *13*, 906038.
- (3) Kavousi, P.; Giamo, T.; Arnold, G.; Allende, M.; Huynh, E.; Lea, J.; Lucine, R.; Tillett Miller, A.; Webre, A.; Yee, A. What do we know about opportunities and challenges for localities from Cannabis legalization? *Review of Policy Research* **2022**, *39*, 143-169.
- (4) Kumar, P.; Mahato, D. K.; Kamle, M.; Borah, R.; Sharma, B.; Pandhi, S.; Tripathi, V.; Yadav, H. S.; Devi, S.; Patil, U.; *et al.* Pharmacological properties, therapeutic potential, and legal status of *Cannabis sativa* L.: an overview. *Phytotherapy Research* **2021**, *35*, 6010-6029.
- (5) Charitos, I. A.; Gagliano-Candela, R.; Santacroce, L.; Bottalico, L. The Cannabis spread throughout the continents and its therapeutic use in history. *Endocrine, Metabolic & Immune Disorders-Drug Targets (Formerly Current Drug Targets-Immune, Endocrine & Metabolic Disorders)* **2021**, *21*, 407-417.
- (6) Daldegan-Bueno, D.; Lindner, S. R.; Kovalski, D.; Fischer, B. Cannabis use, risk behaviours and harms in Brazil: a comprehensive review of available data indicators. *Drug and Alcohol Review* **2023**, *42*, 318-336.
- (7) Tanney, C. A.; Backer, R.; Geitmann, A.; Smith, D. L. Cannabis glandular trichomes: a cellular metabolite factory. *Frontiers in Plant Science* **2021**, *12*, 721986.
- (8) Marzo, V. D.; Petrocellis, L. D. Plant, synthetic, and endogenous cannabinoids in medicine. *Annual Review of Medicine* **2006**, *57*, 553-574.
- (9) Odieka, A. E.; Obuzor, G. U.; Oyediji, O. O.; Gondwe, M.; Hosu, Y. S.; Oyediji, A. O. The medicinal natural products of *Cannabis sativa* Linn.: a review. *Molecules* **2022**, *27*, 1689.
- (10) Janatová, A.; Fraňková, A.; Tlustoš, P.; Hamouz, K.; Božik, M.; Klouček, P. Yield and cannabinoid contents in different Cannabis (*Cannabis sativa* L.) genotypes for medical use. *Industrial Crops and Products* **2018**, *112*, 363-367.
- (11) Walsh, K. B.; McKinney, A. E.; Holmes, A. E. Minor cannabinoids: biosynthesis, molecular pharmacology and potential therapeutic uses. *Frontiers in Pharmacology* **2021**, *12*, 777804.
- (12) Taura, F.; Sirikantaramas, S.; Shoyama, Y.; Shoyama, Y.; Morimoto, S. Phytocannabinoids in *Cannabis sativa*: recent studies on biosynthetic enzymes. *Chemistry & Biodiversity* **2007**, *4*, 1649-1663.
- (13) Grafström, K.; Andersson, K.; Pettersson, N.; Dalgaard, J.; Dunne, S. J. Effects of long term storage on secondary metabolite profiles of Cannabis resin. *Forensic Science International* **2019**, *301*, 331-340.
- (14) Lewis, M. M.; Yang, Y.; Wasilewski, E.; Clarke, H. A.; Kotra, L. P. Chemical profiling of medical Cannabis extracts. *ACS Omega* **2017**, *2*, 6091-6103.
- (15) Gaoni, Y.; Mechoulam, R. Isolation, structure, and partial synthesis of an active constituent of hashish. *Journal of the American Chemical Society* **1964**, *86*, 1646-1647.
- (16) Philips, E.; Erridge, S.; Sodergren, M. H. Cannabis-based medicinal products: a clinical guide. *British Journal of Neuroscience Nursing* **2022**, *18*, 170-174.
- (17) Pertwee, R. G. The diverse CB₁ and CB₂ receptor pharmacology of three plant cannabinoids: Δ^9 -tetrahydrocannabinol, cannabidiol and Δ^9 -tetrahydrocannabivarin. *British Journal of Pharmacology* **2008**, *153*, 199-215.
- (18) Niloy, N.; Hediya, T. A.; Vichitra, C.; Sonali, S.; Chidambaram, S. B.; Gorantla, V. R.; Mahalakshmi, A. M. Effect of Cannabis on memory consolidation, learning and retrieval and its current legal status in India: a review. *Biomolecules* **2023**, *13*, 162.
- (19) Datta, S.; Ramamurthy, P. C.; Anand, U.; Singh, S.; Singh, A.; Dhanjal, D. S.; Dhaka, V.; Kumar, S.; Kapoor, D.; Nandy, S. Wonder or evil?: Multifaceted health hazards and health benefits of *Cannabis sativa* and its phytochemicals. *Saudi Journal of Biological Sciences* **2021**, *28*, 7290-7313.

- (20) Andre, C. M.; Hausman, J.-F.; Guerriero, G. *Cannabis sativa*: the plant of the thousand and one molecules. *Frontiers in Plant Science* **2016**, *7*, 174167.
- (21) Jacob, A.; Todd, A. *Cannabis indica*. Part II. Isolation of cannabidiol from Egyptian hashish. Observations on the structure of cannabinol. *Journal of the Chemical Society (Resumed)* **1940**, *119*, 649-653.
- (22) Mechoulam, R.; Shvo, Y. Hashish—I: the structure of cannabidiol. *Tetrahedron* **1963**, *19*, 2073-2078.
- (23) Noreen, N.; Muhammad, F.; Akhtar, B.; Azam, F.; Anwar, M. I. Is cannabidiol a promising substance for new drug development? A review of its potential therapeutic applications. *Critical Reviews in Eukaryotic Gene Expression* **2018**, *28*, 73-86.
- (24) Laprairie, R.; Bagher, A.; Kelly, M.; Donovan-Wright, E. Cannabidiol is a negative allosteric modulator of the cannabinoid CB₁ receptor. *British Journal of Pharmacology* **2015**, *172*, 4790-4805.
- (25) Russo, E.; Guy, G. W. A tale of two cannabinoids: the therapeutic rationale for combining tetrahydrocannabinol and cannabidiol. *Medical Hypotheses* **2006**, *66*, 234-246.
- (26) Abrams, D. I.; Guzman, M. Cannabis in cancer care. *Clinical Pharmacology & Therapeutics* **2015**, *97*, 575-586.
- (27) Russo, E. B. Taming THC: potential Cannabis synergy and phytocannabinoid-terpenoid entourage effects. *British Journal of Pharmacology* **2011**, *163*, 1344-1364.
- (28) McGregor, I. S.; Cairns, E. A.; Abelev, S.; Cohen, R.; Henderson, M.; Couch, D.; Arnold, J. C.; Gauld, N. Access to cannabidiol without a prescription: a cross-country comparison and analysis. *International Journal of Drug Policy* **2020**, *85*, 102935.
- (29) Golombek, P.; Müller, M.; Barthlott, I.; Sproll, C.; Lachenmeier, D. W. Conversion of cannabidiol (CBD) into psychotropic cannabinoids including tetrahydrocannabinol (THC): a controversy in the scientific literature. *Toxics* **2020**, *8*, 41.
- (30) Tsujikawa, K.; Okada, Y.; Segawa, H.; Yamamuro, T.; Kuwayama, K.; Kanamori, T.; Iwata, Y. T. Thin-layer chromatography on silver nitrate-impregnated silica gel for analysis of homemade tetrahydrocannabinol mixtures. *Forensic Toxicology* **2022**, *40*, 125-131.
- (31) Michael Geci, M. S., and Jordan Tishler. The dark side of cannabidiol: the unanticipated social and clinical implications of synthetic Δ^8 -THC. *Cannabis and Cannabinoid Research* **2023**, *8*, 270-282.
- (32) Small, E. Evolution and classification of *Cannabis sativa* (marijuana, hemp) in relation to human utilization. *The Botanical Review* **2015**, *81*, 189-294.
- (33) Carvalho, V. M.; de Almeida, F. G.; de Macêdo Vieira, A. C.; Rocha, E. D.; Cabral, L. M.; Strongin, R. M. Chemical profiling of Cannabis varieties cultivated for medical purposes in southeastern Brazil. *Forensic Science International* **2022**, *335*, 111309.
- (34) Roman, M. G.; Houston, R. Investigation of chloroplast regions rps16 and clpP for determination of *Cannabis sativa* crop type and biogeographical origin. *Legal Medicine* **2020**, *47*, 101759.
- (35) Cash, M. C.; Cunnane, K.; Fan, C.; Romero-Sandoval, E. A. Mapping cannabis potency in medical and recreational programs in the United States. *Plos One* **2020**, *15*, e0230167.
- (36) Crini, G.; Lichtfouse, E.; Chanet, G.; Morin-Crini, N. Traditional and new applications of hemp. In *Sustainable Agriculture Reviews: Hemp Production and Applications*, Crini, G., Lichtfouse, E. Eds.; Vol. 42; Springer International Publishing, Cham, **2020**; pp 37-87.
- (37) Ahmed, A. T. M. F.; Islam, M. Z.; Mahmud, M. S.; Sarker, M. E.; Islam, M. R. Hemp as a potential raw material toward a sustainable world: a review. *Heliyon* **2022**, *8*, e08753.
- (38) Malone, T.; Gomez, K. Hemp in the United States: a case study of regulatory path dependence. *Applied Economic Perspectives and Policy* **2019**, *41*, 199-214.
- (39) Aloo, S. O.; Mwititi, G.; Ngugi, L. W.; Oh, D.-H. Uncovering the secrets of industrial hemp in food and nutrition: the trends, challenges, and new-age perspectives. *Critical Reviews in Food Science and Nutrition* **2022**, *64*, 5093-5112.
- (40) Farinon, B.; Molinari, R.; Costantini, L.; Merendino, N. The seed of industrial hemp (*Cannabis sativa* L.): nutritional quality and potential functionality for human health and nutrition. *Nutrients* **2020**, *12*, 1935.

- (41) Eastwood, N.; Fox, E.; Rosmarin, A. *A quiet revolution: drug decriminalisation across the globe*; **2016**.
<https://www.release.org.uk/sites/default/files/pdf/publications/A%20Quiet%20Revolution%20-%20Decriminalisation%20Across%20the%20Globe.pdf> (accessed 2024 August 15).
- (42) ProCon. *Legal recreational marijuana States and DC.*; **2024**. <https://marijuana.procon.org/legal-recreational-marijuana-states-and-dc/> (accessed 2024 August 15).
- (43) Simiyu, D. C.; Jang, J. H.; Lee, O. R. Understanding *Cannabis sativa* L.: current status of propagation, use, legalization, and haploid-inducer-mediated genetic engineering. *Plants* **2022**, *11*, 1236.
- (44) Blake, A.; Nahtigal, I. The evolving landscape of cannabis edibles. *Current Opinion in Food Science* **2019**, *28*, 25-31.
- (45) Dilley, J. A.; Graves, J. M.; Brooks-Russell, A.; Whitehill, J. M.; Liebelt, E. L. Trends and characteristics of manufactured Cannabis product and Cannabis plant product exposures reported to US poison control centers, 2017-2019. *JAMA Network Open* **2021**, *4*, e2110925.
- (46) Peng, H.; Shahidi, F. Cannabis and Cannabis edibles: a review. *Journal of Agricultural and Food Chemistry* **2021**, *69*, 1751-1774.
- (47) Hazekamp, A. The trouble with CBD oil. *Medical Cannabis and Cannabinoids* **2018**, *1*, 65-72.
- (48) Manthey, J. Cannabis use in Europe: current trends and public health concerns. *International Journal of Drug Policy* **2019**, *68*, 93-96.
- (49) Langrand, J.; Dufayet, L.; Vodovar, D. Marketing of legalised Cannabis: a concern about poisoning. *The Lancet* **2019**, *394*, 735.
- (50) MacCallum, C. A.; Lo, L. A.; Betts, F.; Koehn, M. Product safety and quality control. In *Cannabinoids and Pain*, Narouze, S. N. Ed.; Springer International Publishing, Cham, **2021**; pp 249-258.
- (51) Evans, D. G. Medical fraud, mislabeling, contamination: all common in CBD products. *Missouri Medicine* **2020**, *117*, 394-399.
- (52) Barrus, D. G.; Capogrossi, K. L.; Cates, S. C.; Gourdet, C. K.; Peiper, N. C.; Novak, S. P.; Lefever, T. W.; Wiley, J. L. Tasty THC: promises and challenges of cannabis edibles. *RTI Press Methods Report Series* **2016**, *2016*, 2-22.
- (53) Goldman, S.; Bramante, J.; Vrdoljak, G.; Guo, W.; Wang, Y.; Marjanovic, O.; Orłowicz, S.; Di Lorenzo, R.; Noestheden, M. The analytical landscape of Cannabis compliance testing. *Journal of Liquid Chromatography & Related Technologies* **2021**, *44*, 403-420.
- (54) Dryburgh, L. M.; Bolan, N. S.; Grof, C. P. L.; Galettis, P.; Schneider, J.; Lucas, C. J.; Martin, J. H. Cannabis contaminants: sources, distribution, human toxicity and pharmacologic effects. *British Journal of Clinical Pharmacology* **2018**, *84*, 2468-2476.
- (55) Pérez-Moreno, M.; Pérez-Lloret, P.; González-Soriano, J.; Santos-Álvarez, I. Cannabis resin in the region of Madrid: adulteration and contamination. *Forensic Science International* **2019**, *298*, 34-38.
- (56) McKernan, K.; Spangler, J.; Helbert, Y.; Lynch, R.; Devitt-Lee, A.; Zhang, L.; Orphe, W.; Warner, J.; Foss, T.; Hudalla, C.; *et al.* Metagenomic analysis of medicinal Cannabis samples; pathogenic bacteria, toxigenic fungi, and beneficial microbes grow in culture-based yeast and mold tests. *F1000Research* **2016**, *5*, 2471.
- (57) Taylor, A.; Birkett, J. W. Pesticides in Cannabis: a review of analytical and toxicological considerations. *Drug Testing and Analysis* **2020**, *12*, 180-190.
- (58) Ray, C. L.; Bylo, M. P.; Pescaglia, J.; Gawenis, J. A.; Greenlief, C. M. Delta-8 tetrahydrocannabinol product impurities. *Molecules* **2022**, *27*, 6924.
- (59) Salvatore, D.; Mok, K.; Garrett, K. K.; Poudrier, G.; Brown, P.; Birnbaum, L. S.; Goldenman, G.; Miller, M. F.; Patton, S.; Poehlein, M.; *et al.* Presumptive contamination: a new approach to PFAS contamination based on likely sources. *Environmental Science & Technology Letters* **2022**, *9*, 983-990.
- (60) Jha, G.; Kankarla, V.; McLennon, E.; Pal, S.; Sihi, D.; Dari, B.; Diaz, D.; Nocco, M. Per- and polyfluoroalkyl substances (PFAS) in integrated crop–livestock systems: environmental exposure and human health risks. *International Journal of Environmental Research and Public Health* **2021**, *18*, 12550.

- (61) Winchell, L. J.; Wells, M. J. M.; Ross, J. J.; Fonoll, X.; Norton, J. W.; Kuplicki, S.; Khan, M.; Bell, K. Y. Per- and polyfluoroalkyl substances presence, pathways, and cycling through drinking water and wastewater treatment. *Journal of Environmental Engineering* **2022**, *148*, 03121003.
- (62) Turner, B. D.; Sloan, S. W.; Currell, G. R. Novel remediation of per- and polyfluoroalkyl substances (PFASs) from contaminated groundwater using *Cannabis sativa* L. (hemp) protein powder. *Chemosphere* **2019**, *229*, 22-31.
- (63) Nassazzi, W.; Wu, T.-C.; Jass, J.; Lai, F. Y.; Ahrens, L. Phytoextraction of per- and polyfluoroalkyl substances (PFAS) and the influence of supplements on the performance of short-rotation crops. *Environmental Pollution* **2023**, *333*, 122038.
- (64) Eze, C. G.; Okeke, E. S.; Nwankwo, C. E.; Nyaruaba, R.; Anand, U.; Okoro, O. J.; Bontempi, E. Emerging contaminants in food matrices: an overview of the occurrence, pathways, impacts and detection techniques of per- and polyfluoroalkyl substances. *Toxicology Reports* **2024**, *12*, 436-447.
- (65) CDR, E. *Union method for the quantitative determination of the Δ^9 -tetrahydrocannabinol content in hemp varieties*; rev. Delegated Regulation (EU) No 639/2014, Annex III as amended by Regulation (EU) 2017/1155; **2017**. Retrieved from Commission Delegated Regulation (EU). https://eur-lex.europa.eu/eli/reg_del/2017/1155/oj (accessed 2024 March 30).
- (66) Mudge, E. M.; Brown, P. N. Determination of cannabinoids in *Cannabis sativa* dried flowers and oils by LC-UV: single-laboratory validation, first action 2018.10. *Journal of AOAC International* **2020**, *103*, 489-493.
- (67) BgVV. *BgVV recommends guidance values for THC (tetrahydrocannabinol) in hemp-containing foods*; **2000**. Retrieved from Federal Institute for Health Protection of Consumers and Veterinary Medicine. <https://mobil.bfr.bund.de/cm/349/tetrahydrocannabinol-levels-are-too-high-in-many-hemp-containing-foods-health-impairments-are-possible.pdf> (accessed 2024 July 24).
- (68) UNODC. *Recommended methods for the identification and analysis of Cannabis and Cannabis products*; **2009**. Retrieved from United Nations Office on Drugs and Crime UNODC. https://www.unodc.org/documents/scientific/ST-NAR-40-Ebook_1.pdf (accessed 2024 March 30).
- (69) García-Valverde, M. T.; Sánchez-Carnerero Callado, C.; Díaz-Liñán, M. C.; Sánchez de Medina, V.; Hidalgo-García, J.; Nadal, X.; Hanuš, L.; Ferreira-Vera, C. Effect of temperature in the degradation of cannabinoids: from a brief residence in the gas chromatography inlet port to a longer period in thermal treatments. *Frontiers in Chemistry* **2022**, *10*, 1038729.
- (70) EU, E. C. *Commission recommendation (EU) 2016/2115 of 1 December 2016 on the monitoring of the presence of Δ^9 -tetrahydrocannabinol, its precursors and other cannabinoids in food*; **2016**. Retrieved from Official Journal of the European Union. <https://eur-lex.europa.eu/legal-content/EN/TXT/PDF/?uri=OJ:L:2016:327:FULL&from=EL> (accessed 2024 March 31).
- (71) AOAC. *AOAC SMPR® 2017.019 Standard method performance requirements (SMPRs®) for quantitation of cannabinoids in edible chocolate*; **2017**. Retrieved from AOAC International. https://www.aoac.org/wp-content/uploads/2020/11/SMPR202017_019.pdf (accessed 2024 July 7).
- (72) AOAC. *AOAC SMPR® 2022.001 Quantitation of cannabinoids in beverages*; **2022**. Retrieved from AOAC International. https://www.aoac.org/wp-content/uploads/2022/11/SMPR-2022_001.pdf (accessed 2024 July 7).
- (73) Deidda, R.; Dispas, A.; De Bleye, C.; Hubert, P.; Ziemons, É. Critical review on recent trends in cannabinoid determination on Cannabis herbal samples: from chromatographic to vibrational spectroscopic techniques. *Analytica Chimica Acta* **2022**, *1209*, 339184.
- (74) Capriotti, A. L.; Cannazza, G.; Catani, M.; Cavaliere, C.; Cavazzini, A.; Cerrato, A.; Citti, C.; Felletti, S.; Montone, C. M.; Piovesana, S.; et al. Recent applications of mass spectrometry for the characterization of Cannabis and hemp phytocannabinoids: from targeted to untargeted analysis. *Journal of Chromatography A* **2021**, *1655*, 462492.
- (75) Bruni, A.; Rodrigues, C.; dos Santos, C.; de Castro, J.; Mariotto, L.; Sinhorini, L. Analytical challenges for identification of new psychoactive substances: a literature-based study for seized drugs. *Brazilian Journal of Analytical Chemistry* **2021**, *9*, 52-78.

- (76) dos Santos, N. A.; Souza, L. M.; Domingos, E.; França, H. S.; Lacerda Jr, V.; Beatriz, A.; Vaz, B. G.; Rodrigues, R. R.; Carvalho, V. V.; Merlo, B. B. Evaluating the selectivity of colorimetric test (fast blue BB salt) for the cannabinoids identification in marijuana street samples by UV–Vis, TLC, ESI (+) FT-ICR MS and ESI (+) MS/MS. *Forensic Chemistry* **2016**, *1*, 13-21.
- (77) Liu, Y.; Brettell, T. A.; Victoria, J.; Wood, M. R.; Staretz, M. E. High performance thin-layer chromatography (HPTLC) analysis of cannabinoids in Cannabis extracts. *Forensic Chemistry* **2020**, *19*, 100249.
- (78) Goutam, S.; Goutam, M.; Yadav, P. Thin layer chromatographic analysis of psychoactive plant *Cannabis sativa* L. *International Journal of Multidisciplinary Approach and Studies* **2015**, *2*, 166-175.
- (79) Xu, L.; Shu, T.; Liu, S. Simplified quantification of representative bioactives in food through TLC image analysis. *Food Analytical Methods* **2019**, *12*, 2886-2894.
- (80) Zhou, B.; Tan, M.; Lu, J.-f.; Zhao, J.; Xie, A.-f.; Li, S.-p. Simultaneous determination of five active compounds in *chimonanthus nitens* by double-development HPTLC and scanning densitometry. *Chemistry Central Journal* **2012**, *6*, 1-5.
- (81) Stroka, J.; Anklam, E. Development of a simplified densitometer for the determination of aflatoxins by thin-layer chromatography. *Journal of Chromatography A* **2000**, *904*, 263-268.
- (82) Chen, W.; Yao, Y.; Chen, T.; Shen, W.; Tang, S.; Lee, H. K. Application of smartphone-based spectroscopy to biosample analysis: a review. *Biosensors and Bioelectronics* **2021**, *172*, 112788.
- (83) Ross, G. M.; Bremer, M. G.; Nielen, M. W. Consumer-friendly food allergen detection: moving towards smartphone-based immunoassays. *Analytical and Bioanalytical Chemistry* **2018**, *410*, 5353-5371.
- (84) Takats, Z.; Wiseman, J. M.; Gologan, B.; Cooks, R. G. Mass spectrometry sampling under ambient conditions with desorption electrospray ionization. *Science* **2004**, *306*, 471-473.
- (85) Zhang, X.-L.; Zhang, H.; Wang, X.-C.; Huang, K.-K.; Wang, D.; Chen, H.-W. Advances in ambient ionization for mass spectrometry. *Chinese Journal of Analytical Chemistry* **2018**, *46*, 1703-1713.
- (86) Chaves, A. R.; Martins, R. O.; Maciel, L. Í. L.; Silva, A. R.; Gondim, D. V.; Fortalo, J. M.; de Souza, S.; Santos, J. V. R.; Vaz, B. G. Ambient ionization mass spectrometry: applications and new trends for environmental matrices analysis. *Brazilian Journal of Analytical Chemistry* **2022**, *2022*, 52-77.
- (87) Cody, R. B.; Laramée, J. A.; Durst, H. D. Versatile new ion source for the analysis of materials in open air under ambient conditions. *Analytical Chemistry* **2005**, *77*, 2297-2302.
- (88) Duvivier, W. F.; van Putten, M. R.; van Beek, T. A.; Nielen, M. W. (Un) targeted scanning of locks of hair for drugs of abuse by direct analysis in real time-high-resolution mass spectrometry. *Analytical Chemistry* **2016**, *88*, 2489-2496.
- (89) Falconer, T. M.; Morales-Garcia, F. Rapid screening of vaping liquids by DART-MS. *Journal of AOAC International* **2023**, *106*, 436-444.
- (90) Chambers, M. I.; Musah, R. A. DART-HRMS as a triage approach for the rapid analysis of cannabinoid-infused edible matrices, personal-care products and *Cannabis sativa* hemp plant material. *Forensic Chemistry* **2022**, *27*, 100382.
- (91) Wang, H.; Liu, J.; Cooks, R. G.; Ouyang, Z. Paper spray for direct analysis of complex mixtures using mass spectrometry. *Angewandte Chemie International Edition* **2010**, *122*, 889-892.
- (92) Taylor, G. I. Disintegration of water drops in an electric field. *Proceedings of the Royal Society of London. Series A. Mathematical and Physical Sciences* **1964**, *280*, 383-397.
- (93) Espy, R. D.; Muliadi, A. R.; Ouyang, Z.; Cooks, R. G. Spray mechanism in paper spray ionization. *International Journal of Mass Spectrometry* **2012**, *325-327*, 167-171.
- (94) Liu, J.; Wang, H.; Manicke, N. E.; Lin, J.-M.; Cooks, R. G.; Ouyang, Z. Development, characterization, and application of paper spray ionization. *Analytical Chemistry* **2010**, *82*, 2463-2471.
- (95) Basuri, P.; Baidya, A.; Pradeep, T. Sub-parts-per-trillion level detection of analytes by superhydrophobic preconcentration paper spray ionization mass spectrometry (SHPPSI MS). *Analytical Chemistry* **2019**, *91*, 7118-7124.

- (96) Bambaauer, T. P.; Maurer, H. H.; Weber, A. A.; Hannig, M.; Pütz, N.; Koch, M.; Manier, S. K.; Schneider, M.; Meyer, M. R. Evaluation of novel organosilane modifications of paper spray mass spectrometry substrates for analyzing polar compounds. *Talanta* **2019**, *204*, 677-684.
- (97) Damon, D. E.; Davis, K. M.; Moreira, C. R.; Capone, P.; Cruttenden, R.; Badu-Tawiah, A. K. Direct biofluid analysis using hydrophobic paper spray mass spectrometry. *Analytical Chemistry* **2016**, *88*, 1878-1884.
- (98) Thomson, J. J. XXVI. Rays of positive electricity. *The London, Edinburgh, and Dublin Philosophical Magazine and Journal of Science* **1911**, *21*, 225-249.
- (99) Mason, E. A.; Schamp Jr, H. W. Mobility of gaseous ions in weak electric fields. *Annals of Physics* **1958**, *4*, 233-270.
- (100) Gabelica, V.; Shvartsburg, A. A.; Afonso, C.; Barran, P.; Benesch, J. L.; Bleiholder, C.; Bowers, M. T.; Bilbao, A.; Bush, M. F.; Campbell, J. L. Recommendations for reporting ion mobility mass spectrometry measurements. *Mass Spectrometry Reviews* **2019**, *38*, 291-320.
- (101) Tose, L. V.; Santos, N. A.; Rodrigues, R. R. T.; Murgu, M.; Gomes, A. F.; Vasconcelos, G. A.; Souza, P. C. T.; Vaz, B. G.; Romão, W. Isomeric separation of cannabinoids by UPLC combined with ionic mobility mass spectrometry (TWIM-MS)—part I. *International Journal of Mass Spectrometry* **2017**, *418*, 112-121.
- (102) Kiselak, T. D.; Koerber, R.; Verbeck, G. F. Synthetic route sourcing of illicit at home cannabidiol (CBD) isomerization to psychoactive cannabinoids using ion mobility-coupled-LC-MS/MS. *Forensic Science International* **2020**, *308*, 110173.
- (103) Hädener, M.; Kamrath, M. Z.; Weinmann, W.; Groessl, M. High-resolution ion mobility spectrometry for rapid Cannabis potency testing. *Analytical Chemistry* **2018**, *90*, 8764-8768.
- (104) Zietek, B. M.; Mengerink, Y.; Jordens, J.; Somsen, G. W.; Kool, J.; Honing, M. Adduct-ion formation in trapped ion mobility spectrometry as a potential tool for studying molecular structures and conformations. *International Journal for Ion Mobility Spectrometry* **2018**, *21*, 19-32.
- (105) van Beek, T. A.; Subrtova, D. Factors involved in the high pressure liquid chromatographic separation of alkenes by means of argentation chromatography on ion exchangers: overview of theory and new practical developments. *Phytochemical Analysis* **1995**, *6*, 1-19.
- (106) Kaneti, J.; de Smet, L. C. P. M.; Boom, R.; Zuilhof, H.; Sudhölter, E. J. R. Computational probes into the basis of silver ion chromatography. II. silver(I)-olefin complexes. *The Journal of Physical Chemistry A* **2002**, *106*, 11197-11204.
- (107) Damyanova, B.; Momtchilova, S.; Bakalova, S.; Zuilhof, H.; Christie, W. W.; Kaneti, J. Computational probes into the conceptual basis of silver ion chromatography: I. silver(I) ion complexes of unsaturated fatty acids and esters. *Journal of Molecular Structure: THEOCHEM* **2002**, *589-590*, 239-249.

Advances in the Fast Analysis of Cannabis and Cannabis products

Huang, S.; van Beek, T. A.; Ma, M.; Chen, B.; Zuilhof, H.; Salentijn, G. IJ.
Manuscript in preparation.



Abstract

The rapid global expansion of the Cannabis industry presents new challenges for analytical methods. Traditional GC and HPLC-based methods are primarily suited for laboratory analysis and are generally time-consuming. However, the accelerated processes of Cannabis cultivation and product use, coupled with increasingly strict legal and quality control requirements, burden traditional laboratory analysis. In this context, new and rapid analytical methods for the analysis of Cannabis and related products across various scenarios will provide new insights and contribute to comprehensive regulation and development of the Cannabis market. This chapter reviews advances over the past decade in the fast analysis of Cannabis and Cannabis products. Different analytical methods, including colorimetric tests, electrochemical, optical spectroscopic, immunochemical, nuclear magnetic resonance (NMR), ion mobility spectrometry (IMS), and ambient ionization mass spectrometry (AIMS) methods, are compared and critically evaluated, providing insights on selecting appropriate analytical approaches for different purposes.

Introduction

Cannabis sativa L. (Cannabis), with thousands of years of cultivation and usage history, has experienced a resurgence in global interest following the legalization of hemp under the US Agriculture Improvement Act of 2018 (2018 Farm Bill).¹ This legislation has catalysed expansive growth in research, cultivation, distribution, and consumption of Cannabis and its derivatives.

Cannabis produces over 500 compounds, with cannabinoids — phytocannabinoids biosynthesized within glandular trichomes of female Cannabis flowers — being the primary biologically active constituents.² Characterized by a typical C₂₁ terpenophenolic skeleton, the most known cannabinoids are Δ^9 -tetrahydrocannabinol (Δ^9 -THC) and cannabidiol (CBD). Δ^9 -THC is psychoactive, whereas CBD offers therapeutic benefits without intoxication, shaping their roles in medical and recreational use. Beyond Δ^9 -THC and CBD, more than 120 cannabinoids have been identified. The chemical and pharmacological diversity of cannabinoids underscores the necessity and complexity of Cannabis analysis. A key focus in Cannabis analysis is its classification, especially the distinction between drug-type marijuana and fiber-type hemp, primarily determined by their Δ^9 -THC content.³

As global Cannabis cultivation rapidly expands, a wide diversity of Cannabis products has emerged.⁴⁻⁶ Apart from normal Cannabis products with phytocannabinoid constituents, a notable trend is the emergence and popularity of "legal high" substitutes of Δ^9 -THC like Δ^8 -THC products. These are semisynthetic cannabinoids, typically derived from legally accessible CBD through simple chemical conversions.⁷⁻⁹ These products exhibit varying degrees of psychoactivity and possess unclear legal status, marketed widely as "legal high" products to evade legal issues. In both conventional Cannabis products and these "legal high" variants, numerous issues have surfaced.¹⁰⁻¹² These include but are not limited to: (i) incorrect labeling, where claims of therapeutic effects prohibited by the FDA are made, alongside inaccuracies in cannabinoid content and absence of health/age warnings;

(ii) instances of illegal Δ^9 -THC levels, despite claims of legal compliance; (iii) presence of unknown substances, such as synthetic cannabinoid byproducts during Δ^8 -THC production, raising concerns due to limited toxicological data.

The evolving Cannabis industry highlights significant concerns regarding legality, safety, and quality. This necessitates appropriate analytical techniques to provide accurate qualitative and quantitative insights into cannabinoid composition across various application scenarios. In recent decades, substantial efforts have been dedicated to developing gas chromatography (GC) and high-performance liquid chromatography (HPLC)-based methods.¹³⁻¹⁵ While these methods have been extensively documented for Cannabis and cannabinoid analysis, their operational parameters vary slightly. Some have been adopted as official methods for Cannabis and Cannabis product analysis,¹⁶⁻²⁰ demonstrating the maturity and robustness of GC and HPLC-based approaches in this field. However, these methods suffer from drawbacks such as decarboxylation in GC and the resulting necessity for derivatization, which can complicate analysis.²¹ HPLC, while versatile and mild, requires significant amounts of organic solvents and encounters challenges with resolving cannabinoid isomers.^{22,23} Additionally, both methods involve sample pretreatment and chromatographic separations, compromising high-throughput capabilities. Finally, they are primarily limited to laboratory settings for the final confirmatory analysis of samples.

As the Cannabis market diversifies, there is an urgent demand for rapid and environmentally friendly methods capable of delivering fast and reliable results across diverse Cannabis and Cannabis product analysis applications. Specifically, three categories — (i) field screening, (ii) portable instrumental testing, and (iii) lab confirmatory methods — show promise in addressing these needs. Field screening methods provide immediate on-site results, enabling rapid decisions in Cannabis classification and quality control of Cannabis products. This initial screening step significantly reduces sample sizes by eliminating negative samples with minimal financial and technical requirements. Portable instrumental testing offers mobility

and versatility, is suitable for further screening analysis with enhanced accuracy, and thus has moderate requirements toward the analytical environment and personnel. Finally, suspected samples can be transported to laboratories for comprehensive confirmatory and regulatory compliance analysis using advanced instrumentation.

In this chapter, recently developed analytical techniques (2013–2023) for the analysis of Cannabis and Cannabis products across various application areas are reviewed. Relevant high-quality literature published between 2013 and 2023 was identified through SciFinder using keywords such as "cannabinoid," "analysis," and "fast" or "rapid" (**Figure 2.1**). The results were systematically screened and are summarized and discussed herein. These methods were primarily classified into: (i) colorimetric spot tests, (ii) electrochemical methods, (iii) spectroscopic methods, (iv) immunochemical methods, (v) nuclear magnetic resonance (NMR) methods, (vi) ion mobility spectrometry (IMS) methods, and (vii) ambient ionization mass spectrometry (AIMS) methods. Detailed information on each developed method, including their advantages, disadvantages, analyzed sample types, targeted cannabinoids, and qualitative and quantitative performance metrics, is presented in tables. Critical comparisons were conducted across these methods regarding their performance in terms of portability, simplicity of sample preparation, eco-friendliness, time efficiency, cost-effectiveness, accuracy, sensitivity, selectivity, and user-friendliness. Based on these evaluations, potential application scenarios were suggested. Other analytical techniques like supercritical fluid chromatography (SFC) have also been applied in the analysis of Cannabis and related products. However, they are not discussed due to yet limited implementation in peer-reviewed publications. Additionally, as previously noted, GC and HPLC-based methods, extensively reviewed elsewhere, are not covered in this chapter.

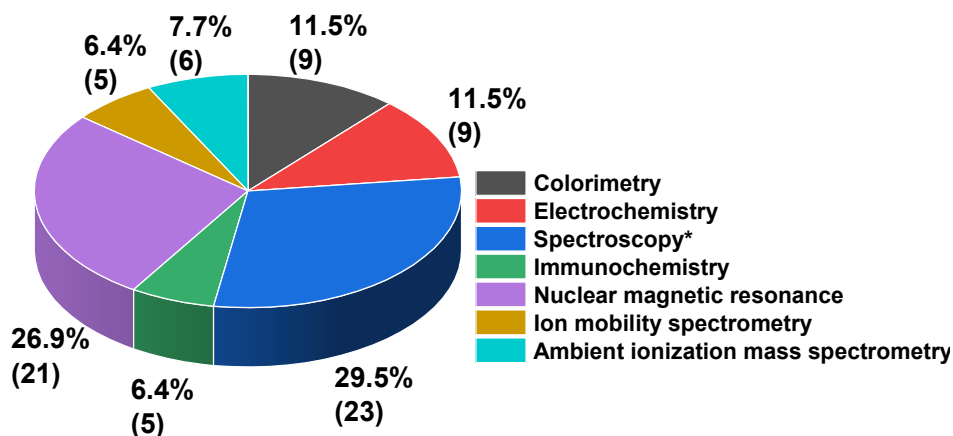


Figure 2.1. Distribution of publications about fast screening methods for Cannabis and cannabinoid analysis from 2013–2023 (78 references in total; for spectroscopy the publications are from 2018–2023).

Colorimetric Spot Tests

Colorimetric spot tests have been widely used as screening methods in commercial test kits for Cannabis plant classification and point-of-need cannabinoid tests, mainly due to their speed, low cost, and ease of use (**Table 2.1**). Since 1941, the most popular colorimetric spot test for identifying Cannabis is the Duquénou–Levine (D-L) field test, in which a purple color is formed by adding a series of reagents to react with cannabinoids.²⁴ However, this method cannot distinguish Δ^9 -THC (marijuana) and CBD (hemp) due to the shared resorcinol backbone and an aliphatic chain triggering the same colorimetric reaction. Also, false positive or inconclusive results have been encountered in multiple non-Cannabis plant materials.²⁵ 4-Aminophenol (4-AP) is a more selective colorimetric reagent; the 4-AP test forms a blue color with THC-rich samples and a pink color with CBD-rich samples. Traditional 4-AP assays need a large volume of solvent (1 mL) and samples (5 mg), and the effective color-observation window is only 1–2 min, which makes color observation and interpretation challenging.²⁶ Acosta et al.²⁷ miniaturized the assay by performing the reaction on a small piece of silicone-treated filter paper (6.35 mm). By such operation, the solvent consumption decreased ($< 50 \mu\text{L}$), and the color-observation window was extended to 5 min. In combination with

chemometric analysis, the miniaturized 4-AP is effective (> 90% correct classification) at distinguishing marijuana from hemp when the ratio $\Delta 9$ -THC:CBD is larger than 2. However, it is ineffective when that ratio is smaller. Other recommended colorimetric reagents by the United Nations Office on Drugs and Crime (UNODC) for cannabinoid analysis include Fast Corinth V and Fast Blue B (FBB) salts.²⁸ Fast Corinth V forms the same purple-red color for $\Delta 9$ -THC, CBD, and CBN, whilst FBB is more selective, producing red for $\Delta 9$ -THC, orange for CBD, and purple for CBN. Fast Blue BB (FBBB) is another popular color reagent with a similar colorimetric reaction as FBB but a higher selectivity. The reaction products formed between FBBB and $\Delta 9$ -THC have been identified by ultraviolet-visible (UV-Vis) spectroscopy, thin layer chromatography (TLC), high-resolution mass spectrometry, ¹H-NMR, and ab initio calculations.^{29,30} Based on these results, FBBB was expected to couple to the para position relative to the phenolic group of $\Delta 9$ -THC.

Similar to the miniaturization of the 4-AP assay, Acosta et al.³¹ also achieved a more sensitive analysis (LOD 500 ng for $\Delta 9$ -THC) of Cannabis through FBBB reaction on a 3.5 mm planar solid phase microextraction (PSPME) substrate. Combined with Linear Discriminant Analysis (LDA), the developed method could successfully distinguish Cannabis and non-Cannabis samples as well as hemp and marijuana. However, again, when the ratio $\Delta 9$ -THC:CBD is smaller than 2, misclassification would be encountered. Moreover, it was suggested that FBBB should be kept in a refrigerator to avoid degradation, which needs to be considered when applying the method in the field.

One significant limitation of conventional colorimetric spot tests is their susceptibility to producing false-positive, false-negative, or inconclusive results. This is primarily due to the complex composition of Cannabis samples, where similar colorimetric reactions can occur for different cannabinoids and non-cannabinoids. Besides, other compounds from the Cannabis matrix, such as pigments, can interfere with color observation. Therefore, separation of components before colorimetric analysis is crucial to enhance accuracy. Thin layer chromatography (TLC) presents a practical method for this purpose, being cost-effective, rapid, and high-throughput.

To observe the separated components, colorless spots from the samples can be seen under ultraviolet (UV) light or through colorimetric reactions.³²

In recent research on cannabinoid analysis, efforts have been made to improve TLC separation and detection. Conventional silica TLC plates provide limited resolution of several common neutral cannabinoids, e.g., Δ^9 -THC, CBD, and CBN.³³⁻³⁶ Instead of using silica TLC plates, Ag(I) modified TLC plates^{37,38} have shown improved separation toward cannabinoids due to various affinities of Ag(I) toward compounds with different numbers or positions of olefinic double bonds.³⁹⁻⁴¹ Tsujikawa et al.³⁷ applied fully impregnated AgNO_3 -silica TLC plates and obtained clear separation of Δ^9 -THC, CBD, CBN, Δ^8 -THC, Δ^{10} -THC, and $\Delta^6\text{a},10\text{a}$ -THC despite THCA tailing and overlap with CBD. After the reaction with FBB, the Ag(I)-TLC plates could provide qualitative information about home-made THC mixtures with the naked eye. Huang et al.³⁸ designed a silica TLC plate with a Ag(I) retention zone and chromogenic smartphone detection zone. The partially modified Ag(I)-TLC plate realized digital chromatographic separation of Δ^9 -THC analogues (THCA, Δ^9 -THC, and CBN) and CBD analogues (CBDA, CBD, and CBG) and showed reliable application in Cannabis classification.

For detecting separated cannabinoids, staining with colorimetric reagents and observing with the naked eye is the cheapest and most common qualitative way, despite the risk of human errors. To minimize such errors, Mano-Sousa et al.³⁶ applied a software tool for color-naming after they achieved the (partial) separation of Δ^9 -THC, CBD, CBN, and CBG by silica TLC plate and stained spots with FBB and Fast Blue RR (FBRR). Such standardized color determination is promising to reduce analytical errors induced by subjectivity. With the development of more detailed and versatile regulations toward cannabinoid contents, (semi)quantitative analysis is needed. For such purposes, densitometric and UV scanners^{33,35} as well as electrospray ionization mass spectrometry³⁴ are used, but have the disadvantages of high cost and low portability. Huang et al.³⁸ applied a smartphone to semiquantify Δ^9 -THC analogues after color development with FBRR, demonstrating the potential of using ubiquitous smartphones as detection tools in colorimetric spot tests.

Table 2.1. Published colorimetric spot tests for Cannabis and cannabinoid analysis from 2013 to 2023.

Method	Portable/ Lab-based	Cannabinoids	Samples	Time	Qualitative/ Quantitative	Advantages	Disadvantages	Year/ Ref
FBB and FBBB colorimetric test of Cannabis plant extracts.	Portable	Δ^9 -THC, CBD, CBN.	8 Cannabis plant samples, parts of Cannabis plant (stalk, flower, leaf and root).	ND	Identification of the presence of Δ^9 -THC, CBN, CBD.	FBBB has better selectivity over FBB toward cannabinoids; colorimetric product of FBBB and Δ^9 -THC was investigated by MS, UV-Vis, and TLC and reaction mechanism was proposed.	Can be only used as a screening assay and false positive results are easily obtained from non-cannabinoids.	2016 ²⁹
FBBB colorimetric test of Cannabis plant extracts using a small polymer strip and a CMV sorbent device.	Portable	Δ^9 -THC, Δ^9 -THC-COOH, Δ^9 -THC-OH, CBN, CBD.	Cannabis plant samples.	ND	Distinction between hemp-type and marijuana-type; LOD 50 ng with small polymer strip and LOD 500 ng with CMV sorbent device.	Fast and portable; colorimetric reaction product of FBBB and Δ^9 -THC was identified by 1H-NMR and HRMS.	Different extraction solvents result in different extents of false positive results.	2020 ³⁰
Miniaturized reaction between FBBB with Δ^9 -THC (red chromophore and fluorophore) and CBD (orange) from plant extracts on a 3.5 mm diameter planar microfiberglass coated with polydimethylsiloxane; RGB image analysis and LDA.	Portable	Δ^9 -THC, CBD.	20 Cannabis plant samples.	~2 min	Distinction between hemp-type and marijuana-type; LOD 500 ng for Δ^9 -THC.	Fast; portable; low solvent consumption (< 50 μ L); ten times more sensitive than the Duquenois-Levine test.	Marijuana with Δ^9 -THC:CBD ratio ≤ 1 could be misclassified as hemp; limited stability of FBBB (survived for a few days at room temperature).	2021 ³¹
HPTLC combined with FBB and ESI-MS.	Lab-based	CBN, CBD, Δ^9 -THC.	15 CBD oils.	30 min	Quantitative; LOD CBN 3.6 ng; CBD 16.6 ng; Δ^9 -THC 7.0 ng.	Sensitive; high-throughput (5 samples/per plate).	Need deuterated IS of CBN, CBD and Δ^9 -THC; specific instrumentation is needed.	2021 ³⁴

Silica gel TLC separation; color-development with FBB or FBRR; Standardization of color names via Sci-Chromus® software.	Lab-based	CBD, Δ9-THC, CBN, CBG.	6 marijuana samples, 1 hemp oil.	ND	Qualitative identification of cannabinoid.	Color-naming by software reduced subjectivity.	Acid cannabinoids which are abundant in Cannabis plant materials are not evaluated; color reaction of FBB and FBRR was only evaluated in acidic condition and one concentration level.	2021 ³⁶
4-AP colorimetric test of Cannabis plant materials without sample pretreatment.	Lab-based	Δ9-THC, THCA, Δ8-THC, Δ9,11-THC, THCV, THCVA, CBD, CBDA, CBDV, CBDVA, CBL, CBLA, CBG, CBGA, CBN, CBNA, CBV, CBC.	66 Cannabis plant samples.	1–2 min	Distinction between THC-rich and CBD-rich Cannabis chemotypes.	Fast; robust (intra-lab, inter-lab consistency); no sample pretreatment.	False positive results from non-Cannabis; inconclusive results when the Δ9-THC:CBD ratios are between 0.3 and 3.0.	2021 ²⁶
Miniaturized 4-AP colorimetric test on a 6.35 mm diameter silicone-treated filter paper substrate with Δ9-THC and CBD from Cannabis extracts; chemometric analysis LDA and DD-SIMCA models.	Portable	Δ9-THC, CBD.	99 marijuana plant samples and 93 hemp plant samples.	5 min	Distinction between hemp-type and marijuana-type.	Fast; portable; low solvent consumption (< 50 µL); > 90% correct classification when Δ9-THC:CBD > 2.	Marijuana could be misclassified as hemp when Δ9-THC:CBD < 2; 4-AP only has 5 min observation window.	2022 ²⁷
Separation by AgNO ₃ fully impregnated silica gel TLC; color development by FBB; visual observation.	Portable	Δ9-THC, Δ8-THC, Δ10-THC, 9S-Δ10-THC, 9R-Δ6a,10a-THC, CBD, CBN, Δ9-THCA.	Acid-treated CBD mixture.	ND	Qualitative identification of cannabinoids; LOD of Δ9-THC, Δ8-THC, CBD, and CBN 0.1 µg.	Δ9-THC, CBD, CBN, and Δ8-THC were resolved; useful for analyzing samples containing THC isomers.	THCA spot was tailing and overlapped with the CBD spot; not suitable for analyzing Cannabis plant samples.	2022 ³⁷

Separation of cannabinoids in Cannabis sample extracts by partially modified AgNO ₃ silica gel TLC; color development by FBBB; smartphone-based color analysis for semiquantification.	Portable	THCA, Δ9-THC, CBN, CBDA, CBD, CBG.	3 Cannabis plant samples and 1 CBD oil.	10 min	Semiquantitative with a LOD of 11 ng for Δ9-THC, 54 ng for CBN, and 50 ng for THCA.	Fast; high-throughput; low solvent consumption; portability; cross-validated with HPLC-UV.	Individual quantification of Δ9-THC and CBN is not feasible due to insufficient separation.	2022 ³⁸
---	----------	------------------------------------	---	--------	---	--	---	--------------------

Abbreviations: Linear Discriminant Analysis (LDA), 4-Aminophenol (4-AP), Data Driven-Soft Independent Modelling of Class Analogies (DD-SIMCA), Fast Blue B salt (FBB, Azoic Diazo No. 48), Fast Blue RR (FBRR, Azoic Diazo No. 24), Fast Blue BB (FBBB), Capillary Microextraction of Volatiles (CMV), High-Performance Thin-Layer Chromatography (HPTLC), Electrospray Ionization Mass Spectrometry (ESI-MS), Internal Standard (IS).

Electrochemical Methods

Due to the merits of miniaturization, low cost, rapidity, and simplicity, electrochemical techniques provide a promising approach for the screening of cannabinoids (**Table 2.2**). The detection principle is mainly based on the irreversible oxidation of the phenol group.⁴² While electrochemical detection offers numerous advantages, detecting Δ^9 -THC poses significant challenges as well. This difficulty is primarily due to the hydrophobic nature of Δ^9 -THC, as electrochemical detection is typically conducted in aqueous solutions. To address this issue, Balbino et al.⁴³⁻⁴⁵ introduced Δ^9 -THC into an organic solution containing tetrabutylammonium tetrafluoroborate in dimethylformamide, enhancing its solubility. Subsequently, they monitored Δ^9 -THC oxidation using a glassy carbon working electrode. Novak et al.⁴⁶ directly loaded Cannabis microparticles on a paraffin-impregnated graphite electrode and immersed the electrode into 0.1 M KNO₃ at pH 7. The attached cannabinoids on the electrode were used as reactants in the square-wave voltammetry analysis to avoid its poor water-solubility issues. Similarly, Nissim et al.⁴⁷ devised an approach involving a recessed Cu wire electrode coated with conductive carbon paste mixed with mineral oil. By doing this, non-polar Δ^9 -THC was preconcentrated from aqueous sample solutions. After that, the Δ^9 -THC-loaded electrode was subjected to an anodic square wave voltammetric scan in a pH 10 buffer solution, resulting in the sensitive detection of Δ^9 -THC. Despite the advantages of non-toxic and easily implemented sampling, reproducibility was found to be challenging due to the complex carbon paste electrode assembly. To avoid the complexity of electrode construction, Renaud-Young et al.⁴⁸ deposited fixed amounts of Δ^9 -THC, OH-THC, or COOH-THC reference standards onto porous carbon electrodes, followed by air-drying. The electrodes were then tested in aqueous solutions with a pH of 10. High sensitivity with LODs of 1 pmol for Δ^9 -THC and THC-OH, as well as 2 pmol for THC-COOH, was achieved with this method, even though the electrochemical signals were not distinct enough to differentiate the three compounds. By using silicon oxide-based materials containing poly-(3,4-ethylenedioxythiophene) (PEDOT) as the working electrode, López-

Iglesias et al.⁴⁹ achieved sensitive detection of reference standards CBD (LOD 0.94 μmol) and CBN (LOD 1.29 μmol). This was possible, because including highly conductive polymer PEDOT inside the electrode improved electrochemical responses. However, due to similar phenol oxidation behavior, no pronounced selectivity between CBD and CBN was observed. To overcome the selectivity issue, Zanfognini et al.⁵⁰ applied Principal Component Analysis (PCA) to distinguish small differences in electrochemical signals and obtained the distinction between reference standards $\Delta^9\text{-THC}$ and CBD. Overall, a significant portion of electrochemical analysis remains confined to cannabinoid reference standards instead of diverse real samples, partly due to their limited ability to resist matrix interferences. This, to some extent, reflects the developmental stage of electrochemical analysis methods in the field of Cannabis and its products.

Table 2.2. Published electrochemical methods for Cannabis and cannabinoid analysis from 2013 to 2023.

Method	Portable/ Lab-based	Cannabinoids	Samples	Time	Qualitative/ Quantitative	Advantages	Disadvantages	Year/ Ref
Voltammetry of microparticles using a paraffin-impregnated graphite electrode in an aqueous solution of 0.1 M KNO ₃ at pH 7.	Lab-based	Δ 9-THC, CBD, CBN.	Cannabis leaves and hemp tea.	ND	Qualitative detection of cannabinoids.	Cannabinoids in microparticles can be directly detected without extraction; avoiding poor solubility in aqueous solutions.	Cannabis samples need to be ground into microparticles and mechanically immobilized into a working electrode first; the oxidation peak potentials of Δ 9-THC, CBD, and CBN, as well as hemp and marijuana samples, are very similar.	2013 ⁴⁶
Δ 9-THC detection by SWV analysis in organic medium DMF; TBATF as supporting electrolyte, and glassy carbon and platinum discs as working electrodes.	Lab-based	Δ 9-THC.	Δ 9-THC reference standard.	ND	Quantitative; LOD of 6.2×10^{-10} mol·L ⁻¹ for glassy carbon and 2.7×10^{-8} mol·L ⁻¹ for platinum.	First work on the direct determination of Δ 9-THC by SWV; more sensitive than other voltammetric methods for Δ 9-THC analysis with glassy carbon work electrode.	Toxic organic solvent DMF used as medium.	2014 ⁴⁴
Absorptive Stripping Voltammetry with a refined carbon paste electrode, composed of graphite powder and mineral oil working in aqueous solutions BBS with a pH of 10.0.	Lab-based	Δ 9-THC.	Synthetic saliva solutions.	> 5 min	Quantitative; LOD 0.50 μ mol·L ⁻¹ .	Sensitive.	Poor reproducibility induced by renewing the surface of the carbon paste electrodes between each scan.	2015 ⁴⁷
Voltammetric analysis using carbon SPE devices in a portable potentiostat.	Portable	Δ 9-THC.	Marijuana extract.	ND	Quantitative; LOD 3.0 μ mol·L ⁻¹ .	No modification on the electrode surface; portable.	Severe interference effects from compounds with phenol group.	2016 ⁴⁵
CV with a glassy carbon working electrode and 0.1 mol·L ⁻¹ TBATFB DMF solution as medium.	Lab-based	Δ 9-THC.	5 Cannabis plant samples.	ND	Qualitative; LOD 1.0 ng·mL ⁻¹ for Δ 9-THC.	Ability to distinguish between Cannabis and non-Cannabis.	Interferences from other cannabinoids were not investigated.	2016 ⁴³
CV and SWV analysis of cannabinoids by infusing them into carbon paper electrodes working in aqueous BBS at pH 10.	Lab-based	Δ 9-THC, Δ 9-THC-OH, Δ 9-THC-COOH.	Reference standards.	ND	Quantitative; LOD: 1 pmol·L ⁻¹ for Δ 9-THC, 1 pmol·L ⁻¹ for OH-THC, 2 pmol·L ⁻¹ for COOH-THC.	Sensitive enough for determination of driver impairment.	Only around 20% of the deposited Δ 9-THC is accessible for electro-oxidation.	2019 ⁴⁸

CuPc- and F16-CuPc-based OTFTs coated with FBBB for detection of cannabinoids in liquid and gas-phase.	Portable	$\Delta 9$ -THC, CBD.	2 Cannabis plant materials.	~2 min	Quantitative estimation of $\Delta 9$ -THC:CBD ratio.	Low cost; simple sample preparation; rapid analysis; capable of liquid- or vapor-phase detection; cross-validated by HPLC-UV.	Large bias from results obtained by HPLC-UV; cannabinolic acids are undifferentiable from the respective neutral forms.	2019 ⁵¹
Voltammetric analysis with Sonogel-Carbon- PEDOT as a working electrode in aqueous buffer solutions mixed with acetonitrile or ethanol.	Lab-based	CBD, CBN.	Reference standards.	> 10 min	Quantitative; LOD of CBD $0.94 \mu\text{mol} \cdot \text{L}^{-1}$ and CBN $1.29 \mu\text{mol} \cdot \text{L}^{-1}$.	High sensitivity due to the inclusion of PEDOT inside the silicon oxide (higher conductivity).	Cannot distinguish CBD and CBN; fouling phenomena needs 10 min of mechanical renewal of the electrode surface.	2020 ⁴⁹
Differential pulse voltammetry method using SPE with a carbon black coating working in 7:3 v/v mixture of BRB (pH 7.0) and MeOH combined with multivariate analysis	Lab-based	$\Delta 9$ -THC, CBD.	Reference standards.	ND	Qualitative.	Identification of $\Delta 9$ -THC without interfering with CBD.	Chemometric analysis is needed to identify the very small difference between $\Delta 9$ -THC and CBD; limited repeatability (RSD 20%).	2022 ⁵⁰

Abbreviations: Square Wave Voltammetric (SWV), N,N-Dimethylformamide (DMF), Tetrabutylammonium Tetrafluoroborate (TBATFB), Borate Buffers (BBS), Screen-Printed Electrode (SPE), Poly-(3,4-Ethylenedioxythiophene) (PEDOT), Cyclic Voltammetry (CV), Copper Phthalocyanine (CuPc), Copper(II) 1,2,3,4,8,9,10,11,15,16,17,18,22,23,24,25-hexadecafluoro-29H,31H-phthalocyanine (F16-CuPc), Organic Thin-Film Transistors (OTFTs).

Optical Spectroscopic Methods

Optical spectroscopic analysis is based on light interacting with the sample, usually ultraviolet, visible, or infrared radiation, and changes in the light are then detected. This process yields information about the composition, structure, and properties of substances.⁵² Among various optical spectroscopic methods, UV-Vis spectroscopy, (near)-infrared ((N)IR) spectroscopy, fluorescence spectroscopy, and Raman spectroscopy have wide applications in cannabinoid analysis.

In the field of Cannabis and cannabinoid analysis, optical spectroscopic techniques are normally combined with chemometrics to interpret complex spectroscopic data sets (**Table 2.3**). Specifically, acquired optical spectra are paired with reference data collected by HPLC-MS or GC-MS to build statistical models by chemometric software for classifying Cannabis or predicting cannabinoid content. The most frequently used chemometrics in this situation is multivariate analysis, including principal component analysis (PCA, to simplify the dataset for better data quality control), partial least squares discriminant analysis (PLS-DA, to classify Cannabis samples), and partial least square regression (PLSR, to predict cannabinoid content). The reliability of the models depends on the quality and quantity of the training set, data transformation, and used algorithms. Among the aforementioned techniques, NIR combined with chemometric analysis has the most published applications due to the advantages of being fast and suitable for a wide range of sample forms and it allows *in situ* and non-invasive detection.⁵³

NIR-chemometric methods have wide applications in the analysis of Cannabis plants. A significant constraint associated with NIR-based techniques pertains to the NIR signal of water. Vibrational overtones (1400–1550 nm) and combination modes (1850–2100 nm) produced by water in wet Cannabis would dampen the vibration frequencies of the target analytes within the same spectral region, consequently hindering the accuracy of predictions and/or classifications.⁵⁴⁻⁵⁶ In order to avoid the water issue, samples need to be dried before NIR analysis through the “curing” step after the harvest (drying in a controlled environment at a temperature of 15–21 °C),⁵⁷ by heat-treatment,⁵⁴ or freeze-drying.⁵⁸ Among them, the heat-treated Cannabis plant

is not suitable for acidic cannabinoid analysis due to decarboxylation. On the other hand, Cannabis samples without drying could also be analyzed by NIR techniques. Su et al.⁵⁹ applied NIR paired with PLSR models to analyze 194 intact samples (consisting of leaf and bud) and 115 ground samples without drying beforehand for the simultaneous quantitative prediction of moisture content and cannabinoids. The predicted moisture content was then used to correct cannabinoid measurements, allowing for the calculation of the adjusted $\Delta 9$ -THC percentage on a dry-weight basis, which can be used to distinguish between legal and illegal Cannabis. However, the NIR signals from water at 980 nm and 1450 nm overlapped with those of CBD, complicating the accurate prediction of CBD levels.

Among NIR applications, hand-held NIR gained more attention due to its portability and potential for in-field analysis. Despite the slightly lower accuracy compared with benchtop equipment,^{58, 60} hand-held NIR devices still have wide applications in discriminating Cannabis from non-Cannabis samples and different Cannabis chemovars, as well as quantitatively predicting cannabinoids in Cannabis plants.⁶¹⁻⁶⁴ According to Deidda et al.,⁶⁵ the choice of device, physical form of sample, and chemometric models have pronounced impacts on the in-field analysis of Cannabis samples by hand-held NIR methods, which should be taken into account. Besides the applications in Cannabis plants, hand-held NIR methods are also employed to analyze Cannabis products, e.g., CBD-based liquid formulations,⁶⁶ commercial hemp flours,⁶⁷ veterinary feeds,⁶⁸ and hemp seed oil.⁶⁹ Efforts have also been made to detect and quantify $\Delta 9$ -THC in oral fluids, and preliminary results showed it was promising to use such a platform for drug tests on the road or in the workplace, despite severe signal overlapping with matrix components, most likely water.⁷⁰ The development of handheld NIR techniques is increasingly trending toward miniaturization,⁶³ automation,⁶⁹ and cloud-based data management.⁷¹

Due to the insensitive fluorescence properties of water molecules, fluorescence spectroscopy is a good option for the analysis of fresh Cannabis. Birenboim et al.^{56,72} employed a lab-based spectrofluorometer combined with different chemometric models to analyze ethanol extracts of fresh Cannabis plant materials and achieved

quantitative prediction of acidic cannabinoids despite the compromised capability to differentiate or quantify neutral cannabinoids. However, the fluorescence spectroscopy technique has an inner filter effect (IFE), which induces a concentration-dependent distortion in the measured fluorescence spectrum. This distortion occurs because of reabsorption phenomena that become increasingly pronounced at higher concentrations. Gilmore et al.⁷³ utilized equipment that integrates UV/Vis/NIR with fluorescence spectroscopy. The absorption spectrum produced by UV/Vis/NIR can be used to correct IFE and thus guarantee more reproducible fluorescence measurements.

Raman spectroscopy is also water-insensitive⁷⁴ but suffers from fluorescence overlapping with Raman signals when using visible or near-IR wavelengths. Porcu et al.⁷⁵ applied Raman spectroscopy with an IR laser (1064 nm) to avoid fluorescence interference and this enabled the analysis of 42 fresh Cannabis plant materials and discrimination between THC-rich and CBD-rich chemotypes. Compared with Raman spectroscopy, surface-enhanced Raman spectroscopy (SERS) has higher sensitivity in general due to the enhanced Raman scattering and thus could achieve lower LOD ($1\text{ }\mu\text{g}\cdot\text{mL}^{-1}$ for $\Delta 9$ -THC reference standard and $65\text{ ng}\cdot\text{mL}^{-1}$ for CBN reference standard).⁷⁶ One limitation of SERS for cannabinoid analysis is the weak surface affinity and inefficient Raman scattering of cannabinoids, which result in low sensitivity compared to other compounds. To achieve sensitive detection of $\Delta 9$ -THC and THC-COOH in biological fluids, Bindesri et al.⁷⁷ utilized electrochemical surface-enhanced Raman spectroscopy (EC-SERS). By applying a voltage to the SERS substrate, the absorption of $\Delta 9$ -THC and $\Delta 9$ -THC-COOH was improved due to the surface charge, and thus, the signal intensity was enhanced.

Despite the fact that spectroscopic-chemometric techniques are intensively studied in this field, there are several challenges with respect to their application and implementation, and improvements are needed in the following aspects: (i) chemometric model suitability, as specific chemometric models are required for different sample types, and model updates are needed when the sample exhibits physicochemical variations; (ii) instrument compatibility, as not all available devices

may be compatible with the complexity of the Cannabis sample; (iii) sample heterogeneity and size, as large sample sizes are needed to capture the natural variabilities within Cannabis samples effectively; (iv) improved accuracy, as in chemometric-related analysis, accuracy depends not only on the instruments but also heavily on the quality and applicability of the calibration models. The selection of the model, the quality and quantity of the training data, and the model validation process all significantly impact the final accuracy. Therefore, the accuracy of chemometric-related analytical methods is generally lower than that of common non-chemometric-related analytical methods.

Table 2.3. Published spectroscopic methods for Cannabis and cannabinoid analysis from 2018 to 2023.

Method	Portable/ Lab-based	Cannabinoids	Samples	Time	Qualitative/ Quantitative	Advantages	Disadvantages	Year/ Ref
NIR and FT-NIR coupled with PLSR model.	Lab-based	CBDV, Δ 9-THCV, CBC, Δ 8-THC, CBD, Δ 9-THC, CBG, CBN.	Cannabis leaves and inflorescences.	ND	Quantitative prediction.	Easy sample pre-treatment (e.g., grinding, drying); no solvent is needed.	Low prediction accuracy for CBN, CBG and Δ 9-THCV.	2018 ⁵⁴
NIR combined with PLSR models.	Lab-based	CBD.	12 different CBD-based liquid formulations.	~30 s	Quantitative.	Fast and no sample pretreatment.	Did not investigate the interferences from other cannabinoids.	2019 ⁶⁶
Miniaturized and portable MicroNIR combined with PLS-DA and PLSR models.	Portable	Δ 9-THC.	Oral fluid specimens from 50 anonymous volunteers and spiked oral fluid.	2.5s	Quantitative prediction; LOD 0.1%.	Fast and easy to use; potential for roadside drug testing and workplace surveillance.	Severe signal overlapping from the matrix.	2019 ⁷⁰
Miniaturized analytical platform based on the MicroNIR combined with PLS-DA and PLSR models.	Portable	Δ 9-THC, CBD, CBG.	10 different hemp flours commercially available were analyzed as such and spiked with CBD, Δ 9-THC, CBG.	2.5 s	Quantitative; LOD 0.001%.	Miniaturized and automated platform.	Large deviation for CBD between quantitative prediction (0.05%) and GC-MS (0.03%).	2020 ⁶⁷
EC-SERS complemented by thorough ab initio calculations of Raman vibrational modes.	Lab-based	Δ 9-THC, Δ 9-THC-COOH.	Artificial saliva, synthetic urine.	30 s	Qualitative.	Ability to electrochemically “clean” the SERS sensor surface prior to analysis to provide more adsorption sites for analytes.	Significant spectral interference from matrix.	2020 ⁷⁷

A benchtop and a handheld NIR device combined with PLS-DA, k-NN and SIMCA models.	Portable & Lab-based	Δ^9 -THC.	189 dried and crushed Cannabis samples (aerial parts).	ND	Qualitative classification Cannabis (binary and tertiary in relation to European legislation).	The handheld device gave similar results as the benchtop device; high prediction accuracy (91% for the handheld device and 95% for the benchtop equipment).	High rate of unclassified samples (21% for the handheld device and 20% for the benchtop equipment); prediction of intermediary class is not so accurate due to limited training sample size (11 samples).	2020 ⁶⁰
Ultra-portable NIR detector connected to a mobile application.	Portable	Δ^9 -THC, CBD.	660 Cannabis specimens.	5 s	Quantitative prediction.	Analysis and results display to end users within 5 s; algorithms and the databases are in the cloud.	Only suitable for the analysis of substances that have been used to train the algorithms; regular updates of models are needed for new species.	2020 ⁷¹
Portable microNIR in combination with PLS-DA and PLSR models.	Portable	CBD, Δ^9 -THC and CBG.	Standard-spiking feeds and 4 real samples with cannabinoids.	ND	Quantitative; detection range for CBD, Δ^9 -THC and CBG 0.001 to 0.01% w/w%.	Non-destructive; solvent-free; easy to use.	Only four real samples were evaluated; correlation $R^2 = 0.96$.	2020 ⁶⁸
Completely automated MicroNIR On-Site spectrometer with prediction models developed by PLSR algorithms.	Portable	Δ^9 -THC, CBD, THCA.	15 commercial Hemp seed oil.	seconds	Quantitative prediction.	On-site prediction in few seconds; automated platform for non-experts.	Limited prediction accuracy; small sample size; low sensitivity for THCA.	2020 ⁶⁹
UV-Vis and NIR combined with PCA and ANNs (prediction) models.	Lab-based	DPPH, Trolox, TPTZ, gallic acid.	46 dried industrial hemp (mixture of leaves, flowers, seeds, and stems).	ND	Quantitative prediction.	Ability to monitor total dissolved solids, extraction yield, total polyphenolic content, antioxidant activity of hemp extracts.	Limited prediction accuracy ($R^2 > 0.7$).	2021 ⁷⁸

Hand-held NIR in couple with PLS models.	Portable	Δ^9 -THC.	Cannabis inflorescence in different physical forms (entire, ground and sieved).	ND	Quantitative.	Portable; direct analysis of entire Cannabis inflorescences and resins.	Sample type-dependent; limited sample size.	2021 ⁶⁵
SERS by using glancing angle deposition and tuned dimensions of AgNRs combined with an open-source ICA algorithm.	Lab-based	Δ^9 -THC, CBN.	Reference standards.	seconds	Quantitative; LOD of Δ^9 -THC 1 $\mu\text{g}\cdot\text{mL}^{-1}$, CBN 65 $\text{ng}\cdot\text{mL}^{-1}$.	SERS substrates could be mass-produced and easily tuned; fast; sensitive; small sample consumption.	Only standard mixtures were tested.	2022 ⁷⁶
FT-NIR coupled with PLS-DA and PLSR models.	Lab-based	CBDA, CBGA, CBG, CBD, Δ^9 -THCV, CBN, Δ^9 -THC, Δ^8 -THC, CBL, CBC, THCA, CBCA; terpenes.	325 dried Cannabis inflorescences.	< 1 min	Quantitative prediction of 10 cannabinoids and 9 terpenes; classification of Cannabis into high-THC, high-CBD, hybrid, and high-CBG, high-CBDA, high-CBGA, high-THCA, and hybrid.	Rapid; high-throughput; non-destructive; no solvent is needed.	Large amount sample is needed (100 mg); only dry samples can be analyzed. Limited accuracy (Correlations R^2 between the predicted and measured concentrations of cannabinoids by HPLC-DAD varied from 0.748 to 0.992.	2022 ⁵⁷
Hand-held NIR in combination with PCA and PLS models.	Portable	Δ^9 -THC, CBD.	35 hemp samples.	ND	Prediction of Δ^9 -THC and CBD.	Simple; low-cost; fast.	Limited sample size for the modelling; limited accuracy.	2022 ⁶⁴

Hand-held Raman spectroscopy in combination with PLS-DA and machine learning.	Portable	Not rely on cannabinoids but carotenoids.	16–25 plants, collecting 50–77 spectra from each group (male, female, hermaphrodites).	1 s	Differentiation between hermaphrodite, male, and female Cannabis.	Label-free; non-invasive; non-destructive.	Limited identification accuracy for hermaphrodites.	2022 ⁶²
NIR combined with PLSR.		CBD, Δ^9 -THC, CBG, CBN, CBC.	Cannabis plant.	< 1 min	Quantitative predictions.	First time used whole hemp materials; moisture content in both ground and whole materials were examined; moisture content was considered for cannabinoid prediction.	Poor prediction accuracy of Δ^9 -THC, CBG and CBN; water signals overlap with CBD signals.	2022 ⁵⁹
Raman spectroscopy with excitation wavelength at 1064 nm combined with multivariate analysis.	Lab-based	Δ^9 -THC, CBD.	42 Cannabis plant samples with different amounts of Δ^9 -THC and CBD.	ND	Qualitative distinction THC-rich and CBD-rich fresh plants samples.	Luminescence contribution in the visible range was avoided; fast; non-invasive; non-destructive; no-sample pretreatment.	Cannabinoid Raman spectra in dry plant samples and fresh samples are different.	2022 ⁷⁵
Miniaturized, battery-operated FT-NIR coupled with PLSR model.	Portable	CBD, Δ^9 -THC, CBDA, THCA.	Hemp.	15 s	Quantitative prediction.	Easy sample preparation.	Large amount of sample (2 g is needed); no distinction between THC & THCA and CBD & CBDA.	2022 ⁶³

Fluorescence spectroscopy method coupled with N-way PLSR (N-PLSR) and PLS-DA models.	Lab-based	THCA, CBDA, CBGA, CBCA, Δ^9 -THC, CBD, CBG.	Ethanol extracts of fresh (wet) Cannabis inflorescences of 16 different chemovars.	ND	Classification of high-THCA chemovars, hybrid THCA/CBDA chemovars, high-CBGA chemovars, and high-CBDA chemovars; quantitative prediction of 4 acidic and 3 neutral cannabinoids.	N-PLSR multilinear model improved prediction performance; high classification accuracy ($R^2 > 0.95$); good prediction accuracy for THCA, CBDA, CBGA, CBCA, and THC ($R^2 > 0.85$).	Poor prediction accuracy for CBG ($R^2 = 0.331$); small sample size.	2023 ⁵⁶
Fluorescence spectroscopic method coupled with PARAFAC model.	Lab-based	THCA, CBDA, CBGA, CBCA, Δ^9 -THC, CBD, CBG.	Ethanol extracts of fresh (wet) Cannabis inflorescences of 16 different chemovars.	ND	Quantitative prediction.	Acceptable prediction accuracy for THCA, CBDA, CBGA.	Poor prediction accuracy for CBCA; cannot distinguish between the neutral cannabinoids Δ^9 -THC, CBD, and CBG.	2023 ⁷²
A-TEEM technique with PCA and XGB models.	Lab-based	Δ^9 -THC, THCA, CBDA, CBD.	49 dry flower extracts into three chemotypes.	< 45 s	Quantification of total Δ^9 -THC:CBD ratio; LOQ: Δ^9 -THC+THCA 0.061%, CBD+CBDA 0.059%.	Low-cost; fast.	Cannot differentiate between THCA and Δ^9 -THC, nor between CBDA and CBD.	2023 ⁷³
Portable NIR with a chemometric analysis platform.	Portable	CBDA, CBD, THCA, Δ^9 -THC, CBGA, CBG, THCVA, Δ^9 -THCV, CBDVA, CBDV, CBN, CBC.	A total of 249 individual female plants, derived from 84 unique accessions.	ND	Quantitative prediction.	Non-destructive; rapid; accurate; economical; ability to discriminate between neutral and acidic forms of cannabinoids as well as between C3-alkyl and C5-alkyl cannabinoids.	High Δ^9 -THCA:CBDA Cannabis samples were underrepresented; cannot accurately predict CBDVA and CBDV.	2023 ⁶¹

Benchtop FT-NIR and handheld NIR coupled with PCA, PLSR and PLS-DA models.	Lab-based & Portable	CBDA, THCA, CBD, THC, CBC, CBGA, CBG, CBDVA, CBDV, THCV, THCVA, CBN, CBNA, CBCA.	734 Cannabis samples with 164 unique chemovars with 4–5 biological repeats.	seconds	Predict cannabinoid concentrations; characterize Cannabis samples into high-CBDA, high-THCA and even-ratio classes.	Large sample size and diversity; high-quality LC-MS data and NIR spectra data for model building; high prediction accuracy (99.4–100% for benchtop instrument and 83.1–100% for the handheld device); rapid, high-throughput; non-destructive screening.	Poor prediction accuracy for CBC, CBG, THCV, and THCVA ($R^2 = 0.34–0.46$); materials need to be ground.	2023 ⁵⁸
--	----------------------	--	---	---------	---	--	--	--------------------

Abbreviations: Principal Component Analysis (PCA), Partial Least Squares Discriminant Analysis (PLS-DA), Fourier Transform Near-Infrared Spectroscopy (FT-NIR), Near-Infrared Spectroscopy (NIR), Partial Least Square Regression (PLSR), Parallel Factor Analysis (PARAFAC), Absorbance-Transmittance Fluorescence Excitation Emission Matrix (A-TEEM), Electrochemical (EC), Surface-Enhanced Raman Spectroscopy (SERS), Silver Nanorods (AgNRs), Partial Least Square (PLS), k-Nearest Neighbors (k-NN), Soft Independent Modelling of Class Analogy (SIMCA), Artificial Neural Network (ANNs), Liquid Chromatography-Mass Spectroscopy (LC-MS), Extreme Gradient Boost (XGB), Independent Component Analysis (ICA); 2,2-Diphenyl-1-picrylhydrazyl (DPPH), 6-Hydroxy-2,5,7,8-tetramethylchromane-2-carboxylic Acid (Trolox), 2,4,6-Tris(2-pyridyl)-s-triazine (TPTZ).

Immunochemical Methods

Immunochemical analysis is a relatively cheap, easy, and fast technique that relies on antibody-antigen interaction for qualitative and quantitative analysis of specific compounds in (biological) samples. Conventional assay formats include enzyme-linked immunosorbent assays (ELISAs), radioimmunoassays (RIAs), and lateral flow assays. The signals produced by antibody-antigen interactions can be detected in different ways, including colorimetry, fluorescence, SERS, and electrochemistry.⁷⁹

In the field of cannabinoid screening, various commercial immunochemical analysis kits have been used for detection of Δ^9 -THC and its metabolites in blood,⁸⁰ urine,^{81,82} saliva⁸³ and hair.⁸⁴ Shared drawbacks include being limited to qualitative analysis with high cutoffs ($5\text{--}50\text{ ng}\cdot\text{mL}^{-1}$), frequent false positive/negative results, and cross-reactivity from structurally similar cannabinoids (isomers) and metabolites. Efforts to develop new immunochemical methods have been made to increase sensitivity, selectivity, quantification ability, and portability (**Table 2.4**).

Detection of Δ^9 -THC in sweat and saliva has many advantages for roadside drug of abuse screening compared with other biological fluids, e.g., non-invasiveness, ease of collection, immediate availability, to name a few.^{85,86} Brunelle et al.⁸⁷ developed a competitive immunochemical sensing surface combined with UV-Vis spectroscopy to qualitatively detect Δ^9 -THC and Δ^9 -THC-COOH in the MeOH extracts of finger sweat collected on polyethylene film, which is a step toward roadside detection. Badawy⁸⁸ developed an end-point dilution lateral flow immunoassay method and achieved semiquantification (with a cutoff value of $50\text{ ng}\cdot\text{mL}^{-1}$) of drugs, including cannabinoids in urine. The process involves consecutive dilutions of the positive test sample with rapid test cassettes until the point of the lowest dilution is reached. At this stage, a colored band appears at the specific cutoff concentration that can be observed by the naked eye, thus avoiding the use of specific detection equipment. However, subjective errors and cross-reactivity are drawbacks. Plouffe et al.⁸⁹ also tried to develop roadside detection methods by constructing a fluorescence-based lateral flow assay to analyze Δ^9 -THC

in saliva. Using polymeric nanoparticle conjugates, sensitive quantification of Δ^9 -THC with an LOD of $0.122 \text{ ng}\cdot\text{mL}^{-1}$ can be achieved within 10 min, using 1 mL of saliva. However, large deviations of -12% – 28% were observed from the actual to measured values with variations of 14% – 40% . Further efforts are needed to improve the repeatability and applicability under real roadside conditions.

Despite the high sensitivity of fluorescence and quantum dots, their performance is compromised by photo-bleaching and low contrast due to the autofluorescence of biomolecules.⁹⁰ Chand et al.⁹¹ developed a lateral-flow immunoassay (LFIA) method using upconverting nanoparticles (UCNPs) as labels instead of fluorescent and quantum dots or gold nanoparticles, which have inadequate color intensity. UCNPs can convert near-infrared excitation into visible emissions and have better signal enhancement performance. With this method, a LOD of $2 \text{ ng}\cdot\text{mL}^{-1}$ was achieved in 20 min. Additionally, Yu et al.⁹² adopted transmission optics for signal detection which can generate larger signal changes than conventional reflective detection. They developed an integrated cartridge that comprises an oral fluid processing kit, a sensor cartridge, and an optical detection cradle for on-site detection of Δ^9 -THC in saliva from Cannabis smokers (Express Probe for On-site Cannabis Inhalation (EPOCH)). Results can be obtained in 5 min with an LOD of $0.17 \text{ ng}\cdot\text{mL}^{-1}$ using $100 \mu\text{L}$ of spiked saliva. Moreover, the quantification of the methanolic THCV reference standard correlated well ($R^2 = 0.987$) with the results obtained by GC-MS. However, interferences from other THC analogues, e.g., Δ^8 -THC, when analyzing real samples, need to be assessed.

Overall, immunochemical methods are typically portable with wide applications in the analysis of cannabinoids from biological matrixes. Cross-reactivity is beneficial for screening a group of structurally similar cannabinoids with varying sensitivities. However, accurate analysis of individual cannabinoids needs to be improved.

Table 2.4. Published Immunochemical Methods for Cannabis and Cannabinoid Analysis from 2013 to 2023.

Method	Portable/ Lab-based	Cannabinoids	Samples	Time	Qualitative/ Quantitative	Advantages	Disadvantages	Year/ Ref
Fluorescent-based immunoassay using polymeric nanoparticles.	Lab-based	Δ^9 -THC.	Oral fluid.	< 10 min	Quantitative; LOD 0.122 ng·mL ⁻¹ .	Easy sampling; sensitive.	Limited reproducibility (variations 14–40%) and accuracy (deviations –12%–28%); not suitable for detection of heavy users.	2017 ⁸⁹
Competitive immunoassay sensing surface combined with UV-Vis spectroscopy.	Lab-based	Δ^9 -THC, Δ^9 -THC-COOH.	Finger sweat.	ND	Qualitative; LOD 5.0 nmol·L ⁻¹ Δ^9 -THC-COOH.	Non-invasive sampling and the ability to avoid tampering; sensitive.	Preparation of sensing surfaces and samples is time-consuming.	2019 ⁸⁷
End-point dilution flow immunochromatographic assay combined with naked-eye evaluation.	Portable	Δ^9 -THC-COOH.	Human urine.	4 min	Semiquantitative analysis; cutoff values of the naked-eye screening 50 ng·mL ⁻¹ .	Fast; ease of use; low cost; semiquantitative analysis by the naked eye; cross-reactivity with Δ^8 -THC, Δ^9 -THC, Δ^8 -THC-COOH, CBN for screening metabolites with similar structures to Δ^9 -THC-COOH.	Inaccurate quantification due to cross-reactivity to different concentrations of cannabinoids with similar structures; subjective errors.	2020 ⁸⁸
LFIA utilizing UCNPs, with nano-conjugates clustered at the test zone for signal enhancement.	Portable	Δ^9 -THC.	Δ^9 -THC spiked saliva.	20 min	Quantitative; LOD 2 ng·mL ⁻¹ .	A 20% increase in the test intensity compared with standard LFIA; good reproducibility (RSD 1–3%) and accuracy for spiked Δ^9 -THC samples (deviation –2.3%–2.3%).	Complex strip fabrication; narrow linear detection range of 2–15 ng·mL ⁻¹ .	2021 ⁹¹
EPOCH test module includes an oral fluid processing kit, sensor cartridge, and optical detection cradle. After oral fluid is collected via swab, it is mixed with gold nanoparticles coated with THC antibodies (AuNPAb) in the processing kit. The mixture is then dispensed onto the detection cartridge, and the optical signal is read by a smartphone.	Portable	Δ^9 -THC, THCV.	Saliva from 43 Cannabis users and 43 controls.	< 5 min	Quantitative; LOD 0.17 ng·mL ⁻¹ .	Fast and sensitive (LOD below the regulatory guideline 1 ng·mL ⁻¹); good correspondence between the developed method and GC-FID for the analysis of THCV reference standard solution ($R^2 = 0.987$); enable on-site test.	Separate modules need to be integrated into a single automated device; did not check the interference from other cannabinoids.	2021 ⁹²

Abbreviations: Ultraviolet-Visible (UV-Vis), Lateral-Flow Immunoassay (LFIA), Upconverting Nanoparticles (UCNPs), Express Probe for On-site Cannabis Inhalation (EPOCH), Direct-Enzyme Linked Immunosorbent Assay (ELISA).

Nuclear Magnetic Resonance (NMR) Methods

In the field of Cannabis and cannabinoid analysis, NMR is increasingly popular, with the merits of strong structure elucidation power, minimal sample preparation, fast analysis, low solvent consumption, good repeatability, and accuracy, as well as the fact that no cannabinoid reference standards are needed.⁹³ Besides, 2D-NMR and quantitative NMR (qNMR) add more possibilities for their analysis.^{94,95} The major applications can be categorized into three categories (**Table 2.5**).

(i) Qualitative analysis of cannabinoids in Cannabis and Cannabis products.

The combination of 1D and 2D NMR enables complete structure elucidation. This advantage has been used to elucidate newly found cannabinoids, for example, cannabicitran (CBT), which is commonly found in commercial CBD products,⁹⁶ minor oxygenated cannabinoids isolated from Cannabis plant materials,^{97,98} as well as synthetic cannabinoid byproducts from commercial Δ 8-THC products.⁹⁹ Such complete structural elucidation is robust and gold standard, but also expertise-demanding and time-consuming. Apart from full structural identification, ^1H NMR provides a fast method for qualitatively detecting the existence of impurities in commercial Δ 8-THC products with minimal sample preparation,^{12,100} which is generally challenging or time-consuming by conventional HPLC or GC-based methods. Additionally, 1D ^1H NMR and COSY could also acquire the fingerprint spectra of Cannabis extracts for authentication of Cannabis¹⁰¹ and distinction of chemotypes at fixed magnet strength, temperature and solvent.¹⁰²

(ii) Quantitative analysis of cannabinoids in Cannabis and Cannabis products.

With 400 MHz ^1H NMR, Ohtsuki et al.¹⁰³ and Barthlott et al.¹⁰⁴ developed quantitative methods to analyze multiple cannabinoids in marketed CBD oils. Compared with the sophisticated, bulky, and expensive NMR with strong magnetic fields, low-resolution benchtop NMR spectrometers, with the merits of being cheap, fast, and easy to measure, provide another possibility for quantification of concentrated cannabinoids. As illustrated by Araneda et al.¹⁰⁵ 60 MHz benchtop ^1H NMR enabled the quantification of Δ 9-THC and CBD in Cannabis concentrates. Apart from ^1H NMR for quantification, ^{13}C NMR has also been used in cannabinoid

quantification, especially because deconvolution is not necessary to achieve precise integration of carbon peaks. As the ^{13}C spectral window is significantly wider than that of ^1H , the chemical shift range is much larger and signal overlapping in complex samples can be reduced to some extent. Pellati and his colleagues^{106,107} applied quantitative ^{13}C spectra at 600 MHz (^1H) to quantify psychoactive and non-psychoactive cannabinoids in different types of Cannabis extracts and comparable results as with HPLC-UV but with much lower solvent consumption and no need for cannabinoid reference standards. Quantitative COSY, in which correlations of neighboring protons are distributed in two dimensions to increase resolution, is another alternative to solve inaccurate quantification by quantitative ^1H NMR due to signal overlap. By constructing calibration curves for specific analytes, accurate and reproducible quantification of cannabinoids in Cannabis and Cannabis products was achieved despite the need for considerable expertise and a higher LOD compared with the quantitative ^1H -NMR method.^{108,109}

In summary, although quantitative ^{13}C NMR offers enhanced resolution and thus accuracy, it is time-consuming due to the low natural abundance of ^{13}C isotopes. Quantitative COSY, on the other hand, requires separate calibration curves for each analyte, as cross-peak intensities are affected by various factors such as concentration, relaxation times, mixing times, evolution times, uneven magnetization transfers, and coupling constants. Conversely, quantitative ^1H NMR is rapid in analysis and allows for the quantification of multiple cannabinoids using a single primary standard with high and known purity, even though sometimes signal overlapping might be a problem.

(iii) Combining NMR and chemometric analysis for cannabinoid metabolomics.

Another application field of NMR in the analysis of Cannabis samples is combining NMR and chemometric analysis for cannabinoid metabolomics, newly termed "cannabinomics" by Aliferis et al.¹¹⁰ The Kayser group did a lot of research¹¹¹⁻¹¹⁴ to differentiate the Cannabis metabolome based on their organs¹¹³ as well as monitor metabolic changes in the trichomes during different growing periods^{111,112,114} with 500 MHz ^1H NMR-based metabolomics. Fernandez et al.¹¹⁵

used 500 MHz ^1H NMR to determine metabolite profiles of high-THCA Cannabis and high-CBDA Cannabis. By comparing the metabolite profiles, they distinguished between two chemotypes and harvests of the same type and obtained information related to fungal infection. Similarly, Leite et al.¹¹⁶ obtained information about regions, seasonality, and degradation of marijuana seizures based on 400 MHz ^1H NMR and chemometric analysis.

Overall, despite the many advantages of the NMR applications discussed, several areas still need improvement: (i) low sensitivity, which is orders of magnitude less sensitive than MS. This limitation can be partly mitigated by using stronger magnetic fields and cryoprobes. In practice, Cannabis and related samples are usually available in sufficient quantities, and instruments operating at 400–800 MHz are usually adequate for the task; (ii) signal overlap, probably leading to missed signals but can be partially alleviated by 2D NMR; (iii) high cost of NMR equipment, posing a barrier to routine analysis; (iv) the commonly used deuterated chloroform in cannabinoid analysis is not environmentally friendly and might be replaced with greener solvents like deuterated MeOH.

Table 2.5. Published nuclear magnetic resonance methods for Cannabis and cannabinoid analysis from 2013 to 2023.

Method	Portable/ Lab-based	Cannabinoids	Samples	Time	Qualitative/ Quantitative	Advantages	Disadvantages	Year/ Ref
¹ H NMR at 500 MHz combined with LC-MS analysis.	Lab-based	THCA, CBDA.	Laser-microdissected samples of capitate-stalked and capitate-sessile trichomes from Cannabis plant.	ND	Qualitative.	NMR enabled the tentative identification of CBCA in the absence of cannabinoid reference standards.	Low sensitivity (cannot detect neutral cannabinoids).	2013 ¹¹¹
¹ H NMR at 500 MHz combined with real time PCR analysis and chemometric analysis.	Lab-based	THCA, CBCA, CBGA, Δ9-THC, non-cannabinoids.	Different organs of two different Cannabis cultivars.	ND	Qualitative.	Easy and fast metabolite profile investigation in different organs.	Low sensitivity, only concentrated cannabinoids in some organs can be quantified.	2014 ¹¹³
¹ H NMR at 400 MHz.	Lab-based	Δ9-THC, CBD, CBG, CBN, THCA, CBDA, CBGA.	4 Cannabis plant samples.	ND	Qualitative; distinction of 4 chemotypes (THC-type, CBD-type, CBG-type, fiber-type).	DMSO-d ₆ is more compatible with analytes having different polarities; differentiation between acidic cannabinoids and their neutral counterparts, as well as between cannabinoid-rich extracts and those with reduced cannabinoid content.	Signal overlap and low sensitivity.	2015 ¹⁰²
¹³ C at 400 MHz (¹ H), ¹ H, COSY, ¹ H- ¹³ C HMBC, ¹ H- ¹ H NOESY and ¹ H- ¹ H ROESY at 400 MHz.	Lab-based	8α-OH-Δ9-THC, 8β-OH-Δ9-THC, 10α-OH-Δ8-THC, 10β-OH-Δ8-THC, 10α-OH-Δ9,11-HHC, 9β,10β-epoxy-HHC, and 11-acetoxy-Δ9-THCA.	Isolated pure compounds.	ND	Qualitative.	Powerful structure elucidation of unknown compounds.	Spectra interpretation needs expertise.	2015 ⁹⁸

¹³ C at 400 MHz (¹ H), ¹ H, COSY ¹ H- ¹³ C HMBBC, ¹ H- ¹ H ROESY at 400 MHz.	Lab-based	9α-OH-HHC, 7-oxo-9α-OH-HHC, 10α-OH-HHC, 10α-OH-HHC, 8-oxo-Δ9-THC, 10α-OH-10-oxo-Δ8-THC, 9α-OH-10-oxo-Δ6a,10a-THC, and 1'S-OH-CBN.	Isolated compound.	ND	Qualitative.	Structure elucidation of new cannabinoids.	Expertise in spectra interpretation.	2015 ⁹⁷
¹ H NMR at 500MHz combined with chemometric analysis.	Lab-based	CBDA, CBD THCA, CBGA and Δ9-THC and non-cannabinoids.	One Cannabis with similar content of THC and CBD; the trichomes were isolated and analyzed from week 5 to week 8 of the flowering period.	ND	Quantitative.	Enabled time-dependent monitoring of biosynthetic processes in the trichomes.	Low sensitivity, only from week 5 onwards, metabolites were quantified by ¹ H-NMR.	2016 ¹¹⁴
¹ H NMR and COSY NMR at 500 MHz in combination with chemometrics.	Lab-based	No cannabinoid reference standards.	25 Cannabis plant samples.	ND	Qualitative; authentication and characterization of Cannabis samples.	Reproducible; fast analysis; labor-saving in analysis.	Low sensitivity.	2017 ¹⁰¹
¹ H NMR at 400 MHz combined with chemometric analysis.	Lab-based	Δ8-THC, Δ9-THC, THCA, 11-OH-CBN, CBV, and CBN.	156 marijuana samples from different regions and seasonality.	ND	Qualitative.	156 marijuana samples can be grouped into two different seizing times.	Unable to distinguish samples from different regions.	2018 ¹¹⁶
¹³ C qNMR at 600 MHz (¹ H).	Lab-based	CBD, CBDA, CBG and CBGA.	8 samples of fibre-type female inflorescences.	~47 min	Quantitative; LOQ for CBD 660 μg·mL ⁻¹ , CBDA 746 μg·mL ⁻¹ , CBG 664 μg·mL ⁻¹ and CBGA 746 μg·mL ⁻¹ .	Good correspondence with HPLC-UV with much less solvent consumption.	Low sensitivity and long analysis time.	2019 ¹⁰⁷

¹ H NMR at 500 MHz combined with chemometric analysis.	Lab-based	THCA, CBCA, Δ9-THC, 20 non-cannabinoids.	Cannabis trichomes isolated at 4 different weeks over the flowering season.	ND	Quantitative.	Metabolomes based on the harvest time can be classified.	Only concentrated cannabinoids can be detected and thus the method is only applicable in the later period of flowering.	2020 ¹¹²
¹ H NMR at 60 MHz benchtop spectrometer.	Lab-based	Δ9-THC, CBD.	3 commercial Cannabis concentrates, 2 CBD spiked Cannabis concentrates.	~16 min	Quantitative.	Minimal sample preparation; cheap instrument; no need for cannabinoid reference standards; easy operation and good correspondence with HPLC-UV.	Low sensitivity, and low resolution (not suitable for multiple analytes), expertise required.	2020 ¹⁰⁵
¹ H qNMR at 500 MHz.	Lab-based	Δ8-THC, Δ(4)8-iso-THC, iso-THCBF.	27 vaporizers from 10 brands.	ND	Quantitative.	Fast analysis; no need for cannabinoid reference standards.	Low sensitivity; spectral overlap.	2021 ¹⁰⁰
¹³ C-qNMR at 600 MHz (¹ H).	Lab-based	CBDA, CBD, CBGA, CBG, Δ9-THCA, Δ9-THC and CBN.	27 different Cannabis inflorescences in 4 chemotypes.	~47 min	Quantitative; LOD 2.3–5.7 μg·mL ⁻¹ .	Deconvolution is not needed to obtain accurate carbon peak integrations; simultaneous identification and quantification of various analytes in complex mixtures with low solvent consumption; good correspondence with HPLC-UV/DAD.	Low sensitivity; long relaxation time of carbon and NOE effect.	2021 ¹⁰⁶
¹ H qNMR at 400 MHz.	Lab-based	CBD, CBDA, Δ9-THC, Δ8-THC, THCA, CBG and CBN.	46 commercial CBD oils.	ND	Quantitative; LOD of CBD 134, 307, 346 mg·kg ⁻¹ for different signals, Δ9-THC: 608 mg·kg ⁻¹ , Δ8-THC 250 mg·kg ⁻¹ , CBN: 504, 517, 623 mg·kg ⁻¹ for different signals.	Simple sample preparation; no need for cannabinoid reference standards.	High LOD not suitable for many CBD oils analysis (below LODs).	2021 ¹⁰⁴

¹³ C at 500 MHz (¹ H), ¹ H, COSY, ¹ H- ¹³ C HMQC, ¹ H J-Res at 500 MHz.	Lab-based	CBD, CBDA, CBG, Δ9-THC.	2 hemp plant materials.	ND	Quantitative.	Good accuracy and reproducibility; ¹³ C qNMR decreases spectral overlap.	Extensive deconvolution processes for ¹ H qNMR due to the severe signal overlapping; low sensitivity of ¹³ C qNMR.	2022 ¹⁰⁹
¹ H qNMR and COSY qNMR at 400 MHz.	Lab-based	CBD, CBDA, CBN, CBC, CBCA, CBG, CBGA, Δ9-THC, Δ9-THCA, Δ8-THC, CBE, CBDV, CBDVA, Δ9-THCVA, CBGV, Δ8-THCV.	Hemp plants; Cannabis extracts; hemp seed oils and cosmetic products with cannabinoids.	< 20 min for COS Y; < 1 min for ¹ H NMR	Quantitative; LOD by ¹ H: CBD 0.018 mg, CBDA 0.018 mg, CBG 0.020 mg, CBGA 0.02 mg, CBN 0.015 mg, Δ9-THCA 0.042 mg, Δ9-THC 0.042 mg; LOD by COSY: CBD 0.11 mg, CBDA 0.12 mg, CBG/CBGA 0.1 mg, CBN 0.08 mg, Δ9-THCA/THC 0.08 mg.	Good accuracy; reproducibility; flexibility; simultaneous quantification of multiple analytes; non-destructive and no need for derivatization; ¹ H NMR is fast in analysis and no need for cannabinoid reference standards; COSY improves resolution.	Severe peak overlapping in ¹ H NMR; ¹ H NMR cannot distinguish CBGV/CBG, Δ8-THCV/Δ8-THC; 2D NMR cannot distinguish Δ9-THCA/THC, CBGA/CBG; COSY needs cannabinoid reference standards.	2022 ¹⁰⁸
¹³ C at 600 MHz (¹ H), ¹ H, ¹ H- ¹³ C HSQC, ¹ H- ¹³ C HMBC, ¹ H- ¹ H NOESY and ¹ H- ¹ H ROESY at 600 MHz combined with DFT calculations for complete ¹ H and ¹³ C NMR assignments.	Lab-based	CBT.	Pure CBT.	ND	Qualitative.	Full assignments of protons and carbons.	Expertise in spectra interpretation.	2022 ⁹⁶

¹ H qNMR at 400 MHz combined with HiFSA.	Lab-based	CBD, trans- Δ^9 -THC, cis- Δ^9 -THC, CBC, CBG, CBN, CBDV.	A commercial CBD oil.	ND	Quantitative.	Resolving overlapping signals in complex mixtures, enhanced quantification.	Need quantum computational resources and expertise for the interpretation of results.	2022 ¹⁰³
¹ H NMR at 800 MHz and 400 MHz.	Lab-based	NA	10 commercial Δ^8 -THC distillates and vaporizer cartridges.	ND	Qualitative.	Finding the existence of impurities.	No identification of impurities.	2022 ¹²
¹³ C at 500 MHz (¹ H), ¹ H, DEPT-135, COSY, ¹ H- ¹³ C HMQC, ¹ H- ¹³ C HMBC, ¹ H- ¹ H NOESY at 500 MHz.	Lab-based	$\Delta(4)8$ -iso-THC, Δ^4 -iso-THC, Δ^8 -cis-iso-THC, 4,8-epoxy-iso-THC, 8-OH-iso-THC, 9 β -OH-HHC, 9 α -OH-HHC, CBT, olivetol, and Δ^9 -THC.	Isolated pure compounds.	ND	Qualitative.	Powerful structure elucidation of unknown compounds.	Spectra interpretation needs expertise.	2023 ⁹⁹
¹³ C at 500 MHz (¹ H), ¹ H, 1D-TOCSY, 1D-NOESY, ¹ H- ¹³ C HSQC, ¹ H- ¹³ C HMBC at 500 MHz combined with HPLC-DAD and multivariate statistical analysis for metabolomic analysis.	Lab-based	CBDA, CBD, CBC, CBN, CBG, THCA, Δ^9 -THC, Δ^8 -THC, THCVA, THCV, CBGA, CBDVA, CBDV, CBGA.	20 plant materials per chemotype (drug chemotype and fiber chemotype) from 3 harvests.	ND	Qualitative; distinction between two Cannabis varieties from different harvest times, as well as identifying a crop with a microbial infection.	The finding of molecular markers related to fungal infection in Cannabis.	Limited sample size.	2023 ¹¹⁵

ND: not described in the paper. Abbreviations: ¹H iterative Full Spin Analysis (HiFSA), One-Dimensional (1D), Two-Dimensional (2D), Quantitative NMR (qNMR), ¹H J-Resolved spectroscopy (J-Res), Nuclear Overhauser Enhancement (NOE)

Ion Mobility Spectrometry (IMS) Methods

Ion mobility spectrometry (IMS)-mass spectrometry (MS) allows the separation of ions based on their mobility through chemically inert gasses under the influence of an electric field, and the mobility depends on their molecular sizes, charges, and shapes.¹¹⁷⁻¹²⁰ Based on the mobility, collision cross sections (CCS), which reflect the size and shape of gaseous ions, can be measured. Through decades of development, various instrument configurations have been developed. Among those, drift tube IMS (DTIMS) and traveling wave IMS (TWIMS) gained interest. Other methods include trapped IMS (TIMS), field asymmetric IMS (FAIMS, also named as differential mobility spectrometry (DMS)), each with different capability, sensitivity, and resolution, as reviewed by Christofi et al.¹²¹ and Delafield et al.¹²²

Due to the extra-dimensional separation capability based on mobility, IMS-MS can also be used to analyze compounds in complex matrixes without chromatographic separations. Some applications for the analysis of Cannabis and cannabinoids without chromatography in the past decade are summarized below (**Table 2.6**). Contreras et al.¹²³ applied thermal desorption (TD) coupled with a hand-held DTIMS to acquire cannabinoid fingerprints from Cannabis plant extracts and residues on hands. Even though multiple cannabinoids share similar or the same reduced mobilities values (K_0), chemometric analysis of data obtained in positive and negative modes enabled the distinction of Cannabis chemotypes. As claimed by the authors, their developed method is portable and fast in analysis and thus holds the potential for on-site classification of Cannabis plants as well as screening of marijuana abuse. Mashmoushi et al.¹²⁴ relied on DMS-MS with the doping of 1.5% (v/v) isopropanol into the carrier gas (N_2) to separate two groups of cannabinoid isomers ($\Delta 9$ -THC/CBD/CBC and THCA/CBDA) in negative ionization mode. The quantification of THCA, CBDA, $\Delta 9$ -THC, CBD, and CBC in a marijuana extract was performed using the standard addition method. However, these results were not compared with those obtained from commonly used methods, such as HPLC or GC. Moreover, while DMS can separate analytes using compensation voltages, it cannot provide CCS information due to the asymmetric waveform and ion structural

changes caused by oscillation between low and high electric field strengths.^{125,126} Zietek et al.¹²⁷ used TIMS to explore the performance of metal ion adducts in the gas phase. Δ^9 -THC, CBD, and another twelve pharmaceutically relevant molecules with various molecular shapes and flexibility were mixed with cesium, lithium, silver or sodium ions and directly infused into TIMS to investigate the conformation changes in different forms of metal adducts compared with protonated species. It was found that the formation of metal ion adducts can lead to different molecular conformations, and in some situations, the radius of cations is correlated with the CCS of adducts. Besides, the presence of rotating bonds can contribute to the formation of dimers. Moreover, the introduction of lithium, sodium, and silver can benefit the resolution of Δ^9 -THC and CBD despite partial overlap ($R \sim 50$). Hädener et al.¹²⁸ used a DTIMS with a resolution higher than 150 to resolve protonated Δ^9 -THC and CBD as well as deprotonated THCA and CBDA. Near-baseline separation of the two isomeric pairs was achieved, and experimental CCS values were obtained using N_2 as the drift gas in drift-tube ion mobility spectrometry ($^{DT}CCS_{N_2}$). Furthermore, by direct infusion, quantification of the four cannabinoids in Cannabis extracts was achieved with LODs between 0.3–7.7 ng·mL⁻¹. Ieritano et al.¹²⁹ applied DMS coupled with tandem MS to differentiate five cannabinoid isomers (Δ^8 -THC, Δ^9 -THC, *exo*-THC, CBC, and CBD) together with two non-isomers (CBC and CBG) based on compensation voltages and MS² fragments of silver ion adducts. They further quantified these cannabinoids in cannabinoid oils with LODs around 10–20 ng·mL⁻¹, but large deviations ($\sim 83\%$) from the claimed value were obtained. Besides, no CCS information was obtained due to the limitations of the instrumentation. Overall, IMS analysis is moving toward the use of more advanced instrumentation, which offers advantages such as high resolution and sensitivity, particularly beneficial for analyzing cannabinoid isomers. Furthermore, obtaining distinct experimental CCS values could serve as an extra means of cannabinoid identification.

Table 2.6. Published ion mobility spectrometry methods for Cannabis and cannabinoid analysis from 2013 to 2023.

Method	Portable/ Lab-based	Cannabinoids	Samples	Time	Qualitative/ Quantitative	Advantages	Disadvantages	Year/ Ref
TIMS-MS with cesium, lithium, silver, and sodium ions doping.	Lab-based	$\Delta 9$ -THC, CBD, and another twelve non-cannabinoids.	Reference standards.	ND	Qualitative.	The introduction of lithium, sodium, and silver can benefit the resolution of $\Delta 9$ -THC and CBD.	Only partial separation of $\Delta 9$ -THC and CBD was achieved ($R \sim 50$).	2018 ¹²⁷
DTIMS with a resolution higher than 150.	Lab-based	$\Delta 9$ -THC, CBD, THCA, CBDA.	Cannabis plant.	~ 1 min	Qualitative; LOD: $\Delta 9$ -THC 6.6 ng·mL ⁻¹ , CBD 7.7 ng·mL ⁻¹ , THCA 0.3 ng·mL ⁻¹ , CBDA 0.5 ng·mL ⁻¹ .	Near-baseline separation of protonated $\Delta 9$ -THC and CBD as well as deprotonated THCA and CBDA; ^{DT} CCS _{N2} values were obtained.	Two pairs of isomers were analyzed in different ionization modes.	2018 ¹²⁸
Handheld TD-IMS combing with PCA-LDA.	portable	CBDV, $\Delta 9$ -THCV, CBD, CBC, $\Delta 8$ -THC, $\Delta 9$ -THC, CBG, CBN, CBDA, CBGA, $\Delta 9$ -THCA.	Cannabis plant.	2-4 min	Qualitative; chemotaxonomic discrimination of Cannabis varieties.	Distinct profiles between non-cannabinoids and cannabinoids; Cannabis plant residues on hands can be easily analyzed with a wipe sampling pad.	Similar profiles of $\Delta 9$ -THCA, $\Delta 9$ -THC, CBDA, $\Delta 8$ -THC and CBN.	2018 ¹²³
DMS-MS (ESI negative) with 1.5% (v/v) isopropanol doping into the N ₂ carrier gas.	Lab-based	$\Delta 9$ -THC, CBD, CBC, THCA, CBDA.	One Cannabis plant material.	seconds	Quantitative; LOD: THCA 13 ng·mL ⁻¹ , CBDA 7 ng·mL ⁻¹ , $\Delta 9$ -THC 7 ng·mL ⁻¹ , CBD 18.9 ng·mL ⁻¹ , CBC 18.4 ng·mL ⁻¹ .	Fast separation of THCA/CBDA and $\Delta 9$ -THC/CBD/CBC was achieved under different conditions.	Quantification results were not verified using an alternative method.	2022 ¹²⁴
DMS and tandem-MS with silver ion doping.	Lab-based	$\Delta 8$ -THC, $\Delta 9$ -THC, $\Delta 9,11$ -THC, CBC, CBD, CBC, CBG.	One $\Delta 8$ -THC oil, and one hemp oil.	ND	Qualitative; LOD: 10–20 ng·mL ⁻¹ .	Fast distinction and quantification of seven cannabinoids, five of which are isomers.	Cannot obtain CCS information.	2023 ¹²⁹

Abbreviations: Trapped Ion Mobility Spectrometry-Mass Spectrometry (TIMS-MS), Differential Mobility Spectrometry (DMS), Drift Tube Ion Mobility Spectrometry (DTIMS), Thermal Desorption (TD)-Ion Mobility Spectrometry (IMS), Principal Component Analysis (PCA)-Linear Discriminant Analysis (LDA).

Ambient Ionization Mass Spectrometry (AIMS) Methods

The advent of ambient ionization mass spectrometry (AIMS) has revolutionized MS analysis by reducing complexity, time, and cost, thereby making MS more accessible and efficient for various applications. AIMS allows fast, direct, *in situ*, and high-throughput analysis of samples without tedious sample preparation. The first AIMS method, desorption electrospray ionization (DESI),¹³⁰ was introduced in 2004. In this technique, charged solvent droplets impact a sample surface at subsonic speeds, causing both the analytes and matrix to be released. Following this, charge transfer occurs from the solvent to the analyte within the rapidly evaporating solvent droplets. Finally, the ionized analytes are detected by MS.

Shortly after DESI, the Direct Analysis in Real Time (DART) technique was published.¹³¹ In this technique, analytes, whether in gas, liquid, or solid phase, are ionized through interactions with electronically or vibrationally excited-state species under atmospheric pressure without the need for solvents. Since its introduction, the field of AIMS has expanded rapidly, with various AIMS methods emerging.^{132,133} Among them, paper spray (PS) ionization¹³⁴ reported in 2010, is known for its fast analysis, ease of use, and low consumable usage. In PS-MS, a spray plume of charged droplets is generated from the sharp tip of a paper substrate via a Taylor cone when solvent and voltage are applied. As these droplets move toward the MS inlet, they repeatedly break up into smaller droplets. Throughout this process, the charge is transferred from the solvent to the analytes, which are then detected by the MS.¹³⁵

No or minimal sample pretreatment is quite attractive for the analysis of Cannabis and Cannabis products considering the complex and diverse sample types, given that sufficient selectivity can be assured in the absence of separation. Therefore, various AIMS techniques have been used for this purpose (**Table 2.7**). Falconer et al.¹³⁶ applied DART-MS for the rapid screening and characterization of approximately 500 vaping liquid samples, with each analysis taking about 1.5 minutes per sample. Cannabinoids were identified by comparing accurate *m/z* values and MS/MS fragments of protonated species with reference standards. However, this

method failed to distinguish between cannabinoid isomers such as Δ^9 -THC, Δ^8 -THC, CBD, and CBC. Similarly, Chambers et al.¹³⁷ qualitatively analyzed cannabinoid-infused edibles, personal-care products, and hemp materials in their native forms by DART-HRMS without the ability to distinguish isomers. The inability to differentiate cannabinoid isomers by AIMS was also encountered by Bills et al.¹³⁸ when using PS-MS to analyze cannabinoids in urine and oral fluid. Cannabinoid isomer distinction is of great importance due to their different psychoactivity and legality. Therefore, efforts have been made to circumvent this issue. Huang et al.¹³⁹ utilized the Ag(I)-alkene complexation mechanism to distinguish cannabinoid isomers with different numbers of C=C double bonds. They successfully achieved the fast and easy distinction of Δ^9 -THC and CBD by Ag(I) impregnated PS-MS and achieved semiquantification of the Δ^9 -THC/CBD ratio in commercial CBD oils. On the other hand, Ogrinc et al.¹⁴⁰ applied water-assisted laser desorption ionization mass spectrometry (SpiderMass), which consisted of a handheld IR-laser and a Q-TOF mass spectrometer and achieved the distinction of the isomers THCA and CBDA by their MS/MS fragments in negative mode. The developed method enabled semiquantification of CBDA/THCA *in situ* from fresh plants even though the results obtained from a small sampling size (a few μm) were not representative of the entire sample. In conclusion, AIMS methods are fast in analyzing a wide variety of Cannabis samples. However, they suffer from resolving cannabinoid isomers even with HRMS and tandem MS. Applying Ag(I) to produce distinct MS fragments provided a solution to this issue. Currently, analyses of Cannabis and related products using AIMS are limited to laboratory settings. Moreover, AIMS typically probes only the surface, which can be a disadvantage because analytes and their concentrations may vary significantly throughout inhomogeneous samples, such as most parts of the Cannabis plant. The development of portable MS technology holds promise for expanding AIMS applications into field settings, making it an area of considerable interest for the analysis of Cannabis and Cannabis products.

Table 2.7. Published ambient ionization mass spectrometry methods for Cannabis and cannabinoid analysis from 2013 to 2023.

Method	Portable/ Lab-based	Cannabinoids	Samples	Time	Qualitative/ Quantitative	Advantages	Disadvantages	Year/ Ref
Solvent assistance thermal desorption with miniature MS combined with PTFE swab sampling.	Portable	CBN, Δ^9 -THC.	Marijuana leaf samples and simulated saliva.	≤ 3 s	Qualitative.	Portable equipment; easy sampling.	Only rely on low-resolution m/z of protonated precursor ions for identification.	2020 ¹⁴¹
PS-MS/MS combined with a half 3D printed autosampler cartridge.	Lab-based	Δ^9 -THC, Δ^9 -THC-OH, Δ^9 -THC-COOH.	Spiked urine and saliva.	ND	Quantitative; LOD: Δ^9 -THC 4 $\text{ng}\cdot\text{mL}^{-1}$ with cartridge; LOD: Δ^9 -THC 1 $\text{ng}\cdot\text{mL}^{-1}$, Δ^9 -THC-OH, 4 $\text{ng}\cdot\text{mL}^{-1}$, Δ^9 -THC-COOH, 5 $\text{ng}\cdot\text{mL}^{-1}$ without cartridge.	Sesame seed oil participating paper strip extraction enables preserving and preconcentration of Δ^9 -THC.	Unable to differentiate isomers.	2020 ¹³⁸
Silver-impregnated PS-MS/MS.	Lab-based	Δ^9 -THC, CBD.	10 commercial CBD oils.	< 30 s	Semiquantification of Δ^9 -THC/CBD ratio; Δ^9 -THC LOD 6 $\text{ng}\cdot\text{mL}^{-1}$ CBD LOD 20 $\text{ng}\cdot\text{mL}^{-1}$.	Fast and easy distinction of Δ^9 -THC and CBD; minimal solvent consumption (15 μL); cross-validated with UHPLC-UV.	Absolute quantification of THC and CBD was not achieved due to the lack of an internal standard.	2021 ¹³⁹
DART-HRMS by matching m/z .	Lab-based	CBD, Δ^9 -THC, CBN, CBG, THCA, CBDA, CBGA.	Hemp plant materials, commercial personal-care products, in-house made edibles infused with THC and CBD.	seconds	Qualitative analysis; LOD 1 $\mu\text{g}\cdot\text{mL}^{-1}$.	Fast; easy; no sample pretreatment.	Cannot distinguish isomers; cannot exclude potential matrix interferences with the same m/z as target cannabinoids.	2022 ¹³⁷

WALDI-MS or (SpiderMass) composed of an IR-laser handheld microsampling probe connected to a mass spectrometer through a transfer tube in combination with multivariate statistical analysis.	Lab-based	THCA, CBDA.	4 Cannabis plant materials.	seconds	Quantitative.	Fast; easy; mini-invasive; <i>in situ</i> analysis; distinction THCA/CBDA by MS/MS in negative ionization mode; differentiation of four Cannabis cultivars by statistical models.	Results cannot be directly compared with absolute quantitative analysis due to the small sampling size (a few μm); the model only has a limited sample size.	2022 ¹⁴⁰
Vaping liquids were dissolved in acetonitrile and sampled using glass capillary tips. The tips were subsequently analyzed via DART-MS.	Lab-based	$\Delta 8$ -THC, $\Delta 9$ -THC, CBD, CBC.	Vaping liquid samples.	< 2 min	Qualitative.	Fast; easy sample pretreatment (just dilution).	Cannot distinguish cannabinoid isomers.	2023 ¹³⁶

Abbreviations: Polytetrafluoroethylene (PTFE), Direct Analysis in Real Time-Mass Spectrometry (DART-MS), High-Resolution Mass Spectrometry (HRMS), Water-Assisted Laser Desorption Ionization Mass Spectrometry (WALDI-MS or SpiderMass), Paper Spray Tandem Mass Spectrometry (PS-MS/MS).

Discussion

Colorimetric spot tests and immunochemical methods employ substrates such as microfiberglass, filter paper, polymer strips, TLC plates, or ELISA plates for reactions involving color reagents and antibodies. Color interpretation can be performed visually, via smartphone, or using densitometric/UV scanners. These assays are highly portable due to their minimal equipment requirements. They consume minimal amounts of solvents, color reagents, and immunoreagents, resulting in lower overall costs. Experimental procedures and result interpretation require minimal expertise, making them accessible to untrained individuals. These advantages make them widely applicable for high-throughput in-field screening, even though they may lack accuracy, sensitivity, and selectivity, particularly in colorimetric spot tests.

Electrochemical methods utilize devices such as potentiostats, electrochemical sensors, or workstations. Spectroscopic analysis employs benchtop or handheld spectrometers, offering varying levels of portability. Advances in portable mass spectrometry (MS) enhance the transportability of AIMS methods. These methods require minimal or no sample preparation, especially in optical spectroscopy, and generate minimal waste, promoting environmental friendliness. They offer improved accuracy, sensitivity, and selectivity compared to colorimetric spot tests, particularly in AIMS techniques. However, proficiency in instrument operation and expertise are necessary due to the complexity involved. These methods bridge high-throughput screening in the field and laboratory confirmatory analysis, reducing the workload and costs associated with lab-based analysis while enhancing real-time testing for timely judicial or quality control decisions.

NMR spectrometers are typically large and heavy due to stringent magnetic and power requirements. Benchtop versions, though transportable, sacrifice resolution compared to high-resolution NMR in complex Cannabis analysis. Similarly, ion mobility spectrometry (IMS) instruments, despite portable options, predominantly use advanced and costly equipment in Cannabis analysis, notably high-end IMS-MS devices introduced in recent years. These high-resolution NMR and IMS-MS

technologies advance speed, accuracy, sensitivity, and selectivity in analysis. However, their high equipment and maintenance costs and technical demands on operators limit their potential primarily to lab-based confirmatory analysis.

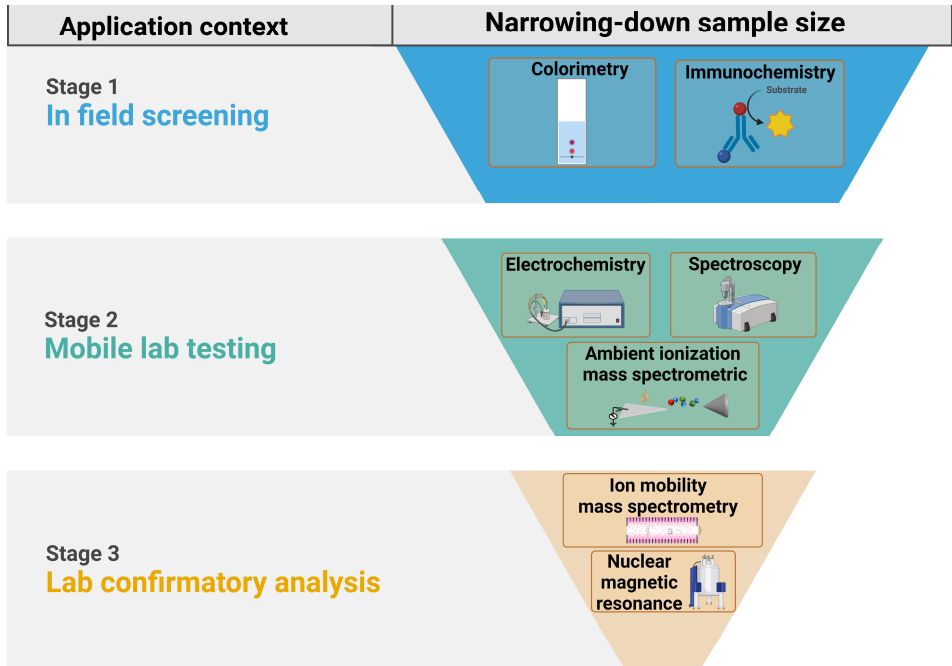


Figure 2.2. Classification of analytical methods reviewed in this chapter according to different application contexts.

Conclusions

Over the past decade, numerous analytical methods have been developed and employed by laboratories and agencies to assess Cannabis and Cannabis products. This chapter reviews analytical techniques beyond classical methods such as HPLC- and GC-based methods, focusing primarily on the rapid analytical technologies that have emerged in the last ten years. There is no universally preferred method for specific samples, and consensus remains inconclusive. Given the diversity of sample types and applications, a one-size-fits-all approach is impractical in this field. Nonetheless, there is an urgent need to establish universally accepted reference methods, likely HPLC- or GC-based, to validate new techniques and facilitate cross-platform comparisons. This is crucial because the analytical results of Cannabis and

its products can significantly impact judicial decisions and actions. While advancements in analytical speed continue, there has been comparatively less emphasis on the environmental impact of these analyses. It is important to address this by developing methods and sample preparation techniques that consider environmental sustainability. Efforts are ongoing to create analytical methods tailored to various application scenarios, such as field screening, mobile lab testing, and laboratory confirmation, with the goal of supporting the sustainable and safe growth of the Cannabis industry. Achieving this objective requires collaboration among legal and regulatory bodies, scientists, marketers, cultivators, and consumers.

References

- (1) Congress. *Agricultural improvement act of 2018*; **2018**. Retrieved from United States Government. <https://www.congress.gov/115/plaws/publ334/PLAW-115publ334.pdf> (accessed 2024 July 24).
- (2) Odieka, A. E.; Obuzor, G. U.; Oyediji, O. O.; Gondwe, M.; Hosu, Y. S.; Oyediji, A. O. The medicinal natural products of *Cannabis sativa* Linn.: a review. *Molecules* **2022**, *27*, 1689.
- (3) Small, E. Evolution and classification of *Cannabis sativa* (marijuana, hemp) in relation to human utilization. *The Botanical Review* **2015**, *81*, 189-294.
- (4) Blake, A.; Nahtigal, I. The evolving landscape of cannabis edibles. *Current Opinion in Food Science* **2019**, *28*, 25-31.
- (5) Dilley, J. A.; Graves, J. M.; Brooks-Russell, A.; Whitehill, J. M.; Liebelt, E. L. Trends and characteristics of manufactured Cannabis product and Cannabis plant product exposures reported to US poison control centers, 2017-2019. *JAMA Network Open* **2021**, *4*, e2110925.
- (6) Peng, H.; Shahidi, F. Cannabis and Cannabis edibles: a review. *Journal of Agricultural and Food Chemistry* **2021**, *69*, 1751-1774.
- (7) McGregor, I. S.; Cairns, E. A.; Abelev, S.; Cohen, R.; Henderson, M.; Couch, D.; Arnold, J. C.; Gauld, N. Access to cannabidiol without a prescription: a cross-country comparison and analysis. *International Journal of Drug Policy* **2020**, *85*, 102935.
- (8) Golombek, P.; Müller, M.; Barthlott, I.; Sproll, C.; Lachenmeier, D. W. Conversion of cannabidiol (CBD) into psychotropic cannabinoids including tetrahydrocannabinol (THC): a controversy in the scientific literature. *Toxics* **2020**, *8*, 41.
- (9) Michael Geci, M. S., and Jordan Tishler. The dark side of cannabidiol: the unanticipated social and clinical implications of synthetic Δ^8 -THC. *Cannabis and Cannabinoid Research* **2023**, *8*, 270-282.
- (10) Evans, D. G. Medical fraud, mislabeling, contamination: all common in CBD products. *Missouri Medicine* **2020**, *117*, 394-399.
- (11) Barrus, D. G.; Capogrossi, K. L.; Cates, S. C.; Gourdet, C. K.; Peiper, N. C.; Novak, S. P.; Lefever, T. W.; Wiley, J. L. Tasty THC: promises and challenges of cannabis edibles. *RTI Press Methods Report Series* **2016**, *2016*, 2-22.
- (12) Ray, C. L.; Bylo, M. P.; Pescaglia, J.; Gawenis, J. A.; Greenlief, C. M. Delta-8 tetrahydrocannabinol product impurities. *Molecules* **2022**, *27*, 6924.
- (13) Capriotti, A. L.; Cannazza, G.; Catani, M.; Cavaliere, C.; Cavazzini, A.; Cerrato, A.; Citti, C.; Felletti, S.; Montone, C. M.; Piovesana, S.; *et al.* Recent applications of mass spectrometry for the characterization of Cannabis and hemp phytocannabinoids: from targeted to untargeted analysis. *Journal of Chromatography A* **2021**, *1655*, 462492.
- (14) Felletti, S.; De Luca, C.; Buratti, A.; Bozza, D.; Cerrato, A.; Capriotti, A. L.; Laganà, A.; Cavazzini, A.; Catani, M. Potency testing of cannabinoids by liquid and supercritical fluid chromatography: where we are, what we need. *Journal of Chromatography A* **2021**, *1651*, 462304.
- (15) Deidda, R.; Dispas, A.; De Bleye, C.; Hubert, P.; Ziemons, É. Critical review on recent trends in cannabinoid determination on Cannabis herbal samples: from chromatographic to vibrational spectroscopic techniques. *Analytica Chimica Acta* **2022**, *1209*, 339184.
- (16) CDR, E. *Union method for the quantitative determination of the Δ^9 -tetrahydrocannabinol content in hemp varieties*; rev. Delegated Regulation (EU) No 639/2014, Annex III as amended by Regulation (EU) 2017/1155; **2017**. Retrieved from Commission Delegated Regulation (EU). https://eur-lex.europa.eu/eli/reg_del/2017/1155/oj (accessed 2024 March 30).
- (17) Mudge, E. M.; Brown, P. N. Determination of cannabinoids in *Cannabis sativa* dried flowers and oils by LC-UV: single-laboratory validation, first action 2018.10. *Journal of AOAC International* **2020**, *103*, 489-493.
- (18) EU, E. C. *Commission recommendation (EU) 2016/2115 of 1 December 2016 on the monitoring of the presence of Δ^9 -tetrahydrocannabinol, its precursors and other cannabinoids in food* **2016**. Retrieved from Official Journal of the European Union. <https://eur-lex.europa.eu/legal-content/EN/TXT/PDF/?uri=OJ:L:2016:327:FULL&from=EL> (accessed 2024 March 31).

- (19) AOAC. *AOAC SMPR®2017.019 Standard method performance requirements (SMPRs®) for quantitation of cannabinoids in edible chocolate*; **2017**. Retrieved from AOAC International. https://www.aoac.org/wp-content/uploads/2020/11/SMPR202017_019.pdf (accessed 2024 July 7).
- (20) AOAC. *AOAC SMPR® 2022.001 Quantitation of cannabinoids in beverages*; **2022**. Retrieved from AOAC International. https://www.aoac.org/wp-content/uploads/2022/11/SMPR-2022_001.pdf (accessed 2024 July 7).
- (21) García-Valverde, M. T.; Sánchez-Carnerero Callado, C.; Díaz-Liñán, M. C.; Sánchez de Medina, V.; Hidalgo-García, J.; Nadal, X.; Hanuš, L.; Ferreiro-Vera, C. Effect of temperature in the degradation of cannabinoids: from a brief residence in the gas chromatography inlet port to a longer period in thermal treatments. *Frontiers in Chemistry* **2022**, *10*, 1038729.
- (22) Chan-Hosokawa, A.; Nguyen, L.; Lattanzio, N.; Adams, W. R. Emergence of delta-8 tetrahydrocannabinol in DUID investigation casework: method development, validation and application. *Journal of Analytical Toxicology* **2022**, *46*, 1-9.
- (23) Reber, J. D.; Karschner, E. L.; Seither, J. Z.; Knittel, J. L.; Dozier, K. V.; Walterscheid, J. P. An enhanced LC-MS-MS technique for distinguishing Δ^8 - and Δ^9 -tetrahydrocannabinol isomers in blood and urine specimens. *Journal of Analytical Toxicology* **2022**, *46*, 343-349.
- (24) Bailey, K. The value of the Duquenois test for Cannabis—a survey. *Journal of Forensic Sciences* **1979**, *24*, 817-841.
- (25) F Kelly, J.; Addanki, K.; Bagasra, O. The non-specificity of the Duquenois-Levine field test for marijuana. *The Open Forensic Science Journal* **2012**, *5*, 4-8.
- (26) Lewis, K.; Wagner, R.; Rodriguez-Cruz, S. E.; Weaver, M. J.; Dumke, J. C. Validation of the 4-aminophenol color test for the differentiation of marijuana-type and hemp-type Cannabis. *Journal of Forensic Sciences* **2021**, *66*, 285-294.
- (27) Acosta, A.; Li, L.; Weaver, M.; Capote, R.; Perr, J.; Almirall, J. Validation of a combined fast blue BB and 4-aminophenol colorimetric test for indication of hemp-type and marijuana-type Cannabis. *Forensic Chemistry* **2022**, *31*, 100448.
- (28) UNODC. *Recommended methods for the identification and analysis of Cannabis and Cannabis products*; **2009**. Retrieved from United Nations Office on Drugs and Crime UNODC. https://www.unodc.org/documents/scientific/ST-NAR-40-Ebook_1.pdf (accessed 2024 March 30).
- (29) dos Santos, N. A.; Souza, L. M.; Domingos, E.; França, H. S.; Lacerda Jr, V.; Beatriz, A.; Vaz, B. G.; Rodrigues, R. R.; Carvalho, V. V.; Merlo, B. B. Evaluating the selectivity of colorimetric test (fast blue BB salt) for the cannabinoids identification in marijuana street samples by UV-Vis, TLC, ESI (+) FT-ICR MS and ESI (+) MS/MS. *Forensic Chemistry* **2016**, *1*, 13-21.
- (30) Franca, H. S.; Acosta, A.; Jamal, A.; Romao, W.; Mulloor, J.; Almirall, J. R. Experimental and *ab initio* investigation of the products of reaction from Δ^9 -tetrahydrocannabinol (Δ^9 -THC) and the fast blue BB spot reagent in presumptive drug tests for cannabinoids. *Forensic Chemistry* **2020**, *17*, 100212.
- (31) Acosta, A.; Almirall, J. Differentiation between hemp-type and marijuana-type Cannabis using the fast blue BB colorimetric test. *Forensic Chemistry* **2021**, *26*, 100376.
- (32) Bele, A. A.; Khale, A. An overview on thin layer chromatography. *International Journal of Pharmaceutical Sciences and Research* **2011**, *2*, 256-267.
- (33) Duffau, B. E.; Alcamán, K. Analysis of Three Main Cannabinoids in Seized Marijuana by Densitometric High-Performance Thin-Layer Chromatography. *Journal of Planar Chromatography* **2019**, *32*, 343-346.
- (34) Schmidt, T.; Stommel, J.; Kohlmann, T.; Kramell, A. E.; Csuk, R. Separating the true from the false: a rapid HPTLC-ESI-MS method for the determination of cannabinoids in different oils. *Results in Chemistry* **2021**, *3*, 100234.
- (35) Fishedick, J. T.; Glas, R.; Hazekamp, A.; Verpoorte, R. A Qualitative and Quantitative HPTLC Densitometry Method for the Analysis of Cannabinoids in *Cannabis sativa* L. *Phytochemical Analysis* **2009**, *20*, 421-426.
- (36) Mano-Sousa, B. J.; Maia, G. A. S.; Lima, P. L.; Campos, V. A.; Negri, G.; Chequer, F. M. D.; Duarte-Almeida, J. M. Color Determination Method and Evaluation of Methods for the

- Detection of Cannabinoids by Thin-Layer Chromatography (TLC). *Journal of Forensic Sciences* **2021**, *66*, 854-865.
- (37) Tsujikawa, K.; Okada, Y.; Segawa, H.; Yamamuro, T.; Kuwayama, K.; Kanamori, T.; Iwata, Y. T. Thin-layer chromatography on silver nitrate-impregnated silica gel for analysis of homemade tetrahydrocannabinol mixtures. *Forensic Toxicology* **2022**, *40*, 125-131.
 - (38) Huang, S.; Qiu, R.; Fang, Z.; Min, K.; Van Beek, T. A.; Ma, M.; Chen, B.; Zuilhof, H.; Salentijn, G. I. Semiquantitative screening of THC analogues by silica gel TLC with an Ag(I) retention zone and chromogenic smartphone detection. *Analytical Chemistry* **2022**, *94*, 13710-13718.
 - (39) van Beek, T. A.; Subrtova, D. Factors involved in the high pressure liquid chromatographic separation of alkenes by means of argentation chromatography on ion exchangers: overview of theory and new practical developments. *Phytochemical Analysis* **1995**, *6*, 1-19.
 - (40) Kaneti, J.; de Smet, L. C.; Boom, R.; Zuilhof, H.; Sudhölter, E. J. Computational probes into the basis of silver ion chromatography. II. silver(I)-olefin complexes. *The Journal of Physical Chemistry A* **2002**, *106*, 11197-11204.
 - (41) Damyanova, B.; Momtchilova, S.; Bakalova, S.; Zuilhof, H.; Christie, W. W.; Kaneti, J. Computational Probes into the Conceptual Basis of Silver Ion Chromatography: I. Silver(I) Ion Complexes of Unsaturated Fatty Acids and Esters. *Journal of Molecular Structure: THEOCHEM* **2002**, *589-590*, 239-249.
 - (42) De Rycke, E.; Stove, C.; Dubruel, P.; De Saeger, S.; Beloglazova, N. Recent developments in electrochemical detection of illicit drugs in diverse matrices. *Biosensors and Bioelectronics* **2020**, *169*, 112579.
 - (43) Balbino, M. A.; de Oliveira, L. S.; Eleotério, I. C.; Oiye, E. N.; Ribeiro, M. F.; McCord, B. R.; Ipolito, A. J.; de Oliveira, M. F. The application of voltammetric analysis of $\Delta(9)$ -THC for the reduction of false positive results in the analysis of suspected marijuana plant matter. *Journal of Forensic Sciences* **2016**, *61*, 1067-1073.
 - (44) Balbino, M. A.; Eleotério, I. C.; Oliveira, L. S. d.; de Menezes, M. M.; Andrade, J. F. d.; Ipólito, A. J.; Oliveira, M. F. d. A comparative study between two different conventional working electrodes for detection of $\Delta 9$ -tetrahydrocannabinol using square-wave voltammetry: a new sensitive method for forensic analysis. *Journal of the Brazilian Chemical Society* **2014**, *25*, 589-596.
 - (45) Balbino, M. A.; Oiye, E. N.; Ribeiro, M. F. M.; Júnior, J. W. C.; Eleotério, I. C.; Ipólito, A. J.; de Oliveira, M. F. Use of screen-printed electrodes for quantification of cocaine and $\Delta 9$ -THC: adaptations to portable systems for forensic purposes. *Journal of Solid State Electrochemistry* **2016**, *20*, 2435-2443.
 - (46) Novak, I.; Mlakar, M.; Komorsky-Lovrić, Š. Voltammetry of immobilized particles of cannabinoids. *Electroanalysis* **2013**, *25*, 2631-2636.
 - (47) Nissim, R.; Compton, R. G. Absorptive stripping voltammetry for Cannabis detection. *Chemistry Central Journal* **2015**, *9*, 1-7.
 - (48) Renaud-Young, M.; Mayall, R. M.; Salehi, V.; Goledzinowski, M.; Comeau, F. J.; MacCallum, J. L.; Birss, V. I. Development of an ultra-Sensitive electrochemical sensor for $\Delta 9$ -tetrahydrocannabinol (THC) and its metabolites using carbon paper electrodes. *Electrochimica Acta* **2019**, *307*, 351-359.
 - (49) López-Iglesias, D.; García-Guzmán, J. J.; Zanardi, C.; Palacios-Santander, J. M.; Cubillana-Aguilera, L.; Pigani, L. Fast electroanalytical determination of cannabidiol and cannabinol in aqueous solution using sonogel-carbon-PEDOT devices. *Journal of Electroanalytical Chemistry* **2020**, *878*, 114591.
 - (50) Zanfognini, B.; Monari, A.; Foca, G.; Ulrici, A.; Pigani, L.; Zanardi, C. Preliminary evaluation of the use of a disposable electrochemical sensor for selective identification of $\Delta 9$ -tetrahydrocannabinol and cannabidiol by multivariate analysis. *Microchemical Journal* **2022**, *183*, 108108.
 - (51) Comeau, Z. J.; Boileau, N. T.; Lee, T.; Melville, O. A.; Rice, N. A.; Troung, Y.; Harris, C. S.; Lessard, B. H.; Shuhendler, A. J. On-the-spot detection and speciation of cannabinoids using organic thin-film transistors. *ACS Sensors* **2019**, *4*, 2706-2715.

- (52) Gauglitz, G.; Dakin, J. P. Spectroscopic analysis. In *Handbook of Optoelectronics*, CRC Press, Boca Raton, **2017**; pp 569-600.
- (53) Nobari Moghaddam, H.; Tamiji, Z.; Akbari Lakeh, M.; Khoshayand, M. R.; Haji Mahmoodi, M. Multivariate analysis of food fraud: a review of NIR based instruments in tandem with chemometrics. *Journal of Food Composition and Analysis* **2022**, *107*, 104343.
- (54) Callado, C. S.-C.; Núñez-Sánchez, N.; Casano, S.; Ferreiro-Vera, C. The potential of near infrared spectroscopy to estimate the content of cannabinoids in *Cannabis sativa* L.: a comparative study. *Talanta* **2018**, *190*, 147-157.
- (55) Burns, D. A.; Ciurczak, E. W. *Handbook of near-infrared analysis*; CRC Press, Boca Raton, **2007**.
- (56) Birenboim, M.; Kenigsbuch, D.; Shimshoni, J. A. Novel fluorescence spectroscopy method coupled with N-PLS-R and PLS-DA models for the quantification of cannabinoids and the classification of Cannabis cultivars. *Phytochemical Analysis* **2023**, *34*, 280-288.
- (57) Birenboim, M.; Kengisbuch, D.; Chalupowicz, D.; Maurer, D.; Barel, S.; Chen, Y.; Fallik, E.; Paz-Kagan, T.; Shimshoni, J. A. Use of Near-Infrared Spectroscopy for the Classification of Medicinal Cannabis Cultivars and the Prediction of Their Cannabinoid and Terpene Contents. *Phytochemistry* **2022**, *204*, 113445.
- (58) Tran, J.; Vassiliadis, S.; Elkins, A. C.; Cogan, N. O.; Rochfort, S. J. Developing prediction models using near-infrared spectroscopy to quantify cannabinoid content in *Cannabis sativa*. *Sensors* **2023**, *23*, 2607.
- (59) Su, K.; Maghirang, E.; Tan, J. W.; Yoon, J. Y.; Armstrong, P.; Kachroo, P.; Hildebrand, D. NIR Spectroscopy for Rapid Measurement of Moisture and Cannabinoid Contents of Industrial Hemp (*Cannabis sativa*). *Industrial Crops and Products* **2022**, *184*, 115007.
- (60) Duchateau, C.; Kauffmann, J. M.; Canfyn, M.; Stévigny, C.; De Braekeleer, K.; Deconinck, E. Discrimination of legal and illegal *Cannabis spp.* according to European legislation using near infrared spectroscopy and chemometrics. *Drug Testing and Analysis* **2020**, *12*, 1309-1319.
- (61) Gloerfelt-Tarp, F.; Hewavitharana, A. K.; Mieog, J.; Palmer, W. M.; Fraser, F.; Ansari, O.; Kretschmar, T. Using a global diversity panel of *Cannabis sativa* L. to develop a near infrared-based chemometric application for cannabinoid quantification. *Scientific Reports* **2023**, *13*, 2253.
- (62) Goff, N. K.; Guenther, J. F.; Roberts III, J. K.; Adler, M.; Molle, M. D.; Mathews, G.; Kurouski, D. Non-invasive and confirmatory differentiation of hermaphrodite from both male and female Cannabis plants using a hand-held Raman spectrometer. *Molecules* **2022**, *27*, 4978.
- (63) Yao, S.; Ball, C.; Miyagusuku-Cruzado, G.; Giusti, M. M.; Aykas, D. P.; Rodriguez-Saona, L. E. A novel handheld FT-NIR spectroscopic approach for real-time screening of major cannabinoids content in hemp. *Talanta* **2022**, *247*, 123559.
- (64) Jarén, C.; Zambrana, P. C.; Pérez-Roncal, C.; López-Maestresalas, A.; Ábrego, A.; Arazuri, S. Potential of NIRS technology for the determination of cannabinoid content in industrial hemp (*Cannabis sativa* L.). *Agronomy* **2022**, *12*, 938.
- (65) Deidda, R.; Coppey, F.; Damergi, D.; Schelling, C.; Coïc, L.; Veuthey, J.-L.; Sacré, P.-Y.; De Bleye, C.; Hubert, P.; Esseiva, P. New perspective for the in-field analysis of Cannabis samples using handheld near-infrared spectroscopy: a case study focusing on the determination of Δ^9 -tetrahydrocannabinol. *Journal of Pharmaceutical and Biomedical Analysis* **2021**, *202*, 114150.
- (66) Espel Grekopoulos, J. Construction and validation of quantification methods for determining the cannabidiol content in liquid pharma-grade formulations by means of near-infrared spectroscopy and partial least squares regression. *Medical Cannabis and Cannabinoids* **2019**, *2*, 43-55.
- (67) Risoluti, R.; Gullifa, G.; Battistini, A.; Materazzi, S. Monitoring of cannabinoids in hemp flours by microNIR/chemometrics. *Talanta* **2020**, *211*, 120672.
- (68) Risoluti, R.; Gullifa, G.; Battistini, A.; Materazzi, S. The detection of cannabinoids in veterinary feeds by microNIR/chemometrics: a new analytical platform. *Analyst* **2020**, *145*, 1777-1782.

- (69) Risoluti, R.; Gullifa, G.; Battistini, A.; Materazzi, S. Development of a “single-click” analytical platform for the detection of cannabinoids in hemp seed oil. *RSC Advances* **2020**, *10*, 43394-43399.
- (70) Risoluti, R.; Gullifa, G.; Battistini, A.; Materazzi, S. MicroNIR/chemometrics: a new analytical platform for fast and accurate detection of Δ^9 -tetrahydrocannabinol (THC) in oral fluids. *Drug and Alcohol Dependence* **2019**, *205*, 107578.
- (71) Coppey, F.; Bécue, A.; Sacré, P.-Y.; Ziemons, E. M.; Hubert, P.; Esseiva, P. Providing illicit drugs results in five seconds using ultra-portable NIR technology: an opportunity for forensic laboratories to cope with the trend toward the decentralization of forensic capabilities. *Forensic Science International* **2020**, *317*, 110498.
- (72) Birenboim, M.; Rinnan, Å.; Kengisbuch, D.; Shimshoni, J. A. Novel fluorescence spectroscopy coupled with PARAFAC modeling for major cannabinoids quantification and identification in Cannabis extracts. *Chemometrics and Intelligent Laboratory Systems* **2023**, *232*, 104717.
- (73) Gilmore, A. M.; Elhendawy, M. A.; Radwan, M. M.; Kidder, L. H.; Wanas, A. S.; Godfrey, M.; Hildreth, J. B.; Robinson, A. E.; ElSohly, M. A. Absorbance-transmittance excitation emission matrix method for quantification of major cannabinoids and corresponding acids: a rapid alternative to chromatography for rapid chemotype discrimination of *Cannabis sativa* varieties. *Cannabis and Cannabinoid Research* **2023**, *8*, 911-922.
- (74) Sun, Y.; Tang, H.; Zou, X.; Meng, G.; Wu, N. Raman spectroscopy for food quality assurance and safety monitoring: a review. *Current Opinion in Food Science* **2022**, *47*, 100910.
- (75) Porcu, S.; Tuveri, E.; Palanca, M.; Melis, C.; La Franca, I. M.; Satta, J.; Chiriu, D.; Carbonaro, C. M.; Cortis, P.; De Agostini, A. Rapid *in situ* detection of THC and CBD in *Cannabis sativa* L. by 1064 nm Raman spectroscopy. *Analytical Chemistry* **2022**, *94*, 10435-10442.
- (76) Botta, R.; Limwichean, S.; Limsuwan, N.; Moonlek, C.; Horprathum, M.; Eiamchai, P.; Chananonawathorn, C.; Patthanasettakul, V.; Chindaudom, P.; Nuntawong, N. An efficient and simple SERS approach for trace analysis of tetrahydrocannabinol and cannabinol and multi-cannabinoid detection. *Spectrochimica Acta Part A: Molecular and Biomolecular Spectroscopy* **2022**, *281*, 121598.
- (77) Bindesri, S. D.; Jebailey, R.; Albarghouthi, N.; Pye, C. C.; Brosseau, C. L. Spectroelectrochemical and computational studies of tetrahydrocannabinol (THC) and carboxy-tetrahydrocannabinol (THC-COOH). *Analyst* **2020**, *145*, 1849-1857.
- (78) Valinger, D.; Jurina, T.; Šain, A.; Matešić, N.; Panić, M.; Benković, M.; Gajdoš Kljusurić, J.; Jurinjak Tušek, A. Development of ANN models based on combined UV-Vis-NIR spectra for rapid quantification of physical and chemical properties of industrial hemp extracts. *Phytochemical Analysis* **2021**, *32*, 326-338.
- (79) Terzapulo, X.; Kassenova, A.; Bukasov, R. Immunoassays: analytical and clinical performance, challenges, and perspectives of SERS detection in comparison with fluorescent spectroscopic detection. *International Journal of Molecular Sciences* **2024**, *25*, 2080.
- (80) Moody, M. T.; Ringel, M. M.; Mathews, C. M.; Midthun, K. M. Determination of cross-reactivity of contemporary cannabinoids with THC direct immunoassay (ELISA) in whole blood. *Journal of Analytical Toxicology* **2022**, *46*, 844-851.
- (81) Vikingsson, S.; Winecker, R. E.; Cone, E. J.; Kuntz, D. J.; Dorsey, B.; Jacques, M.; Senter, M.; Flegel, R. R.; Hayes, E. D. Prevalence of cannabidiol, Δ^9 - and Δ^8 -tetrahydrocannabinol and metabolites in workplace drug testing urine specimens. *Journal of Analytical Toxicology* **2022**, *46*, 866-874.
- (82) Mullen, L. D.; Hart, E. D.; Vikingsson, S.; Winecker, R. E.; Hayes, E.; Flegel, R. Δ^8 -THC-COOH cross-reactivity with cannabinoid immunoassay kits and interference in chromatographic testing methods. *Journal of Analytical Toxicology* **2023**, *47*, 557-562.
- (83) Desrosiers, N. A.; Milman, G.; Mendu, D. R.; Lee, D.; Barnes, A. J.; Gorelick, D. A.; Huestis, M. A. Cannabinoids in oral fluid by on-site immunoassay and by GC-MS using two different oral fluid collection devices. *Analytical and Bioanalytical Chemistry* **2014**, *406*, 4117-4128.
- (84) Tassoni, G.; Cippitelli, M.; Ottaviani, G.; Frolidi, R.; Cingolani, M. Detection of cannabinoids by ELISA and GC-MS methods in a hair sample previously used to detect other drugs of abuse. *Journal of Analytical Toxicology* **2016**, *40*, 408-413.

- (85) Futane, A.; Senthil, M.; S, J.; Srinivasan, A.; R, K.; Narayanamurthy, V. Sweat analysis for urea sensing: trends and challenges. *Analytical Methods* **2023**, *15*, 4405-4426.
- (86) Boroumand, M.; Olinas, A.; Cabras, T.; Manconi, B.; Fanni, D.; Faa, G.; Desiderio, C.; Messina, I.; Castagnola, M. Saliva, a bodily fluid with recognized and potential diagnostic applications. *Journal of Separation Science* **2021**, *44*, 3677-3690.
- (87) Brunelle, E.; Thibodeau, B.; Shoemaker, A.; Halánek, J. Step toward roadside sensing: noninvasive detection of a THC metabolite from the sweat content of fingerprints. *ACS Sensors* **2019**, *4*, 3318-3324.
- (88) Badawy, S. M. Semi-quantitative analysis of drugs of abuse in human urine by end-point dilution flow immunochromatographic assay. *Journal of Planar Chromatography* **2020**, *33*, 419-425.
- (89) Plouffe, B. D.; Murthy, S. K. Fluorescence-based lateral flow assays for rapid oral fluid roadside detection of Cannabis use. *Electrophoresis* **2017**, *38*, 501-506.
- (90) Gong, X.; Cai, J.; Zhang, B.; Zhao, Q.; Piao, J.; Peng, W.; Gao, W.; Zhou, D.; Zhao, M.; Chang, J. A review of fluorescent signal-based lateral flow immunochromatographic strips. *Journal of Materials Chemistry B* **2017**, *5*, 5079-5091.
- (91) Chand, R.; Mittal, N.; Srinivasan, S.; Rajabzadeh, A. R. Upconverting nanoparticle clustering based rapid quantitative detection of tetrahydrocannabinol (THC) on lateral-flow immunoassay. *Analyst* **2021**, *146*, 574-580.
- (92) Yu, H.; Lee, H.; Cheong, J.; Woo, S. W.; Oh, J.; Oh, H.-K.; Lee, J.-H.; Zheng, H.; Castro, C. M.; Yoo, Y.-E. A rapid assay provides on-site quantification of tetrahydrocannabinol in oral fluid. *Science Translational Medicine* **2021**, *13*, eabe2352.
- (93) Hazekamp, A.; Choi, Y. H.; Verpoorte, R. Quantitative analysis of cannabinoids from *Cannabis sativa* using ¹H-NMR. *Chemical and Pharmaceutical Bulletin* **2004**, *52*, 718-721.
- (94) Pauli, G. F. qNMR—a versatile concept for the validation of natural product reference compounds. *Phytochemical Analysis* **2001**, *12*, 28-42.
- (95) Santos, A.; Dutra, L.; Menezes, L.; Santos, M.; Barison, A. Forensic NMR spectroscopy: just a beginning of a promising partnership. *TrAC Trends in Analytical Chemistry* **2018**, *107*, 31-42.
- (96) Wood, J. S.; Gordon, W. H.; Morgan, J. B.; Williamson, R. T. Calculated and experimental ¹H and ¹³C NMR assignments for cannabicitran. *Magnetic Resonance in Chemistry* **2022**, *60*, 196-202.
- (97) Ahmed, S. A.; Ross, S. A.; Slade, D.; Radwan, M. M.; Khan, I. A.; ElSohly, M. A. Minor oxygenated cannabinoids from high potency *Cannabis sativa* L. *Phytochemistry* **2015**, *117*, 194-199.
- (98) Radwan, M. M.; ElSohly, M. A.; El-Alfy, A. T.; Ahmed, S. A.; Slade, D.; Husni, A. S.; Manly, S. P.; Wilson, L.; Seale, S.; Cutler, S. J. Isolation and pharmacological evaluation of minor cannabinoids from high-potency *Cannabis sativa*. *Journal of Natural Products* **2015**, *78*, 1271-1276.
- (99) Radwan, M. M.; Wanas, A. S.; Gul, W.; Ibrahim, E. A.; ElSohly, M. A. Isolation and characterization of impurities in commercially marketed Δ^8 -THC products. *Journal of Natural Products* **2023**, *86*, 822-829.
- (100) Meehan-Atrash, J.; Rahman, I. Novel Δ^8 -tetrahydrocannabinol vaporizers contain unlabeled adulterants, unintended byproducts of chemical synthesis, and heavy metals. *Chemical Research in Toxicology* **2021**, *35*, 73-76.
- (101) Wang, X.; Harrington, P. d. B.; Baugh, S. F. Comparative study of NMR spectral profiling for the characterization and authentication of Cannabis. *Journal of AOAC International* **2017**, *100*, 1356-1364.
- (102) Peschel, W.; Politi, M. ¹H NMR and HPLC/DAD for *Cannabis sativa* L. chemotype distinction, extract profiling and specification. *Talanta* **2015**, *140*, 150-165.
- (103) Ohtsuki, T.; Friesen, J. B.; Chen, S.-N.; McAlpine, J. B.; Pauli, G. F. Selective preparation and high dynamic-range analysis of cannabinoids in “CBD oil” and other *Cannabis sativa* preparations. *Journal of Natural Products* **2022**, *85*, 634-646.
- (104) Barthlott, I.; Scharinger, A.; Golombek, P.; Kuballa, T.; Lachenmeier, D. W. A quantitative ¹H NMR method for screening cannabinoids in CBD oils. *Toxics* **2021**, *9*, 136.

- (105) Araneda, J. F.; Chu, T.; Leclerc, M. C.; Riegel, S. D.; Spingarn, N. Quantitative analysis of cannabinoids using benchtop NMR instruments. *Analytical Methods* **2020**, *12*, 4853-4857.
- (106) Brighenti, V.; Marchetti, L.; Anceschi, L.; Protti, M.; Verri, P.; Pollastro, F.; Mercolini, L.; Bertelli, D.; Zanardi, C.; Pellati, F. Separation and non-separation methods for the analysis of cannabinoids in *Cannabis sativa* L. *Journal of Pharmaceutical and Biomedical Analysis* **2021**, *206*, 114346.
- (107) Marchetti, L.; Brighenti, V.; Rossi, M. C.; Sperlea, J.; Pellati, F.; Bertelli, D. Use of ^{13}C -qNMR spectroscopy for the analysis of non-psychoactive cannabinoids in fibre-type *Cannabis sativa* L. (hemp). *Molecules* **2019**, *24*, 1138.
- (108) Dadiotis, E.; Mitsis, V.; Melliou, E.; Magiatis, P. Direct quantitation of phytocannabinoids by one-dimensional ^1H qNMR and two-dimensional ^1H - ^1H COSY qNMR in complex natural mixtures. *Molecules* **2022**, *27*, 2965.
- (109) Colella, M. F.; Salvino, R. A.; Gaglianò, M.; Litrenta, F.; Oliviero Rossi, C.; Le Pera, A.; De Luca, G. NMR spectroscopy applied to the metabolic analysis of natural extracts of *Cannabis sativa*. *Molecules* **2022**, *27*, 3509.
- (110) Aliferis, K. A.; Bernard-Perron, D. Cannabinomics: application of metabolomics in *Cannabis* (*Cannabis sativa* L.) research and development. *Frontiers in Plant Science* **2020**, *11*, 517837.
- (111) Happyana, N.; Agnolet, S.; Muntendam, R.; Van Dam, A.; Schneider, B.; Kayser, O. Analysis of cannabinoids in laser-microdissected trichomes of medicinal *Cannabis sativa* using LCMS and cryogenic NMR. *Phytochemistry* **2013**, *87*, 51-59.
- (112) Happyana, N.; Kayser, O. Metabolic changes in the trichomes of *Cannabis sativa* var. *bedrobinol* analyzed by ^1H -NMR-based metabolomics. *Indonesian Journal of Chemistry* **2020**, *20*, 1246-1254.
- (113) Happyana, N.; Kayser, O. ^1H NMR-based metabolomics differentiation and real time PCR analysis of medicinal *Cannabis* organs. In *XXIX International Horticultural Congress on Horticulture: Sustaining Lives, Livelihoods and Landscapes (IHC2014): V World 1125*, **2014**; pp 25-32.
- (114) Happyana, N.; Kayser, O. Monitoring metabolite profiles of *Cannabis sativa* L. trichomes during flowering period using ^1H NMR-based metabolomics and real-time PCR. *Planta Medica* **2016**, 1217-1223.
- (115) Fernández, S.; Castro, R.; López-Radcenko, A.; Rodriguez, P.; Carrera, I.; García-Carnelli, C.; Moyna, G. Beyond cannabinoids: application of NMR-based metabolomics for the assessment of *Cannabis sativa* L. crop health. *Frontiers in Plant Science* **2023**, *14*, 1025932.
- (116) de A Leite, J.; de Oliveira, M. V.; Conti, R.; Borges, W. d. S.; Rosa, T. R.; Filgueiras, P. R.; Lacerda Jr, V.; Romão, W.; Neto, Á. C. Extraction and isolation of cannabinoids from marijuana seizures and characterization by ^1H NMR allied to chemometric tools. *Science & Justice* **2018**, *58*, 355-365.
- (117) Thomson, J. J. XXVI. Rays of positive electricity. *The London, Edinburgh, and Dublin Philosophical Magazine and Journal of Science* **1911**, *21*, 225-249.
- (118) Mason, E. A.; Schamp Jr, H. W. Mobility of gaseous ions in weak electric fields. *Annals of Physics* **1958**, *4*, 233-270.
- (119) Mason, E. A.; McDaniel, E. W. *Transport properties of ions in gases*;
- (120) Gabelica, V.; Shvartsburg, A. A.; Afonso, C.; Barran, P.; Benesch, J. L.; Bleiholder, C.; Bowers, M. T.; Bilbao, A.; Bush, M. F.; Campbell, J. L. Recommendations for reporting ion mobility mass spectrometry measurements. *Mass Spectrometry Reviews* **2019**, *38*, 291-320.
- (121) Christofi, E.; Barran, P. Ion Mobility Mass Spectrometry (IM-MS) for Structural Biology: Insights Gained by Measuring Mass, Charge, and Collision Cross Section. *Chemical Reviews* **2023**, *123*, 2902-2949.
- (122) Delafield, D. G.; Lu, G.; Kaminsky, C. J.; Li, L. High-End Ion Mobility Mass Spectrometry: A Current Review of Analytical Capacity in Omics Applications and Structural Investigations. *TrAC Trends in Analytical Chemistry* **2022**, *157*, 116761.
- (123) del Mar Contreras, M.; Jurado-Campos, N.; Callado, C. S.-C.; Arroyo-Manzanares, N.; Fernandez, L.; Casano, S.; Marco, S.; Arce, L.; Ferreira-Vera, C. Thermal desorption-ion mobility

- spectrometry: a rapid sensor for the detection of cannabinoids and discrimination of *Cannabis sativa* L. chemotypes. *Sensors and Actuators B: Chemical* **2018**, 273, 1413-1424.
- (124) Mashmoushi, N.; Campbell, J. L.; di Lorenzo, R.; Hopkins, W. S. Rapid separation of cannabinoid isomer sets using differential mobility spectrometry and mass spectrometry. *Analyst* **2022**, 147, 2198-2206.
 - (125) Campbell, J. L.; Blanc, J. Y. L.; Kibbey, R. G. Differential mobility spectrometry: a valuable technology for analyzing challenging biological samples. *Bioanalysis* **2015**, 7, 853-856.
 - (126) Dodds, J. N.; Baker, E. S. Ion mobility spectrometry: fundamental concepts, instrumentation, applications, and the road ahead. *Journal of the American Society for Mass Spectrometry* **2019**, 30, 2185-2195.
 - (127) Zietek, B. M.; Mengerink, Y.; Jordens, J.; Somsen, G. W.; Kool, J.; Honing, M. Adduct-ion formation in trapped ion mobility spectrometry as a potential tool for studying molecular structures and conformations. *International Journal for Ion Mobility Spectrometry* **2018**, 21, 19-32.
 - (128) Hädener, M.; Kamrath, M. Z.; Weinmann, W.; Groessl, M. High-resolution ion mobility spectrometry for rapid Cannabis potency testing. *Analytical Chemistry* **2018**, 90, 8764-8768.
 - (129) Ieritano, C.; Thomas, P.; Hopkins, W. S. Argentation: A Silver Bullet for Cannabinoid Separation by Differential Mobility Spectrometry. *Analytical Chemistry* **2023**, 95, 8668-8678.
 - (130) Takats, Z.; Wiseman, J. M.; Gologan, B.; Cooks, R. G. Mass spectrometry sampling under ambient conditions with desorption electrospray ionization. *Science* **2004**, 306, 471-473.
 - (131) Cody, R. B.; Laramée, J. A.; Durst, H. D. Versatile new ion source for the analysis of materials in open air under ambient conditions. *Analytical Chemistry* **2005**, 77, 2297-2302.
 - (132) Zhang, X.-L.; Zhang, H.; Wang, X.-C.; Huang, K.-K.; Wang, D.; Chen, H.-W. Advances in ambient ionization for mass spectrometry. *Chinese Journal of Analytical Chemistry* **2018**, 46, 1703-1713.
 - (133) Kuo, T.-H.; Dutkiewicz, E. P.; Pei, J.; Hsu, C.-C. Ambient ionization mass spectrometry today and tomorrow: embracing challenges and opportunities. *Analytical Chemistry* **2020**, 92, 2353-2363.
 - (134) Wang, H.; Liu, J.; Cooks, R. G.; Ouyang, Z. Paper spray for direct analysis of complex mixtures using mass spectrometry. *Angewandte Chemie International Edition* **2010**, 122, 889-892.
 - (135) Espy, R. D.; Muliadi, A. R.; Ouyang, Z.; Cooks, R. G. Spray mechanism in paper spray ionization. *International Journal of Mass Spectrometry* **2012**, 325-327, 167-171.
 - (136) Falconer, T. M.; Morales-Garcia, F. Rapid screening of vaping liquids by DART-MS. *Journal of AOAC International* **2023**, 106, 436-444.
 - (137) Chambers, M. I.; Musah, R. A. DART-HRMS as a triage approach for the rapid analysis of cannabinoid-infused edible matrices, personal-care products and *Cannabis sativa* hemp plant material. *Forensic Chemistry* **2022**, 27, 100382.
 - (138) Bills, B.; Manicke, N. Using sesame seed oil to preserve and preconcentrate cannabinoids for paper spray mass spectrometry. *Journal of the American Society for Mass Spectrometry* **2020**, 31, 675-684.
 - (139) Huang, S.; Claassen, F. W.; van Beek, T. A.; Chen, B.; Zeng, J.; Zuilhof, H.; Salentijn, G. I. J. Rapid distinction and semiquantitative analysis of THC and CBD by silver-impregnated paper spray mass spectrometry. *Analytical Chemistry* **2021**, 93, 3794-3802.
 - (140) Ogrinc, N.; Schneider, S.; Bourmaud, A.; Gengler, N.; Salzter, M.; Fournier, I. Direct *in vivo* analysis of CBD- and THC-acid cannabinoids and classification of Cannabis cultivars using SpiderMass. *Metabolites* **2022**, 12, 480.
 - (141) Wang, W.; Xu, C.; Ruan, H.; Li, H.; Xing, Y.; Hou, K.; Li, H. Solvent assisted thermal desorption for the on-site detection of illegal drugs by a miniature ion trap mass spectrometer. *Analytical Methods* **2020**, 12, 264-271.

Rapid Distinction and Semiquantitative Analysis of Δ^9 -THC and CBD by Silver-Impregnated Paper Spray Mass Spectrometry

This chapter was published as:

Huang, S.; Claassen, F. W.; van Beek, T. A.; Chen, B.; Zeng, J.; Zuilhof, H.; Salentijn, G. IJ. Rapid distinction and semiquantitative analysis of THC and CBD by silver-impregnated paper spray mass spectrometry. *Analytical Chemistry* **2021**, 93, 3794-3802. <https://doi.org/10.1021/acs.analchem.0c04270>.



Abstract

The control over the amount of psychoactive Δ 9-tetrahydrocannabinol (Δ 9-THC) in commercial cannabidiol (CBD) products has to be strict. A fast and simple semiquantitative Ag(I)-impregnated paper spray mass spectrometric method for differentiating between Δ 9-THC and CBD, which shows no difference in standard single-stage or tandem MS, was established. Because of a different binding affinity to Ag(I) ions, quasi-molecular Ag(I) adducts [Δ 9-THC + Ag]⁺ and [CBD + Ag]⁺ at m/z 421 and 423 give different fragmentation patterns. The product ions at m/z 313 for Δ 9-THC and m/z 353 and 355 for CBD can be used to distinguish Δ 9-THC and CBD and to determine their ratio. Quantification of Δ 9-THC/CBD ratios in commercial CBD oils was accomplished with a low matrix effect ($-2.2 \pm 0.4\%$ for Δ 9-THC and $-2.0 \pm 0.3\%$ for CBD). After simple methanol extraction (recovery of $87.3 \pm 1.2\%$ for Δ 9-THC and $92.3 \pm 1.4\%$ for CBD), Ag(I)-impregnated paper spray analysis was employed to determine this ratio. A single run can be completed in a few minutes. This method was benchmarked against the UHPLC-UV method. Ag(I)-impregnated paper spray MS had the same working range (Δ 9-THC/CBD = 0.001–1) as UHPLC-UV analysis ($R^2 = 0.9896$ and $R^2 = 0.9998$, respectively), as well as comparable accuracy (-2.7% to 14%) and precision (RSD 1.7–11%). The method was further validated by the analysis of 10 commercial oils by Ag(I)-impregnated paper spray MS and UHPLC-UV analysis. Based on the determined relative concentration ratios of Δ 9-THC/CBD and the declared CBD concentration, 6 out of 10 CBD oils appear to contain more Δ 9-THC than the Dutch legal limit of 0.05%.

Introduction

Cannabis (*Cannabis sativa* L.) has been cultivated for medicinal, recreational, and industrial purposes since ancient times and remains a widely cultivated plant.¹ Among its identified cannabinoids, Δ^9 -tetrahydrocannabinol (THC) and cannabidiol (CBD), and their carboxylated forms, Δ^9 -tetrahydrocannabinolic acid (THCA) and cannabidiolic acid (CBDA), are the most sought after by people because of their psychoactive and therapeutic effects.² Δ^9 -THC is responsible for the psychoactive effects and has some potential analgesic, anti-emetic, anti-kinetotic, and appetite-stimulating properties.³ CBD is not psychoactive but exhibits similar beneficial effects as Δ^9 -THC.⁴ The absence of psychoactive effects and the abundance of anecdotal claims of the effectiveness of CBD across a wide variety of conditions in both mainstream and social media have created significant public interest in CBD products, typically as oils. Such interest has led to increased consumer availability. Generally, commercially available CBD oils mainly consist of CBD and carrier oil and may contain flavorings, terpenes, or other cannabinoids like CBDA or trace amounts of THCA and Δ^9 -THC.⁵ Incorrect or misleading labels for the cannabinoid content of CBD products and indiscriminate use of CBD may lead to various issues. The presence of Δ^9 -THC in commercial CBD oils can occur because of the fact that even CBD-rich varieties of Cannabis produce a small amount of Δ^9 -THC.⁶ Therefore, naturally derived CBD extracts may contain some Δ^9 -THC in the final products, and oil consumers could thus be taking Δ^9 -THC without knowing so. Additionally, if the Δ^9 -THC content of a CBD product exceeds the maximally allowed limit, this could lead to legal problems. Many nations stipulate a zero-tolerance policy or a maximum Δ^9 -THC level (0.05–1%) for CBD products.^{6,7}

As Δ^9 -THC and CBD are structural isomers (accurate molecular weight of 314.2246 Da), differentiating as well as quantifying Δ^9 -THC and CBD is challenging. Generally, gas chromatography (GC)- or liquid chromatography (LC)-based techniques are employed, and typically run times of 10–20 min are required to achieve baseline separation.⁸ Additionally, for GC-based techniques, the detection

of the acidic precursors THCA and CBDA (accurate molecular weight of 358.2144 Da) is not feasible without derivatization.⁹

Simple and rapid methods to screen Δ 9-THC and CBD have been developed, including electrochemical² and colorimetric^{10,11} approaches. However, these methods cannot differentiate cannabinolic acids (THCA and CBDA) from the respective cannabinol forms (Δ 9-THC and CBD)² or distinguish Δ 9-THC and CBD;¹¹ moreover, these methods cannot achieve quantitative results.¹⁰

Even with mass spectrometry (MS), it is difficult to differentiate between Δ 9-THC and CBD as they have the same mass and give identical collision-induced dissociation (CID) fragmentation patterns in positive ionization mode.¹² In negative mode, it has been reported that there may exist a unique Δ 9-THC MS/MS fragment (m/z 191) under specific conditions, which could allow the differentiation of these two compounds to some extent.¹³ However, in another report, this fragment — under different conditions — has also been demonstrated for CBD.¹⁴ Therefore, only relying on this fragment for distinguishing between the isomers and their quantification remains challenging.

To enhance MS performance and improve ionization efficiency, adduct formation with Ag(I) ions has been exploited in ion mobility spectrometry,¹⁵ electrospray ionization mass spectrometry (ESI-MS),¹⁶⁻¹⁸ secondary ion mass spectrometry,¹⁹ and matrix-assisted laser desorption ionization mass spectrometry.²⁰ Ag(I) coordinates strongly with alkenes and weakly with polar groups like hydroxyls. The presence of multiple isolated C=C bonds, especially 1,5-dienes, strongly increases complexation, which is used in the analysis of certain olefinic compounds.²¹⁻²³ However, to the best of our knowledge, Ag(I) adduct formation has been rarely applied to ambient ionization mass spectrometry (AIMS),²⁴ with the notable exception of improving the detection of olefins with desorption electrospray ionization (DESI)-MS.²⁵

Paper spray ionization mass spectrometry (PS-MS), first reported in 2010,²⁶ is an AIMS method, well known for its fast analysis at low cost of consumables.²⁷ In

PS-MS, analytes are ionized from a paper tip by application of a solvent and an electric field, and thus it is one of the many variants of electrospray ionization.²⁸ Importantly, paper can be readily modified to enhance PS-MS selectivity and sensitivity through surface modification or coating.²⁷⁻³⁰

In this work, we investigated the combination of Ag(I) ions and PS-MS for the rapid and selective analysis of Δ 9-THC and CBD, in particular for detecting low concentrations of Δ 9-THC in CBD oils. Based on the different complexations of Δ 9-THC (weak; single alkene C=C bond) and CBD (strong; 1,5-diene moiety) with Ag(I) ions,²¹ we hypothesized that the formed Δ 9-THC and CBD Ag(I) adducts will exhibit different stabilities. In turn, this could lead to different fragmentation patterns in tandem MS. If so, simple and fast differentiation of Δ 9-THC and CBD as well as semiquantitative analysis should be achievable. As hypothesized, the quasi-molecular Ag(I) adducts of Δ 9-THC [Δ 9-THC + Ag]⁺ and CBD [CBD + Ag]⁺ at m/z 421 and 423 give different product ions in tandem MS, at m/z 313 for Δ 9-THC and m/z 353 and 355 for CBD. These product ions were then used to distinguish between Δ 9-THC and CBD and to determine their ratio within a few minutes in commercial CBD oils.

Materials and Methods

Chemicals and Reagents. Acetonitrile, methanol, and *tert*-butyl methyl ether (MTBE; HPLC-grade) were purchased from Biosolve Chimie SARL (Dieuze, France). Formic acid (HPLC-grade) and silver nitrate (analytical grade) were purchased from Fisher Scientific (Loughborough, Leicestershire). Deionized water was obtained from a Milli-Q direct ultrapure water system (Millipore, USA). Δ 9-THC and CBD standards were obtained from Cannabis flowers and CBD oil, respectively. According to nuclear magnetic resonance (NMR), thin layer chromatography (TLC), and UHPLC-UV data (**Supporting Information (SI), Figures S1–S3**), their purity was > 98%. Chromatography paper was purchased from Hangzhou Special Paper Co., Ltd. (Hangzhou, China). Different brands of pure CBD oils were purchased from health shops (Wageningen, the Netherlands) or

ordered online. Information on all CBD oils is shown in the **SI, Table S1**. Ammonium acetate (analytical grade) was obtained from Merck (Darmstadt, Germany). Santonin (analytical grade) was purchased from Sigma (St. Louis, MO, USA).

Preparation of Paper Substrate. Chromatography paper was cut into isosceles triangles with a height of 10 mm and a base of 5 mm, employing a paper cutter made in-house. These paper tips were put in a bottle with methanol and washed for 30 min in an ultrasonic bath at room temperature. Afterward, methanol was decanted, and the bottle with tips was placed in a fume hood for 30 min at room temperature and then dried at 60 °C in a vacuum oven for 12 h. The resulting paper tips are referred to as *clean*.

Preparation of Ag(I)-Impregnated Paper Substrate. For the preparation of Ag(I)-impregnated tips, 60 mL of ultrapure water was added to 1.02 g silver nitrate in a 125 mL wide-mouth brown bottle, which was placed in an ultrasonic bath for 2 min to obtain a 0.10 mol·L⁻¹ AgNO₃ solution. *Clean* paper tips were immersed in the AgNO₃ solution, and after capping, the bottle was placed in an ultrasonic bath. After 15 min of sonication, water in the ultrasound bath was replaced because otherwise the temperature of water would become too high (should not be above *ca.* 40 °C), making the surface of the paper rough or even damaging the tips. After another 15 min, the AgNO₃ solution was decanted, and the bottle without a cap was heated in an oven at 100 °C for at least 1 h to evaporate most water. Finally, the tips were taken out of the bottle and dried in a vacuum oven at 60 °C for 12 h. Ag(I)-impregnated paper was put in tin foil and stored in a desiccator away from light. *Clean* paper tips were used for PS-MS, and the Ag(I)-impregnated paper tips were used for Ag(I)-impregnated paper spray MS (AgPS-MS).

Paper Spray Setup. The paper tip was positioned by an alligator clip, which was part of a modified DESI ion source (Prosolia, USA) equipped with a rotational and *x-y-z* positioner, and was directly connected to the HV supply of the ion

source. The front of the paper tip was pointing toward the MS inlet at 4–6 mm. A sample solution of 15 μL was added using an Eppendorf pipette (10–100 μL). After this, a voltage of 4 kV was applied. The paper spray ion source was connected to either a high-resolution MS or to a linear ion trap MS.

Linear Ion Trap Mass Spectrometer. A Thermo LXQ linear ion trap mass spectrometer (Thermo Fisher Scientific, San Jose, CA, USA) was used in positive mode, with a capillary voltage of 49 V, tube lens of 85 V, and a capillary temperature of 350 °C, unless indicated otherwise. All full-scan measurements were performed with a scan range of m/z 100.0–2000.0. For all MS^n fragmentation measurements, CID energy was determined as the energy at which the target product ions had the highest abundance while the precursor ion or ions had not yet disappeared completely. The isolation width was set to include all desired target precursor ions.

Quadrupole Orbitrap High-Resolution Mass Spectrometer. For accurate mass measurements, the paper spray device was coupled to a Q-Exactive quadrupole orbitrap high-resolution MS (Thermo Fischer Scientific). All measurements were performed in positive mode with a mass resolution of 140,000 fwhm and a maximum injection time of 100 ms. The capillary temperature was 350 °C, and the S-lens RF level was 47. All full-scan measurements were performed with a scan range of m/z 100.0–2000.0. For molecular formula confirmation of the main peaks in MS^1 and MS^2 spectra, full-scan and CID fragmentation scan modes were used, respectively. For the determination of the molecular formula of the main peaks in MS^3 and MS^4 spectra from the LXQ analysis, in-source fragmentation and CID fragmentation were combined to provide higher energies for further fragmentation. Thermo Scientific Xcalibur 2.2 software was used for data acquisition and processing. The intensity of ions with m/z values within ± 5 ppm of the theoretical m/z is shown in the extracted ion chromatogram (EIC).

Ag(I) Complexation (Argentation) Chromatography-Mass Spectrometry.

Following a previously described method,²¹ a strong cation exchange HPLC column (Nucleosil SA, 100 Å, 5 μ m, 2.1 \times 250 mm; Grace) was flushed with an aqueous 1% NH₄OAc solution at 0.50 mL \cdot min⁻¹ for 1 h, followed by distilled water for 1 h. An aqueous AgNO₃ solution (0.20 g \cdot mL⁻¹) was injected onto the column *via* an autosampler in 50 μ L aliquots at 1 min intervals; 20 min after the last injection, the column was washed with MeOH for 1 h. A 1220 Infinity II LC system (Agilent Technologies, Santa Clara, USA) was coupled to the LXQ MS. Separation of Δ 9-THC and CBD was achieved using the loaded Ag(I) column, with MeOH as the mobile phase, at a flow rate of 0.80 mL \cdot min⁻¹. The complexes of eluted compounds were directed into the LXQ MS and analyzed under full-scan or product ion scan mode. The LXQ settings were identical to those described for the PS-MS measurements except for the sheath gas flow rate of 15 (arbitrary units).

UHPLC-UV Analysis. A Zorbax Eclipse Plus C18 column (2.1 mm \times 50 mm, 1.8 μ m; Agilent Technologies, Santa Clara, CA, USA) was coupled to a 1290 Infinity ultra-high performance liquid chromatography (UHPLC) system (Agilent Technologies, Santa Clara, USA), with a diode array detector. The mobile phase consisted of 5 mM formic acid in both water (mobile phase A) and acetonitrile (mobile phase B), and the flow rate was 0.80 mL \cdot min⁻¹. Isocratic elution for 2 min with 25% B was followed by a gradient toward 100% B in 7 min. After being in this condition for 4 min, the system was returned to 25% B in 1 min and then re-equilibrated for 3 min at 25% B.³¹

Sample Preparation and Extraction. Stock solutions of Δ 9-THC and CBD were prepared in MeOH at 1.00 mg \cdot mL⁻¹. Samples for the determination of recovery, matrix effects, and calibration curves were constructed by spiking sunflower oil with Δ 9-THC or CBD stock solutions (see following sections). For extraction, 50.0 mg of spiked or blank oil was precisely weighed and 2.00 mL of MeOH was added. The extraction was performed by stirring samples with a magnetic stirring bar and a

magnetic stirrer (IKA Labortechnik, IKAMAG RCT basic, Germany) for 1, 5, 10, 20, or 30 min. Afterward, 1.00 mL of the supernatant of each extracted sample was collected for analysis. Commercial CBD oil samples were diluted with sunflower oil to 0.2% (w/w%) CBD in oil based on the labeled concentration. A magnetic stirring bar was used to stir the oil vigorously for 1 min. A 50.0 mg of the diluted CBD oil was precisely weighed for the following analysis. A 2.00 mL of MeOH was added to 50.0 mg of the diluted CBD oil for extraction. The extraction procedure was performed in triplicate by stirring these samples with a magnetic stirring bar for 1 min. A volume of 1.00 mL of the supernatant of each extracted sample was taken for further MS or UHPLC analysis.

Determination of Recovery and Matrix Effects. Extraction recovery and matrix effects were determined according to the procedure by Gottardo *et al.*,³² with minor modifications, as described below (see also **SI, Table S2**).

Sunflower oil samples containing 0.20% Δ^9 -THC (Δ^9 -THC/oil, w/w%) and 0.20% CBD (CBD/oil, w/w%) were extracted with MeOH for 1, 5, 10, 20, and 30 min (sample type III, $n = 3$), whereas, for comparison, analogous extractions of the blank matrix (sunflower oil) were performed. These blank matrix extracts were then spiked with the same amount of Δ^9 -THC and CBD per mL of methanol (sample type II, $n = 3$). The final methanolic solutions were analyzed by the UHPLC-UV method, and the recovery was calculated as the ratio of the averaged peak areas from set III to set II, expressed as a percentage (recovery (%) = $\text{III/II} \times 100$) for both Δ^9 -THC and CBD.

For the matrix effect measurements, the same amounts of Δ^9 -THC and CBD were spiked in the blank matrix extract (sample type II, $n = 3$) or pure MeOH (sample type I, $n = 3$). These methanolic solutions were analyzed by AgPS-MS. The EIC was normalized to the total ion chromatogram (TIC) to correct for the spray instability and irreproducibility (EIC/TIC). The matrix effect was calculated as the ratio of the Δ^9 -THC MS² characteristic signal (m/z 313) from set II to set I, subtracted by 1, and expressed as a percentage (matrix effect (%) = $(\text{II/I} - 1) \times 100$). The matrix effect of

CBD (m/z 353 + 355) was measured and calculated with the same methods as that for Δ 9-THC. A negative matrix effect percentage represents signal suppression and a positive percentage represents signal enhancement.

Calibration Curve Construction and Evaluation of Accuracy, Precision, LOD, and LOQ. Δ 9-THC and CBD stock solutions were used to prepare oil samples with different Δ 9-THC/CBD ratios (0.001, 0.002, 0.005, 0.01, 0.02, 0.05, 0.1, 0.2, 0.5, and 1; $n = 3$ per ratio), keeping the CBD content constant at 0.20% (CBD/oil, w/w%). To achieve this, appropriate volumes of methanolic stock solutions were mixed and dried under nitrogen and then reconstituted in 50.0 mg sunflower oil. These samples were extracted as described above, and the methanolic extract was analyzed with UHPLC-UV and AgPS-MS methods. The peak area ratios of Δ 9-THC/CBD at 215 nm or the characteristic MS² EIC area ratios of Δ 9-THC/CBD were plotted against the concentration ratios of Δ 9-THC/CBD for constructing the calibration curves for UHPLC-UV detection and AgPS-MS, respectively.

The accuracy and precision of the method were evaluated at three Δ 9-THC/CBD ratios (low (0.004), medium (0.07), and high (0.3) in sunflower oil, $n = 3$ per ratio). The preparation of these three samples was identical to the preparation of calibration curve samples. Precision was calculated as the relative standard deviation (RSD%) ($n = 3$). Accuracy was calculated as the relative deviation (%) of the calculated mean value from the respective reference value.

Santonin with an accurate molecular weight of 246.1256 Da was used as the internal standard for the determination of the absolute LOD and LOQ of the AgPS-MS method for Δ 9-THC. The characteristic MS² peaks are m/z 309 and 311 from their precursor ions, m/z 353 and 355, when analyzed by AgPS-MS. A 100.0 μ L of 300.0 μ g·mL⁻¹ santonin in MeOH was mixed with 0.0, 1.0, 2.5, 5.0, 10.0, 25, 50, or 100 μ L of a 200.0 μ g·mL⁻¹ Δ 9-THC solution in MeOH, and MeOH was added to 1.00 mL to prepare 0.0, 0.2, 0.5, 1.0, 2.0, 5.0, 10.0, or 20.0 μ g·mL⁻¹ Δ 9-THC solutions, with 30 μ g·mL⁻¹ santonin ($n = 3$ per concentration). The samples were analyzed by AgPS-MS under the same conditions as those used for the Δ 9-THC/CBD

ratio analysis. The characteristic MS² fragment EIC area ratios of Δ 9-THC (m/z 313) to santonin (m/z 309) were plotted against the concentrations of Δ 9-THC for constructing a curve. LOD and LOQ were calculated as follows: LOD = 3 \times SD of blank/slope of the curve; LOQ = 10 \times SD of blank/slope of the curve.

Quantum Chemical Computations. Calculations of the binding energies of Δ 9-THC and CBD toward Ag(I) were performed with the Gaussian16 suite of programs, with the B3LYP and wB97XD functionals as implemented in there; a 6-311+G(d,p) basis set was used throughout. The electrostatic potential map was generated using Gaussview 6.

Results and Discussion

Δ 9-THC and CBD are isomers with an accurate molecular weight of 314.2246 Da. It is difficult to distinguish between these two species by AIMS,^{31,33,34} including MS/MS analysis, as both compounds fragment into product ions with the same mass. When analyzed by PS-MS in (+) mode and setting m/z 315 as the precursor ion with an isolation width of 1.5, Δ 9-THC (**Figure 3.1A**) and CBD (**Figure 3.1B**) indeed yield the same MS² spectrum with the main fragments of m/z 193 and m/z 259, making differentiation impossible.

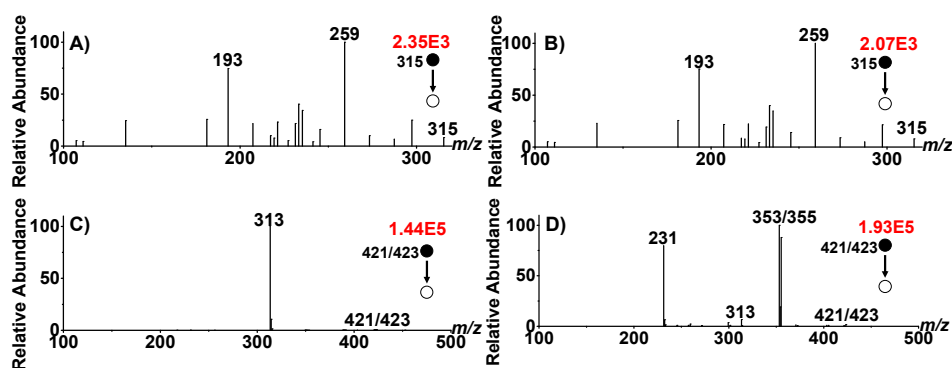


Figure 3.1. PS-MS² spectrum of A) Δ 9-THC, B) PS-MS² spectrum of CBD; AgPS-MS² spectrum of C) Δ 9-THC, and D) AgPS-MS² spectrum of CBD.

In order to effectively combine the advantages of AIMS and the potential of

Ag(I) ions to bind differently to different olefinic compounds, Ag(I) was combined with PS-MS by using an Ag(I)-impregnated paper. Quasi-molecular species at m/z 421 and 423 were observed for both Δ 9-THC and CBD because of the existence of two silver isotopes, ^{107}Ag (52%) and ^{109}Ag (48%). By setting m/z 422 as the precursor ion and using an isolation width of 4 (thus including both m/z 421 and 423), different fragmentation patterns for Δ 9-THC (**Figure 3.1C**) and CBD (**Figure 3.1D**) were observed. Specifically, there was only one product ion at m/z 313 for Δ 9-THC, and for CBD, the most pronounced fragments appeared at m/z 353 and 355, which is the same fragment, with the mass difference because of two silver isotopes. The accurate masses and molecular formulas of the characteristic peaks for both Δ 9-THC and CBD Ag(I) adducts, as well as their fragments, were determined with MS/HRMS (**Figure 3.2**). After CID, $[\Delta\text{9-THC} + \text{Ag}]^+$ loses its Ag(I) during the MS² stage, whereas the majority of $[\text{CBD} + \text{Ag}]^+$ retains Ag(I) until the MS³ stage (**SI, Figure S4**). This finding suggests — as hypothesized — that Ag(I) binds more strongly to CBD than to Δ 9-THC and that this indeed leads to substantial differences in CID patterns.

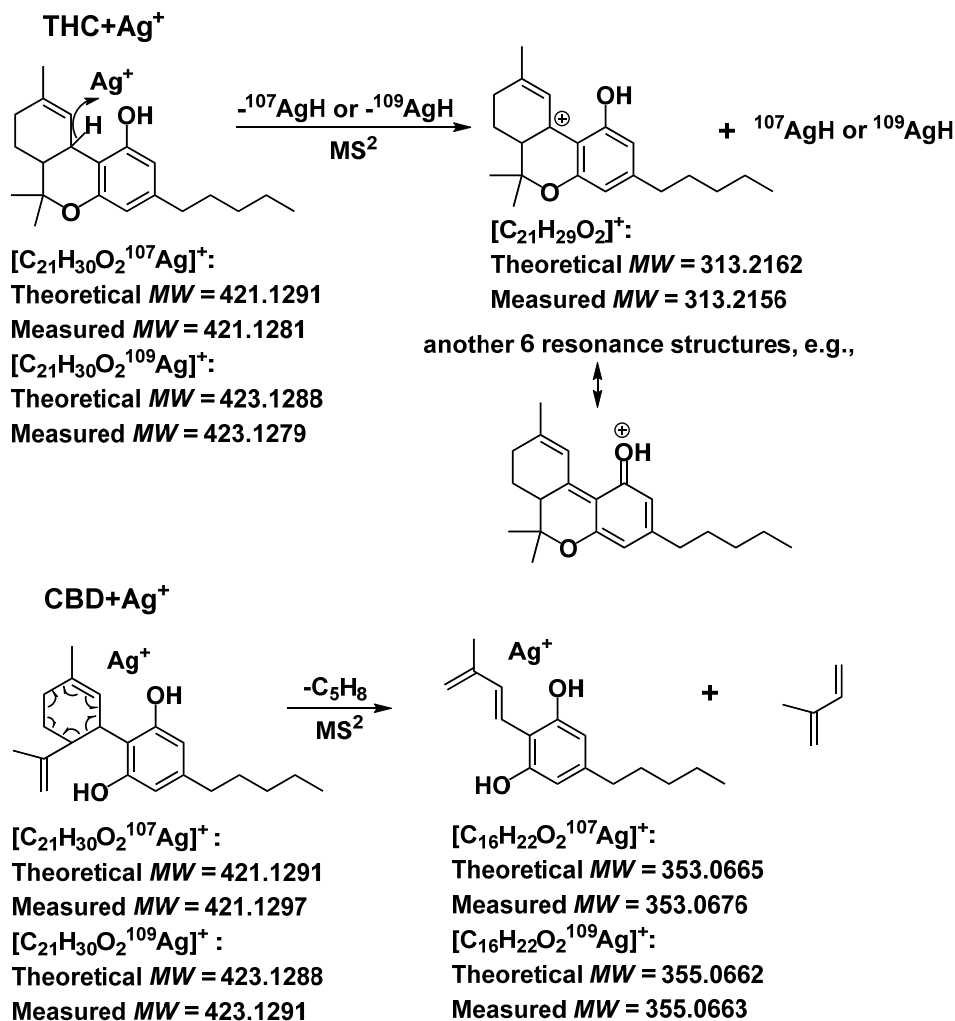


Figure 3.2. Proposed mechanism for MS² fragmentation of Δ⁹-THC and CBD in the presence of Ag(I).

This hypothesis was further substantiated by argentation HPLC-MS/MS results (SI, **Figure S5**). CBD [capacity factor (*k'*) = 11.2] eluted much later than Δ⁹-THC (*k'* = 0.2), which means that CBD has a much stronger retention than Δ⁹-THC on the Ag(I) column. Moreover, by quantum chemical wB97XD/6-311+G(d,p) simulations, the CBD + Ag(I) complex was found to be ~12 kcal·mol⁻¹ more stable than the Δ⁹-THC + Ag(I) complex (SI, **Figure S6**), which means that a higher

energy is required for the CBD + Ag(I) complex to lose its Ag(I) compared to the Δ 9-THC + Ag(I) complex.

Based on the above findings, a mechanism for the MS fragmentation of Δ 9-THC and CBD in the presence of Ag(I) was proposed. As shown in **Figure 3.2**, the $[\Delta$ 9-THC + Ag]⁺ adducts lose AgH during the MS² stage, but the majority of [CBD + Ag]⁺ adducts lose C₅H₈ during the MS² stage, most likely the neutral loss of 2-methyl-1,3-butadiene. The Ag(I) ion of [CBD + Ag]⁺ adducts is lost from CBD as AgCH₃ during the MS³ stage (**SI, Figure S4**). This difference reflects the much stronger binding of Ag(I) to CBD than to Δ 9-THC, which is attributed to the 1,5-diene system of CBD.²¹⁻²³ The loss of the Ag(I) ion during the MS³ stage can be explained too because in the *m/z* 353/355 CBD fragment, Ag(I) complexes with a 1,3-diene system. This complexation is weaker than that with the 1,5-diene system in the quasi-molecular ion (*m/z* 421 and *m/z* 423) of CBD.²¹ In the case of the $[\Delta$ 9-THC + Ag]⁺ adduct, because of the oxygen-*gem*-dimethyl carbon bond in Δ 9-THC, methyl-butadiene cannot be split off, and the loss of the only weakly bound Ag(I) is to be expected. The neutral loss of either AgH or AgCH₃ is supported by the literature.^{35,36}

AgPS-MS/MS can clearly be employed to distinguish Δ 9-THC from CBD. However, in the MS² spectrum of CBD (**Figure 3.1D**), there is also a minor peak at *m/z* 313, which equals the mass of the characteristic MS² fragment of Δ 9-THC. This finding complicates the determination of the Δ 9-THC/CBD ratio. If this *m/z* 313 fragment would originate from a CBD-to- Δ 9-THC conversion, and would therefore be variable, this would preclude an accurate determination of the Δ 9-THC/CBD ratio. However, if it is a product ion directly originating from the fragmentation of CBD, its intensity can potentially be corrected for.

To elucidate whether the *m/z* 313 fragment in the CBD spectrum originated from CBD or Δ 9-THC, further fragmentation analysis was carried out for Δ 9-THC and CBD. The Δ 9-THC *m/z* 313 fragment yielded the main fragment at *m/z* 217 with some other minor fragments during the MS³ stage (**SI, Figure S7**). For CBD, the fragmentation of *m/z* 313 yielded a similar MS³ spectrum in which the peak at *m/z*

243 reproducibly had double relative intensity compared to the Δ^9 -THC spectrum. For the fragments from m/z 313 of Δ^9 -THC, m/z 243 and m/z 245 had equal abundance. For the fragments from m/z 313 of CBD, the abundance of m/z 243 almost doubled that of m/z 245. This suggests that the fragment of m/z 313 in the CBD MS³ spectrum is structurally different from the m/z 313 fragment in the Δ^9 -THC MS³ spectrum.

To further exclude the possibility of conversion from CBD to Δ^9 -THC, the peak area ratio of m/z 313/(353 + 355) was measured for pure CBD under different MS parameters ($n = 3$ per parameter), namely various source temperatures, CID energies, and CBD concentrations, as well as on two different mass spectrometers. The ratio was always constant within 2.7–3.0%, regardless of the parameter changes (SI, Figure S8), strongly suggesting that the fragment at m/z 313 in the MS² CBD spectrum is a genuine fragment of CBD, and not due to *in situ* conversion to Δ^9 -THC, as that would have likely led to a change in the m/z 313/(353 + 355) ratio with a change in any of these parameters. Taking all the above into consideration, we argue that the m/z 313 signal in the CBD AgPS-MS² spectrum is derived from CBD itself and not from Δ^9 -THC.

When keeping all equipment parameters unchanged, the EIC area ratio of m/z 313 to (m/z 353 + m/z 355) in the CBD MS² spectrum is constant (0.028 ± 0.001) for a range of CBD concentrations (0.5 – $1000 \mu\text{g}\cdot\text{mL}^{-1}$). As a result, the m/z 313 signal resulting from the CBD spectrum can, in the MS data from samples, be subtracted as the background value. Quantitative analysis of the Δ^9 -THC/CBD ratio in samples can thus be achieved by measuring in the MS² spectra the EIC area ratio of m/z 313 to (m/z 353 + m/z 355) and then subtracting the background value of 0.028 ± 0.001 from pure CBD.

An important consideration for the cannabinoid analysis is that cannabinoids from plants are effectively in a “prodrug” form, existing as cannabinolic acids that must be decarboxylated to their respective cannabinol form to have pharmacological effects.² This decarboxylation, for example, occurs while smoking; however, upon oral consumption, no CBDA or THCA present is converted to CBD or Δ^9 -THC by enzymatic or other processes.^{37,38} If the production and processing of CBD oils does

not remove all THCA and CBDA, some THCA and CBDA might still be present in the final CBD oil products. To evaluate whether THCA and CBDA would decarboxylate to their respective cannabinol forms during the AgPS-MS analysis and would thus interfere with the quantification of the Δ 9-THC/CBD ratio, standard solutions of THCA and CBDA were analyzed with AgPS-MS (**SI, Figure S9**), UHPLC-UV (**SI, Figure S10**), and HRMS (**SI, Figures S11 and 12**). Both THCA and CBDA formed quasi-molecular ions (Ag(I) adducts) at m/z 465 and 467, and no fragments at m/z 421 and 423 can be observed. Therefore, any CBDA or THCA present does not interfere with the analysis of Δ 9-THC and CBD when choosing m/z 421/423 as the precursor ions for fragmentation to obtain the characteristic MS² fragments of Δ 9-THC and CBD.

Recovery and Matrix Effect. To apply the findings in the practical analysis of Δ 9-THC and CBD in CBD oil samples, an analytical method consisting of an easy sample pretreatment step and a fast AgPS-MS procedure was developed. To determine the recovery and matrix effect, sunflower oil was selected as the matrix for Δ 9-THC and CBD because of the similar fatty acid composition³⁹ as hempseed oil (the main constituent of commercial CBD oil). Additionally, Δ 9-THC and CBD do not occur in sunflower oil.

The recovery was calculated by comparing the extract of a spiked sample to the extract of a blank matrix sample that was spiked with the same amount after extraction. In both cases, the co-extracted matrix compounds will be the same in the extract, and the only difference is caused by the recovery of the analytes. These samples were analyzed by the UHPLC-UV method, and the extraction recovery was calculated as the ratio of the average UHPLC chromatogram Δ 9-THC or CBD peak areas from extracted samples and non-extracted samples, and expressed as a percentage (**Figure 3.3 A**). Different extraction times have a limited effect on the recovery of both Δ 9-THC (86.7–90.0%) and CBD (92.3–95.6%). The slightly lower recovery of Δ 9-THC can be explained by the fact that Δ 9-THC is less polar than CBD and more likely to remain in the non-polar sunflower oil.

The matrix effect was assessed by comparing spiked methanol with a spiked matrix extract. In both solutions, Δ^9 -THC and CBD do not undergo any extraction step, that is, the recovery is 100%. However, pure MeOH does not contain extracted matrix compounds, whereas the blank matrix sample does. Matrix compounds might interfere with the analysis through ion suppression. The calculated ME for AgPS-MS from sunflower oil is shown in **Figure 3.3B** for various extraction times (-2.2% to -4.8% for Δ^9 -THC and -2.0% to -3.2% for CBD). Both Δ^9 -THC and CBD suffer the least from ion suppression when the extraction time is 1 min ($-2.2 \pm 0.4\%$ for Δ^9 -THC and $-2.0 \pm 0.3\%$ for CBD), and the ion suppression becomes more pronounced when extending the extraction time (**Figure 3.3B**). However, in view of the tolerant limit for matrix effects ($\pm 25\%$),⁴⁰ longer extraction times would also be possible if desired.

To correct for the extraction efficiency and matrix effects in the quantification, a matrix-based calibration curve was constructed. As extraction for 1 min resulted in acceptable recoveries for Δ^9 -THC and CBD ($87.3 \pm 1.2\%$ for Δ^9 -THC and $92.3 \pm 1.4\%$ for CBD), and minimal matrix effects ($-2.2 \pm 0.4\%$ for Δ^9 -THC, $-2.0 \pm 0.3\%$ for CBD) as well as high time efficiencies, the 1 min extraction time was used in all subsequent experiments.

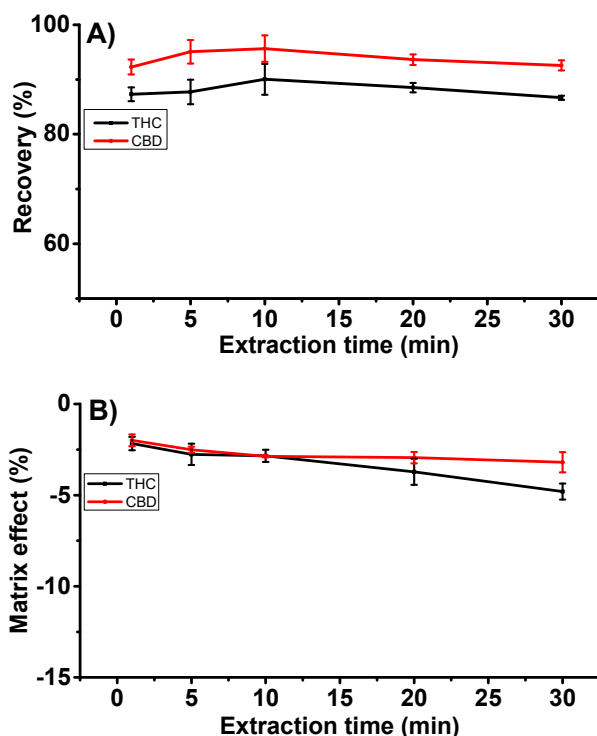


Figure 3.3. A) Recovery and B) matrix effect for Δ^9 -THC and CBD analysis after extraction versus the extraction times. Error bars represent standard deviation ($n = 3$).

Calibration Curve, Precision, and Accuracy. An AgPS-MS calibration curve was constructed relating the characteristic MS² EIC area ratio of Δ^9 -THC/CBD to the concentration ratio of Δ^9 -THC/CBD in samples (SI, **Figure S13A**). The y -intercept of this curve is 0.0280, which means that when the sample does not contain Δ^9 -THC, the characteristic signal ratio of Δ^9 -THC to CBD is 0.0280, consistent with the formation of the minor fragment at m/z 313 purely by CBD. For comparison, a UHPLC-UV curve was established associating the characteristic peak area ratio of Δ^9 -THC/CBD with the concentration ratio of Δ^9 -THC/CBD in samples. There is good linearity ($R^2 = 0.9896$) of the AgPS-MS signal intensity over the full working range of Δ^9 -THC/CBD ratios from 0.001 to 1 (SI, **Figure S13**). Even though the UHPLC-UV curve has a better linearity ($R^2 = 0.9998$), each run takes 17 min, which is much longer than that of an AgPS-MS experiment (< 30 s).

Accuracy and precision of the methods were evaluated at three $\Delta 9$ -THC/CBD ratios of 0.004, 0.07, and 0.3 (low, medium, and high levels) in spiked sunflower oil samples and are shown in **Table 3.1**. The AgPS-MS method has comparable analytical performance as the UHPLC-UV method, with accuracy and precision for medium and high concentrations as well as acceptable accuracy and precision at low $\Delta 9$ -THC concentrations.

Table 3.1. Precision (% RSD) and accuracy (% deviation from true value) of spiked sunflower oil samples.

Spiked $\Delta 9$ -THC:CBD ratio in samples	Spiked absolute $\Delta 9$ -THC in samples ($\mu\text{g}\cdot\text{mL}^{-1}$)	Spiked absolute CBD in samples ($\mu\text{g}\cdot\text{mL}^{-1}$)	UHPLC-UV result		AgPS-MS result	
			Precision ($n = 3$)	Accuracy	Precision ($n = 3$)	Accuracy
Low (0.004)	0.200	50.0	2.3	8.3	11	14
Medium (0.07)	3.50	50.0	2.8	4.3	7.2	-0.1
High (0.3)	15.0	50.0	1.2	1.3	1.7	-2.7

The LOD and LOQ of the AgPS-MS method to determine $\Delta 9$ -THC were determined at 6 and 20 $\text{ng}\cdot\text{mL}^{-1}$, respectively. As the intensities in PS-MS are not very reproducible and quantification almost always relies on the use of an internal standard, santonin was used as the internal standard for $\Delta 9$ -THC. The [santonin + Ag]⁺ adduct (m/z 353 and 355) produces characteristic MS² fragments at m/z 309 and 311, which can be differentiated from the characteristic MS² fragment of the [$\Delta 9$ -THC + Ag]⁺ adduct at m/z 313 and thus used as the internal standard.

Application to Commercial CBD Oil Samples. Ten commercial samples were analyzed with the AgPS-MS and UHPLC-UV methods as benchmarks for their $\Delta 9$ -THC/CBD ratios (**Figure 3.4A**). Sunflower oil was used for the dilution of CBD samples to 0.20% CBD. Because of the similar triacylglycerol composition as hemp oil, any matrix effects will be similar. The additional advantages of using sunflower oil for dilution instead of organic solvents are its availability, lack of toxicity, low

cost, and environmental friendliness. Moreover, by assuming that the absolute CBD concentration as provided by the supplier is correct and taking the dilution factors into consideration, the absolute Δ 9-THC concentrations in these CBD oil products can be calculated. Although these do not provide direct absolute quantitative data, these estimates can serve as a screening tool to identify suspect samples that require further investigation to determine their compliance with legal standards. The clear advantage of this screening method is that it requires no addition of internal standards to the sample because of the use of the ratio between Δ 9-THC and CBD.

According to the results, in CBD oil_2, based on the detected ratio of Δ 9-THC/CBD by AgPS-MS, the calculated absolute Δ 9-THC concentration is $0.0226 \pm 0.0010\%$, which is almost identical with the UHPLC-UV result of $0.0236 \pm 0.0020\%$. For CBD oil_6 and CBD oil_8, AgPS-MS is unable to detect the presence of Δ 9-THC because of their very low Δ 9-THC content, which was confirmed by the UHPLC-UV analysis result. For oils with an even lower Δ 9-THC content, like CBD oil_1, no Δ 9-THC signal was detected by either the UHPLC-UV or AgPS-MS method. Both methods revealed that CBD oils 3, 4, 5, 9, and 10 contained a relatively high Δ 9-THC content and are actually over the Dutch legal limit of 0.05% if the declared CBD content is correct. In other words, if the actual CBD concentration is much lower than the declared value, the calculated Δ 9-THC concentration may be within the legal limit, but then the CBD content on the label is incorrect. In either case, it warrants further investigation by, for example, UHPLC-UV analysis. For CBD oil_7, further analysis would be needed because the predicted result is around the legal limit, that is, $0.0571 \pm 0.0126\%$ Δ 9-THC based on AgPS-MS and $0.0418 \pm 0.0008\%$ based on UHPLC-UV detection.

In short, the developed method can quickly screen for the presence of Δ 9-THC in CBD oil by measuring the ratio of Δ 9-THC/CBD and determine whether the Δ 9-THC content is below the legal limit based on the declared CBD content. Although from the perspective of linearity, RSD, and accuracy, the UHPLC-UV methodology has a better performance, AgPS-MS greatly shortens the analysis time (from 17 min to less than 30 s). Apart from this, AgPS-MS analysis does not require any mobile

phase, as only 15 μL of MeOH is needed for spraying, making it more environmentally friendly and cheaper. Moreover, for relative quantification analysis, that is, the determination of the $\Delta^9\text{-THC/CBD}$ ratio, the developed method does not require the use of deuterated standards, which are difficult to obtain and are expensive.

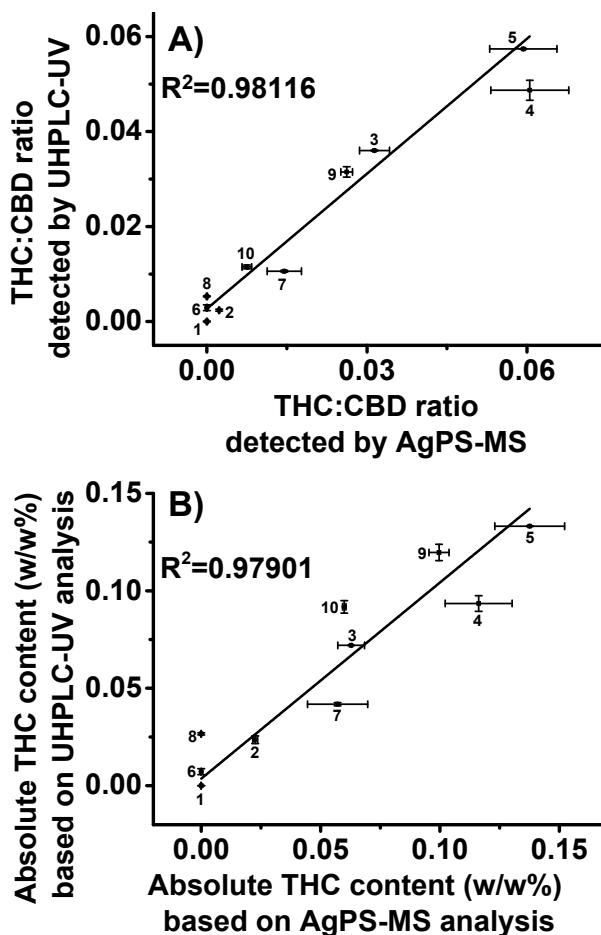


Figure 3.4. A) $\Delta^9\text{-THC/CBD}$ ratio detected by AgPS-MS versus UHPLC-UV; B) absolute $\Delta^9\text{-THC}$ content based on AgPS-MS versus UHPLC-UV. Error bars represent standard deviation ($n = 3$).

Conclusions

Ag(I)-impregnated paper spray tandem MS allows for a fast distinction of $\Delta^9\text{-THC}$ and CBD, as well as for a reliable quantitative analysis of their concentration

ratio. The method is based on a different complexation of Δ 9-THC and CBD with Ag(I) ions, leading in turn to different mass spectrometric fragmentation pathways. Samples with a wide range of Δ 9-THC/CBD ratios (Δ 9-THC/CBD = 0.001–1) can be analyzed by the developed method within tens of seconds, requiring only minimal amounts of solvent. The good correspondence between the UHPLC-UV and AgPS-MS data of commercial CBD oils confirms the applicability of the method. Thus, it could be used for quality control of CBD oils. Another application area for this screening method could be the legal control of Δ 9-THC-poor hemp varieties for fiber production. Positive samples can then be retested in the lab by a validated quantitative method, such as UHPLC-UV.

Supporting Information

The supporting information is available free of charge at <https://pubs.acs.org/doi/10.1021/acs.analchem.0c04270>, and the table of contents is presented below.

Supporting Information Table of Contents

Figure S1	¹ H NMR spectra of CBD and Δ 9-THC	Page S3
Figure S2	TLC of Δ 9-THC and CBD	Page S4
Figure S3	UHPLC-UV profiles of CBD and CBD, Δ 9-THC mixture	Page S5
Table S1	Information on purchased CBD oils	Page S6
Table S2	The preparation of sample sets I, II and III	Page S7
Figure S4	Exact masses of fragments and proposed mechanism for MS fragmentation of Δ 9-THC and CBD in the presence of Ag(I)	Page S8
Figure S5	Argentation HPLC-MS profiles of Δ 9-THC and CBD	Page S9
Figure S6	Computational structures of Δ 9-THC + Ag(I) and CBD + Ag(I)	Page S10
Figure S7	AgPS-MS ³ spectrum of Δ 9-THC and CBD	Page S10
Figure S8	EIC area ratio of m/z 313:(353 + 355) in CBD AgPS-MS ² spectrum under different capillary temperatures, different CID energies, and different CBD concentrations	Page S11
Figure S9	AgPS-MS of THCA and CBDA	Page S12

Figure S10	UHPLC-UV profiles of THCA and CBDA	Page S13
Figure S11	Blank PS-MS and MS ² (Q-Exactive) of THCA	Page S14
Figure S12	Blank PS-MS and MS ² (Q-Exactive) of CBDA	Page S15
Figure S13	Calibration curve of THC:CBD ratio constructed by AgPS-MS and UHPLC-UV	Page S16
Table S3	Commercial CBD oils analyzed by AgPS-MS and UHPLC-UV	Page S17
References		Page S18

Acknowledgments

The authors thank Prof. Michel Nielen (Wageningen Food Safety Research) for helpful discussions and acknowledge support from the National Natural Science Foundation of China (21775040, 21775041, and 21575040), the China Scholarship Council 2020 International Cooperation Training Program for Innovative Talents, the Aid Program for S&T innovation research team in higher education institutions, the construction program of key disciplines of Hunan Province (2015JC1001), the project of Hunan Provincial Department of Education (17C0947), and the Hunan Province 100 experts project.

References

- (1) Chandra, S.; Radwan, M. M.; Majumdar, C. G.; Church, J. C.; Freeman, T. P.; ElSohly, M. A. New trends in Cannabis potency in USA and Europe during the last decade (2008–2017). *European Archives of Psychiatry and Clinical Neuroscience* **2019**, *269*, 5–15.
- (2) Comeau, Z. J.; Boileau, N. T.; Lee, T.; Melville, O. A.; Rice, N. A.; Troung, Y.; Harris, C. S.; Lessard, B. H.; Shuhendler, A. J. On-the-spot detection and speciation of cannabinoids using organic thin-film transistors. *ACS Sensors* **2019**, *4*, 2706–2715.
- (3) Pertwee, R. The diverse CB₁ and CB₂ receptor pharmacology of three plant cannabinoids: Δ 9-tetrahydrocannabinol, cannabidiol and Δ 9-tetrahydrocannabivarin. *British Journal of Pharmacology* **2008**, *153*, 199–215.
- (4) Pertwee, R. G. Emerging strategies for exploiting cannabinoid receptor agonists as medicines. *British Journal of Pharmacology* **2009**, *156*, 397–411.
- (5) Marinotti, O.; Sarill, M. Differentiating full-spectrum hemp extracts from CBD isolates: implications for policy, safety and science. *Journal of Dietary Supplements* **2020**, *17*, 517–526.
- (6) Hazekamp, A. The trouble with CBD oil. *Medical Cannabis and Cannabinoids* **2018**, *1*, 65–72.
- (7) Manthey, J. Cannabis use in Europe: current trends and public health concerns. *International Journal of Drug Policy* **2019**, *68*, 93–96.
- (8) Borges, G. R.; Birk, L.; Scheid, C.; Morés, L.; Carasek, E.; Kitamura, R. O. S.; Roveri, F. L.; Eller, S.; de Oliveira Merib, J.; de Oliveira, T. F. Simple and straightforward analysis of cannabinoids in medicinal products by fast-GC-FID. *Forensic Toxicology* **2020**, *38*, 531–535.
- (9) Zivovinic, S.; Alder, R.; Allenspach, M. D.; Steuer, C. Determination of cannabinoids in *Cannabis sativa* L. samples for recreational, medical, and forensic purposes by reversed-phase liquid chromatography-ultraviolet detection. *Journal of Analytical Science and Technology* **2018**, *9*, 1–10.
- (10) Hädener, M.; Gelmi, T. J.; Martin-Fabritius, M.; Weinmann, W.; Pfäffli, M. Cannabinoid concentrations in confiscated Cannabis samples and in whole blood and urine after smoking CBD-rich Cannabis as a “tobacco substitute”. *International Journal of Legal Medicine* **2019**, *133*, 821–832.
- (11) Amjadi, M.; Sodouri, T. A surface plasmon resonance-based method for detection and determination of cannabinoids using silver nanoparticles. *Journal of Applied Spectroscopy* **2014**, *81*, 232–237.
- (12) Kauppila, T. J.; Flink, A.; Laakkonen, U. M.; Aalberg, L.; Ketola, R. A. Direct analysis of Cannabis samples by desorption atmospheric pressure photoionization-mass spectrometry. *Drug Testing and Analysis* **2013**, *5*, 186–190.
- (13) Ifa, D. R.; Manicke, N. E.; Dill, A. L.; Cooks, R. G. Latent fingerprint chemical imaging by mass spectrometry. *Science* **2008**, *321*, 805–805.
- (14) Berman, P.; Futoran, K.; Lewitus, G. M.; Mukha, D.; Benami, M.; Shlomi, T.; Meiri, D. A new ESI-LC/MS approach for comprehensive metabolic profiling of phytocannabinoids in Cannabis. *Scientific Reports* **2018**, *8*, 14280.
- (15) Hädener, M.; Kamrath, M. Z.; Weinmann, W.; Groessl, M. High-resolution ion mobility spectrometry for rapid Cannabis potency testing. *Analytical Chemistry* **2018**, *90*, 8764–8768.
- (16) Grossert, J. S.; Herrera, L. C.; Ramaley, L.; Melanson, J. E. Studying the chemistry of cationized triacylglycerols using electrospray ionization mass spectrometry and density functional theory computations. *Journal of The American Society for Mass Spectrometry* **2014**, *25*, 1421–1440.
- (17) Lévêque, N. L.; Héron, S.; Tchaplal, A. Regioisomer characterization of triacylglycerols by non-aqueous reversed-phase liquid chromatography/electrospray ionization mass spectrometry using silver nitrate as a postcolumn reagent. *Journal of Mass Spectrometry* **2010**, *45*, 284–296.
- (18) Acheampong, A.; Leveque, N.; Tchaplal, A.; Heron, S. Simple complementary liquid chromatography and mass spectrometry approaches for the characterization of

- triacylglycerols in *Pinus koraiensis* seed oil. *Journal of Chromatography A* **2011**, *1218*, 5087-5100.
- (19) Grade, H.; Winograd, N.; Cooks, R. Cationization of organic molecules in secondary ion mass spectrometry. *Journal of the American Chemical Society* **1977**, *99*, 7725-7726.
- (20) Cohen, L. H.; Gusev, A. I. Small molecule analysis by MALDI mass spectrometry. *Analytical and Bioanalytical Chemistry* **2002**, *373*, 571-586.
- (21) van Beek, T. A.; Subrtova, D. Factors involved in the high pressure liquid chromatographic separation of alkenes by means of argentation chromatography on ion exchangers: overview of theory and new practical developments. *Phytochemical Analysis* **1995**, *6*, 1-19.
- (22) Kaneti, J.; de Smet, L. C.; Boom, R.; Zuilhof, H.; Sudhölter, E. J. Computational probes into the basis of silver ion chromatography. II. silver(I)-olefin complexes. *The Journal of Physical Chemistry A* **2002**, *106*, 11197-11204.
- (23) Damyanova, B.; Momtchilova, S.; Bakalova, S.; Zuilhof, H.; Christie, W. W.; Kaneti, J. Computational probes into the conceptual basis of silver ion chromatography: I. silver(I) ion complexes of unsaturated fatty acids and esters. *Journal of Molecular Structure: THEOCHEM* **2002**, *589*, 239-249.
- (24) Feider, C. L.; Krieger, A.; DeHoog, R. J.; Eberlin, L. S. Ambient ionization mass spectrometry: recent developments and applications. *Analytical Chemistry* **2019**, *91*, 4266-4290.
- (25) Jackson, A. U.; Shum, T.; Sokol, E.; Dill, A.; Cooks, R. G. Enhanced detection of olefins using ambient ionization mass spectrometry: Ag⁺ adducts of biologically relevant alkenes. *Analytical and Bioanalytical Chemistry* **2011**, *399*, 367-376.
- (26) Wang, H.; Liu, J.; Cooks, R. G.; Ouyang, Z. Paper spray for direct analysis of complex mixtures using mass spectrometry. *Angewandte Chemie International Edition* **2010**, *122*, 889-892.
- (27) Liu, J.; Wang, H.; Manicke, N. E.; Lin, J.-M.; Cooks, R. G.; Ouyang, Z. Development, characterization, and application of paper spray ionization. *Analytical Chemistry* **2010**, *82*, 2463-2471.
- (28) Basuri, P.; Baidya, A.; Pradeep, T. Sub-parts-per-trillion level detection of analytes by superhydrophobic preconcentration paper spray ionization mass spectrometry (SHPPSI MS). *Analytical chemistry* **2019**, *91*, 7118-7124.
- (29) Bambauer, T. P.; Maurer, H. H.; Weber, A. A.; Hannig, M.; Pütz, N.; Koch, M.; Manier, S. K.; Schneider, M.; Meyer, M. R. Evaluation of novel organosilane modifications of paper spray mass spectrometry substrates for analyzing polar compounds. *Talanta* **2019**, *204*, 677-684.
- (30) Damon, D. E.; Davis, K. M.; Moreira, C. R.; Capone, P.; Cruttenden, R.; Badu-Tawiah, A. K. Direct biofluid analysis using hydrophobic paper spray mass spectrometry. *Analytical Chemistry* **2016**, *88*, 1878-1884.
- (31) Duvivier, W. F.; van Beek, T. A.; Pennings, E. J.; Nielen, M. W. Rapid analysis of Δ^9 -tetrahydrocannabinol in hair using direct analysis in real time ambient ionization orbitrap mass spectrometry. *Rapid Communications in Mass Spectrometry* **2014**, *28*, 682-690.
- (32) Gottardo, R.; Sorio, D.; Ballotari, M.; Tagliaro, F. First application of atmospheric-pressure chemical ionization gas chromatography tandem mass spectrometry to the determination of cannabinoids in serum. *Journal of Chromatography A* **2019**, *1591*, 147-154.
- (33) Cody, R. B.; Laramée, J. A.; Durst, H. D. Versatile new ion source for the analysis of materials in open air under ambient conditions. *Analytical Chemistry* **2005**, *77*, 2297-2302.
- (34) Duvivier, W. F.; van Putten, M. R.; van Beek, T. A.; Nielen, M. W. (Un) targeted scanning of locks of hair for drugs of abuse by direct analysis in real time-high-resolution mass spectrometry. *Analytical Chemistry* **2016**, *88*, 2489-2496.
- (35) Shoeib, T.; Zhao, J.; Aribi, H. E.; Hopkinson, A. C.; Michael Siu, K. Dissociations of complexes between monovalent metal ions and aromatic amino acid or histidine. *Journal of the American Society for Mass Spectrometry* **2012**, *24*, 38-48.
- (36) Sigsworth, S.; Castleman Jr, A. Rates of hydride abstraction from amines via reactions with ground-state silver (+) and copper (+). *Journal of the American Chemical Society* **1989**, *111*, 3566-3569.

- (37) Jung, J.; Kempf, J.; Mahler, H.; Weinmann, W. Detection of Δ 9-tetrahydrocannabinolic acid A in human urine and blood serum by LC-MS/MS. *Journal of Mass Spectrometry* **2007**, *42*, 354-360.
- (38) Eichler, M.; Spinedi, L.; Unfer-Grauwiler, S.; Bodmer, M.; Surber, C.; Luedi, M.; Drewe, J. Heat exposure of *Cannabis sativa* extracts affects the pharmacokinetic and metabolic profile in healthy male subjects. *Planta Medica* **2012**, *78*, 686-691.
- (39) Ariffin, A. A.; Bakar, J.; Tan, C. P.; Rahman, R. A.; Karim, R.; Loi, C. C. Essential fatty acids of pitaya (dragon fruit) seed oil. *Food Chemistry* **2009**, *114*, 561-564.
- (40) SWGTOX. Scientific working group for forensic toxicology (SWGTOX) standard practices for method validation in forensic toxicology. *Journal of Analytical Toxicology* **2013**, *37*, 452-474.

Semiquantitative Screening of Δ^9 -THC Analogues by Silica Gel TLC with an Ag(I) Retention Zone and Chromogenic Smartphone Detection

This chapter was published as:

Huang, S.; Qiu, R.; Fang, Z.; Min, K.; Van Beek, T. A.; Ma, M.; Chen, B.; Zuilhof, H.; Salentijn, G. IJ. Semiquantitative screening of THC analogues by silica gel TLC with an Ag(I) retention zone and chromogenic smartphone detection. *Analytical Chemistry* **2022**, 94, 13710-13718. <https://doi.org/10.1021/acs.analchem.2c01627>.



Abstract

With the ever-evolving Cannabis industry, low-cost and high-throughput analytical methods for cannabinoids are urgently needed. Normally, (potentially) psychoactive cannabinoids, typically represented by Δ^9 -tetrahydrocannabinol (THC), and non-psychoactive cannabinoids with therapeutic benefits, typically represented by cannabidiol (CBD), are the target analytes. Structurally, the former (tetrahydrocannabinolic acid (THCA), cannabinol (CBN), and Δ^9 -THC) have one olefinic double bond and the latter (cannabidiolic acid (CBDA), cannabigerol (CBG), and CBD) have two, which results in different affinities for Ag(I) ions. Thus, a silica gel thin-layer chromatography (TLC) plate with the lower third impregnated with Ag(I) ions enabled within minutes a digital chromatographic separation of strongly retained CBD analogues and poorly retained Δ^9 -THC analogues. The resolution (R_s) between the closest two spots from the two groups was 4.7, which is almost 8 times higher than the resolution on unmodified TLC. After applying Fast Blue BB as a chromogenic reagent, smartphone-based color analysis enabled semiquantification of the total percentage of Δ^9 -THC analogues (with a limit of detection (LOD) of 11 ng for Δ^9 -THC, 54 ng for CBN, and 50 ng for THCA when the loaded volume is 1.0 μL). The method was validated by analyzing mixed Cannabis extracts and Cannabis extracts. The results correlated with those of high-performance liquid chromatography with ultraviolet detection (HPLC-UV) ($R^2 = 0.97$), but the TLC approach had the advantages of multi-minute analysis time, high throughput, low solvent consumption, portability, and ease of interpretation. In a desiccator, Ag(I)-TLC plates can be stored for at least 3 months. Therefore, this method would allow rapid distinction between high and low Δ^9 -THC varieties of Cannabis, with the potential for on-site applicability.

Introduction

Cannabis (*Cannabis sativa* L.) has been used by man since the Stone Age as a source of food, fiber, medicine, and psychoactives. It contains a specific class of phytochemicals called cannabinoids.¹ The most abundant cannabinoids are tetrahydrocannabinolic acid (THCA) and cannabidiolic acid (CBDA), derived from the same precursor cannabigerolic acid (CBGA) with THCA synthase and CBDA synthase, respectively. These acidic cannabinoids are rather unstable and may lose CO₂ by exposure to light, air, or heat to produce cannabidiol (CBD), Δ⁹-tetrahydrocannabinol (THC), and cannabigerol (CBG) with different bioactivities.² Further degradation can occur, for example, cannabinol (CBN) as an oxidative degradation product of Δ⁹-THC is found in aged Cannabis.³ Chemically, these cannabinoids can be roughly divided into two groups: (1) Δ⁹-THC analogues that have a pyran ring and (2) CBD analogues that have a disubstituted double bond and a second phenolic group instead of the pyran ring. THCA is not psychoactive, but it can be converted to Δ⁹-THC, the main psychoactive cannabinoid, during smoking or baking.⁴ CBN is also psychoactive but has only 10% of the potency of Δ⁹-THC.⁵ Congeners of the other group like CBG, CBDA, and CBD are not psychoactive but possess various therapeutic properties (**Figure 4.1**).⁶

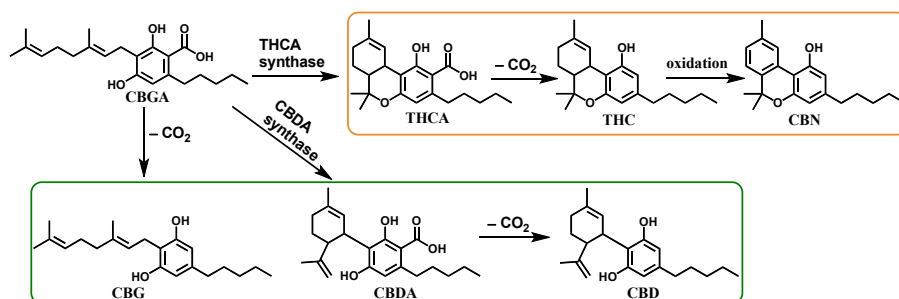


Figure 4.1. Structures and formation process of important cannabinoids: cannabigerolic acid (CBGA), tetrahydrocannabinolic acid (THCA), Δ⁹-tetrahydrocannabinol (THC), cannabinol (CBN), cannabigerol (CBG), cannabidiolic acid (CBDA) and cannabidiol (CBD).

Although there are many classification systems based on the content of psychotropic components, the drug-type (marijuana) and the fiber-type (hemp) are

the most important Cannabis types for forensic and legislative considerations. Marijuana is characterized by a high content of the psychoactive compound $\Delta 9$ -THC (> 0.3% of dry weight).⁷ Given that CBN is a degradation product of $\Delta 9$ -THC, it can be included as a relevant parameter when evaluating the initial $\Delta 9$ -THC concentration.⁸ For assessing the total $\Delta 9$ -THC potential of Cannabis, both its precursor THCA and degradation product CBN should thus be taken into consideration.^{9,10} In contrast to marijuana, hemp is characterized by non-psychoactive cannabinoids including CBDA and its decarboxylated form, namely, CBD, as well as some minor cannabinoids, e.g., CBGA and CBG.¹¹ Since THCA, CBDA, and CBG are all formed from the common precursor CBGA,¹² many Cannabis plants contain THCA, CBDA, and CBG at the same time. Moreover, in many screening and instrumental analyses, it is difficult to differentiate between different cannabinoids from those different groups. As a result, the separation of CBD analogues from $\Delta 9$ -THC analogues is necessary to prevent interference.

The growing Cannabis industry and increasing pressure on forensic testing have pushed the development of portable, high-throughput, and easy-to-use tests that can be performed directly in the field for qualitative and quantitative analysis of Cannabis.¹³ Kurouski et al.^{14,15} proposed a non-invasive and non-destructive method to distinguish between freshly frozen plants rich in THCA and rich in CBD using a handheld Raman spectrometer. Due to the variation in intensities of characteristic vibrational bands from cellulose, xylan, carotenoids, lignin, and THCA in different plant materials, this method could be used to classify Cannabis varieties. However, this method only enables qualitative analysis by comparison with previously collected Raman spectroscopic signatures from various Cannabis varieties. Valid quantification of individual cannabinoids still needs further study. Arce et al.¹⁶ applied thermal desorption (TD)-ion mobility spectrometry (IMS) to analyze dried leaves and flowers of plant samples for potentially on-site discrimination of Cannabis varieties. However, most signals in the TD-IMS spectra under both positive and negative ionization modes could not be clearly identified.

Compared with the above-mentioned instrument-dependent in-field screening methods, colorimetric tests are attractive alternatives, as they are cheap and require minimal operational training. Colorimetric test kits based on fast blue BB salt or Duquenois–Levine reagent are commonly used by forensic laboratories for the analysis of marijuana samples. However, without any pre-separation, false-positive results can be obtained from non-psychoactive cannabinoids, e.g., CBD analogues, as well as non-cannabinoids.¹⁷ Therefore, separation of individual cannabinoids before color development is a necessity.

To achieve such separation, the combination of thin-layer chromatography (TLC) and a chromogenic reagent for visualization of spots has been demonstrated, leading to simple, fast, and qualitative or semiquantitative analysis of Cannabis. Different stationary phases,^{18,19} solvent systems,¹³ and methods for semiquantitative image analysis have been tested.²⁰ Liu et al.¹³ evaluated different mobile phases for analysis of possibly illegal Cannabis products on silica gel and a reversed-phase (C18) plate. Both systems provided good separation for Δ 9-THC, CBD, and CBN in hemp and marijuana samples but could not adequately separate the acidic cannabinoids like THCA, CBDA, and CBGA. In other studies, the stationary phase has been modified to obtain better separations.^{18,19} Tsujikawa et al.¹⁹ recently analyzed five THC isomers (Δ 9-THC, Δ 8-THC, a pair of diastereomers of Δ 10-THC, and Δ 6a,10a-THC), CBD, CBN, and THCA in samples of CBD heated in acidic ethanol on silica gel TLC plates modified with 10% AgNO_3 and toluene as solvent. After chromogenic detection, this system resolved Δ 9-THC, CBD, CBN, and Δ 8-THC relying on the specific affinity of Ag(I) toward compounds with different numbers or different positions of olefinic double bonds, which has been described in previous work.^{21–23} This mechanism has also been used in our recent work for the differentiation of isomers Δ 9-THC and CBD by Ag(I) -impregnated paper spray mass spectrometry.²⁴ However, a disadvantage of the method developed by Tsujikawa et al. was that the THCA spot was tailing and overlapped with the CBD spot. Considering this overlap and the fact that Δ 8-THC is not a target compound for analysis of herbal Cannabis, the authors explicitly stated that this system is not

suitable for Cannabis plant samples. Furthermore, because the entire TLC plate was modified by AgNO_3 , significant background color from the reaction of Ag(I) ions with the basic ammonia solution interfered with the detection of cannabinoids.

In addition to the use of a TLC for the separation of different cannabinoids, the listed applications are based on the use of chromogenic reagents for qualitative analysis. For TLC-based quantitative analysis, research has relied on using a photoelectric densitometer to scan spots,^{20,25,26} which is not suitable for instrument-free on-site analysis. The portability, low cost, versatility, and wide availability of smartphones create opportunities for the instrument-free analysis of TLC plates. Scientific efforts have focused on smartphone-based qualitative and quantitative analyses and led to applications in the detection of (heavy) metals, herbicides, pesticides, antibiotics, biochemical indicators, allergens, bacteria, viruses, and so on.²⁷⁻²⁹

The aim of this research was to improve both the TLC separation of Δ^9 -THC analogues using a partially modified silica gel TLC plate with Ag(I) ions and the detection step by semiquantitatively scanning the colored THC spots with a smartphone. This combination of techniques would allow for a fast, instrument-free, in-field screening of Cannabis varieties in a greenhouse setting or for on-site forensic purposes with a low solvent consumption.

Materials and Methods

Overview of the Experiments. The aim of this work is to semiquantify psychoactive cannabinoids with a fast and portable tool. To achieve this, the experimental design, given in **Figure 4.2**, was followed. This started with sample preparation, including standard solutions, Cannabis extracts, and mixed Cannabis extracts. Next, Ag(I) -TLC plates were designed and optimized for the digital chromatographic separation of Δ^9 -THC analogues from CBD analogues, and their storage stability was investigated with respect to light, humidity, and time. Following that, samples were loaded on the optimized Ag(I) -TLC plates and went through the separation and color development process. The quality of the separation was then

validated by HPLC-MS/MS, by recovering cannabinoids from different regions of the TLC plates, and analyzing those. Subsequently, calibration curves were constructed, based on smartphone analysis of the colored spots on the TLC plate, and the LODs of THCA, Δ^9 -THC, and CBN were evaluated. Finally, the total Δ^9 -THC potential percentages of Cannabis extracts and mixed Cannabis extracts were semiquantified by the developed smartphone analysis and benchmarked against HPLC-UV.

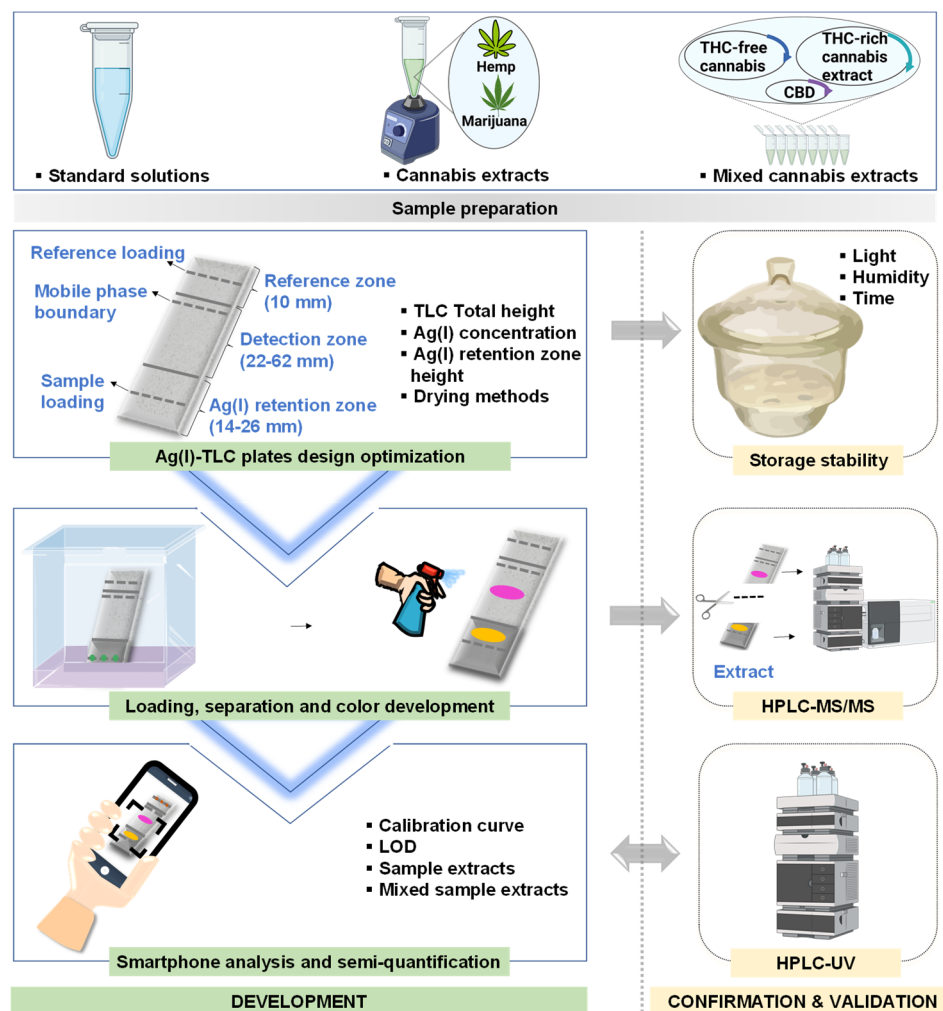


Figure 4.2. Overview of the experimental workflow.

Chemicals and Reagents. Acetonitrile (ACN, HPLC-grade) and methanol (MeOH; HPLC-grade) were purchased from Sigma-Aldrich (St. Louis). Hexane (HPLC-grade), *tert*-butyl methyl ether (MTBE; HPLC-grade), and acetic acid (AcOH; HPLC-grade) were purchased from Sinopharm Chemical Reagent Co., Ltd. (Shanghai, China). Deionized water was prepared by a Milli-Q water purification system (Millipore). AgNO₃ (AR, 99.8%) and NaOH (AR, 99.8%) were purchased from Aladin Biochemical Technology Co. Ltd. (Shanghai, China). 4-Benzoylamino-2,5-diethoxybenzenediazonium chloride hemi (zinc chloride) salt (Fast Blue BB; FBBB; AR grade) was obtained from Sigma-Aldrich (St. Louis). Olivetol (5-pentylbenzene-1,3-diol, AR, 99.7%) was bought from Shanghai Haohong Biomedical Technology Co., Ltd. (Shanghai, China). Aluminum-backed silica gel 60 F₂₅₄ 20 × 20 cm² TLC plates were purchased from Merck (Darmstadt, Germany). THCA (99.2%), Δ^9 -THC (99.0%), CBN (99.2%), CBDA (99.3%), CBD (99.8%), and CBG (99.1%) standards were obtained from Henan Wanjia Reference Material R&D Center Co., Ltd. (Zhengzhou, China). Pure CBD powder (99.5%) and 10% (w/w%) CBD oil (hemp seed oil as matrix) were bought from Yuxi Hongbao Biological Technology Co., Ltd. (Yunnan, China). Dry plant materials were purchased online in China, and are referred to as Cannabis_1, Cannabis_2, and Cannabis_3. Marijuana extract was prepared from marijuana inflorescence and concentrated by the evaporation of most solvents.

HPLC-(PDA) MS/MS Setup. A high-performance liquid chromatograph (HPLC Prominence; Shimadzu, Kyoto, Japan), equipped with an Ultimate LP-C18 column (4.6 × 150 mm², 5 μ m; Welch Materials, Inc., West Haven) and an SPD-M20A photodiode array detector was coupled to a triple-quadrupole mass spectrometer (MS8050; Shimadzu, Kyoto, Japan). The mobile phase consisted of 0.1% (v/v%) formic acid in both water (mobile phase A) and acetonitrile (mobile phase B), and the flow rate was 1.0 mL·min⁻¹: 0–12 min 80% B; 12–13 min linear ramping to 100%; 13–18 min 100% B; 18–19 min linear decrease to 80% B; 19–28 min reequilibration at 80% B. Mass spectrometry was performed in positive multiple

reaction monitoring (MRM) mode (see **Supporting Information (SI), Table S3** for settings) with an atomizer flow rate of $3 \text{ L} \cdot \text{min}^{-1}$, a heating gas flow rate of $10 \text{ L} \cdot \text{min}^{-1}$, a drying gas flow rate of $10 \text{ L} \cdot \text{min}^{-1}$, DL temperature 250°C , ion source interface voltage of 4 kV, and heating block temperature of 400°C .

Sample Preparation. Standard Solutions. THCA, $\Delta 9$ -THC, CBN, CBDA, CBD, and CBG methanol stock solutions ($1.00 \mu\text{g} \cdot \mu\text{L}^{-1}$) were diluted with MeOH to obtain a series of standard solutions for subsequent analysis. A “standard_mixture” was prepared containing $83.3 \text{ ng} \cdot \mu\text{L}^{-1}$ THCA, $\Delta 9$ -THC, CBN, CBG, CBDA, and CBD in MeOH.

Cannabis Extracts. MeOH ($300 \mu\text{L}$) was added to 100.0 mg of dried, homogenized, and ground herbal Cannabis_1, Cannabis_2, and Cannabis_3 one by one with a pipette (Eppendorf 3120000267, $100\text{--}1000 \mu\text{L}$). The extraction was performed by vortexing for 3 min with Vortex-Genie 2 (Scientific Industries, Inc.). The extracted samples were filtered using a $0.2 \mu\text{m}$ PTFE membrane syringe filter ($\varnothing 13 \text{ mm}$). Marijuana extract concentrate was diluted with MeOH to 10.00 and $1.00 \text{ mg} \cdot \text{mL}^{-1}$. 10% CBD oil was diluted with MeOH 50-fold. All solutions except for $10.00 \text{ mg} \cdot \text{mL}^{-1}$ marijuana extract concentrate were analyzed by HPLC-UV at 228 nm for quantification of six cannabinoids according to external standard calibration curves (**SI, Figure S1 and Table S1**). A “sample_mixture” was prepared by mixing $60.0 \mu\text{L}$ of Cannabis_1 extract, $120.0 \mu\text{L}$ of Cannabis_2 extract, $60.0 \mu\text{L}$ of Cannabis_3 extract, $60.0 \mu\text{L}$ of marijuana extract, and $60.0 \mu\text{L}$ of CBD oil extract.

Mixed Cannabis Extracts. Different volumes of marijuana extract (high levels of $\Delta 9$ -THC analogues) were spiked into Cannabis_3 plant material (no $\Delta 9$ -THC analogues, blank matrix) to produce samples containing different concentrations of $\Delta 9$ -THC analogues (mixed Cannabis extracts set I, **SI, Table S2**). Next, different volumes of marijuana extract (high levels of $\Delta 9$ -THC analogues) and 1.00 mg of CBD powder were spiked into Cannabis_3 plant material (no $\Delta 9$ -THC analogues, blank matrix) to produce samples containing both $\Delta 9$ -THC analogues and CBD (mixed Cannabis extracts set II, **SI, Table S2**).

Ag(I)-TLC Plates Design, Optimization, and Storage Stability. *Ag(I)-TLC Plate Design.* The 20×20 cm² aluminum-backed silica gel TLC plates were cut with scissors into rectangular plates. The plates were made with three regions: (1) Ag(I) retention zone, (2) detection zone, and (3) reference zone, as shown in **Figure 4.2** (see **SI, Figure S2** for more details).

Ag(I)-TLC Plate Optimization. THCA, Δ^9 -THC, CBN, CBDA, CBD, and CBG standard solutions were analyzed (see protocol below) and the resolution between the pairs THCA-CBD, Δ^9 -THC-THCA, and Δ^9 -THC-CBN were investigated to optimize (i) the total height of the TLC plate, (ii) AgNO₃ concentration for TLC modification, (iii) Ag(I) retention zone height, and (iv) drying method of modified TLC plates step by step (see **SI, Protocol S1** for details).

Ag(I)-TLC Plates Storage Stability. A batch of Ag(I)-TLC plates was prepared and stored in sealed plastic bags with the aluminum side up, under three different conditions: on a desk, in a black box, and in a brown desiccator with anhydrous calcium chloride as a drying agent at room temperature (**SI, Figure S3**). At regular intervals, three pieces of Ag(I)-TLC plates under each storage condition were tested with Δ^9 -THC and CBD standards to evaluate the separation performance over time.

Sample Loading, Separation, and Color Development. *Sample Loading and Separation.* To load a sample on the TLC plate, 1.0 μ L of an extract solution was applied on both the sample loading line and the reference sample loading line of the TLC plate with a pipette (Eppendorf 3120000216, 0.1–2.5 μ L). After drying, the TLC plate was placed into a sealed chamber (width 4 cm, height 10.5 cm, with removable lid) conditioned with mobile phase (MTBE/hexane = 1:4 v/v with 0.1% AcOH) vapor for at least 5 min with a piece of filter paper on the wall of the tank to facilitate the equilibration.³⁰ When the mobile phase reached the mobile phase boundary line, the TLC plate was taken out and dried in a fume hood. The loaded samples on the reference sample line were not eluted by the mobile phase but were included in the color development procedure.

Color Development. The color developing procedure needs A and B solutions consisting of 0.2 M NaOH solution in water/MeOH (1:9 v/v) and a 5 mg·mL⁻¹ FBBB MeOH solution, respectively. A and B solutions were ready for use in glass spray bottles (SI, **Figure S4**). For color development, solution A was evenly sprayed by applying five pumps on the developed TLC plate, and then solution B was evenly sprayed by applying 10 pumps. After 2 min, the TLC plate was moved to a custom-made light box (SI, **Figure S5**) and an Apple iPhone 11 camera was used for image acquisition.

Confirmation by HPLC-MS/MS. Extracts were made of the scraped-off silica from the different regions of the TLC plates, and these were evaluated by HPLC-MS/MS to (i) confirm the identity of the cannabinoids present in the different regions, (ii) to quantify those cannabinoids to assess the separation efficiency, and (iii) to evaluate whether other cannabinoids are present at low levels that are missed by the colorimetric analysis. The detailed procedures can be found in SI, **Protocol S2**. In short, the “standard_mixture” and “sample_mixture” were analyzed by both unmodified TLC plate and Ag(I)-TLC plate. The silica gel in the upper part and lower part of each plate was scraped off separately and extracted with MeOH for HPLC-MS/MS analysis of separated cannabinoids.

Smartphone Analysis and Semiquantification. *Calibration Curve Construction.* To achieve semiquantification of major psychoactive cannabinoids with smartphone analysis, calibration curves of THCA, Δ^9 -THC, and CBN were constructed and the LODs were evaluated. THCA, Δ^9 -THC, and CBN methanol solutions (0.20, 0.50, 0.80, and 1.00 $\mu\text{g}\cdot\mu\text{L}^{-1}$) (1.0 μL) were loaded on the sample loading line of an Ag(I)-TLC plate, and 1.0 μL of a 1.00 $\mu\text{g}\cdot\mu\text{L}^{-1}$ solution of each analyte was loaded twice to have an absolute amount of 2.00 μg . Each solution was analyzed on three different TLC plates. Olivetol (1.0 μL of 0.10 $\mu\text{g}\cdot\mu\text{L}^{-1}$ in MeOH loaded on a square TLC plate) was chosen as a reference to correct for variation in color development and image acquisition because it also reacts with FBBB to form a colored product. ImageJ (NIH) software was used to obtain three image

parameters, namely, hue (H), saturation (S), and brightness (B).²⁷ Each spot on the image was analyzed, and the obtained value for saturation was normalized against the obtained saturation value of the olivetol reference spot. The normalized saturation values for THCA, $\Delta 9$ -THC, and CBN were plotted as a function of their concentration.

Evaluation of LOD. The LOD was calculated as follows: $\text{LOD} = 3 \times \text{SD of blank/slope of the curve}$, in which the blank is the normalized background saturation of analyzed TLC plates. Additionally, to check whether the calculated LODs match with actual observations by the naked eye, 1.0 μL of 62.5, 31.3, 15.6, and 7.8 $\text{ng} \cdot \mu\text{L}^{-1}$ of THCA, $\Delta 9$ -THC, and CBN was loaded on Ag(I)-TLC plate and went through solvent-development as well as color development processes.

Analysis of (Mixed) Cannabis Extracts. (Mixed) Cannabis extracts (1.0 μL) (**SI, Table S2**) were analyzed by Ag(I)-TLC plates with smartphone detection. The normalized THCA saturation value was used to calculate THCA content in samples by the above-constructed THCA calibration curve. The normalized $\Delta 9$ -THC and CBN saturation value was used to calculate the sum content of $\Delta 9$ -THC + CBN in samples by the above-constructed $\Delta 9$ -THC calibration curve unless noted otherwise. Further image analysis in RGB space was explored to assess if the color of the $\Delta 9$ -THC and CBN spot could be used to assess whether it is high in $\Delta 9$ -THC or CBN, as pure spots produce purple and orange, respectively. Subsequently, total $\Delta 9$ -THC potential percentage was expressed as follows:

$$\% \text{THCA} = [\text{THCA}] \times (\text{VOL}/\text{DW}) \times 100$$

$\% \Delta 9$ -THC and $\% \text{CBN}$ were calculated similarly.

$$\text{total } \Delta 9\text{-THC potential percentage} = (\% \text{THCA} \times 0.877) + \% \Delta 9\text{-THC} + \% \text{CBN}$$

where $[\text{THCA}]$ is the measured concentration of THCA ($\mu\text{g} \cdot \text{mL}^{-1}$), VOL is the external volume (300 μL), DW is the dry sample weight (100.0 mg), and 0.877 is the molecular weight ratio of cannabinoids to cannabinoid acids under study.^{31,32}

Validation by HPLC-UV. The concentration of THCA, $\Delta 9$ -THC, and CBN in Cannabis extracts was determined by external standard calibration curves (**SI, Figure S1** and **Table S1**) with HPLC-UV at 228 nm. The total $\Delta 9$ -THC potential

percentages in (mixed) Cannabis extracts were calculated in the same way as for smartphone analysis except for the following difference in mixed Cannabis extracts.

$$\%THCA = ([THCA] \times 10 \times \text{spiked volume}) / DW \times 100$$

[THCA] ($\mu\text{g}\cdot\text{mL}^{-1}$) is the measured concentration in $1.00\text{ mg}\cdot\text{mL}^{-1}$ marijuana solution from HPLC-UV at 228 nm, and the spiked volume is 0, 0.12, 0.14, 0.2, 0.3, 0.4, 0.5 or 0.6 mL, DW is the dry sample weight (100.0 mg), and $\%\Delta^9\text{-THC}$ and $\%\text{CBN}$ were calculated similarly.

Results and Discussion

Comparison of Ag(I)-TLC and Unmodified TLC for Separation of Standards. As colored products are formed by coupling FBBB to the para position relative to the phenolic group in a slightly alkaline solution, the colorimetric reaction is highly selective for phenols but does not distinguish individual members within the cannabinoid group.³³ There are many varieties of Cannabis containing both $\Delta^9\text{-THC}$ analogues and CBD analogues, which are difficult to separate by traditional TLC methods.³⁴ The difference in affinity of Ag(I) ions with a single alkene C=C bond (weak) versus a 1,5-diene (strong)²¹ was exploited here to allow the separation of these two groups.

As shown in **Figure 4.3A**, when applying unmodified TLC, $\Delta^9\text{-THC}$ and CBD (isomers) have similar R_f values (0.55 and 0.60, respectively) as well as the pair THCA and CBDA (isomers) (0.29 and 0.34, respectively). The resolution of the closest two spots (one from $\Delta^9\text{-THC}$ analogues and the other one from CBD analogues) was only 0.6, making it difficult to distinguish the $\Delta^9\text{-THC}$ analogues and CBD analogues, which is necessary for assessing the total $\Delta^9\text{-THC}$ potential without interference from CBD analogues. However, after extensive optimization (**SI, Figures S6 and S7**), a partially coated Ag(I)-TLC plate was successfully developed and could be used to separate CBD analogues from $\Delta^9\text{-THC}$ analogues (**Figure 4.3B**). The resolution between the highest CBD analogue and the lowest $\Delta^9\text{-THC}$ analogue was 4.7, which is almost 8 times the resolution on an unmodified TLC plate.

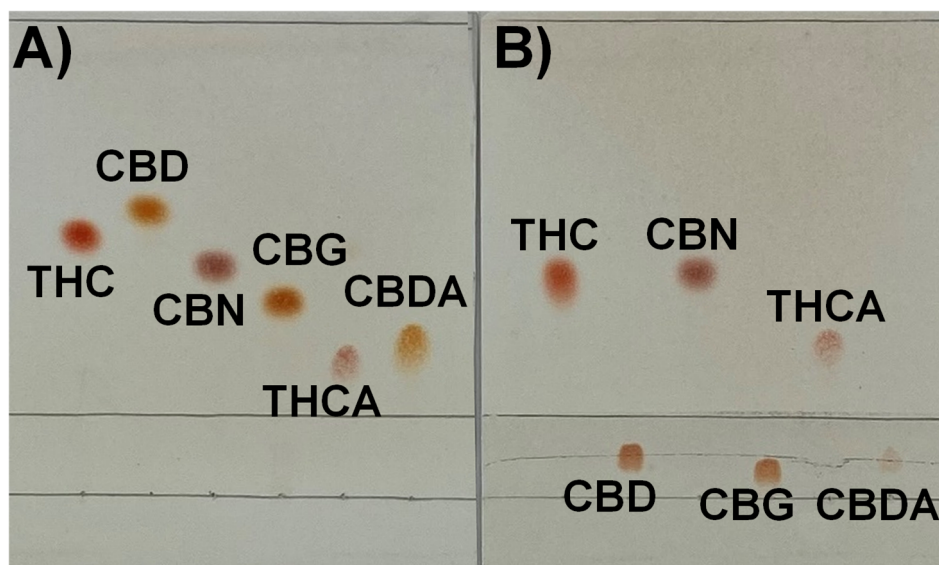


Figure 4.3. Δ^9 -THC, CBD, CBN, CBG, THCA and CBDA standards (from left to right) loaded and separated on A) an unmodified silica gel TLC plate and B) an Ag(I)-TLC plate.

Storage Stability of Ag(I)-TLC Plates. After obtaining the optimized Ag(I)-TLC plates, storage stability was investigated for robust applicability, considering the sensitivity of Ag(I) toward light and humidity (**Figure 4.4** and **SI, Figure S8**).³⁵ There is little difference in separation between Δ^9 -THC and CBD for the first 37 days between plates stored under different conditions. This is probably because all Ag(I)-TLC plates were put in plastic, sealed bags with the aluminum side up so that the influence of light and humidity could be somewhat prevented during the initial storage stage. With extended storage time, however, the separation performance of Ag(I)-TLC plates stored on the desk dropped sharply. During this process, the Ag(I) retention zone became visibly and increasingly darker due to the photodegradation of Ag(I) (**SI, Figure S8**), which resulted in the compromised retention effect toward CBD. Moreover, the absolute R_f of Δ^9 -THC and CBD increased (**SI, Figure S9**), possibly due to the competitive binding of water molecules on silica. When these plates are stored in a black box, the effect from light can be excluded, and the separation quality was constant for 44 days but did eventually deteriorate upon storage between 44 and 88 days. Storage in the brown desiccator with a drying agent

yielded the best result, as separation performance remained good during the entire stability study, which lasted 88 days. Therefore, when suitably stored, mass-produced Ag(I)-TLC plates could be used for large-scale applications.

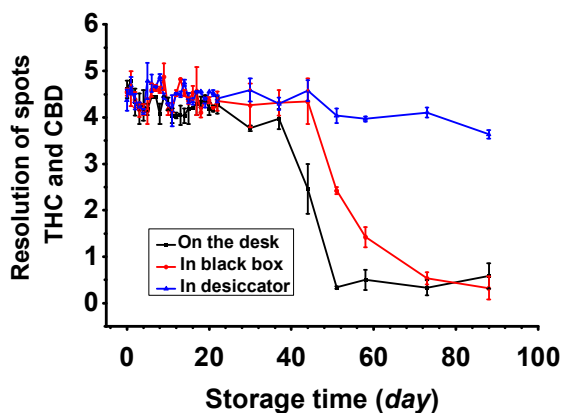


Figure 4.4. Changes in resolution between Δ^9 -THC and CBD during storage in plastic sealed bags and put on a desk, in a black box or in a brown desiccator. Error bars represent standard deviation ($n = 3$).

Assessment of Ag(I)-TLC Separation by HPLC-MS/MS. After obtaining a digital chromatographic separation (SI, Figure S10), HPLC-MS/MS was used to identify and quantify the cannabinoids in the upper and lower parts of the TLC plate, in the “standard_mixture” and “sample_mixture.” THCA, CBDA, Δ^9 -THC, CBD, CBN, and CBG were identified by comparing with standards to match retention time and MRM signals (see Figure 4.5A and SI, Figure S11). Other cannabinoids found in sample extracts were identified by matching MRM signals and relative retention times with the literature (SI, Figures S12 and S13).³⁶⁻³⁸ Δ^9 -THC, CBN, and THCA were identified in the detection zone, while CBD, CBG, and CBDA were detected in the retention zone of the Ag(I)-TLC plate (Figure 4.5B,C), which is consistent with the observed colorimetric results. In contrast, when applying unmodified silica TLC, all of these six standards were found in the detection zone (SI, Figure S11). During the HPLC-MS/MS analysis of the “sample_mixture,” 12 cannabinoids could be identified. On unmodified silica TLC, signals of all 12 cannabinoids were found in the upper part, and most cannabinoids, except CBDV, CBG, and CBDA, were also

found in the bottom part (**SI, Figure S12**). For Ag(I)-TLC plates, all $\Delta 9$ -THC analogues (THCV, $\Delta 9$ -THC, CBN, THCVA, THCA, CBLA) were found in the upper part (detection zone) and there were no signals of any CBD analogues (CBDA, CBD, CBG, CBDVA, CBDV, CBGA); in the bottom part (Ag(I) retention zone), the main signals were from the CBD analogues (CBDV, CBD, CBG, CBDVA, CBDA, and CBGA) (**SI, Figure S12**). Two minor signals of THCVA and THCA were also found in the Ag(I) retention zone. However, the peak area of THCVA only accounts for $4.0 \pm 1.0\%$ of the corresponding signal peak area found in the upper part (detection zone), while for THCA the value is $4.7 \pm 1.0\%$. The retention of these two acidic compounds in the bottom part is also found on normal TLC plates, probably due to the interaction between the carboxyl moieties and silica-based silanol.

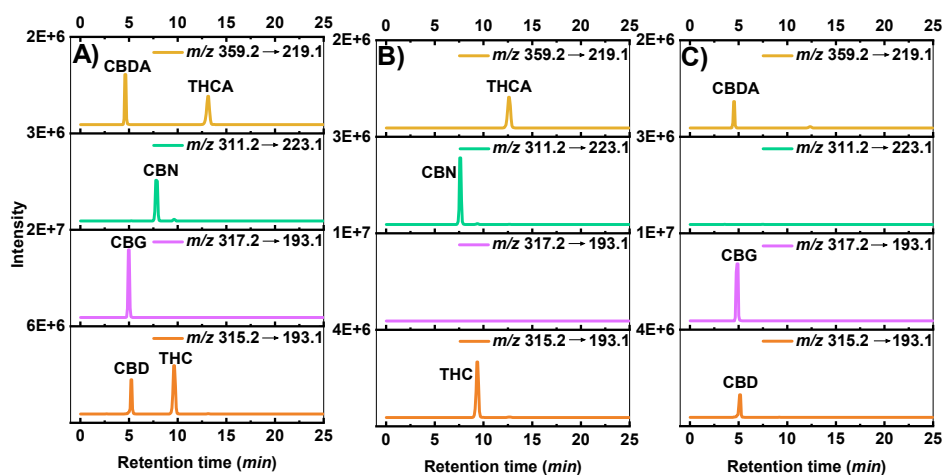


Figure 4.5. HPLC-MRM chromatograms of detected cannabinoids in A) ‘standard_mixture’, B) extract of Ag(I)-TLC detection zone silica after separating ‘standard_mixture’, C) extract of Ag(I) retention zone silica after separating ‘standard_mixture’.

Based on the colorimetric detection and mass spectrometric identification of cannabinoids separated with Ag(I)-TLC plate, it can be seen the Ag(I)-TLC plate has the ability to divide cannabinoids into two groups. Structurally, in the bottom part (Ag(I) retention zone), all cannabinoids share a 1,5-diene moiety, while the cannabinoids in the detection zone have no or only one double olefinic bond (**SI,**

Figure S13). From the perspective of psychoactive effects, two compounds are most relevant: THCV, which is the decarboxylated product resulting from (non-psychoactive) THCVA, and possesses ~25% of the psychoactive potency of Δ^9 -THC,³⁹ while CBLA is a rare and poorly investigated cannabinoid, whose decarboxylated product CBL was initially named “THC III”.⁴⁰ For the CBD analogues, CBD (decarboxylated from CBDA), CBG, and CBDV (decarboxylated from CBDVA) are not psychoactive and have various therapeutic properties. Thus, it appears that the cannabinoids found in the detection zone tend to be (potentially) psychoactive, while those retained in the Ag(I) retention zone are non-psychoactive.

Ag(I)-TLC Coupling with Smartphone for Semiquantitative Analysis of Δ^9 -THC Analogues. After fully assessing the separation performance of Ag(I)-TLC plates, smartphone analysis was used for semiquantification of Δ^9 -THC analogues.

Calibration Curves and LOD. Calibration curves between the absolute amount of THCA, Δ^9 -THC, or CBN loaded on the plate and the saturation values were first constructed (**SI, Figure S14**), which showed good linearity ($R^2 = 0.96$ – 0.98) in the range of 0.2–2 μg and LODs of 11 ng for Δ^9 -THC, 54 ng for CBN, 50 ng for THCA. The lowest visible amount on a developed TLC plate was 15.6 ng for Δ^9 -THC, 31.3 ng for CBN, and 31.3 ng for THCA (see **SI, Figure S15**), which are similar to the calculated values.

Distinction between Δ^9 -THC and CBN by Image Analysis. By applying the smartphone calibration curves, separate semiquantitative analysis of THCA in samples can be achieved. However, since the spots of Δ^9 -THC and CBN on Ag(I)-TLC plates overlap (**Figure 4.3B**), separate analysis of Δ^9 -THC and CBN is challenging. In a previous study, the sum of Δ^9 -THC + CBN has been used to assess the initial Δ^9 -THC level and thus indirectly Cannabis potency.³² Similarly, in this work, the combined Δ^9 -THC and CBN spot was used to estimate the total amount of Δ^9 -THC + CBN from the Δ^9 -THC calibration curve. Due to the slightly different smartphone signal contributions from individual Δ^9 -THC and CBN (as shown in their separate calibration curves in **SI, Figure S14**), some error can be expected when

analyzing samples containing various relative compositions of $\Delta 9$ -THC and CBN. To investigate this, a series of $\Delta 9$ -THC + CBN standard mixtures with same absolute amount but different CBN/($\Delta 9$ -THC + CBN) ratios were analyzed by the Ag(I)-TLC plates (**SI, Figure S16A**), and the smartphone saturation signal from each spot was compared with that from the pure $\Delta 9$ -THC spot. When the CBN/($\Delta 9$ -THC + CBN) ratio is between 0 and 0.6, the saturation signals showed little differences with that from pure $\Delta 9$ -THC; however, when the CBN/($\Delta 9$ -THC + CBN) ratio is larger than 0.6, saturation signals accounted for around 70% of the signal from pure $\Delta 9$ -THC (**SI, Figure S16B**). Under this circumstance, applying a $\Delta 9$ -THC-only calibration curve to calculate the sum content of $\Delta 9$ -THC + CBN would end up with an underestimation of the $\Delta 9$ -THC + CBN content. Considering the fact that fresh Cannabis or relevant products normally contain little CBN (CBN/($\Delta 9$ -THC + CBN) < 0.6),^{32,41} this would not lead to issues with our semiquantitative method in most cases. However, samples could contain higher CBN content (CBN/($\Delta 9$ -THC + CBN) > 0.6) due to long storage, possibly at ambient temperature or without protection from light.³² It was thus investigated whether smartphone image analysis could be used to at least identify when this would be the case. This check is based on the fact that pure $\Delta 9$ -THC produces an orange color, whereas pure CBN produces a purple color, after reacting with FBBB. The distinction between such high and low CBN samples could be achieved by RGB color analysis. In short, the relative difference between the R and B components was measured in ImageJ and normalized to a value ranging between 100% $\Delta 9$ -THC (1) and 100% CBN (0) (see **SI, Figures S17 and S18** for more details). This method allows identification of samples containing higher ratios of CBN/($\Delta 9$ -THC + CBN) (> 0.6), for which the application of the CBN calibration curve would then be appropriate.

Analysis of (Mixed) Cannabis Extracts. Mixed Cannabis extracts set 1 and mixed Cannabis extracts set II (see **SI, Table S2**) were analyzed by Ag(I)-TLC coupled with smartphone detection (**SI, Figure S19A,B**). The $\Delta 9$ -THC calibration curve was applied to calculate the sum content of $\Delta 9$ -THC + CBN since the RGB color analysis showed that the marijuana extract has a CBN/($\Delta 9$ -THC + CBN) ratio

smaller than 0.6 (SI, **Figures S17 and S18**). The total Δ^9 -THC potential percentage was calculated and plotted against the spiked total Δ^9 -THC potential percentage. As shown in **Figure 4.6**, the calculated total Δ^9 -THC potential percentages have a good correlation with the spiked total Δ^9 -THC potential percentages for these two sets of samples ($R^2 = 0.97$), up to $\sim 1\%$. Apart from that, the curves representing two sets of samples almost overlap, which means that there is no obvious interference from CBD for the analysis of Δ^9 -THC analogues, due to the digital chromatographic separation by the developed Ag(I)-TLC plate. The results of CBD spiked samples also show the potential application of screening illegal CBD products according to diverse legislative status toward Δ^9 -THC (legal limit varies from 0.05% to 1%) and CBN (controlled substance in the U.K.) in CBD-related products among the world.^{42,43} Considering that the Ag(I) retention zone has the ability to retain CBD, CBG, and CBDA up to 10 μg (SI, **Figure S20**) and the linear range for Δ^9 -THC and CBN is 0.2–2 μg , the detectable ratio range of Δ^9 -THC/CBD would be limited to 0.02–0.2. However, according to our previous analysis results of commercially available oils labeled as “CBD oil,” four out of 10 CBD oils contained a Δ^9 -THC/CBD ratio higher than 0.02,²¹ which means they could also have been detected by this Ag(I)-TLC coupled with a smartphone.

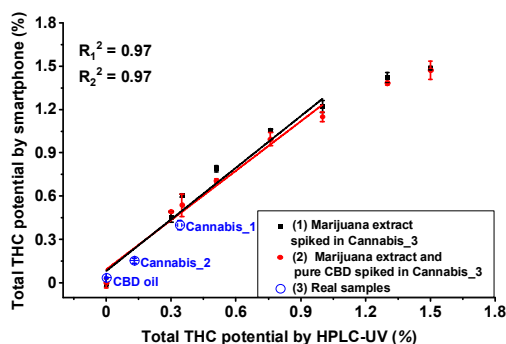


Figure 4.6. Relationship between total Δ^9 -THC potential percentage and normalized saturation of Δ^9 -THC analogues.

To explore the method for real samples, two Cannabis samples and one commercial CBD oil were analyzed as well (**SI, Figure S19C**). When performing RGB color analysis, Cannabis_1 and Cannabis_2 gave a result that indicated a CBN/(Δ^9 -THC + CBN) ratio higher than 0.6 (**SI, Figures S17 and S18**), which matches with the HPLC-UV results with a CBN/(Δ^9 -THC + CBN) ratio 0.7 for Cannabis_1 and 0.9 for Cannabis_2 (**SI, Table S1**). Therefore, the CBN calibration curve instead of Δ^9 -THC calibration curve was applied for calculating the sum of Δ^9 -THC + CBN. The obtained total Δ^9 -THC potential percentages from Cannabis_1, Cannabis_2, and CBD oil were compared with the HPLC-UV analysis (**Figure 4.6**). These results were consistent with HPLC-UV results, although the precision was worse (for HPLC-UV, RSD varies from 1.2% to 3.1%; for smartphone, RSD varies from 5.9% to 10.8%). The calculation of total Δ^9 -THC potential in this study may result in an overestimation of the psychoactive effects of the tested samples considering the lower potency of CBN (around 10%) compared with Δ^9 -THC. However, as a screening method, it can minimize false-negative results by reflecting the maximum psychoactive potential.

Conclusions

The Ag(I)-TLC smartphone method that we describe in this paper allows for a reliable semiquantitative analysis of total THCA, Δ^9 -THC, and CBN, which could be potentially applied in the field as a fast screening method for the classification of Cannabis varieties. The method is based on a different complexation of Δ^9 -THC analogues and CBD analogues with Ag(I) ions, leading in turn to good separation of these cannabinoid classes. As Δ^9 -THC analogues migrate out of the Ag(I) area, interference from Ag(I) with the color analysis is avoided. Afterward, smartphone image analysis affords a semiquantitative tool for determining total Δ^9 -THC analogues percentage. Furthermore, based on different RGB color information of Δ^9 -THC and CBN spots, a distinction between high ratio (> 0.6) of CBN/(Δ^9 -THC + CBN) and low ratio (≤ 0.6) of CBN/(Δ^9 -THC + CBN) could be achieved. Multiple Cannabis herbal samples can be analyzed simultaneously by the developed method

within 10 min, requiring only a few milliliters of solvent. The good correspondence between HPLC-UV and the Ag(I)-TLC methods for different samples confirms the applicability of the current method. Samples identified as positive by our cheap and fast screening method can then be retested in the lab by a validated quantitative method, such as HPLC-UV. The developed method reinvigorates TLC analysis of Δ^9 -THC analogues and requires no special instruments. Thus, it could be useful on-site and affordable to local authorities and small laboratories due to its simplicity, low operating cost, and use of inexpensive and general instruments, and seems an ideal approach to conduct large-scale surveillance programs for the rapid detection and content determination of cannabinoids. Apart from that, this method is also promising to be applied for Cannabis freshness identification and Δ^9 -THC screening in CBD products.

Supporting Information

The supporting information is available free of charge at <https://pubs.acs.org/doi/10.1021/acs.analchem.2c01627>, and the table of contents is presented below.

Supporting Information Table of Contents

Figure S1	HPLC-UV calibration curves of Δ^9 -THC, CBN, THCA, CBD, CBG and CBDA	Page S3
Table S1	THCA, CBN, Δ^9 -THC, CBD, CBG and CBDA content in samples	Page S4
Table S2	Preparation of mixed Cannabis extracts	Page S5
Figure S2	Design of Ag(I)-TLC plate	Page S6
Protocol S1	Optimization of TLC plates	Page S7
Figure S3	Images of different storage conditions for Ag(I)-TLC plates	Page S8
Figure S4	Glass spray bottle for spraying color reagents	Page S8
Figure S5	Images of light box for controlling photographing conditions	Page S9
Figure S6	Photographs of Ag(I)-TLC plates for parameter optimization	Page S10
Figure S7	Resolution of standards and analysis time under different experimental parameters by Ag(I)-TLC	Page S11
Protocol S2	Procedure for extracting cannabinoids from TLC plates	Page S13

Table S3	LC-MS/MS acquisitions parameters for the 12 cannabinoids	Page S14
Figure S8	Image of separation of THC and CBD on Ag(I)-TLC plates stored under different conditions and duration	Page S15
Figure S9	Absolute R_f of Δ^9 -THC and CBD obtained by Ag (I)-TLC plates stored under different conditions and duration	Page S16
Figure S10	Photographs of preparative normal TLC and Ag(I)-TLC for separation of 'standard_mixture' and 'sample_mixture'	Page S17
Figure S11	HPLC-MRM chromatograms of cannabinoids in 'standard_mixture' before and after separation by normal TLC and Ag(I)-TLC	Page S18
Figure S12	HPLC-MRM chromatograms of cannabinoids in 'sample_mixture' before and after separating by normal TLC and Ag(I)-TLC	Page S19
Figure S13	Chemical structures of cannabinoids separated by Ag(I)-TLC plate	Page S20
Figure S14	Calibration curves between Δ^9 -THC, CBN, THCA amount on Ag(I)-TLC plate and smartphone signal	Page S20
Figure S15	Images of various amounts of Δ^9 -THC, CBN and THCA analyzed by Ag(I)-TLC plate	Page S20
Figure S16	Photographs of Ag(I)-TLC plates with Δ^9 -THC + CBN standard mixtures and relationship between normalized saturation signal and CBN/(Δ^9 -THC + CBN) ratio	Page S21
Figure S17	Relationship between normalized (B-R) signal and CBN/(Δ^9 -THC + CBN) ratio	Page S23
Figure S18	Images of samples accompanied with standards analyzed by Ag(I)-TLC plate	Page S24
Figure S19	Images of samples analyzed by Ag(I)-TLC plate	Page S25
Figure S20	Images of various amounts of CBD, CBG and CBDA analyzed by Ag(I)-TLC plate	Page S27
References		Page S28

Acknowledgments

The authors acknowledge support from the National Natural Science Foundation of China (21775040, 21775041, 21575040), the China Scholarship Council 2020 International Cooperation Training Program for Innovative Talents, the Aid Program for S&T Innovation Research Team in Higher Education Institutions, the Construction Program of Key Disciplines of Hunan Province

(2015JC1001), the Project of Hunan Provincial Department of Education (17C0947), and the Hunan Province 100 Experts Project.

References

- (1) Fishedick, J. T. Identification of terpenoid chemotypes among high (–)-trans- Δ^9 -tetrahydrocannabinol-producing *Cannabis sativa* L. cultivars. *Cannabis and Cannabinoid research* **2017**, *2*, 34–47.
- (2) Nachnani, R.; Raup-Konsavage, W. M.; Vrana, K. E. The pharmacological case for cannabigerol. *Journal of Pharmacology and Experimental Therapeutics* **2021**, *376*, 204–212.
- (3) Trofin, I. G.; Vlad, C. C.; Noja, V. V.; Dabija, G. Identification and characterization of special types of herbal Cannabis. *UPB Buletin Stiintific, Series B: Chemistry and Materials Science* **2012**, *74*, 119–130.
- (4) Radwan, M. M.; Chandra, S.; Gul, S.; ElSohly, M. A. Cannabinoids, phenolics, terpenes and alkaloids of Cannabis. *Molecules* **2021**, *26*, 2774.
- (5) Sharma, P.; Murthy, P.; Bharath, M. S. Chemistry, metabolism, and toxicology of Cannabis: clinical implications. *Iranian Journal of Psychiatry* **2012**, *7*, 149–156.
- (6) Martínez, V.; Iriondo De-Hond, A.; Borrelli, F.; Capasso, R.; Del Castillo, M. D.; Abalo, R. Cannabidiol and other non-psychoactive cannabinoids for prevention and treatment of gastrointestinal disorders: useful nutraceuticals? *International Journal of Molecular Sciences* **2020**, *21*, 3067.
- (7) Roman, M. G.; Houston, R. Investigation of chloroplast regions rps16 and clpP for determination of *Cannabis sativa* crop type and biogeographical origin. *Legal Medicine* **2020**, *47*, 101759.
- (8) Pavlovic, R.; Nenna, G.; Calvi, L.; Panzeri, S.; Borgonovo, G.; Giupponi, L.; Cannazza, G.; Giorgi, A. Quality traits of “cannabidiol oils”: cannabinoids content, terpene fingerprint and oxidation stability of European commercially available preparations. *Molecules* **2018**, *23*, 1230.
- (9) Hazekamp, A.; Tejkalová, K.; Papadimitriou, S. Cannabis: from cultivar to chemovar II—a metabolomics approach to Cannabis classification. *Cannabis and Cannabinoid Research* **2016**, *1*, 202–215.
- (10) Fishedick, J. T.; Glas, R.; Hazekamp, A.; Verpoorte, R. A qualitative and quantitative HPTLC densitometry method for the analysis of cannabinoids in *Cannabis sativa* L. *Phytochemical Analysis* **2009**, *20*, 421–426.
- (11) Brighenti, V.; Protti, M.; Anceschi, L.; Zanardi, C.; Mercolini, L.; Pellati, F. Emerging challenges in the extraction, analysis and bioanalysis of cannabidiol and related compounds. *Journal of Pharmaceutical and Biomedical Analysis* **2021**, *192*, 113633.
- (12) Gülck, T.; Möller, B. L. Phytocannabinoids: origins and biosynthesis. *Trends in Plant Science* **2020**, *25*, 985–1004.
- (13) Liu, Y.; Brettell, T. A.; Victoria, J.; Wood, M. R.; Staretz, M. E. High performance thin-layer chromatography (HPTLC) analysis of cannabinoids in Cannabis extracts. *Forensic Chemistry* **2020**, *19*, 100249.
- (14) Sanchez, L.; Baltensperger, D.; Korouski, D. Raman-based differentiation of hemp, cannabidiol-rich hemp, and Cannabis. *Analytical Chemistry* **2020**, *92*, 7733–7737.
- (15) Sanchez, L.; Filter, C.; Baltensperger, D.; Korouski, D. Confirmatory non-invasive and non-destructive differentiation between hemp and Cannabis using a hand-held Raman spectrometer. *RSC Advances* **2020**, *10*, 3212–3216.
- (16) del Mar Contreras, M.; Jurado-Campos, N.; Callado, C. S.-C.; Arroyo-Manzanares, N.; Fernández, L.; Casano, S.; Marco, S.; Arce, L.; Ferreira-Vera, C. Thermal desorption-ion mobility spectrometry: a rapid sensor for the detection of cannabinoids and discrimination of *Cannabis sativa* L. chemotypes. *Sensors and Actuators B: Chemical* **2018**, *273*, 1413–1424.
- (17) Bruni, A.; Rodrigues, C.; dos Santos, C.; de Castro, J.; Mariotto, L.; Sinhorini, L. Analytical challenges for identification of new psychoactive substances: a literature-based study for seized drugs. *Brazilian Journal of Analytical Chemistry* **2021**.
- (18) Goutam, S.; Goutam, M.; Yadav, P. Thin layer chromatographic analysis of psychoactive plant *Cannabis sativa* L. *International Journal of Multidisciplinary Approach and Studies* **2015**, *2*, 166–175.

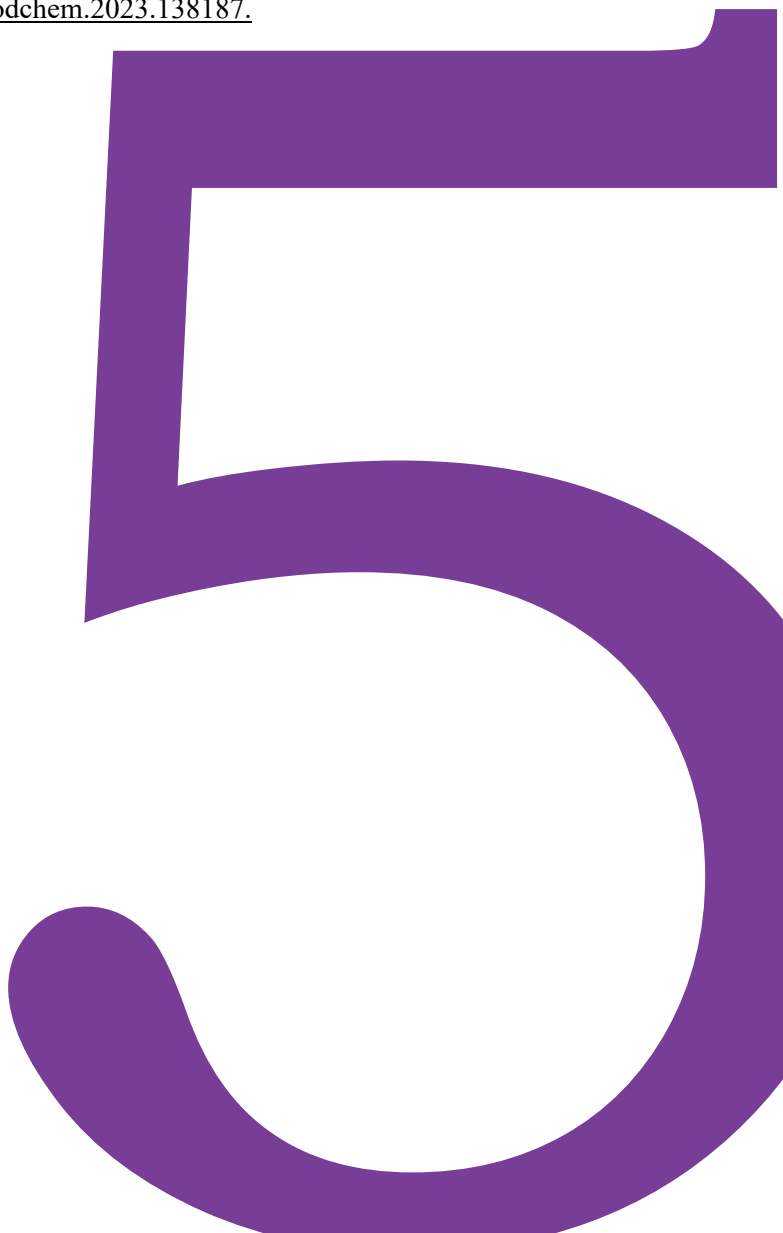
- (19) Tsujikawa, K.; Okada, Y.; Segawa, H.; Yamamuro, T.; Kuwayama, K.; Kanamori, T.; Iwata, Y. T. Thin-layer chromatography on silver nitrate-impregnated silica gel for analysis of homemade tetrahydrocannabinol mixtures. *Forensic Toxicology* **2022**, *40*, 125-131.
- (20) Xu, L.; Shu, T.; Liu, S. Simplified quantification of representative bioactives in food through TLC image analysis. *Food Analytical Methods* **2019**, *12*, 2886-2894.
- (21) van Beek, T. A.; Subrtova, D. Factors involved in the high pressure liquid chromatographic separation of alkenes by means of argentation chromatography on ion exchangers: overview of theory and new practical developments. *Phytochemical Analysis* **1995**, *6*, 1-19.
- (22) Kaneti, J.; de Smet, L. C.; Boom, R.; Zuilhof, H.; Sudhölter, E. J. Computational probes into the basis of silver ion chromatography. II. silver(I)-olefin complexes. *The Journal of Physical Chemistry A* **2002**, *106*, 11197-11204.
- (23) Damyanova, B.; Momtchilova, S.; Bakalova, S.; Zuilhof, H.; Christie, W. W.; Kaneti, J. Computational probes into the conceptual basis of silver ion chromatography: I. silver (I) ion complexes of unsaturated fatty acids and esters. *Journal of Molecular Structure: THEOCHEM* **2002**, *589*, 239-249.
- (24) Huang, S.; Claassen, F. W.; van Beek, T. A.; Chen, B.; Zeng, J.; Zuilhof, H.; Salentijn, G. I. Rapid distinction and semiquantitative analysis of THC and CBD by silver-impregnated paper spray mass spectrometry. *Analytical Chemistry* **2021**, *93*, 3794-3802.
- (25) Zhou, B.; Tan, M.; Lu, J.-f.; Zhao, J.; Xie, A.-f.; Li, S.-p. Simultaneous determination of five active compounds in *chimonanthus nitens* by double-development HPTLC and scanning densitometry. *Chemistry Central Journal* **2012**, *6*, 1-5.
- (26) Stroka, J.; Anklam, E. Development of a simplified densitometer for the determination of aflatoxins by thin-layer chromatography. *Journal of Chromatography A* **2000**, *904*, 263-268.
- (27) Chen, W.; Yao, Y.; Chen, T.; Shen, W.; Tang, S.; Lee, H. K. Application of smartphone-based spectroscopy to biosample analysis: a review. *Biosensors and Bioelectronics* **2021**, *172*, 112788.
- (28) Fan, Y.; Li, J.; Guo, Y.; Xie, L.; Zhang, G. Digital image colorimetry on smartphone for chemical analysis: a review. *Measurement* **2021**, *171*, 108829.
- (29) Ross, G. M.; Bremer, M. G.; Nielen, M. W. Consumer-friendly food allergen detection: moving towards smartphone-based immunoassays. *Analytical and Bioanalytical Chemistry* **2018**, *410*, 5353-5371.
- (30) Silver, J. Let us teach proper thin layer chromatography technique! *Journal of Chemical Education* **2020**, *97*, 4217-4219.
- (31) Sarma, N. D.; Waye, A.; ElSohly, M. A.; Brown, P. N.; Elzinga, S.; Johnson, H. E.; Marles, R. J.; Melanson, J. E.; Russo, E.; Deyton, L. Cannabis inflorescence for medical purposes: USP considerations for quality attributes. *Journal of Natural Products* **2020**, *83*, 1334-1351.
- (32) Tsumura, Y.; Aoki, R.; Tokieda, Y.; Akutsu, M.; Kawase, Y.; Kataoka, T.; Takagi, T.; Mizuno, T.; Fukada, M.; Fujii, H. A survey of the potency of Japanese illicit Cannabis in fiscal year 2010. *Forensic Science International* **2012**, *221*, 77-83.
- (33) Franca, H. S.; Acosta, A.; Jamal, A.; Romao, W.; Mulloor, J.; Almirall, J. R. Experimental and *ab initio* investigation of the products of reaction from Δ^9 -tetrahydrocannabinol (Δ^9 -THC) and the fast blue BB spot reagent in presumptive drug tests for cannabinoids. *Forensic Chemistry* **2020**, *17*, 100212.
- (34) Galand, N.; Ernouf, D.; Montigny, F.; Dollet, J.; Pothier, J. Separation and identification of Cannabis components by different planar chromatography techniques (TLC, AMD, OPLC). *Journal of Chromatographic Science* **2004**, *42*, 130-134.
- (35) Momtchilova, S.; Nikolova-Damyanova, B. Stationary phases for silver ion chromatography of lipids: preparation and properties. *Journal of Separation Science* **2003**, *26*, 261-270.
- (36) McRae, G.; Melanson, J. E. Quantitative determination and validation of 17 cannabinoids in Cannabis and hemp using liquid chromatography-tandem mass spectrometry. *Analytical and Bioanalytical Chemistry* **2020**, *412*, 7381-7393.
- (37) Scheunemann, A.; Elsner, K.; Germerott, T.; Hess, C.; Röhrich, J. Simultaneous quantification of 18 different phytocannabinoids in serum using a highly sensitive liquid chromatography-

- tandem mass spectrometry (LC-MS/MS) method. *Journal of Chromatography B* **2021**, 1173, 122685.
- (38) Gul, W.; Gul, S. W.; Radwan, M. M.; Wanas, A. S.; Mehmedic, Z.; Khan, I. I.; Sharaf, M. H.; ElSohly, M. A. Determination of 11 cannabinoids in biomass and extracts of different varieties of Cannabis using high-performance liquid chromatography. *Journal of AOAC International* **2015**, 98, 1523-1528.
- (39) Casajuana Kögel, C.; López-Pelayo, H.; Balcels-Olivero, M. M.; Colom, J.; Gual, A. Psychoactive constituents of Cannabis and their clinical implications: a systematic review. *Adicciones* **2018**, 30, 140-151.
- (40) Gaoni, Y.; Mechoulam, R. Isolation and structure of DELTA.-tetrahydrocannabinol and other neutral cannabinoids from hashish. *Journal of the American Chemical Society* **1971**, 93, 217-224.
- (41) Jang, E.; Kim, H.; Jang, S.; Lee, J.; Baeck, S.; In, S.; Kim, E.; Kim, Y.-u.; Han, E. Concentrations of THC, CBD, and CBN in commercial hemp seeds and hempseed oil sold in Korea. *Forensic Science International* **2020**, 306, 110064.
- (42) Hazekamp, A. The trouble with CBD oil. *Medical Cannabis and Cannabinoids* **2018**, 1, 65-72.
- (43) Liebling, J. P.; Clarkson, N. J.; Gibbs, B. W.; Yates, A. S.; O'Sullivan, S. E. An analysis of over-the-counter cannabidiol products in the United Kingdom. *Cannabis and Cannabinoid Research* **2022**, 7, 207-213.

Comprehensive Cannabinoid Profiling of Acid-Treated CBD Samples and Δ^8 -THC-Infused Edibles

This chapter was published as:

Huang, S.; van Beek, T. A.; Claassen, F. W.; Janssen, H.-G.; Ma, M.; Chen, B.; Zuilhof, H.; Salentijn, G. IJ. Comprehensive cannabinoid profiling of acid-treated CBD samples and Δ^8 -THC-infused edibles. *Food Chemistry* **2024**, 440, 138187. <https://doi.org/10.1016/j.foodchem.2023.138187>.



Abstract

Δ^8 -Tetrahydrocannabinol (THC) is increasingly popular as a controversial substitute for Δ^9 -THC in cannabinoid-infused edibles. Δ^8 -THC is prepared from cannabidiol (CBD) by treatment with acids. Side products including Δ^9 -THC and other isomers that might end up in Δ^8 -THC edibles are less studied. In this paper, three orthogonal methods, namely reversed-phase (RP)-UHPLC-DAD/HRMS, normal-phase/argentation (silica-Ag(I))-HPLC-DAD/MS, and GC-FID/MS were developed for analysis of cannabinoid isomers, namely Δ^8 -THC, Δ^9 -THC, CBD, Δ^8 -iso-THC, $\Delta(4)8$ -iso-THC, and hydrated THC isomers. Eight acid-treated CBD mixtures contained various amounts of Δ^8 -THC (0–89%, w/w%), high levels of Δ^9 -THC (up to 49%), Δ^8 -iso-THC (up to 55%), $\Delta(4)8$ -iso-THC (up to 17%), and three hydrated THC isomers. Commercial Δ^8 -THC gummies were also analyzed, and issues like overclaimed Δ^8 -THC, excessive Δ^9 -THC, undeclared Δ^8 -iso-THC, and $\Delta(4)8$ -iso-THC were found. These findings highlight the urgency of improving regulations toward converting CBD to Δ^8 -THC for use as food ingredients.

Introduction

Cannabinoid-infused edibles containing e.g., cannabidiol (CBD) and recently $\Delta 8$ -tetrahydrocannabinol ($\Delta 8$ -THC), but lacking $\Delta 9$ -tetrahydrocannabinol ($\Delta 9$ -THC), are becoming increasingly popular for therapeutic or recreational purposes.^{1,2} The U.S. Agriculture Improvement Act of 2018 (2018 Farm Bill) legalized hemp and hemp-derived products containing no more than 0.3% of $\Delta 9$ -THC on a dry weight basis.³ However, the 2018 Farm Bill does not regulate $\Delta 8$ -THC, which possesses similar therapeutic and mild psychoactive effects as $\Delta 9$ -THC.⁴ In 1995, $\Delta 8$ -THC underwent its initial assessment as an anti-emetic remedy in a trial involving eight children undergoing chemotherapy.⁵ Subsequently, $\Delta 8$ -THC was found to produce a dose-dependent response leading to euphoria, blurred vision, mental confusion, and lethargy with around 75% of the potency of $\Delta 9$ -THC.⁶ It is therefore not surprising that $\Delta 8$ -THC-infused edibles are pursued as a legal substitution of $\Delta 9$ -THC by consumers.⁷

Due to the negligible occurrence of natural $\Delta 8$ -THC in Cannabis,⁸ $\Delta 8$ -THC for consumption is typically produced by acid-catalyzed intramolecular cyclization of CBD.⁹ $\Delta 8$ -THC-infused products are often marked as “hemp-derived” or “legal high” products in different formulations, e.g., vape oils, gummies, and chocolates, with attractive packaging and are easy to acquire in stores or online. Some “home-kitchen” protocols for making $\Delta 8$ -THC edibles from CBD are also easily available on websites. However, there is no regulation or monitoring for producing $\Delta 8$ -THC from CBD, and such acid induced intramolecular cyclization is normally versatile with not only $\Delta 8$ -THC but also $\Delta 9$ -THC and other cannabinoids formed. Subsequent infusing into a food matrix would result in concomitant concerns about the safety and legal status of $\Delta 8$ -THC edibles. We summarized 53 analysis reports of commercial $\Delta 8$ -THC products reported by the US Cannabis Council and the New Leafreport Research in 2021,^{10,11} and there were several issues concerning $\Delta 8$ -THC products including (i) unknown ingredients, (ii) no content label or incorrect $\Delta 8$ -THC content, and (iii) illegal levels of $\Delta 9$ -THC ($> 0.3\%$, **Supporting Information (SI), Figure S1**). While the latter is already worrisome, the presence of unknown

compounds from the Δ 8-THC producing process, without toxicity data, is potentially of even greater concern. Moreover, increasing hospitalizations induced by consuming Δ 8-THC edibles and other products further underlines the need to analyze the compositions after converting CBD to Δ 8-THC.⁷

Cannabinoids in edibles that should at least be analyzed are Δ 9-THC, tetrahydrocannabinolic acid (THCA), CBD, cannabidiolic acid (CBDA), and cannabinol (CBN).^{12,13} Recent research expanded the analytical scope with Δ 8-THC.¹⁴⁻¹⁶ As mentioned earlier, most Δ 8-THC found in the market is synthesized and thus unavoidably accompanied by other THC isomers.^{17,18} Advanced analytical methods to analyze Δ 8-THC, Δ 9-THC, and CBD in the presence of synthetic isomers have recently been published. These include a 2D high-performance liquid chromatography (HPLC) system (C6 Phenyl column as the first dimension and C18 as the second dimension) for analysis of Δ 8-THC, Δ 9-THC, CBD, Δ 6a,10a-THC, and Δ 10-THC in e-cigarettes,¹⁹ and poroshell C18 column with complex multi-step gradient conditions for analysis of Δ 8-THC, Δ 9-THC, Δ 6a,10a-THC, Δ 10-THC, and Δ 9,11-THC.²⁰ All these methods rely on reversed-phase separations and multiple reaction monitoring (MRM) mass spectrometry (MS), with the same MS/MS transitions for different isomers. As a consequence, multiple challenges remain to be addressed. First, due to their near-identical retention times, baseline separation between Δ 8-THC and Δ 9-THC is only achieved by resorting to highly efficient HPLC systems such as ultra-high-pressure liquid chromatography (UHPLC), or to the use of core-shell particles. Even then, isomers, e.g., Δ 9,11-THC that are coeluting with Δ 9-THC, interfere with their analysis.²⁰ Second, the lack of unique MRM transitions makes the identification of isomers problematic. Thus, given their near-identical retention times and lack of MS-based identification, a small variation in retention time can easily lead to misassignments. Kiselak et al.²¹ coupled RP-HPLC-MS with ion mobility spectrometry (IMS) to investigate formed cannabinoids when converting CBD to Δ 9-THC (or Δ 8-THC) at home. Even though they identified multiple unnatural cannabinoids, the isomers Δ 9-THC and Δ 8-THC were just partially separated and had the same MS fragments and collision cross sections,

hampering identification by IMS. Apart from that, two compounds eluting closely to $\Delta 8$ -THC and $\Delta 9$ -THC with identical MS fragments and collision cross sections as $\Delta 8$ -THC and $\Delta 9$ -THC could not be unambiguously identified. Ciolino et al.²² identified $\Delta 8$ -THC, $\Delta 9$ -THC, $\Delta 6a,10a$ -THC, $\Delta 10$ -THC and $\Delta 9,11$ -THC in commercial vaping liquids by GC-MS. However, all these THC isomers had to be silylated prior to separation, and no absolute quantification of $\Delta 8$ -THC and $\Delta 9$ -THC was achieved. Thus, despite the attention given to synthetic THC isomers when analyzing $\Delta 8$ -THC-related products, more efforts are needed in developing analytical methods and understanding product compositions, especially regarding the synthetic THC isomers, for both forensic purposes and health considerations.

In the current paper, we therefore set out to improve the analysis of cannabinoid isomers formed in the process of converting CBD to $\Delta 8$ -THC as well as their occurrence in cannabinoid-infused edibles ($\Delta 8$ -THC gummies). We thus aimed to first evaluate eight common synthetic protocols using acid catalysis to convert CBD to $\Delta 8$ -THC (including methods suggested for ‘use at home’). Different chromatographic methods, that are based on different principles were expected to jointly achieve improved separation and profiling of the cannabinoids from those mixtures: a) an RP-UHPLC-diode array detector (DAD)/high-resolution mass spectrometer (HRMS) method; b) a GC-flame ionization detector (FID)/MS method; c) a silica-Ag(I) HPLC-DAD/MS method. For the silica-Ag(I) HPLC-DAD/MS method, we hypothesized that Ag(I) affinity combined with the normal-phase separation mechanism could lead to improved separation of cannabinoids. Apart from that, Ag(I) adduct formation and unique MS/MS transitions were expected due to selective affinities of Ag(I) toward olefins with different numbers and positions of C=C double bonds.²³⁻²⁵ If so, characteristic fragments in the presence of Ag(I) could be used for more reliable identification of isomeric cannabinoids.

Materials and Methods

Chemicals and Reagents. Formic Acid (HPLC grade) and silver nitrate (analytical grade) were purchased from Fisher Scientific (Loughborough,

Leicestershire, UK). Acetonitrile (ACN, HPLC grade) and methanol (MeOH, HPLC grade) were obtained from VWR Chemicals (Gliwice, Poland). n-Hexane (hexane, HPLC grade) was obtained from Honeywell Riedel-de Haën (Seelze, Germany). Ethanol (EtOH, HPLC-grade) was purchased from Biosolve Chimie SARL (57260 Dieuze, France). Methyl *tert*-butyl ether (MTBE) was bought from Biosolve BV (Valkenswaard, the Netherlands). Deionized water was obtained from a Milli-Q direct ultrapure water system (18.2 M Ω ·cm, Milli-Q Integral 3 system, Millipore, USA). Δ^9 -THC standard was purified from Cannabis flowers. Crystalline CBD was purchased from CBDolie.nl. Δ^8 -THC and Δ^8 -iso-THC standards were isolated from acid-treated CBD.²⁶ The group of Prof. Passarella²⁷ kindly provided Δ^8 -iso-THC (for comparison with our isolated standard Δ^8 -iso-THC) and $\Delta(4)$ -iso-THC. According to NMR and peak integrations at DAD 215 nm (**SI, Figures S2 and S3**), the purity of these five standards was > 98 %. Normal gummies without cannabinoids were purchased from a local supermarket in Wageningen, the Netherlands, and labeled as N#1, N#2, and N#3. Δ^8 -THC gummies were bought online and named as C#1 and C#2.

RP-UHPLC-DAD/HRMS. A 1290 Infinity UHPLC system (Agilent Technologies, Santa Clara, United States) equipped with a Zorbax Eclipse Plus C18 column (2.1 \times 100 mm, 1.8 μ m; Agilent Technologies) was used with DAD and coupled to a Q-Exactive quadrupole orbitrap high-resolution mass spectrometer (Thermo Fisher Scientific, San Jose, CA, USA) via an electrospray ionization (ESI) interface. The mobile phase consisted of 5 mM formic acid in water (mobile phase A) and ACN (mobile phase B). The injection volume was 8 μ L. Isocratic elution was applied with 58% B at a flow rate of 0.50 mL·min⁻¹, unless otherwise specified. The resolution (R_s) of two peaks was calculated as follows:

$$R_s = \frac{(t_{R2} - t_{R1})}{0.85 \times (W_{1,h/2} + W_{2,h/2})}$$

t_{R1} , t_{R2} : retention time of two adjacent peaks; $W_{1,h/2}$, $W_{2,h/2}$: peak width at

half-height of two adjacent peaks.

Positive ionization mode MS was used with a mass resolution of 70,000 FWHM, a maximum injection time of 200 ms, a sheath gas flow rate of 36 (arbitrary units), and an auxiliary gas flow rate of 18 (arbitrary units). The capillary temperature was 320 °C and the S-lens RF level was 50 (arbitrary units). All full-scan measurements were performed with a scan range of m/z 100.0–1500.0. A normalized collision energy (NCE) of 40 V was applied for MS/MS fragmentation. Thermo Scientific Xcalibur 2.2 software was used for data acquisition and processing. The intensity of ions with m/z values within ± 5 ppm of the theoretical m/z was shown in the extracted ion chromatogram (EIC).

GC-FID/MS. An Agilent 5975C VL MSD GC-MS system (Agilent, Amstelveen, the Netherlands) equipped with a HP-5MS capillary column (5% phenylmethylpolysiloxane, 30 m \times 0.25 mm i.d. and 0.25 μ m film thickness, Agilent J&W GC column, Amstelveen, the Netherlands) was used for GC-FID/MS analysis with a split ratio of 1:1 to the FID and MS detector. The injection temperature was 250 °C and the carrier gas was He at a linear velocity of 29 cm·s⁻¹. For the fast analysis of $\Delta 8$ -THC, $\Delta 9$ -THC and CBD, the initial column temperature was 200 °C, which was ramped with 10 °C·min⁻¹ to 275 °C and kept at this temperature for 5 min (total analysis time is 12.5 min). For the analysis of the five isomers and samples, a two-step gradient temperature program was used with an initial column temperature of 200 °C, ramped with 1 °C·min⁻¹ to 222.5 °C. Then, the column temperature was ramped to 250 °C with 5 °C·min⁻¹ and kept at this temperature for 5 min (total analysis time of 33 min). 1 μ L of sample was injected with a split ratio of 1:10. The mass spectrometer was operated in the 70 eV electron ionization (EI) mode, scanning from m/z 35 to 500 at 4 spectra·s⁻¹. Actual measurements started 3.0 min after injection to protect the filament of the mass spectrometer.

Silica-Ag(I) HPLC-DAD/MS. A 1220 Infinity II liquid chromatography system (Agilent Technologies) equipped with a Nucleosil Ag(I) phase column (100

$\times 4.6$ mm, 3 μm ; custom packed at Agilent, Middelburg, the Netherlands) was used with DAD, or with a Linear Ion Trap mass spectrometer (ESI-LXQ, Thermo Fisher Scientific) via a custom-built ESI interface. Isocratic elution was applied with 1% ACN in hexane (v/v%) as mobile phase at a flow rate of $1.00\text{ mL}\cdot\text{min}^{-1}$. 5 μL of sample was injected. Since hexane cannot be easily used for stable ESI,²⁸ post-column mixing with a solution of AgNO_3 ($2.5 \times 10^{-5}\text{ M}$) in EtOH was used to assist ESI ionization and form silver adducts (see **SI, Protocol S1, Figure S4**). Ionization was performed in positive mode with capillary voltage 49 V, tube lens 85 V, capillary temperature $350\text{ }^\circ\text{C}$, and sheath gas flow rate of 15 (arbitrary units). All full-scan measurements were performed with a scan range of m/z 100.0–2000.0. For all MS/MS fragmentation measurements, collision induced dissociation (CID) energies were determined as the energy at which the target product ions had the highest abundance while the precursor ions had not yet disappeared completely. The isolation width was set to include all desired precursor ions. For accurate mass measurements of Ag(I) adducts and relevant fragments, a previously published Ag(I)-paper spray ionization method was used, in combination with a Q-Exactive mass spectrometer.²³

Calibration Curve Construction and Evaluation of LOD and LOQ. Stock solutions of Δ^8 -THC, Δ^9 -THC, and CBD were prepared in MeOH at $1.00\text{ mg}\cdot\text{mL}^{-1}$. Mixed standard solutions of 333, 167, 100, 10.0, 5.00 $\mu\text{g}\cdot\text{mL}^{-1}$ and $0.500\text{ }\mu\text{g}\cdot\text{mL}^{-1}$ were prepared in triplicate by mixing stock solutions and serially diluting them with MeOH, and were analyzed by RP-UHPLC-DAD and GC-FID. For silica-Ag(I) HPLC-DAD analysis, considering the incompatibility of the sample solvent with the mobile phase, 100 μL of the mixed standard solution was first blow-dried with N_2 and re-dissolved in 100 μL of mobile phase in a 1.8 mL HPLC vial with a micro-insert (200 μL , Fisher Scientific, Warsaw, Poland). Characteristic peak areas were plotted against the concentration to construct calibration curves for external standard quantification. For the determination of the limit of detection (LOD) and limit of quantification (LOQ), the peak height was used. Blanks (MeOH for RP-UHPLC-

DAD and GC-FID; MeOH blow-dried and redissolved in 1% ACN in hexane (v/v%) for silica-Ag(I) HPLC-DAD) were injected and standard deviations (SD) of the signal at the respective retention times of the analytes were determined. The LODs and LOQs were calculated as follows: $\text{LOD} = 3 \times \text{SD of blank/slope of the calibration curve}$; $\text{LOQ} = 10 \times \text{SD of blank/slope of the calibration curve}$.^{29,30} Samples with concentrations close to the calculated LODs were tested for confirmation.

Preparation of Mixtures Containing $\Delta 8$ -THC by Treatment of CBD with Acid. Eight reported methods (see SI, Figure S5 and Table S1) for producing “ $\Delta 8$ -THC” samples from CBD were carried out with minor modifications.^{21,27} In summary, different catalytic conditions were employed: p-toluenesulfonic acid with varying acid quantities and solvent types (Entries 1–4), boron trifluoride diethyl etherate ($\text{BF}_3 \cdot \text{OEt}_2$) catalysis in acetonitrile (Entry 5), sulfuric acid in ethanol (Entry 6), acetic acid in ethanol (Entry 7), and hydrochloric acid in ethanol (Entry 8). After workup (quenched with base solutions, washed with saturated aqueous NaHCO_3 and NaCl solutions, dried with Na_2SO_4 and filtered through filter paper. All eight reaction solutions were filtered through 0.2 μm PTFE membrane syringe filters (\varnothing 13 mm, Pall Corporation, Port Washington, NY, USA), and the solvent was evaporated under N_2 flow, followed by freeze-drying (FreeZone 2.5 L, Labconco, Kansas City, MO, USA) at -84°C for more than 24 h. The reaction products obtained by each method were dissolved in MeOH at $100\ \mu\text{g} \cdot \text{mL}^{-1}$ unless otherwise stated for RP-UHPLC-DAD/MS and GC-FID/MS analysis. For silica-Ag(I) HPLC-DAD/MS analysis, 100 μL of the methanolic solution was first blow-dried with N_2 and re-dissolved in 100 μL of 1% ACN in hexane (v/v%).

Gummy Extraction. 1.00 ± 0.06 g of normal gummy or $\Delta 8$ -THC gummy was weighed in a conical stopper flask and extracted with 200.00 mL of an MTBE/water 1/1 (v/v) solution by ice bath ultrasonication (Bandelin Sonorex, Rangendingen, Germany) for up to 40 min to fully dissolve the gummies. After waiting 10 min for

phase separation, the MTBE layer was filtered over 0.2 μm PTFE membrane syringe filters and then used for subsequent analysis.

Extraction Recovery. Four aliquots (1.00 mL each) of 100 $\mu\text{g}\cdot\text{mL}^{-1}$ CBD methanolic solution were blow-dried. After that, one aliquot was redissolved in MTBE and subjected to GC-FID/MS analysis. The remaining three aliquots were reconstituted with 1.00 mL of MTBE and 1.00 mL of water, followed by hand-shaking of 10 min. After a waiting period of 10 min for phase separation, 60 μL of the MTBE layer was taken for GC-FID/MS analysis.

$$\text{Extraction recovery(\%)} = (A_{\text{after extraction}}/A_{\text{without extraction}}) \times 100.$$

A is the GC-FID peak area of a specific cannabinoid.

Four aliquots (100 μL each) of methanolic solution consisting of 100 $\mu\text{g}\cdot\text{mL}^{-1}$ of Δ^8 -THC, Δ^9 -THC, Δ^8 -iso-THC, $\Delta(4)$ 8-iso-THC, and CBD (five-cannabinoid solution) went through the above procedure (volumes of 100 μL of MTBE and 100 μL of water) to evaluate the extraction recovery of each cannabinoid.

Matrix Effects, Accuracy, and Precision. *Matrix Effects.* Hundred μL of 100 $\mu\text{g}\cdot\text{mL}^{-1}$ five-cannabinoid methanolic solution was blow-dried and redissolved in 100 μL of normal gummy extract for GC-FID/MS and silica-Ag(I) HPLC-DAD analysis. The characteristic peak area of each cannabinoid in spiked normal gummy extract (sample type II) was compared with that in solvent (sample type I).

$$\text{Matrix effect(\%)} = ((A_{\text{II}}/A_{\text{I}}) - 1) \times 100.$$

A is the peak area of GC-FID or silica-Ag(I) HPLC-DAD (215 nm) of a specific cannabinoid.

Accuracy and Precision. Accuracy and precision of the method were evaluated at three concentration levels (weight percentage w/w%: low (0.02%), medium (0.1%) and high (0.2%)) in normal gummy N#2 extract ($n = 3$ per concentration). 100 μL of 20, 100, 200 $\mu\text{g}\cdot\text{mL}^{-1}$ five-cannabinoid methanolic solution was spiked in 1.00 mL of normal gummy extract N#2 (0.01 times of the total gummy weight) and blow-dried. Subsequently, 100 μL of MeOH was added for GC-FID/MS analysis

and 100 μL of 1% ACN in hexane (v/v%) was added for silica-Ag(I) HPLC-DAD analysis. The concentration of each cannabinoid was calculated by the established calibration curves.

The weight percentage was expressed as:

$$\text{Weight percentage (\%)} = (C \times V) / W \times 100$$

C: calculated concentration in extract ($\mu\text{g} \cdot \text{mL}^{-1}$); V: volume of extraction (mL); W: total gummy weight (μg).

Precision was calculated as the relative standard deviation (RSD%) ($n = 3$). Accuracy was calculated as the relative deviation (%) of the calculated mean value of weight percentage from the respective reference value.

Cannabinoid Gummy Analysis. Cannabinoid gummy C#1 and C#2 were extracted as described above ($n = 3$). 1.00 mL of the MTBE layer was filtered and then subjected to the analysis by GC-FID/MS and silica-Ag(I) HPLC-DAD methods for quantification of $\Delta 8$ -THC. For the quantification of other cannabinoids, the filtrate of the MTBE layer was concentrated 20 times by blow-drying and reconstitution before analysis. The percentage was expressed as aforementioned with a concentrating factor taken into account if used.

Results and Discussion

RP-UHPLC-DAD/HRMS for Separation and Identification of $\Delta 8$ -THC, $\Delta 9$ -THC, and CBD Standards. The ever-popular $\Delta 9$ -THC and CBD and increasingly popular $\Delta 8$ -THC are isomers, but have a different pharmacology, toxicology, and legal status. Therefore, discrimination and characterization of these three cannabinoids are of great importance. Methods applying RP-HPLC coupled to ultraviolet (UV) detection or DAD have been most frequently used, as reviewed recently by La Maida et al.⁶ Generally, long separation times (> 20 min) with high flow rates ($> 1 \text{ mL} \cdot \text{min}^{-1}$) have been used to achieve partial or baseline separation of $\Delta 8$ -THC and $\Delta 9$ -THC, and UV absorption spectra show no differences for the three isomers. Very recently, a RP-2D-HPLC system¹⁹ and a RP-superficially porous

column under a multi-step gradient elution²⁰ achieved separation of $\Delta 8$ -THC and $\Delta 9$ -THC in 10 min with R_s 2.5 and 1.4, respectively. Subsequently, ESI-MS/MS (MRM mode) with identical transitions was used for quantification.

In the present study, $\Delta 8$ -THC and $\Delta 9$ -THC were, after optimization, also resolved ($R_s = 1.8$) by RP-UHPLC (Figure 5.1A, and SI, Table S2 and Figure S6). When coupled to DAD and HRMS detectors, as expected, there was no selectivity in the UV absorption (SI, Figure S7), nor in the high-resolution mass spectra in positive ionization mode (Figure 5.1B), as described in other references.^{19,20,31} The attribution of compounds can thus only be made by comparison of chromatographic retention times (RTs) with the standards. However, if the RT shifts slightly across samples due to e.g., column degradation, sample overloading, variations of mobile phase, column temperature, pressure, incorrect analysis might ensue.³² Moreover, any co-eluting matrix compound or isomer would be detrimental to the performance, due to many shared fragments between those. Therefore, improved chromatographic separation and more specific MS information are needed.

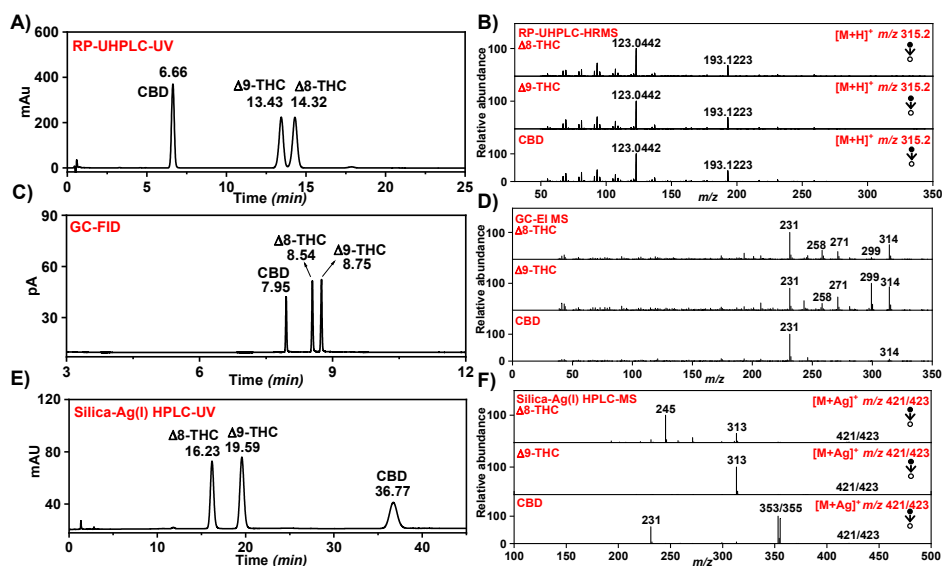


Figure 5.1. $\Delta 8$ -THC, $\Delta 9$ -THC, and CBD standards analyzed by A) RP-UHPLC-DAD, B) RP-UHPLC-HRMS/MS of $[M + H]^+$, C) GC-FID, D) GC-EI-MS, E) silica-Ag(I) HPLC-DAD and F) silica-Ag(I) HPLC-MS/MS of $[M + Ag]^+$.

GC-FID/MS for Separation and Identification of Δ 8-THC, Δ 9-THC, and CBD Standards. As second standard method, GC-FID/MS was applied for the analysis of the three neutral cannabinoids. Thermal decomposition should not pose a problem as these synthetic products typically do not contain acidic cannabinoids. Even if the starting CBD would contain acidic cannabinoids, acids were used in treating CBD and this would lead to decarboxylation.³³ As shown in **Figures 5.1C** and **5.1D**, Δ 8-THC, Δ 9-THC, and CBD were well resolved by the GC method (R_s of Δ 8-THC and Δ 9-THC is 3.1) in 9 min, and have distinct EI spectra. Combined with the merit of a short analysis time, GC-FID/MS is promising in the analysis of Δ 8-THC, Δ 9-THC, and CBD. However, a very recent study³⁴ observed the thermal decomposition of CBD to Δ 9-THC in the injector of the GC-MS system if the splitless mode was used, due to the longer residence time in the injector compared to split mode. Therefore, some caution is required and split injection with the injector temperature at 200 °C should be applied to avoid such decomposition.

Silica-Ag (I) HPLC-DAD/MS for Separation and Identification of Δ 8-THC, Δ 9-THC, and CBD Standards. In previous work, we separated Δ 9-THC from CBD by Ag(I)-loaded cation exchange HPLC-MS with MeOH as mobile phase and observed unique fragmentation of silver adducts.²³ This was based on the different affinity of Ag(I) for a single C=C bond versus that for two C=C bonds in 1,5-dienes. Therefore, we further explored whether Ag(I) affinity could enable improved separation and characterization of Δ 8-THC, Δ 9-THC, and CBD. Not unexpectedly, both Δ 8-THC and Δ 9-THC eluted close to the dead time with Δ 8-THC eluting 0.18 min earlier than Δ 9-THC on the Ag(I)-loaded cation exchanger (**SI, Figure S8**), due to their much weaker interactions with Ag(I) compared to CBD. As demonstrated by previous quantum chemical results,²³ CBD is bound to Ag(I) about 12 kcal·mol⁻¹ stabler than Δ 9-THC, and further quantum chemical computation (**SI, Figure S9**) showed that Δ 9-THC is bound to Ag(I) 5 kcal·mol⁻¹ more strongly than Δ 8-THC. Due to the lack of separation on the Ag(I)-loaded cation exchange column, an alternative approach was chosen, in which an Ag(I)-coated

silica gel column with 1% ACN in hexane (v/v%) as mobile phase was used for the separation of the three analytes. As shown in **Figure 5.1E**, excellent separation of Δ 8-THC and Δ 9-THC was obtained ($R_s = 4.5$), due to the combined contributions from normal-phase adsorption, Ag(I) complexation effects and long separation times.^{35,36} However, the applied mobile phase (1% ACN in hexane (v/v%)) cannot be used to produce a stable ESI spray, making it difficult to obtain MS information after the Ag(I)-coated silica chromatographic separation.

To overcome this, we employed the setup as shown in **Figure S4 (SI, Figure S4)**, by which both DAD and mass spectra could be collected after separation. This was achieved by combining the effluent of the HPLC column in a mixer with AgNO₃ in EtOH (2.5×10^{-5} M) to produce a stable spray to introduce Ag(I)-cannabinoid adducts to the MS. These adducts have unique fragmentation patterns, even for THC isomers (**Figure 5.1F**). Quasi-molecular species at m/z 421 and 423 were found for Δ 8-THC, Δ 9-THC and CBD with characteristic silver isotopes, ¹⁰⁷Ag (52%) and ¹⁰⁹Ag (48%). Different fragmentation patterns for Δ 8-THC, Δ 9-THC and CBD were found by utilizing m/z 422 as the precursor ion with an isolation width of 4 (thus containing both m/z 421 and 423). For CBD, main fragments were observed at m/z 353/355. For Δ 9-THC, there was only one product ion at m/z 313. However, for Δ 8-THC, apart from a minor fragment at m/z 313, the most prominent fragment was found at m/z 245.

Resolving THC Isomers by RP-UHPLC-DAD/HRMS, GC-FID/MS, and Silica-Ag(I) HPLC-DAD/MS. When treating CBD with acids for producing Δ 8-THC, the formation of various other THC isomers is hardly avoidable as reviewed by Golombek et al.¹⁷ The existence of multiple isomers may ruin the analysis of Δ 8-THC, Δ 9-THC and CBD when less selective methods are used.³⁷ Relatively few papers are devoted to chemical analysis of cannabinoids (only around 2% of all publications on Cannabis).³⁸ Recently published methods for the analysis of THC isomers mainly focus on resolving Δ 8-THC, Δ 9-THC and CBD from Δ 6a,10a-THC, Δ 10-THC, and Δ 9,11-THC.¹⁹⁻²² Still, there are also other THC isomers, namely Δ 8-

iso-THC and $\Delta(4)8$ -iso-THC, which are also found in acid-treated CBD mixtures,^{27,39} and even in commercial products.⁴⁰ However, apart from NMR^{27,40} there are hardly any other methods available to analyze these isomers in the presence of $\Delta 8$ -THC, $\Delta 9$ -THC and CBD. Marzullo et al.²⁷ applied RP-HPLC in an attempt to resolve $\Delta 8$ -iso-THC and $\Delta(4)8$ -iso-THC from $\Delta 8$ -THC and $\Delta 9$ -THC, but $\Delta 8$ -THC coeluted with $\Delta 8$ -iso-THC, and $\Delta 9$ -THC coeluted with $\Delta(4)8$ -iso-THC. Even $\Delta 8$ -THC and $\Delta 9$ -THC were only partially separated. Therefore, in the end, NMR was used together with the RP-HPLC method for the distinction and identification of these isomers in mixtures. However, larger amounts of samples are needed for NMR.

Here, we further evaluated the separation ability of the three chromatography-based methods with $\Delta 8$ -iso-THC and $\Delta(4)8$ -iso-THC being present in the standard mixture. As shown in **Figure 5.2A**, with RP-UHPLC, $\Delta 8$ -iso-THC had the same retention time as $\Delta 8$ -THC, and $\Delta(4)8$ -iso-THC overlapped with $\Delta 8$ -THC and $\Delta 9$ -THC. Furthermore, these two isomers have the same UV spectra (**SI, Figure S7**) and fragmentation patterns for protonated precursor ions (**SI, Figure S10**) as $\Delta 8$ -THC, $\Delta 9$ -THC and CBD. Therefore, when $\Delta 8$ -iso-THC and $\Delta(4)8$ -iso-THC are present, it is not possible to identify $\Delta 8$ -THC and $\Delta 9$ -THC by RP-UHPLC-DAD/HRMS (**Figure 5.2A** and **5.2B**).

With GC, using the aforementioned 12.5 min temperature program, $\Delta 8$ -THC, $\Delta 9$ -THC and CBD can be resolved, but $\Delta(4)8$ -iso-THC overlapped with CBD (**SI, Figure S11**). In this case, a two-step gradient and a longer (33 min) temperature program was applied for the separation of the five isomers (**Figure 5.2C**), and all of them produced distinct EI spectra (**Figure 5.2D**). Ciolino et al.²² also applied a two-step gradient temperature program with an analysis time of 39.9 min, and resolved various THC isomers that differ in the position of the C=C bond and/or stereochemistry (6aR,10aR- $\Delta 8$ -THC, 6aR,10aR-exo-THC, 6aR,10aR- $\Delta 9$ -THC, $\Delta 6a$,10a-THC, 6aR,9S- $\Delta 10$ -THC and 6aR,9R- $\Delta 10$ -THC), despite the partial overlap of $\Delta 6a$,10a-THC and $\Delta 10$ -THC. Even though their targets did not include acidic cannabinoids, they still carried out silylation before GC analysis, which took an additional 30 min.

When applying silica-Ag(I) HPLC-DAD/MS, both Δ^8 -iso-THC and $\Delta(4)$ 8-iso-THC were separated from the three major cannabinoids (**Figure 5.2E**). Apart from that, each isomer gave a different fragmentation pattern in the presence of Ag(I), with a unique fragment at m/z 419 for $\Delta(4)$ 8-iso-THC, and a characteristic favored fragment at m/z 299 for Δ^8 -iso-THC when fragmenting precursor ions at m/z 422 with an isolation width of 4 (thus including both m/z 421 and m/z 423) (**Figure 5.2F**). We further investigated the fragmentation of precursor ions at m/z 421 (isolation width of 1) and m/z 423 (isolation width of 1) separately (**SI, Figure S12**). It was shown that, for Δ^8 -iso-THC, this gave the characteristic fragment at m/z 299 in both cases. For $\Delta(4)$ 8-iso-THC, the precursor ion at m/z 423 yielded the fragment at m/z 421, while the precursor ion at m/z 421 yielded the fragment at m/z 419, which seemed to follow the fragmentation pathway $[M + Ag - 2H]^+$.

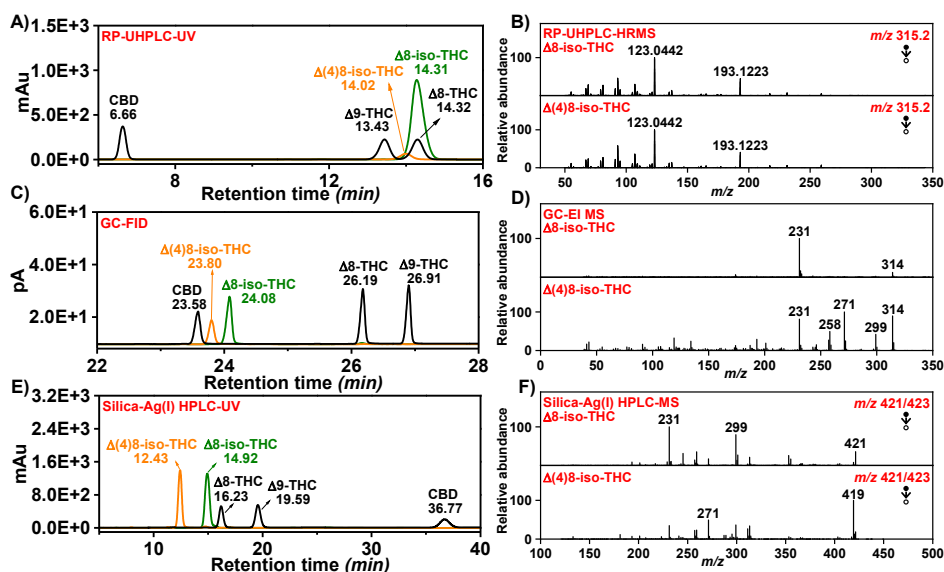


Figure 5.2. Δ^8 -iso-THC, $\Delta(4)$ 8-iso-THC, Δ^8 -THC, Δ^9 -THC, and CBD were analyzed by A) RP-UHPLC-DAD, B) RP-UHPLC-HRMS/MS of $[M + H]^+$, C) GC-FID, D) GC-EI-MS, E) silica-Ag(I) HPLC-DAD and F) silica-Ag(I) HPLC-MS/MS of $[M + Ag]^+$.

In our previous work, the MS fragmentation pathways of CBD and Δ^9 -THC with Ag(I) were proposed.²³ Here, we further propose a mechanism for the MS fragmentation of Δ^8 -THC in the presence of Ag(I). The accurate mass of Δ^8 -THC

Ag(I) adducts and their fragments were determined by Ag(I) paper spray-HRMS and plausible structures and their formation are presented in **Figure 5.3**. The $[\Delta 8\text{-THC} + \text{Ag}]^+$ adduct loses AgH during the MS² stage to form a tertiary carbocation (path ①). This carbocation undergoes methyl migration and rearrangement to form a new carbocation, stabilized by the lone pair on the oxygen. Afterward, a stable structure at m/z 245 was formed by the retro-Diels–Alder rearrangement.⁴¹ On the other hand, similar to $\Delta 9\text{-THC}$,²³ $[\Delta 8\text{-THC} + \text{Ag}]^+$ adducts could lose AgH during the MS² stage to form the fragment at m/z 313 stabilized by the aromatic ring with the phenolic group (path ②). However, since the C=C double bond of $\Delta 8\text{-THC}$ is between carbon atoms 8 and 9 instead of 9 and 10, the fragment is less stable than that of $\Delta 9\text{-THC}$. Additionally, the steric hindrance from the aromatic ring makes the H⁺ loss from carbon atom 10 as AgH less favored compared with path ①. Combined, for $\Delta 8\text{-THC}$, the signal at m/z 313 is less abundant than the signal at m/z 245. These distinctive MS² signals could thus be used for further confirmation of $\Delta 8\text{-THC}$, $\Delta 9\text{-THC}$, and CBD, in addition to assignments according to HPLC retention times of standards.

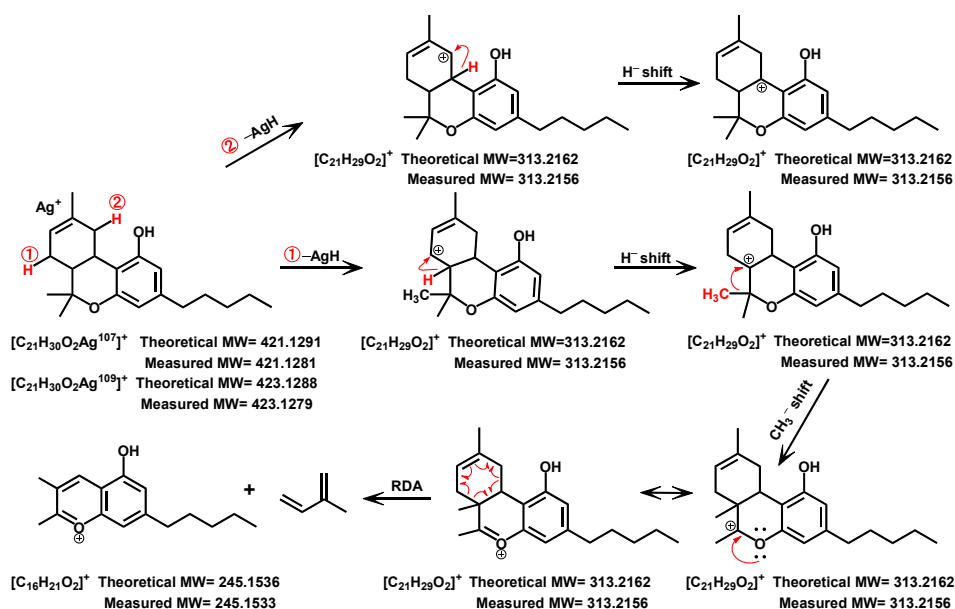


Figure 5.3. Proposed mechanism for MS² fragmentation of $\Delta 8\text{-THC}$ in the presence of Ag(I).

Investigation of Acid-treated CBD Mixtures by RP-UHPLC-DAD/HRMS, GC-FID/MS, and Silica-Ag(I) HPLC-DAD/MS. The increasing popularity of Δ^8 -THC products and the insufficient analysis of their composition threaten consumer health and induce potential legal issues. By following several common acid catalysis-based protocols to produce Δ^8 -THC from CBD, a better understanding is expected of the possible byproducts or impurities accompanying Δ^8 -THC. Briefly, different acids, solvents, and conditions were used to treat CBD. Among those protocols, concerning, some materials and procedures can be easily accessed and followed, and thus are described online for home-making of Δ^8 -THC. These acid-treated CBD mixtures were then analyzed by the developed methods in this study to investigate the composition. Even though the optimized RP-UHPLC-DAD/MS method properly resolved Δ^8 -THC, Δ^9 -THC, and CBD, it still cannot provide accurate identification of all compounds in the samples, as these (by the other two methods) were shown to contain multiple THC isomers like Δ^8 -iso-THC and $\Delta(4)$ 8-iso-THC. Therefore, GC-FID/MS and silica-Ag(I) HPLC-DAD/MS were used to investigate these acid-treated CBD mixtures.

First, the occurrence of Δ^8 -THC, Δ^9 -THC, CBD, Δ^8 -iso-THC and $\Delta(4)$ 8-iso-THC was checked by comparing the respective retention times and mass spectra (**SI, Figure S13**) with those of the standards. As shown in **Figure 5.4**, the product profiles vary substantially from protocol to protocol. In mixtures #1 and #2, CBD was not fully consumed and the major product is Δ^9 -THC followed by Δ^8 -THC, and then a little Δ^8 -iso-THC. Increasing the amount of acid (molar ratio of acid to CBD from 0.1 to 2) increased the conversion of CBD. In mixtures #3 and #4, the main product is Δ^8 -THC accompanied by trace amounts of Δ^9 -THC. $\Delta(4)$ 8-iso-THC was also detected in these two mixtures. When applying hexane as solvent (#4), $\Delta(4)$ 8-iso-THC signal was more pronounced, and additionally, Δ^8 -iso-THC was found. Compared with #1 and #2 (toluene as solvent), there was a trend of solvent selectivity, with toluene yielding more Δ^9 -THC and DCM or hexane yielding more Δ^8 -THC. When using $\text{BF}_3 \cdot \text{OEt}_2$ as a catalyst and performing the reaction at -10°C in ACN, Δ^8 -THC and Δ^9 -THC concentrations decreased, and instead, Δ^8 -iso-THC

and $\Delta(4)8$ -iso-THC dominated. In #6, #7 and #8, easily-accessible materials, namely ethanol (solvent), and battery acid (37% sulfuric acid), vinegar (5.4% acetic acid), or muriatic acid (30% hydrochloric acid) were used, respectively, and the reactions were conducted at 70 °C, which can be performed with ease in a home kitchen. In #6, four THC isomers were formed, predominately $\Delta 8$ -iso-THC, and only a bit of CBD remained unreacted. A similar profile was found for #8, except that no CBD was found and less $\Delta 8$ -THC was detected. Contrary to #6, in #7, no THC isomers were formed and mainly unreacted CBD was detected.

Except for the peaks identified by comparison with the five reference cannabinoids, there are multiple additional peaks in each. Three of them (initially named X1, X2, and X3) were isolated and RP-UHPLC-DAD/HRMS, GC-FID/MS, and silica-Ag(I) HPLC-DAD/MS (**SI, Figure S14**) analysis were performed. RP-UHPLC could resolve them and X3 had the same RT as CBD. The three isolated compounds also had the same UV spectra (**SI, Figure S7**), identical MS signals at m/z 315.2319 ($[M + H]^+$, $C_{21}H_{31}O_2$) (**SI, Figure S10**), and MS^2 fragments (**SI, Figure S15**) as $\Delta 8$ -THC, $\Delta 9$ -THC and CBD of m/z 315.2319. Apart from that, they all showed an extra signal in full-scan MS at m/z 333.2408 ($C_{21}H_{33}O_3$) (**SI, Figure S10**), which during fragmentation produced $[M - 18]^+$, likely resulting from the loss of H_2O , at m/z 315.2319 ($C_{21}H_{31}O_2$) (**SI, Figure S16**). Separation by the GC method showed molecular ion at m/z 332 (**SI, Figure S17**) for all three, confirming a molecular weight of 332 Da. Furthermore, the three compounds shared EI fragments at m/z 314 and 231 with $\Delta 8$ -THC, $\Delta 9$ -THC and CBD, implying a similar chemical structure. On the silica-Ag(I) HPLC column, the three compounds showed similar retention time (7.57 min for X1, 7.89 min for X2, and 7.48 min for X3) and clear Ag(I) adduct signals at m/z 439/441 ($[M + Ag]^+$) and m/z 771/773 ($[2M + Ag]^+$) (**SI, Figure S18**), again confirming a molecular weight of 332 Da for the three compounds. All combined, the three compounds were expected to be hydrated forms of $\Delta 8$ -THC, $\Delta 9$ -THC or CBD. Finally, by performing 700 MHz NMR analysis (**SI, Figure S19**) and comparison with recently identified cannabinoids,^{42,43} the compounds were assigned as follows: X1 = 9 β -hydroxyhexahydrocannabinol; X2 =

9 α -hydroxyhexahydrocannabinol; X3 = 8-hydroxy-isotetrahydrocannabinol. These compounds were observed in mixtures #3, 4, 6, and 8 by the GC-FID method, and in mixtures #1, 2, 3, 4, 5, 6, and 8 by the more sensitive RP-UHPLC-DAD method (SI, Figure S20). These findings suggest that these compounds, of which there is currently no toxicological knowledge, occur in many of these CBD reaction mixtures, which warrants further investigation.

In addition to these five THC isomers and three hydrated THC isomers, several minor peaks (especially in the last three samples) can be observed, reflecting the complexity of the product mixtures obtained by treating CBD with acids. There is little information regarding the toxicity and pharmacology of Δ^8 -THC, and nothing about Δ^8 -iso-THC, $\Delta(4)$ 8-iso-THC. Since these eight samples were converted from CBD by both lab-based protocols and kitchen-based protocols, they reflect, to some extent, the uncertainties about the composition of existing Δ^8 -THC products in the market, and point to potential risks for Δ^8 -THC consumers.

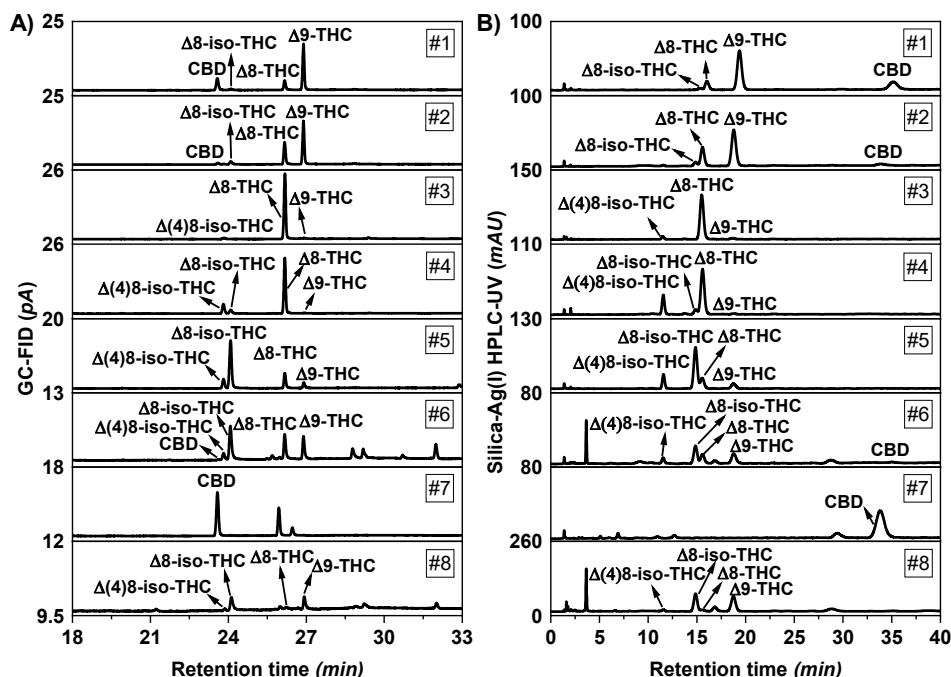


Figure 5.4. Detection of Δ^8 -THC, Δ^9 -THC, CBD, Δ^8 -iso-THC, and $\Delta(4)$ 8-iso-THC in acid-treated CBD mixtures by A) GC-FID and B) silica-Ag(I) HPLC-DAD (215 nm).

Quantification of Δ 8-THC, Δ 9-THC, CBD, Δ 8-iso-THC, and Δ (4)8-iso-THC by RP-UHPLC-DAD, GC-FID, and silica-Ag(I) HPLC-DAD. As mentioned earlier, there are many issues with commercially available Δ 8-THC products such as incorrectly labeled Δ 8-THC content, and high levels of Δ 9-THC. As such, it is important to understand how much of the different cannabinoids are present in acid-treated CBD mixtures for both investigative and legislative purposes. Therefore, further quantitative analysis of three major cannabinoids (Δ 8-THC, Δ 9-THC, and CBD) in the acid-treated CBD mixtures was conducted.

External calibration curves based on RP-UHPLC-DAD, silica-Ag(I) HPLC-DAD, and GC-FID were constructed (**SI, Figure S21**). LODs were calculated and solutions with cannabinoid concentrations close to the calculated LODs were analyzed (**SI, Figure S22**) to confirm the calculated LOD. The GC-FID method and the silica-Ag(I) HPLC-DAD method have the same linear range ($5.00\text{--}333\text{ }\mu\text{g}\cdot\text{mL}^{-1}$) (**SI, Table S3**). GC-FID has an LOD of $0.30\text{ }\mu\text{g}\cdot\text{mL}^{-1}$ for both Δ 8-THC and Δ 9-THC, and $1.3\text{ }\mu\text{g}\cdot\text{mL}^{-1}$ for CBD and the silica-Ag(I) HPLC-DAD method has LODs of $0.50\text{ }\mu\text{g}\cdot\text{mL}^{-1}$ for Δ 8-THC, $0.40\text{ }\mu\text{g}\cdot\text{mL}^{-1}$ for Δ 9-THC and $0.90\text{ }\mu\text{g}\cdot\text{mL}^{-1}$ for CBD. As a comparison, the RP-UHPLC-DAD method could achieve a wider linear range of $0.500\text{--}333\text{ }\mu\text{g}\cdot\text{mL}^{-1}$ with the lowest LOD: $0.020\text{ }\mu\text{g}\cdot\text{mL}^{-1}$ for all the three major cannabinoids. Even though the developed RP-UHPLC-DAD method cannot be used for analyzing the samples prepared in this study, it is a more sensitive method for quantifying Δ 8-THC, Δ 9-THC, and CBD, when there are no interferences of other THC isomers.

Next, all eight acid-treated CBD mixtures were analyzed by the GC-FID method and the silica-Ag(I) HPLC-DAD method. The results are summarized in **Table 5.1**. The plot of the quantitative HPLC results against the GC results of the three cannabinoids shows good correspondence between the two methods ($R^2 > 0.99$) (**SI, Figure S23**). Still, there is a large discrepancy for the Δ 8-THC percentage in sample #6 between the two methods (8.1% versus 6.5%) due to the insufficient separation of the Δ 8-iso-THC and Δ 8-THC peaks by the silica-Ag(I) HPLC-DAD method, resulting in an overestimation of Δ 8-THC. Also, for the quantification of

CBD, a deviation (6.9% versus 8.6%) is observed in sample #2, which is probably caused by the combined effects of a low CBD concentration in the sample and the relatively high detection limit for CBD by the GC-FID method ($1.3 \mu\text{g}\cdot\text{mL}^{-1}$), resulting an underestimation of CBD. Δ^9 -THC shows excellent correspondence between the various methods in all eight mixtures. This is especially important due to the strict legal limit for Δ^9 -THC. From the perspective of cannabinoid concentrations in the samples, Δ^8 -THC percentages vary from 0 to 89%. Despite Δ^8 -THC being advertised as a “legal high” product, there is little knowledge about its toxicity and pharmacology. Thus, consumers are inhaling or ingesting various amounts of Δ^8 -THC without knowing the consequences. On the other hand, with the exception of sample #7, all other samples contain considerable amounts of Δ^9 -THC (1.1–49%, w/w%), which are obviously all above the legal limit of 0.3%.¹¹ With respect to CBD, half of the mixtures contain residual CBD, with levels ranging from 3.5% to 53%. In the other mixtures, the complete reaction of CBD under acid and heat is obvious, even when using the mild reactions condition of procedure #8. It would be of interest to investigate to which extent such conversion might occur during the consumption of CBD from e-liquid, which is also heated during vaping.⁴⁴

Apart from the three major cannabinoids, the existence of Δ^8 -iso-THC and $\Delta(4)^8$ -iso-THC in some acid-treated CBD mixtures was significant and thus they were semiquantified by silica-Ag(I) HPLC-DAD and GC-FID methods using response factors (**SI, Protocol S2, Table S4**).⁴⁵ The majority of these acid-treated CBD mixtures contain Δ^8 -iso-THC (six out of eight, with percentages of 1.9–55%) and $\Delta(4)^8$ -iso-THC (five out of eight, with percentages of 0.32–17%). If such acid-treated CBD mixtures or infused samples are analyzed by commonly used RP-chromatography-based methods, overestimation of Δ^8 -THC content would occur due to the coelution of Δ^8 -iso-THC and Δ^8 -THC and the partial overlap of $\Delta(4)^8$ -iso-THC and Δ^8 -THC.²⁷ Such lack of separation in the most commonly used chromatographic approach could potentially explain issues with incorrectly labeled Δ^8 -THC content encountered in Δ^8 -THC products.

Table 5.1. Percentage (w/w%, after solvent evaporation) of Δ^8 -THC, Δ^9 -THC and CBD in acid-treated CBD mixtures analyzed by silica-Ag(I) HPLC-DAD (215 nm) and GC-FID.

Sample	Δ^8 -THC (w/w%)		Δ^9 -THC (w/w%)		CBD (w/w%)	
	GC-FID	Ag-LC-DAD	GC-FID	Ag-LC-DAD	GC-FID	Ag-LC-DAD
#1	11 (2.6%)	9.4 (2.1%)	49 (0.3%)	49 (2.6%)	26 (2.0%)	28 (2.4%)
#2	26 (4.0%)	25 (3.9%)	48 (0.1%)	49 (3.0%)	6.9 (0.4%)	8.6 (5.2%)
#3	78 (2.1%)	89 (4.0%)	1.6* (1.1%)	1.5* (11%)	ND	ND
#4	70 (1.8%)	70 (4.6%)	1.1* (5.6%)	1.1** (7.0%)	ND	ND
#5	14 (3.7%)	14 (6.7%)	6.3 (5.2%)	5.9 (5.7%)	ND	ND
#6	8.1 (0.5%)	6.5 (14.4%)	8.9 (1.2%)	8.2 (6.3%)	4.2 (0.2%)	3.5 (6.9%)
#7	ND	ND	ND	ND	48 (0.7%)	53 (12%)
#8	1.4 (1.1%)	1.6* (4.6%)	5.0 (2.5%)	4.8* (3.6%)	ND	ND

ND, non-detectable, i.e., <LOD. Values in brackets represent relative standard deviations ($n = 3$).

*Calculated based on 10 times concentrated sample; **calculated based on 50 times concentrated sample.

Analysis of Cannabinoid-infused Gummies and Evaluation of Extraction Recovery, Matrix Effects, Accuracy, and Precision. Previous experiments were focused on analyzing acid-treated CBD mixtures to understand which cannabinoids might be present after the chemistry, prior to infusion into edibles. While complex due to presence of isomers, as alluded to, the analysis is not complicated in terms of the matrix, as a fairly clean solution is obtained. To further explore the application potential of the developed methods, the composition of cannabinoid-infused edibles was assessed. An extraction and analysis protocol was developed for infused gummies, and extraction recovery, matrix effects, accuracy, and precision were evaluated.

Extraction Recovery. Neutral cannabinoids are relatively non-polar and are

well-soluble in e.g., ethanol, hexane, and MTBE.⁴⁶ Major components of gummies (gelatin, starch, sugars, flavors, and colorants), are well-soluble in water.⁴⁷ Therefore, a liquid-liquid extraction (LLE) with MTBE and water (1/1, v/v) was applied considering the higher polarity and lower toxicity of MTBE compared with hexane, as well as lower polarity than ethanol to exclude co-extracting of flavors and colorants.⁴⁶ Three normal gummies and two $\Delta 8$ -THC gummies were dissolved during ice-bath sonication for 20–40 min. After phase separation, a colorless, clear, and transparent MTBE layer was obtained (**SI, Figure S24**). To evaluate the partitioning of cannabinoids between MTBE and water phases, CBD was first used as a representative cannabinoid and showed an extraction recovery of $101 \pm 0.3\%$ with a total volume of extraction solvent of 2.00 mL, as determined by GC-FID. Afterwards, the five cannabinoid mixtures were also tested in the same way with a smaller volume of extraction solvent (200 μ L), and the extraction recovery for different cannabinoids varied from $100 \pm 17\%$ to $101 \pm 16\%$ (**SI, Table S5**). Despite the large relative standard deviation (RSD 15–17%), which can be attributed to the small extraction volume as it was not observed during the CBD extraction with 2 mL, all tested cannabinoids show approximately 100% extraction recovery.

Matrix Effects. Next, matrix effects of the two analytical methods were evaluated. Considering the unclear compositional information of commercial $\Delta 8$ -THC gummies, as well as the diversity of gummies in terms of composition, texture, and solubility (**SI, Table S6**), three varieties of normal gummies without cannabinoids were tested. For the GC-FID/MS method, the extractions of three normal gummies showed minor peaks, which were all distinct from peaks of the tested cannabinoids (**SI, Figure S25**). Matrix effects for the five cannabinoids varied from -2.6% to 14% (**SI, Table S7**). For the silica-Ag(I) HPLC-DAD method, extractions of all three normal gummies exhibited a clean background (**SI, Figure S26**), possibly due to the reconstitution step by a different solvent (mobile phase, 1% ACN in hexane (v/v%)) with different polarity from the extraction solvent MTBE, which provided further selectivity. At the same time, the additional blow-drying and reconstitution potentially introduced experimental errors, especially due to the small

sample volume (100 μL). Therefore, even though theoretically the silica-Ag(I) HPLC-DAD method should have limited matrix effects with the three tested normal gummies, deviations of -9.6% to 11% were observed for different cannabinoids (**SI, Table S7**), although this can likely be improved when larger sample volumes are used. In summary, the two developed methods showed acceptable matrix effects⁴⁸ with signal suppression $< 10\%$ and signal enhancement $< 14\%$ for five cannabinoids in three tested normal gummies.

Accuracy and Precision. Furthermore, accuracy and precision were evaluated by spiking standards into normal gummy #2, which was most similar in texture and solubility to the tested commercial $\Delta 8$ -THC gummies. Five-point calibration curves of $\Delta 8$ -THC, $\Delta 9$ -THC, CBD, $\Delta(4)8$ -iso-THC, and $\Delta 8$ -iso-THC were established (**SI, Figure S27**) and accuracy and precision at three different spiking weight percentages 0.02%, 0.1%, and 0.2% (low, medium, and high) were assessed. As shown in **Table S8 (SI, Table S8)**, both methods showed acceptable accuracy (bias from -12% to 19%)⁴⁸ and good precision (RSD 0.26–6.1%) for all investigated cannabinoids at different spiking weight percentages. The silica-Ag(I) HPLC-DAD method exhibited better accuracy than the GC-FID/MS method in general (bias -12 – 8.6% vs 3.0 – 19%).

Analysis of $\Delta 8$ -THC gummies. Finally, two $\Delta 8$ -THC gummies were analyzed by the developed methods (**SI, Figure S28**) and weight percentages of five isomeric cannabinoids were compared with the declared information in the certificate of analysis (**Table 5.2**). The results obtained by the two developed methods nicely corresponded. For sample C#1, $\Delta 8$ -THC (0.63% by silica-Ag(I) HPLC-DAD and 0.68% by GC-FID in this study vs 0.65% as declared), $\Delta 9$ -THC (0.015% by silica-Ag(I) HPLC-DAD and 0.014% by GC-FID in this study vs $< 0.050\%$ as declared) and CBD (not detected in all cases) results matched well with the declared contents. However, for sample #2, a lower content of $\Delta 8$ -THC (2.8% by silica-Ag(I) HPLC-DAD and 2.9% by GC-FID in this study vs 3.1% as declared) and higher content of $\Delta 9$ -THC (0.099% by silica-Ag(I) HPLC/DAD and 0.086% by GC-FID in this study vs $< 0.074\%$ as declared) were detected by the developed methods in this study,

whereas the declared CBD content matches with our results (not detected in this study vs $< 0.0010\%$ as declared). Moreover, Δ^8 -iso-THC and $\Delta(4)$ 8-iso-THC, about which no information is provided in the certificate of analysis, were found in both tested samples. C#1 only contained a small amount of $\Delta(4)$ 8-iso-THC (0.031% by silica-Ag(I) HPLC-DAD and 0.033% by GC-FID) and no Δ^8 -iso-THC but C#2 contained higher amounts of $\Delta(4)$ 8-iso-THC (0.13% by silica-Ag(I) HPLC-DAD and 0.12% by GC-FID) and Δ^8 -iso-THC (0.0072% by silica-Ag(I) HPLC-DAD and 0.0069% by GC-FID). On the one hand, the presence of $\Delta(4)$ 8-iso-THC and Δ^8 -iso-THC could partly explain the overestimation of Δ^8 -THC in the certificate of analysis (RP-HPLC-UV method was used). Crucially, such analysis highlights the necessity of methods to distinguish between THC isomers, such as demonstrated in this work. Moreover, it demonstrates the importance of providing qualitative and quantitative information to consumers, especially due to the fact that intoxication cases induced by consuming Δ^8 -THC gummies have already been reported.⁴⁹

Table 5.2. Percentage (w/w%) of $\Delta 8$ -THC, $\Delta 9$ -THC, $\Delta 8$ -iso-THC, $\Delta(4)8$ -iso-THC in $\Delta 8$ -THC gummies analyzed by silica-Ag(I) HPLC-DAD (215 nm) and GC-FID and compared with claimed information.

Sample	$\Delta 8$ -THC (w/w%)			$\Delta 9$ -THC (w/w%)			CBD (w/w%)			$\Delta 8$ -iso-THC (w/w%)			$\Delta(4)8$ -iso-THC (w/w%)		
	GC-FID	Ag(I) HPLC-DAD	Declared*	GC-FID	Ag(I) HPLC-DAD	Declared*	GC-FID	Ag(I) HPLC-DAD	Declared*	GC-FID	Ag(I) HPLC-DAD	Declared*	GC-FID	Ag(I) HPLC-DAD	Declared*
C#1	0.68 (1.8%)	0.63 (2.6%)	0.65	0.014 (4.4%)	0.015 (4.7%)	< 0.050	ND	ND	ND	ND	ND	NI	0.033 (2.3%)	0.031 (2.6%)	NI
C#2	2.9 (1.3%)	2.8 (1.4%)	3.1	0.086 (3.4%)	0.099 (3.1%)	0.074	ND	ND	< 0.0010	0.0069 (2.6%)	0.0072 (3.7%)	NI	0.12 (1.9%)	0.13 (6.8%)	NI

*Information provided by the certificate of analysis. ND, non-detectable, i.e., <LOD. NI, no information.

Conclusions

Three methods based on RP-UHPLC-DAD/HRMS, silica-Ag(I) HPLC-DAD/MS, and GC-FID/MS have been developed for the analysis of Δ^8 -THC related products with special emphasis on THC isomers. RP-UHPLC-DAD/MS provides sufficient separation of Δ^8 -THC, Δ^9 -THC, and CBD and is the most sensitive method. However, this method cannot resolve Δ^8 -THC from the interferences $\Delta(4)$ 8-iso-THC and Δ^8 -iso-THC in “ Δ^8 -THC” samples and gives identical MS/HRMS spectra for all five isomers. GC-FID/MS separated the five isomers with a two-step gradient temperature program in 33 min, and all isomers showed different EI spectra that thus allows identification. With an analysis time of 40 min, silica-Ag(I) HPLC-DAD/MS also achieved sufficient separation of the five isomers. Importantly, unique Ag(I) adduct fragmentation mass spectra for Δ^8 -THC, Δ^9 -THC, CBD, Δ^8 -iso-THC, and $\Delta(4)$ 8-iso-THC were obtained, which cannot be achieved by HRMS with protonated adducts. The GC-FID/MS method is faster and more robust in the analysis of cannabinoid mixtures, such as “ Δ^8 -THC” products, while silica-Ag(I) HPLC-DAD/MS provides an orthogonal method and distinct ESI spectra toward THC isomers. By analyzing eight of such “ Δ^8 -THC” samples from lab-based and kitchen-based syntheses starting from CBD, potential issues are revealed with regard to Δ^8 -THC edibles and other products in the market, including various amounts of Δ^8 -THC (0–89%), illegal levels of Δ^9 -THC of up to nearly 50%, and the presence of other known THC isomers and hydrated THC isomers. Subsequently, commercially available normal gummies were analyzed to evaluate matrix effects, accuracy, and precision of the developed methods in the situation of complex food analysis. Our silica-Ag(I) HPLC-DAD/MS method shows limited matrix effects and a higher accuracy for all five cannabinoid isomers compared to the GC-FID/MS method. Finally, two commercial Δ^8 -THC gummies were analyzed, and both Δ^8 -iso-THC and $\Delta(4)$ 8-iso-THC were observed. The existence of such, typically unspecified, THC isomers tends to result in overestimated Δ^8 -THC content, as evidenced by the certificate of analysis in which a RP-HPLC-UV method (with limited resolution toward Δ^8 -THC, Δ^8 -iso-THC and $\Delta(4)$ 8-iso-THC) was used. On

the other hand, underestimation of Δ^9 -THC in the certificate of analysis was found for one of the two gummies. In short, the developed silica-Ag(I) HPLC-DAD/MS method and GC-FID/MS method showed good applicability in the analysis of cannabinoid products. From a food science perspective, attention should be paid to cannabinoid isomers when analyzing cannabinoid products, considering their common existence, varied health effects and legal status. Moreover, analytical methods that can distinguish and quantify multiple isomers can provide consumers and regulation agencies with more accurate and complete information. From the analysis of real food products in this work, it is clear that such analytical methods are needed to provide a more complete overview of their cannabinoid profile. Moreover, such methods could lay the foundation for future investigations toward the toxicity of (un)known compounds, as well as for the identification of unknown compounds in cannabinoid products.

Supporting Information

The supporting information is available free of charge at <https://doi.org/10.1016/j.foodchem.2023.138187>, and the table of contents is presented below.

Supporting Information Table of Contents

Figure S1	Percentages of Δ^8 -THC and Δ^9 -THC in 53 commercial Δ^8 -THC products	Page S4
Figure S2	^1H NMR spectra of Δ^8 -THC, Δ^9 -THC, CBD, and Δ^8 -iso-THC	Page S6
Figure S3	RP-UHPLC-DAD (215nm) chromatograms of Δ^8 -THC, Δ^9 -THC, CBD, Δ^8 -iso-THC, and $\Delta(4)$ 8-iso-THC	Page S7
Protocol S1	Post-column introduction of AgNO_3 EtOH solution to normal-phase HPLC	Page S8
Figure S4	Setup of silica-Ag(I) HPLC coupled with DAD and MS detectors	Page S8
Figure S5	General reaction scheme of acid-treated cyclization of CBD for the synthesis of Δ^8 -THC	Page S9
Table S1	Reaction conditions of acid-treated cyclization of CBD for the synthesis of Δ^8 -THC	Page S9

Table S2	Conditions for RP-UHPLC separation of Δ 8-THC, Δ 9-THC, and CBD mixture	Page S11
Figure S6	RP-UHPLC-MS chromatograms of a mixture of Δ 8-THC, Δ 9-THC, and CBD under different conditions	Page S12
Figure S7	UV spectra of Δ 8-THC, Δ 9-THC, CBD, Δ 8-iso-THC, Δ (4)8-iso-THC, compound X1 (9 β -hydroxyhexahydrocannabinol), compound X2 (9 α -hydroxyhexahydrocannabinol), and compound X3 (8-hydroxy-iso-tetrahydrocannabinol)	Page S13
Figure S8	Strong cation exchange Ag(I) HPLC-DAD (215nm) chromatograms of Δ 8-THC, Δ 9-THC and CBD	Page S14
Figure S9	Computational structures of Δ 8-THC + Ag(I) and Δ 9-THC + Ag(I)	Page S15
Figure S10	Protonated HRMS full-scan spectra of Δ 8-THC, Δ 9-THC, CBD, Δ 8-iso-THC, Δ (4)8-iso-THC, compound X1 (9 β -hydroxyhexahydrocannabinol), 9 α -hydroxyhexahydrocannabinol, compound X2 (9 α -hydroxyhexahydrocannabinol), and compound X3 (8-hydroxy-iso-tetrahydrocannabinol).	Page S16
Figure S11	GC-FID profiles of Δ 8-iso-THC, Δ (4)8-iso-THC, Δ 8-THC, Δ 9-THC, and CBD	Page S17
Figure S12	Fragmentation of [Δ 8-iso-THC + Ag] ⁺ with precursor ions at m/z 422 (an isolation width of 4), m/z 423 (an isolation width of 1), m/z 421 (an isolation width of 1), and [Δ (4)8-iso-THC + Ag] ⁺ with precursor ions at m/z 422 (an isolation width of 4), m/z 423 (an isolation width of 1), m/z 421 (an isolation width of 1)	Page S18
Figure S13	Identification of cannabinoids in samples and compared to standards with GC-EI and silica-Ag(I) HPLC-MS/MS of [M + Ag] ⁺	Page S19–25
Figure S14	Compounds X1 (9 β -hydroxyhexahydrocannabinol), X2 (9 α -hydroxyhexahydrocannabinol), and X3 (8-hydroxy-iso-tetrahydrocannabinol) were analyzed by RP-UHPLC-DAD, GC-FID, and silica-Ag(I) HPLC-DAD	Page S26
Figure S15	Protonated HRMS MS ² spectra with m/z 315.2 as precursor ion of Δ 8-THC, Δ 9-THC, CBD, Δ 8-iso-THC, Δ (4)8-iso-THC, X1 (9 β -hydroxyhexahydrocannabinol), X2 (9 α -hydroxyhexahydrocannabinol), and X3 (8-hydroxy-iso-tetrahydrocannabinol) at normalized collision energy (NCE) of 40 V	Page S27
Figure S16	Protonated HRMS MS ² spectra with m/z 333.2 as precursor ion of X1 (9 β -	Page S28

	hydroxyhexahydrocannabinol), X2 (9 α -hydroxyhexahydrocannabinol), and X3 (8-hydroxy-iso-tetrahydrocannabinol) at normalized collision energy (NCE) of 20 V	
Figure S17	GC-EI spectrum of X1 (9 β -hydroxyhexahydrocannabinol), X2 (9 α -hydroxyhexahydrocannabinol), and X3 (8-hydroxy-iso-tetrahydrocannabinol)	Page S29
Figure S18	Ag(I) adduct signals of X1 (9 β -hydroxyhexahydrocannabinol), X2 (9 α -hydroxyhexahydrocannabinol), and X3 (8-hydroxy-iso-tetrahydrocannabinol)	Page S29
Figure S19	¹ H NMR spectra of X1 (9 β -hydroxyhexahydrocannabinol), X2 (9 α -hydroxyhexahydrocannabinol), and X3 (8-hydroxy-iso-tetrahydrocannabinol)	Page S32
Figure S20	Detection of X1 (9 β -hydroxyhexahydrocannabinol), X2 (9 α -hydroxyhexahydrocannabinol), and X3 (8-hydroxy-iso-tetrahydrocannabinol) in acid-treated CBD mixtures by RP-UHPLC-DAD (215 nm), RP-UHPLC-HRMS, and silica-Ag(I) HPLC-DAD	Page S33
Figure S21	Calibration curves of Δ 8-THC, Δ 9-THC, and CBD between characteristic peak areas and concentrations constructed by RP-UHPLC-DAD (215 nm), GC-FID, and silica-Ag(I) HPLC-DAD (215 nm)	Page S33
Figure S22	Δ 8-THC, Δ 9-THC, and CBD mixture analyzed by RP-UHPLC-DAD (215 nm), silica-Ag(I) HPLC-DAD (215 nm), and GC-FID	Page S34
Table S3	Calibration curves and LODs of Δ 8-THC, Δ 9-THC, and CBD by RP-UHPLC-DAD(215 nm), silica-Ag(I) HPLC-DAD (215 nm), and GC-FID	Page S34
Figure S23	Correlation of percentage (w/w%) of Δ 8-THC, Δ 9-THC, and CBD in acid-treated CBD mixtures analyzed by silica-Ag(I) HPLC-DAD (215 nm) and GC-FID	Page S35
Protocol S2	Semiquantification of Δ 8-iso-THC, and Δ (4)8-iso-THC in acid-treated CBD mixtures by silica-Ag(I) HPLC-DAD (215 nm) and GC-FID using response factor	Page S36
Table S4	Percentage of Δ 8-THC, Δ 9-THC, CBD, Δ 8-iso-THC, and Δ (4)8-iso-THC in acid-treated CBD mixtures analyzed by silica-Ag(I) HPLC-DAD (215 nm) and GC-FID	Page S36
Figure S24	Photos of dissolved gummies after phase separation by liquid-liquid extraction (water/MTBE)	Page S37

Table S5	Extraction recovery of Δ^8 -THC, Δ^9 -THC, CBD, Δ^8 -iso-THC, and $\Delta(4)$ 8-iso-THC	Page S37
Table S6	Ingredients, texture, and solubility of gummies investigated in this study	Page S38
Figure S25	GC-FID profiles of normal gummies and standard spiked normal gummy	Page S39
Figure S26	Silica-Ag(I) HPLC-DAD (215 nm) profiles of normal gummies and standard spiked normal gummy	Page S40
Table S7	Matrix effect of GC-FID/MS and silica-Ag(I) HPLC-DAD methods	Page S41
Table S8	Accuracy and precision of GC-FID/MS and silica-Ag(I) HPLC-DAD methods	Page S41
Figure S27	Calibration curves of Δ^8 -THC, Δ^9 -THC, CBD, Δ^8 -iso-THC, and $\Delta(4)$ 8-iso-THC between characteristic peak areas and concentrations constructed by silica-Ag(I) HPLC-DAD (215 nm) and GC-FID	Page S42
Figure S28	Silica-Ag(I) HPLC-DAD (215 nm) and GC-FID profiles of Δ^8 -THC gummies	Page S43
References		Page S44

Acknowledgments

The authors thank prof. Daniele Passarella group from the Dipartimento di Chimica, Università degli Studi di Milano, Milano, Italy for kindly providing Δ^8 -iso-THC and $\Delta(4)$ 8-iso-THC, dr. Muthusamy Subramaniam for helpful discussions, and Hans Beijleveld for technical support. We acknowledge support from the National Natural Science Foundation of China (22276050, 22276049), the China Scholarship Council 2020 International Cooperation Training Program for Innovative Talents, and the Hunan Province 100 experts project.

References

- (1) Leas, E. C.; Nobles, A. L.; Shi, Y.; Hendrickson, E. Public interest in Δ 8-tetrahydrocannabinol (Δ 8-THC) increased in US states that restricted Δ 9-tetrahydrocannabinol (Δ 9-THC) use. *International Journal of Drug Policy* **2022**, *101*, 103557.
- (2) Peng, H.; Shahidi, F. Cannabis and Cannabis edibles: a review. *Journal of Agricultural and Food Chemistry* **2021**, *69*, 1751-1774.
- (3) Congress. *Agricultural improvement act of 2018*; **2018**. Retrieved from United States Government. <https://www.congress.gov/115/plaws/publ334/PLAW-115publ334.pdf> (accessed 2024 July 24).
- (4) Casajuana Kögel, C.; López-Pelayo, H.; Balcells-Olivero, M. M.; Colom, J.; Gual, A. Psychoactive constituents of Cannabis and their clinical implications: a systematic review. *Adicciones* **2018**, *30*, 140-151.
- (5) Abrahamov, A.; Abrahamov, A.; Mechoulam, R. An efficient new cannabinoid antiemetic in pediatric oncology. *Life Sciences* **1995**, *56*, 2097-2102.
- (6) La Maida, N.; Di Giorgi, A.; Pichini, S.; Busardò, F. P.; Huestis, M. A. Recent challenges and trends in forensic analysis: Δ 9-THC isomers pharmacology, toxicology and analysis. *Journal of Pharmaceutical and Biomedical Analysis* **2022**, *220*, 114987.
- (7) LoParco, C. R.; Rossheim, M. E.; Walters, S. T.; Zhou, Z.; Olsson, S.; Sussman, S. Y. Δ 8-tetrahydrocannabinol: a scoping review and commentary. *Addiction* **2023**, *118*, 1011-1028.
- (8) Gülck, T.; Möller, B. L. Phytocannabinoids: origins and biosynthesis. *Trends in Plant Science* **2020**, *25*, 985-1004.
- (9) Duffy, B. C.; Li, L.; Lu, S.; Dittmar, M. A.; Delaney-Baldwin, E.; Durocher, L. A.; Spink, D. C. Chemotyping of Δ 8-THC-containing e-liquids analyzed during the 2019–2020 New York State EVALI investigation. *Journal of Analytical Toxicology* **2022**, *46*, 743-749.
- (10) Council, U. S. C. *The unregulated distribution and sale of consumer products marketed as delta-8 THC*; **2021**. <https://irp.cdn-website.com/6531d7ca/files/uploaded/USCC%20Delta-8%20Kit.pdf> (accessed 2024 May 27).
- (11) Gleb, O. *New leafreport research reveals more than 50% of delta-8 THC hemp-derived products tested had illegal levels of delta-9 THC*; **2022**. <https://www.leafreport.com/education/delta-8-thc-products-market-report-11339> (accessed May 27, 2024).
- (12) AOAC. *AOAC SMPR® 2017.019 Standard method performance requirements (SMPRs®) for quantitation of cannabinoids in edible chocolate*; **2017**. Retrieved from AOAC International. https://www.aoac.org/wp-content/uploads/2020/11/SMPR202017_019.pdf (accessed 2024 July 7).
- (13) AOAC. *AOAC SMPR® 2022.001 Quantitation of cannabinoids in beverages*; **2022**. Retrieved from AOAC International. https://www.aoac.org/wp-content/uploads/2022/11/SMPR-2022_001.pdf (accessed 2024 July 7).
- (14) Christinat, N.; Savoy, M.-C.; Mottier, P. Development, validation and application of a LC-MS/MS method for quantification of 15 cannabinoids in food. *Food Chemistry* **2020**, *318*, 126469.
- (15) Pisciotto, I. D. M.; Guadagnuolo, G.; Soprano, V.; Esposito, M.; Gallo, P. A survey of Δ 9-THC and relevant cannabinoids in products from the Italian market: A study by LC-MS/MS of food, beverages and feed. *Food Chemistry* **2021**, *346*, 128898.
- (16) Song, L.; Meyer, G.; Adejumo, E.; Jovanovich, E.; LeBlanc, L.; Provis, J. Potency testing of up to sixteen cannabinoids in hemp-infused edibles using liquid chromatography diode array detector with optional confirmation of identity by electrospray ionization time-of-flight mass spectrometry. *Food Chemistry* **2023**, *417*, 135819.
- (17) Golombek, P.; Müller, M.; Barthlott, I.; Sproll, C.; Lachenmeier, D. W. Conversion of cannabidiol (CBD) into psychotropic cannabinoids including tetrahydrocannabinol (THC): a controversy in the scientific literature. *Toxics* **2020**, *8*, 41.
- (18) Helander, A.; Johansson, M.; Andersson, A.; Villén, T. Analytical and medico-legal problems linked to the presence of Δ 8-tetrahydrocannabinol (Δ 8-THC): results from urine drug testing in Sweden. *Drug Testing and Analysis* **2022**, *14*, 371-376.

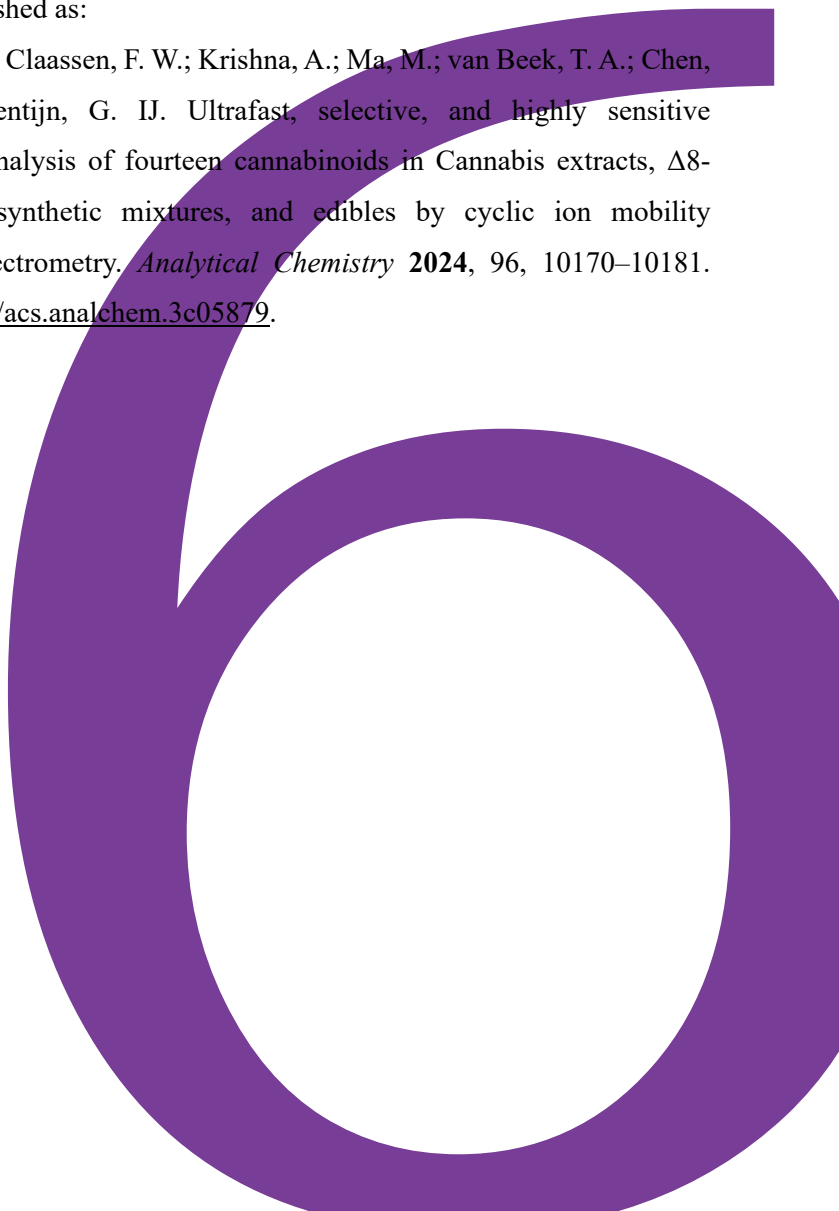
- (19) Chan-Hosokawa, A.; Nguyen, L.; Lattanzio, N.; Adams, W. R. Emergence of delta-8 tetrahydrocannabinol in DUID investigation casework: method development, validation and application. *Journal of Analytical Toxicology* **2022**, *46*, 1-9.
- (20) Reber, J. D.; Karschner, E. L.; Seither, J. Z.; Knittel, J. L.; Dozier, K. V.; Walterscheid, J. P. An enhanced LC-MS-MS technique for distinguishing Δ^8 - and Δ^9 -tetrahydrocannabinol isomers in blood and urine specimens. *Journal of Analytical Toxicology* **2022**, *46*, 343-349.
- (21) Kiselak, T. D.; Koerber, R.; Verbeck, G. F. Synthetic route sourcing of illicit at home cannabidiol (CBD) isomerization to psychoactive cannabinoids using ion mobility-coupled-LC-MS/MS. *Forensic Science International* **2020**, *308*, 110173.
- (22) Ciolino, L. A.; Ranieri, T. L.; Brueggemeyer, J. L.; Taylor, A. M.; Mohrhaus, A. S. EVALI vaping liquids part 1: GC-MS cannabinoids profiles and identification of unnatural THC isomers. *Frontiers in Chemistry* **2021**, *9*, 746479.
- (23) Huang, S.; Claassen, F. W.; van Beek, T. A.; Chen, B.; Zeng, J.; Zuilhof, H.; Salentijn, G. I. Rapid distinction and semiquantitative analysis of THC and CBD by silver-impregnated paper spray mass spectrometry. *Analytical Chemistry* **2021**, *93*, 3794-3802.
- (24) Kaneti, J.; de Smet, L. C.; Boom, R.; Zuilhof, H.; Sudhölter, E. J. Computational probes into the basis of silver ion chromatography. II. silver(I)-olefin complexes. *The Journal of Physical Chemistry A* **2002**, *106*, 11197-11204.
- (25) van Beek, T. A.; Subrtova, D. Factors involved in the high pressure liquid chromatographic separation of alkenes by means of argentation chromatography on ion exchangers: overview of theory and new practical developments. *Phytochemical Analysis* **1995**, *6*, 1-19.
- (26) Citti, C.; Linciano, P.; Forni, F.; Vandelli, M. A.; Gigli, G.; Laganà, A.; Cannazza, G. Analysis of impurities of cannabidiol from hemp. Isolation, characterization and synthesis of cannabidibutol, the novel cannabidiol butyl analog. *Journal of pharmaceutical and biomedical analysis* **2019**, *175*, 112752.
- (27) Marzullo, P.; Foschi, F.; Coppini, D. A.; Fanchini, F.; Magnani, L.; Rusconi, S.; Luzzani, M.; Passarella, D. Cannabidiol as the substrate in acid-catalyzed intramolecular cyclization. *Journal of Natural Products* **2020**, *83*, 2894-2901.
- (28) Zhang, J.-T.; Wang, H.-Y.; Zhu, W.; Cai, T.-T.; Guo, Y.-L. Solvent-assisted electrospray ionization for direct analysis of various compounds (complex) from low/nonpolar solvents and eluents. *Analytical Chemistry* **2014**, *86*, 8937-8942.
- (29) Shrivastava, A.; Gupta, V. B. Methods for the determination of limit of detection and limit of quantitation of the analytical methods. *Chronicles of Young Scientists* **2011**, *2*, 21-25.
- (30) Villela, A.; Van der Klift, E. J.; Mattheussens, E. S.; Derksen, G. C.; Zuilhof, H.; Van Beek, T. A. Fast chromatographic separation for the quantitation of the main flavone dyes in Reseda luteola (weld). *Journal of Chromatography A* **2011**, *1218*, 8544-8550.
- (31) Lin, L.; Amaratunga, P.; Reed, J.; Huang, P.; Lemberg, B. L.; Lemberg, D. Quantitation of Δ^8 -THC, Δ^9 -THC, cannabidiol and 10 other cannabinoids and metabolites in oral fluid by HPLC-MS-MS. *Journal of Analytical Toxicology* **2022**, *46*, 76-88.
- (32) Wang, Y.; Ma, L.; Zhang, M.; Chen, M.; Li, P.; He, C.; Yan, C.; Wan, J.-B. A simple method for peak alignment using relative retention time related to an inherent peak in liquid chromatography-mass spectrometry-based metabolomics. *Journal of Chromatographic Science* **2019**, *57*, 9-16.
- (33) Zhang, X.; Geng, Z.; Wang, Y. Density functional theory study of the mechanism of the acid-catalyzed decarboxylation of pyrrole-2-carboxylic acid and mesitoic acid. *Science China Chemistry* **2011**, *54*, 762-768.
- (34) Tsujikawa, K.; Okada, Y.; Segawa, H.; Yamamuro, T.; Kuwayama, K.; Kanamori, T.; Iwata, Y. T. Thermal decomposition of CBD to Δ^9 -THC during GC-MS analysis: a potential cause of Δ^9 -THC misidentification. *Forensic Science International* **2022**, *337*, 111366.
- (35) Adlof, R. O. Normal-phase separation effects with lipids on a silver ion high-performance liquid chromatography column. *Journal of Chromatography A* **1997**, *764*, 337-340.
- (36) Huang, S.; Qiu, R.; Fang, Z.; Min, K.; Van Beek, T. A.; Ma, M.; Chen, B.; Zuilhof, H.; Salentijn, G. I. Semiquantitative screening of THC analogues by silica gel TLC with an Ag(I) retention zone and chromogenic smartphone detection. *Analytical Chemistry* **2022**, *94*, 13710-13718.

- (37) Lachenmeier, D. W.; Habel, S.; Fischer, B.; Herbi, F.; Zerbe, Y.; Bock, V.; de Rezende, T. R.; Walch, S. G.; Sproll, C. Are adverse effects of cannabidiol (CBD) products caused by tetrahydrocannabinol (THC) contamination? *F1000Research* **2023**, *8*, 1394.
- (38) Gertsch, J. Analytical and pharmacological challenges in Cannabis research. *Planta Medica* **2018**, *84*, 213-213.
- (39) Gaoni, Y.; Mechoulam, R. The iso-tetrahydrocannabinols. *Israel Journal of Chemistry* **1968**, *6*, 679-690.
- (40) Meehan-Atrash, J.; Rahman, I. Novel Δ 8-tetrahydrocannabinol vaporizers contain unlabeled adulterants, unintended byproducts of chemical synthesis, and heavy metals. *Chemical Research in Toxicology* **2021**, *35*, 73-76.
- (41) Tureček, F.; Hanuš, V. Retro-Diels-Alder reaction in mass spectrometry. *Mass Spectrometry Reviews* **1984**, *3*, 85-152.
- (42) Cheng, L.-J.; Xie, J.-H.; Chen, Y.; Wang, L.-X.; Zhou, Q.-L. Enantioselective total synthesis of (–)- Δ 8-THC and (–)- Δ 9-THC via catalytic asymmetric hydrogenation and SNAr cyclization. *Organic Letters* **2013**, *15*, 764-767.
- (43) Radwan, M. M.; Wanas, A. S.; Gul, W.; Ibrahim, E. A.; ElSohly, M. A. Isolation and characterization of impurities in commercially marketed Δ 8-THC products. *Journal of Natural Products* **2023**, *86*, 822-829.
- (44) Czégény, Z.; Nagy, G.; Babinszki, B.; Bajtel, Á.; Sebestyén, Z.; Kiss, T.; Csupor-Löffler, B.; Tóth, B.; Csupor, D. CBD, a precursor of THC in e-cigarettes. *Scientific Reports* **2021**, *11*, 8951.
- (45) Cuadros-Rodríguez, L.; Bagur-González, M. G.; Sánchez-Vinas, M.; González-Casado, A.; Gómez-Sáez, A. M. Principles of analytical calibration/quantification for the separation sciences. *Journal of Chromatography A* **2007**, *1158*, 33-46.
- (46) López-Olmos, C.; García-Valverde, M. T.; Hidalgo, J.; Ferrerio-Vera, C.; Sánchez de Medina, V. Comprehensive comparison of industrial cannabinoid extraction techniques: Evaluation of the most relevant patents and studies at pilot scale. *Frontiers in Natural Products* **2022**, *1*, 1043147.
- (47) Burey, P.; Bhandari, B.; Rutgers, R.; Halley, P.; Torley, P. Confectionery gels: a review on formulation, rheological and structural aspects. *International Journal of Food Properties* **2009**, *12*, 176-210.
- (48) SWGTOX. Scientific working group for forensic toxicology (SWGTOX) standard practices for method validation in forensic toxicology. *Journal of Analytical Toxicology* **2013**, *37*, 452-474.
- (49) Akpunonu, P.; Baum, R. A.; Reckers, A.; Davidson, B.; Ellison, R.; Riley, M.; Trecki, J.; Gerona, R. Sedation and acute encephalopathy in a pediatric patient following ingestion of delta-8-tetrahydrocannabinol gummies. *The American Journal of Case Reports* **2021**, *22*, e933488-933481.

Ultrafast, Selective, and Highly Sensitive Non-chromatographic Analysis of Fourteen Cannabinoids in Cannabis Extracts, Δ^8 -Tetrahydrocannabinol Synthetic Mixtures, and Edibles by Cyclic Ion Mobility Spectrometry-Mass Spectrometry

This chapter was published as:

Huang, S.; Righetti, L.; Claassen, F. W.; Krishna, A.; Ma, M.; van Beek, T. A.; Chen, B.; Zuilhof, H.; Salentijn, G. IJ. Ultrafast, selective, and highly sensitive nonchromatographic analysis of fourteen cannabinoids in Cannabis extracts, Δ^8 -tetrahydrocannabinol synthetic mixtures, and edibles by cyclic ion mobility spectrometry-mass spectrometry. *Analytical Chemistry* **2024**, 96, 10170–10181. <https://doi.org/10.1021/acs.analchem.3c05879>.



Abstract

The diversity of cannabinoid isomers and complexity of Cannabis products pose significant challenges for analytical methodologies. In this study, we developed a method to analyze 14 different cannabinoid isomers in diverse samples within milliseconds by leveraging the unique adduct-forming behavior of silver ions in advanced cyclic ion mobility spectrometry-mass spectrometry. The developed method achieved the separation of isomers from four groups of cannabinoids: Δ^3 -tetrahydrocannabinol (THC) (**1**), Δ^8 -THC (**2**), Δ^9 -THC (**3**), cannabidiol (CBD) (**4**), Δ^8 -iso-THC (**5**), and $\Delta^4(8)$ -iso-THC (**6**) (all MW = 314); 9α -hydroxyhexahydrocannabinol (**7**), 9β -hydroxyhexahydrocannabinol (**8**), and 8-hydroxy-iso-THC (**9**) (all MW = 332); tetrahydrocannabinolic acid (THCA) (**10**) and cannabidiolic acid (CBDA) (**11**) (both MW = 358); Δ^8 -tetrahydrocannabivarin (THCV) (**12**), Δ^8 -iso-THCV (**13**), and Δ^9 -THCV (**14**) (all MW = 286). Moreover, experimental and theoretical traveling wave collision cross section values in nitrogen ($^{TW}CCS_{N_2}$) of cannabinoid-Ag(I) species were obtained for the first time with an average error between experimental and theoretical values of 2.6%. Furthermore, a workflow for the identification of cannabinoid isomers in Cannabis and Cannabis-derived samples was established based on three identification steps (m/z and isotope pattern of Ag(I) adducts, $^{TW}CCS_{N_2}$, and MS/MS fragments). Afterward, calibration curves of three major cannabinoids were established with a linear range of 1–250 ng·ml⁻¹ for Δ^8 -THC (**2**) ($R^2 = 0.9999$), 0.1–25 ng·ml⁻¹ for Δ^9 -THC (**3**) ($R^2 = 0.9987$), and 0.04–10 ng·ml⁻¹ for CBD (**4**) ($R^2 = 0.9986$) as well as very low limits of detection (0.008–0.2 ng·ml⁻¹). Finally, relative quantification of Δ^8 -THC (**2**), Δ^9 -THC (**3**), and CBD (**4**) in eight complex acid-treated CBD mixtures was achieved without chromatographic separation. The results showed good correspondence ($R^2 = 0.999$) with those obtained by gas chromatography-flame ionization detection/mass spectrometry.

Introduction

Given the continuous growth of the Cannabis market and the variable composition of Cannabis products, comprehensive, sensitive, selective, and reliable analytical methods for the determination of cannabinoids, which are diverse and broad in occurrence, are needed to facilitate forensic oversight and understand health impact.¹ Special focus is required on cannabinoid isomers, which — although similar in structure — can have highly varied pharmacology and legal status. The isomeric complexity of Cannabis-derived products extends far beyond the common isomers in Cannabis extracts, such as tetrahydrocannabinolic acid (THCA), cannabidiolic acid (CBDA), Δ^9 -tetrahydrocannabinol (THC), and cannabidiol (CBD). For instance, the common reaction of treating CBD with acid yields multiple classes of structural isomers, such as the THC isomers: Δ^8 -THC, Δ^9 -THC, Δ^3 -THC, Δ^8 -iso-THC, and $\Delta(4)$ 8-iso-THC and hydrated THC isomers such as 8-hydroxy-iso-THC and 9 α -hydroxyhexahydrocannabinol.²⁻⁴ The pharmacological effects of these byproducts have not been extensively studied, yet these compounds end up in popular Δ^8 -THC-containing products. These are bought by consumers for recreational or medicinal purposes, alarmingly resulting in increasing hospitalization cases.⁵

Comprehensive separation and distinction of these isomers are particularly challenging due to insufficient resolution of typical high-pressure liquid chromatography (HPLC)-based methods and the incompatibility of acidic cannabinoids with gas chromatography (GC)-based methods.^{3,4} Alternatively, NMR can be used, but large amounts of samples are needed due to limited sensitivity, potentially resulting in undetected compounds with lower concentrations.^{3,6} Moreover, despite advancements in high-field NMR instruments, there are still significant challenges related to chemical shift resolution.⁷

Recently, efforts have been made to include ion mobility spectrometry (IMS) for the analysis of cannabinoid isomers in a more rapid, comprehensive, and sensitive way. IMS is a gas-phase separation technique for ions based on their

mobility in an inert gas under an electric field. The mobility of ions is influenced not only by their size and charge but also by their three-dimensional conformation. This three-dimensional conformation property is different from chromatographic retention times, m/z values, and MS fragmentation, and it is unaffected by various experimental conditions such as matrix, concentration, and specific equipment. Consequently, the collision cross section (CCS) can serve as a standardized molecular descriptor for both targeted and untargeted analysis.^{8,9} However, currently reported research on IMS-based separation for cannabinoid isomers suffers from limitations: (i) insufficient resolution toward cannabinoid isomers, especially THC isomers, (ii) limited types of cannabinoid isomers investigated, typically focusing mainly on the well-known THCA, CBDA, CBD, Δ 8-THC, and Δ 9-THC, (iii) no or indistinctive reporting of CCS values. Specifically, Tose et al.⁸ used traveling wave ion mobility spectrometry (TWIMS) and could resolve three out of five protonated cannabinoid isomers (assigned as Δ 9-THC, Δ 8-THC, cannabicyclol (CBL), cannabichromene (CBC), and CBD) but were unable to separate Δ 9-THC and Δ 8-THC. Similarly, by using TWIMS, Kiselak et al.⁹ could resolve protonated CBD and CBC but could not separate protonated Δ 8-THC and Δ 9-THC. Likewise, Zietek et al.¹⁰ were unable to distinguish protonated Δ 9-THC and CBD by trapped IMS (TIMS), but Hädener et al.¹¹ effectively resolved two isomeric pairs, Δ 9-THC and CBD, as well as THCA and CBDA with a high-resolution drift-tube IMS (DTIMS, $R > 150$). Near-baseline separation was achieved, and experimental $^{DT}CCS_{N_2}$ values were obtained for protonated Δ 9-THC and CBD as well as deprotonated THCA and CBDA. Clearly, it has been challenging to separate such isomeric cannabinoids by IMS. A major improvement of separation performance was obtained by leveraging the unique adduct-formation behavior of cannabinoids with silver ions to amplify structural differences and thus enhance isomer separation in the gas phase, first reported in 2018.¹⁰ In our previous work, we have subsequently reported that Ag(I) allows the distinction of cannabinoid isomers in both chromatography and mass spectrometry-based analysis due to different Ag(I) affinities.^{4,12,13} In 2021, we demonstrated, for the first time, that cannabinoid isomers with identical MS/MS

product ion spectra of protonated precursor ions have completely different product ion spectra when selecting the silver adducts as precursor ions.¹³ Very recently, this effect was further studied for a wider range of cannabinoids, thus obtaining unique fragmentation for Δ^8 -THC (compound **2**), Δ^9 -THC (compound **3**), Δ^8 -iso-THC (compound **5**), $\Delta(4)$ 8-iso-THC (compound **6**), cannabichromene (CBC), *exo*-THC, and CBD (compound **4**).^{4,14} In terms of IMS separation, Zietek et al.¹⁰ have demonstrated that the introduction of Ag(I) to TIMS allows the partial separation of Δ^9 -THC and CBD, despite the limited resolution of the instrument. Also, Ieritano et al.¹⁴ applied this strategy for differential mobility spectrometry (DMS) and could distinguish the isomers Δ^8 -THC, Δ^9 -THC, CBD, *exo*-THC, and CBC in oils. While this is a major step forward, those cannabinoids had previously been separated by reversed-phase HPLC.¹⁵ On the contrary, two cannabinoids that are typically found in synthetic Δ^8 -THC products and are known to interfere with HPLC analysis of Δ^8 -THC products remain to be addressed,^{6,16} namely, the Δ^8 -THC iso-forms (Δ^8 -iso-THC (compound **5**) and $\Delta(4)$ 8-iso-THC (compound **6**)). Moreover, to the best of our knowledge, no reports of IMS separation of diastereomeric hydrated cannabinoids are available, while these compounds have recently been demonstrated to occur in Δ^8 -THC products for consumption.¹⁷ Finally, currently, no CCS values of any cannabinoid-Ag(I) adducts have been reported. The aim of the current work has thus been to address these challenges and to arrive at a broadly applicable set of operations that allows separation, identification, and quantification of many classes of isomeric cannabinoids, even those that are inseparable on chromatographic equipment, in a matter of milliseconds. Logically, this would require more advanced operations in the ion mobility space, mass spectrometry space, and interface between these than used in previous works, which is why cyclic IMS (cIMS) coupled to a quadrupole time-of-flight (qTOF) MS was selected for this purpose.

cIMS, first reported in 2019, greatly improves the resolving power of conventional TWIMS by the multipass running of ions in a 98-cm cyclic ion mobility tube to increase the separation path length.¹⁸ It has shown excellent separation performance for isomeric saponin,¹⁹ oligosaccharides,²⁰ and flavonoids,²¹ but it has

not yet been tried for isomeric cannabinoids. This novel state-of-the-art equipment has superior resolving power (a resolution (R) of ~ 78 in 1 pass up to ~ 750 in 100 passes, $\text{CCS}/\Delta\text{CCS}$) compared to linear IMS-MS ($R < 40$ for a standard linear TWIMS cell, $\text{CCS}/\Delta\text{CCS}$). Moreover, it incorporates high-resolution mass spectrometry (TOF) for accurate mass-to-charge ratio (m/z) measurements after IMS separation. Finally, also MS/MS fragments can be further separated with IMS, providing a powerful technique for studies on fragmentation products and their 3D conformation.¹⁸⁻²¹ The latter is especially interesting to further study the interaction between analytes and less common adduct ions such as Ag(I)-cannabinoid interactions. These interactions are known to be quite diverse for different cannabinoids^{4,12-14} and could help in explaining the differences in 3D shape (and thus in their CCS) of these silver adduct ions and why they can be separated. This also means that through comparison of experimental and theoretical CCS values, potentially new insights can be gained into the interactions between silver ions and cannabinoids. Such studies have, to the best of our knowledge, not been performed in the context of cannabinoid analysis. Addressing these challenges is important to further allow the development of an analytical workflow, including multiple molecular descriptors, for the unambiguous analysis of a wide range of cannabinoids (**Figure 6.1**, 14 cannabinoids, four groups of isomers) in Cannabis and Cannabis-derived samples. Establishing such a workflow as well as benchmarking it against gold standard chromatography-based methods has been the objective of this paper.

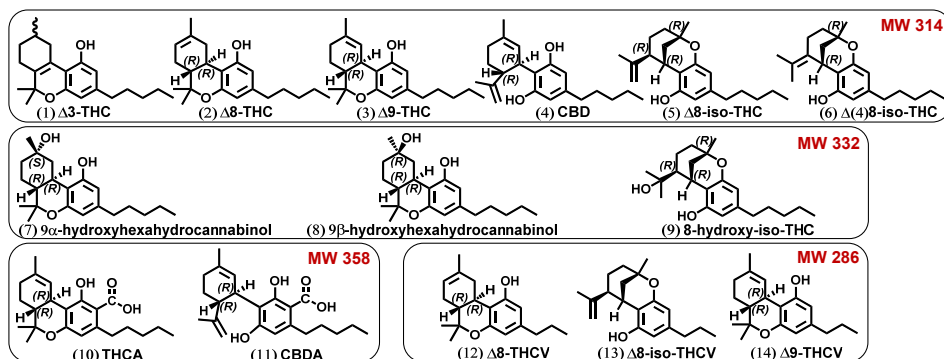


Figure 6.1. Structures of investigated cannabinoids (four groups of isomers) in this study.

Materials and Methods

Chemicals and Reagents. Silver nitrate (AgNO_3 , analytical grade) was purchased from Fisher Scientific (Loughborough, Leicestershire). Methanol (MeOH , HPLC-grade) was obtained from VWR Chemicals (Gliwice, Poland). Methyl *tert*-butyl ether (MTBE) was purchased from Biosolve BV (Valkenswaard, the Netherlands). Major Mix IMS/ToF calibration kit was purchased from Waters (Wilmslow, UK). Acid-treated CBD mixtures were prepared in our previous study (**Supporting Information (SI), Table S1**, data from our previous study)⁴ and abbreviated as R#1–R#8. Cannabis materials (C#1–C#3) were purchased locally, and Δ^8 -THC gummies (G#1–G#2) were purchased online (**SI, Table S2**). $\Delta(4)$ 8-iso-THC (**6**) was kindly provided by Danielle Passarella (Dipartimento di Chimica, Università degli Studi di Milano, Milano, Italy).³ Crystalline CBD (**4**) (99%) was purchased from CBDolie.nl. CBDA isolate (90%–95%) was obtained from GVB Biopharma (Tygh Valley, USA). Δ^8 -THC (**2**), Δ^9 -THC (**3**), CBD (**4**), Δ^8 -iso-THC (**5**), 9α -hydroxyhexahydrocannabinol (**7**), 9β -hydroxyhexahydrocannabinol (**8**), and 8-hydroxy-iso-THC (**9**) standards (purity > 98%) were isolated and identified in our previous study.⁴ THCA (**10**) was purified from Cannabis flowers. Δ^3 -THC (named as $\Delta^6\text{a},10\text{a}$ -THC in the general introduction) (**1**) was purified from Δ^{10} -THC vape oil obtained online. Δ^9 -THCV (**14**) and the mixture containing Δ^8 -THCV (**12**) and Δ^8 -iso-THCV (**13**) (with a mole ratio of 1:2) were isolated from 4% THCV oil purchased online. The newly isolated cannabinoids in the current study Δ^3 -THC (**1**), THCA (**10**), Δ^9 -THCV (**13**) were identified by 1D and 2D NMR (Bruker 700 MHz Avance, Bruker GmbH, Rheinstetten, Germany) and analyzed by reversed-phase UHPLC-UV/MS. The isolated mixture containing Δ^8 -THCV (**13**) and Δ^8 -iso-THCV (**14**) (with a mole ratio of 1:2) was identified by ^1H NMR (Bruker 700 MHz Avance, Bruker GmbH, Rheinstetten, Germany), reversed-phase UHPLC-UV/MS, GC-FID/MS, and silica-Ag(I) HPLC-DAD (**SI, Figures S1–S4**).⁴ According to NMR and peak integrations at UV 215 nm, the purity of compounds **1**, **14**, and the mixture of **12** and **13** (mole ratio 1:2) was > 90%; the purity of compound **10** was > 75%.

Solutions and Samples. The stock solution of each standard cannabinoid and acid-treated CBD mixtures (R#1–R#8) were prepared in MeOH at $100\ \mu\text{g}\cdot\text{mL}^{-1}$. 6.0 mg, 6.4 mg, and 7.7 mg of Cannabis (C#1, C#2, and C#3) were accurately weighed (Mettler Instrumente AG, CH-8606 Greifensee-Zurich) in 1.5 mL Eppendorf safe-lock tubes (Eppendorf Nederland B.V., Nijmegen, Netherlands). 600 μL , 640 μL , and 770 μL of MeOH were added individually with a micropipette (Eppendorf research plus, 100–1000 μL , Nijmegen, Netherlands). After a 10-min sonication extraction (Bandelin Sonorex, Rangendingen, Germany), the solutions were filtered over 0.2 μm PTFE membrane syringe filters (Pall Corporation, Port Washington, NY, USA) and diluted with MeOH by 100 times to $100\ \mu\text{g}\cdot\text{mL}^{-1}$ (= Cannabis stock solution). 10.0 mg of Δ^8 -THC gummies (G#1 and G#2) were extracted by 1.00 mL MTBE/ H_2O (v/v = 1:1) in 1.5 mL Eppendorf safe-lock tubes with handshaking for 15 min. After waiting 10 min for phase separation, 300 μL of the MTBE layer was filtered over 0.2 μm PTFE membrane syringe filters. After that, 100 μL of the filtered solution was blow-dried and reconstituted in 2.00 mL of MeOH to $100\ \mu\text{g}\cdot\text{mL}^{-1}$ (gummy stock solution). The MeOH or 10^{-4} M AgNO_3 in MeOH (in a brown bottle) was used to further dilute the stock solutions ten times for cIMS analysis, unless otherwise stated. For CBD (**4**), CBDA (**11**), Δ^8 -THCV (**13**), and Δ^8 -iso-THCV (**14**), the dilution was $100\times$ by a 10^{-4} M AgNO_3 MeOH solution. For the analysis of standard mixtures, diluted cannabinoid stock solutions were mixed in equal volumes.

cIMS-qTOF-MS Analysis. A Select Series Cyclic Ion Mobility Mass Spectrometer (cIMS, Waters Corporation, Wilmslow, U.K.) was used in this study. Direct infusion analysis at a flow rate of $15\ \mu\text{L}\cdot\text{min}^{-1}$ was used, unless otherwise stated. For ionization, the capillary voltage was 2.5 kV when there was no Ag(I) and 1.2 kV when Ag(I) ions were present. The cone voltage was 40 V with the source temperature at 100 $^\circ\text{C}$, the nitrogen desolvation gas flow at $800\ \text{L}\cdot\text{h}^{-1}$, and the desolvation temperature at 300 $^\circ\text{C}$. TOF (V) mode was used for general MS analysis

without mobility separation. Mobility mode was aimed at mobility separation and analysis. Major settings of the mobility mode (Cyclic Control) were 5 pushes per bin, traveling wave (TW) velocity $375 \text{ m}\cdot\text{s}^{-1}$, TW static height and start height 15 V, and inject time 10 ms. Multiple-pass separation was achieved by using the manual function with a slider. The qualitative analysis of standards and samples was conducted by MS full-scan in TOF mode, isolating targeted m/z for mobility separation, trap fragmentation (by adjusting trap energy) before mobility separation, and transfer fragmentation (by adjusting the transfer energy) after mobility separation. For experiments without fragmentation, 6 V trap energy and 4 V transfer energy were used. Nitrogen was used as collision and cIMS gas. For quantitative analysis, loop injection ($5 \text{ }\mu\text{L}$) instead of direct infusion was used. MeOH was used to thoroughly flush the system between different samples. Acquisition and processing were performed using MassLynx (version 4.2), DriftScope (version 3.0), and Microsoft Excel. The instrument was mass calibrated with a Major Mix IMS/ToF Calibration Kit (Waters Corp, Wilmslow UK) in both positive and negative ion electrospray mode at 60 000 resolution (FWHM) over an m/z range of 50–1000. $50 \text{ pg}\cdot\mu\text{L}^{-1}$ of leucine enkephalin in water/acetonitrile (50:50, v/v) was infused at $1 \text{ }\mu\text{L}\cdot\text{min}^{-1}$ to be used as lockmass calibrant ($[\text{M} + \text{H}]^+ m/z 556.2766$).

Multipass CCS Calibration and Experimental Measurement. Multipass CCS calibration and experimental measurements were performed according to instructions from the manufacturer.^{22–26} Major Mix calibration standards were measured under 1-pass and 2-pass separation settings. Only six out of twenty-nine calibrants were selected in this study (SI, Table S3), considering m/z values below and above the m/z of interest (cannabinoids range $m/z 287$ – 467). These compounds were peak detected and the arrival times (t_a , Eq 1) of the calibrant ions were determined for both 1-pass and 2-pass separation data sets. The drift time (t_d) for a single pass of each calibrant ion (Eq 2) and the dead time (t_0 , Eq 3) of the cIM-ToF system were then calculated using the arrival times (Eq 1). The CCS calibration curve was then constructed by using the 1-pass drift time (t_d) values and the power

function $y = ax^b$. To measure CCS values of unknown analytes in multipass separation settings, a corrected single-pass transit time ($^c t_i$) should be calculated with Eq 4, in which the multipass drift time ($^{mp} t_d$) was obtained from multiple-pass arrival times (t_a) minus dead time (t_0). After that, the plotted CCS calibration curve (**SI, Figure S5**) was used to obtain CCS values of unknowns. Cannabinoid standards prepared at different concentrations ($10.0 \mu\text{g}\cdot\text{mL}^{-1}$ unless otherwise stated) in MeOH or 10^{-4} M AgNO_3 in MeOH were injected in triplicate, thus obtaining the $^{TW}\text{CCS}_{\text{N}_2}$ from the average of $n = 3$, unless otherwise specified.

$$\text{Arrival time } (t_a) = \text{Drift time } (t_d) + \text{Dead time } (t_0) \quad (\text{Eq 1})$$

$$\text{Drift time } (t_d) = \text{Arrival time 2 pass } (^2 t_a) - \text{Arrival time 1 pass } (^1 t_a) \quad (\text{Eq 2})$$

$$\text{Dead time } (t_0) = \text{Arrival time 1 pass } (^1 t_a) - \text{Drift time } (t_d) \quad (\text{Eq 3})$$

$$\text{Corrected single-pass drift time } (^c t_i) = \text{multipass drift time } (^{mp} t_d) / \text{number of passes } (n) \quad (\text{Eq 4})$$

Chromatography. Cannabis extracts (C#1–C#3) were analyzed by the reversed-phase UHPLC-UV/MS method developed in our previous study.⁴ $\Delta 8$ -THC gummy extracts (G#1–G#2) were analyzed by a slightly modified GC-FID/MS method developed in the same study.⁴ Specifically, a DB-5MS UI capillary column (Agilent J and W GC column, USA) instead of HP-5MS capillary column was used with a prolonged temperature program. The temperature program started with an initial column temperature of 200°C , followed by a gradual increase at a rate of $1^\circ\text{C}\cdot\text{min}^{-1}$ until reaching 223°C . Subsequently, the column temperature was further elevated at a rate of $5^\circ\text{C}\cdot\text{min}^{-1}$ to 250°C and maintained at this level for 15 min, resulting in a total analysis time of 43 min. A $1 \mu\text{L}$ sample was injected with a 1:10 split ratio. The injection temperature was 200°C . Helium was used as the carrier gas with a linear velocity of $26 \text{ cm}\cdot\text{s}^{-1}$, and the flow was constant during the entire analysis. The mass spectrometer was operated in 70 eV electron ionization (EI) mode, scanning from m/z 35 to 500 at $4 \text{ spectra}\cdot\text{s}^{-1}$. Measurements were delayed by 3.0 min following an injection to safeguard the filament of the mass spectrometer.

Quantification of $\Delta 8$ -THC, $\Delta 9$ -THC, and CBD. 1.00 $\mu\text{g}\cdot\text{mL}^{-1}$ of $\Delta 8$ -THC (**2**), $\Delta 9$ -THC (**3**), and CBD (**4**) in 10^{-4} M AgNO_3 MeOH were prepared as stock solutions. 250 μL of 1.00 $\mu\text{g}\cdot\text{mL}^{-1}$ $\Delta 8$ -THC (**2**), 25.0 μL of 1.00 $\mu\text{g}\cdot\text{mL}^{-1}$ $\Delta 9$ -THC (**3**), and 10.0 μL of 1.00 $\mu\text{g}\cdot\text{mL}^{-1}$ CBD (**4**) were mixed and diluted with 10^{-4} M AgNO_3 MeOH to 1.00 mL to obtain a mixed standard solution of $\Delta 8$ -THC (**2**) (250 $\text{ng}\cdot\text{mL}^{-1}$), $\Delta 9$ -THC (**3**) (25.0 $\text{ng}\cdot\text{mL}^{-1}$), and CBD (**4**) (10.0 $\text{ng}\cdot\text{mL}^{-1}$). The obtained mixed standard solution was then diluted to obtain a series of working solutions with the concentration range 1.00–250 $\text{ng}\cdot\text{mL}^{-1}$ for $\Delta 8$ -THC (**2**), 0.100–25.0 $\text{ng}\cdot\text{mL}^{-1}$ for $\Delta 9$ -THC (**3**), and 0.0400–10.0 $\text{ng}\cdot\text{mL}^{-1}$ for CBD (**4**). 5.00 μL portion of each working solution was injected by a loop injector to perform a multipass ion mobility separation and postmobility fragmentation (transfer energy 30 V) of the precursor ion at m/z 421. Calibration curves for $\Delta 8$ -THC, $\Delta 9$ -THC, and CBD were made by plotting areas of the extracted mobiligram of the characteristic fragment at m/z 245 for $\Delta 8$ -THC (**2**), m/z 313 for $\Delta 9$ -THC (**3**), and m/z 353 for CBD (**3**) against the used concentrations. Limit of detection (LOD) of $\Delta 8$ -THC (**2**), $\Delta 9$ -THC (**3**), and CBD (**4**) was calculated as follows: $\text{LOD} = 3 \times \text{SD}$ of the lowest concentration of the calibration curve/slope of the calibration curve.

Prediction of and Calculation of the Theoretical CCS Values (tCCS).

Theoretical CCS of protonated and sodiated species were predicted using AllCCS (<http://allccs.zhulab.cn/>).^{27,28} In brief, using a training set of experimentally measured CCS, the software employs a machine learning algorithm that is able to predict CCS values for novel structures. To calculate the predicted CCS for $[\text{M} + \text{H}]^+$ and $[\text{M} + \text{Na}]^+$ species, the SMILES string of each cannabinoid was imported to the web interface of AllCCS Predictor. CCS values for Ag^+ adducts could not be predicted by AllCCS because no Ag^+ ions were used to build the training set. Therefore, density functional theory (DFT)-based methods were used to obtain theoretical CCS values of cannabinoid- Ag(I) species by a two-step procedure.²⁹ Specifically, quantum chemistry-based optimization of cannabinoid- Ag(I) structures was used as an input in Collidoscope³⁰ to obtain tCCS values, and a Boltzmann-

weighted distribution of possible structures was considered to produce the final averaged tCCS values. The optimization was conducted through B97XD/def2TZVP calculations, utilizing the corresponding parameters in Gaussian 16. All structures were fully optimized, and vibrational frequency calculations were performed to confirm that these were minima and to obtain the free energy.

Results and Discussion

cIMS Multiple-pass Separation of Cannabinoid Isomers. Despite the isomeric separation power of IMS, only limited research has been performed toward the analysis of cannabinoid isomers, and the maximum number of resolved isomeric cannabinoids reported so far is five.¹⁴ In the current study, the comprehensive investigation of 14 acidic and neutral cannabinoids (**Figure 6.1**), forming four groups each with a specific MW, was carried out with advanced cIMS-MS. First, the separation of six THC isomers (a mixture of compounds **1–6**) was investigated. The six protonated species (**SI, Figure S6a–c**) showed no or little separation with 1 pass up to 7 passes (**Figure 6.2A**). Even increasing the number of passes to 11 resulted in only a shoulder peak. As the number of passes was further increased, peak broadening became increasingly prominent as opposed to yielding enhancements in separation. Alternatively, sodiated species (**SI, Figure S6d–e**), which were more intense than the protonated signals, showed two peaks for the mixtures containing six isomers in the mobiligram after 1-pass separation. At best, three peaks could be observed after a 7-pass separation of sodiated species (**Figure 6.2B**), which is still not enough for the distinction of these six isomers. As revealed in our previous research,^{31–33} Ag(I) has different affinities for compounds with different numbers or positions of olefinic double bonds, and recent work^{4,10,12–14} also proved cannabinoid isomers have different interactions with Ag(I). Therefore, we investigated whether Ag(I) complexation in combination with advanced cIMS would further benefit the analysis of more complex mixtures and diverse cannabinoids. While a 1-pass separation of Ag(I) adducts showed limited separation (**Figure 6.2C**), the 6-pass separation exhibited obvious improvement compared to its Na⁺-counterpart, with six

identified peaks in the mobiligram for the six THC isomers (**Figure 6.2D**). Further increasing the number of passes would result in wrap-around effects (the fastest ions catching up with the slowest ones). The **Supporting Information** provides a full comparison of the various charged species (**SI, Figure S6a–c** for protonated species, **S6d–f** for Na^+ adducts, and **S6f–h** for Ag^+ adducts).

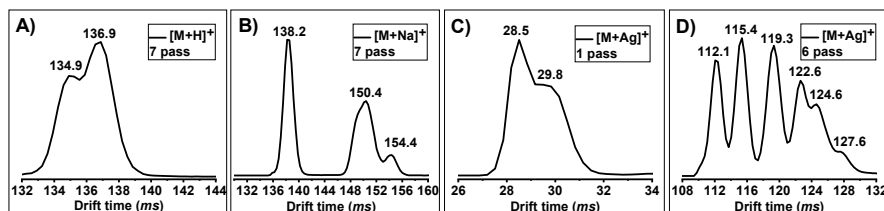


Figure 6.2. Mobiligrams of the mixture of six isomers (compounds **1–6**) A) as protonated species (extracting $[\text{M} + \text{H}]^+$ signal at m/z 315; drift time at 134.9 ms: $\Delta 8$ -iso-THC and $\Delta(4)8$ -iso-THC; drift time at 136.9 ms: CBD, $\Delta 8$ -THC, $\Delta 9$ -THC, and $\Delta 3$ -THC) after 7-pass separation; B) as sodiated species (extracting $[\text{M} + \text{Na}]^+$ signal at m/z 337; drift time = 138.2 ms: CBD; drift time = 150.4 ms: $\Delta 9$ -THC, $\Delta 8$ -iso-THC, $\Delta(4)8$ -iso-THC, and $\Delta 8$ -THC, drift time = 154.4 ms: $\Delta 3$ -THC) after 7-pass separation; C) as Ag(I) species (extracting $[\text{M} + \text{Ag}]^+$ signal = m/z 421; drift time = 28.5 ms: CBD and $\Delta 9$ -THC; drift time = 29.8 ms: $\Delta(4)8$ -iso-THC, $\Delta 8$ -iso-THC, $\Delta 8$ -THC, and $\Delta 3$ -THC) after 1-pass separation; and D) as Ag(I) species (extracting $[\text{M} + \text{Ag}]^+$ signal = m/z 421; drift time = 112.1 ms: CBD; drift time = 115.4 ms: $\Delta 9$ -THC; drift time = 119.3 ms: $\Delta(4)8$ -iso-THC; drift time = 122.6 ms: $\Delta 8$ -iso-THC; drift time = 124.6 ms: $\Delta 8$ -THC; drift time = 127.6 ms: $\Delta 3$ -THC) after 6-pass separation.

Postmobility Fragmentation for Improved Identification. *THC/CBD Isomers (Compounds 1–6, MW 314)*. Though multiple-pass separation of Ag(I) adducts could already resolve all six THC isomers, a more selective strategy was explored for the unambiguous identification of each isomer. Based on previous research, different Ag(I) adducts are known to produce different ESI-MS fragmentation patterns, which thus can facilitate cannabinoid isomer distinctions.^{4,12-14} Therefore, postmobility fragmentation was performed. Since postmobility fragmentation happens after mobility separation, fragment and precursor drift times are aligned, which can facilitate the assignment of fragments to specific precursors. Indeed, the six isomers exhibited distinct fragmentation patterns with major characteristic fragments for $\Delta 3$ -THC (**1**) at m/z 299, $\Delta 8$ -THC (**2**) at m/z 245, $\Delta 9$ -

THC (**3**) at m/z 313, CBD (**4**) at m/z 353, Δ 8-iso-THC (**5**) at m/z 259, and Δ (4)8-iso-THC (**6**) at m/z 419 (**SI, Figure S7a**). By extracting the major characteristic fragment signal for each isomer after the 6-pass separation, six distinct traces can be observed (**Figure 6.3A**), even for cannabinoids, which have been impossible to separate to date by RP-UHPLC. Therefore, distinct fragments can provide extra evidence apart from drift time for cannabinoid identification.

THCV Isomers (Compounds 12–14, MW 286). Compared with Δ 9-THC (**3**), Δ 8-THCV (**12**), Δ 8-iso-THCV (**13**), and Δ 9-THCV (**14**) contain a propyl rather than a pentyl side chain. Δ 9-THCV exists in Cannabis and shows pharmacological effects similar to those of Δ 9-THC.³⁴ Δ 8-THCV (**13**) and Δ 8-iso-THCV (**14**), while structurally similar to Δ 8-THC (**2**) and Δ 8-iso-THC (**5**), likely originate from organic synthesis,³⁵ and there is only limited information about the pharmacological effects of these two cannabinoids. Despite the coelution in RP-UHPLC (**SI, Figure S2**), with the cIMS method, the three isomeric THCV were well distinguished. Δ 9-THCV (**14**) had a characteristic fragment at m/z 285, which is 28 Da less than the characteristic fragment of Δ 9-THC (**3**) at m/z 313 (**SI, Figure S7b**). Similarly, Δ 8-iso-THCV (**13**) was characterized by fragments at m/z 231, 28 Da less than the corresponding fragments of Δ 8-iso-THC (**5**) (m/z 259). This also worked for Δ 8-THCV (**13**) and Δ 8-THC (**2**), showing a difference of 28 Da between the characteristic fragments (m/z 217 vs m/z 245). Also, due to the shorter side chain, small conformational differences of Ag(I) adducts resulted in a slightly lower resolution of THCV isomers compared with their THC counterparts (**Figure 6.3B**).

THCA/CBDA (Compounds 10–11, MW 358). The Ag(I)-enhanced-multiple-pass separation combined with postmobility fragmentation works not only for the neutral cannabinoid isomers Δ 3-THC (**1**), Δ 8-THC (**2**), Δ 9-THC (**3**), CBD (**4**), Δ 8-iso-THC (**5**), Δ (4)8-iso-THC (**6**), Δ 9-THCV (**14**), Δ 8-THCV (**12**), and Δ 8-iso-THCV (**13**) but also for the distinction of acidic cannabinoids THCA (**10**) (characteristic fragment at m/z 339) and CBDA (**11**) (characteristic fragment at m/z 379) (**Figure 6.3C** and **SI, Figure S7c**). This is highly valuable for the direct analysis of Cannabis extracts since they mainly contain such acidic cannabinoids.³⁶

Hydrated THC Isomers (Compounds 7–9, MW 332). It was recently demonstrated that in addition to THC isomers, hydrated THC isomers occur in commercial Δ^8 -THC products.¹⁷ Three hydrated THC isomers were isolated and identified as 9α -hydroxyhexahydrocannabinol (**7**), 9β -hydroxyhexahydrocannabinol (**8**), and 8-hydroxy-iso-THC (**9**) in our previous study.⁴ cIMS was then also applied to their analysis. Unfortunately, these isomers could not be resolved by mobility separation alone (**SI, Figure S8**), and thus, relying on drift time for compound assignments is insufficient. Through postmobility fragmentation and extracting characteristic fragments, three hydrated THC species, of which two are stereoisomers, could also be distinguished (**Figure 6.3D**). On the contrary, without cIMS separation, it would be impossible to separate these compounds based on their traces alone as several fragments also occur as minor fragments for other isomers (e.g., characteristic fragment of 8-hydroxy-iso-THC (**9**) at m/z 259 also occurs in 9α -hydroxyhexahydrocannabinol (**7**), and both 9α -hydroxyhexahydrocannabinol (**7**) and 9β -hydroxyhexahydrocannabinol (**8**) share the characteristic fragment at m/z 313) (**SI, Figure S7d**). Therefore, these two techniques are truly complementary and together exhibit excellent distinction power for a comprehensive range of cannabinoid isomers.

Additionally, in both ESI-qTOF-MS and GC-MS, the three hydrated THC isomers tend to lose H_2O and thus form a product with the same molecular weight as compounds **1–6** (**SI, Figures S9 and S10**). In order to investigate whether the existence of hydrated THC isomers would interfere with the analysis of compounds **1–6**, the three hydrated THC isomers were analyzed individually by cIMS with or without Ag(I) being present. When selecting the protonated species at m/z 333 in the absence of Ag(I), apart from the signals at m/z 333.2420, there were peaks at m/z 315.2311 (dehydrated forms of signals at m/z 333.2420) detected for all three hydrated THC isomers (**SI, Figure S11a**), which matches the results obtained by RP-UHPLC-ESI-Orbitrap-MS (**SI, Figure S9**). However, with Ag(I), when the silver adduct was selected at m/z 439, no dehydrated silver adducts were detected under the same conditions (**SI, Figure S11b**). Therefore, the formation of Ag(I)

adducts is hypothesized to stabilize the hydrated THC isomers and prevent H₂O loss during ionization to form products that might interfere with the analysis of THC isomers. That is very meaningful for preventing false-positive THC results when Cannabis products, e.g., Δ^8 -THC products, are analyzed without chromatographic separation.

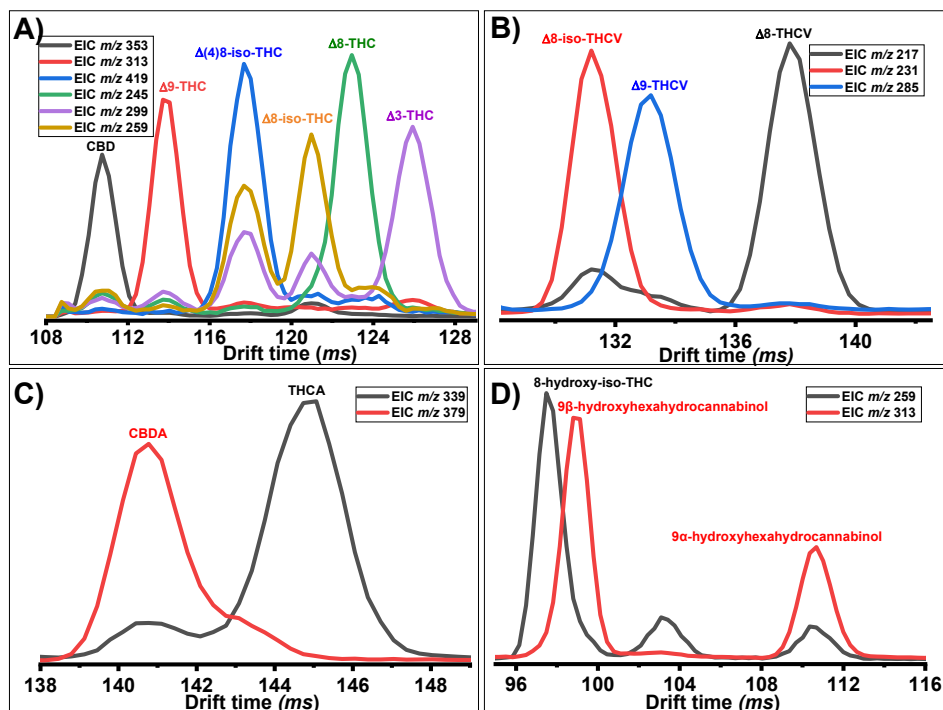


Figure 6.3. Extracted mobiligram of the characteristic fragment of A) Δ^8 -THC, Δ^9 -THC ($\div 5$), Δ^3 -THC, CBD, Δ^8 -iso-THC ($\times 2$) and $\Delta(4)$ 8-iso-THC ($\times 4$) after 6-pass separation; B) Δ^9 -THCV ($\div 5$), Δ^8 -THCV and Δ^8 -iso-THCV after 7-pass separation; C) THCA and CBDA after 7-pass separation; D) 9 α -hydroxyhexahydrocannabinol ($\div 10$), 9 β -hydroxyhexahydrocannabinol ($\div 10$), and 8-hydroxy-iso-THC after 5-pass separation in the presence of Ag(I).

Experimental and Theoretical CCS Determination of Ag(I) Adducts for Unambiguous Identification. Apart from providing the extra dimension of separation to increase peak capacity, one of the most attractive parts of IMS is the ability to obtain CCS values, a structure-dependent parameter, for compound identification.³⁷ Among the prominent ion mobility techniques, the Field

Asymmetric IMS (FAIMS) also known as DMS cannot provide CCS information because of their asymmetric waveform and ion structural alterations induced by the oscillation between low and high electric field strengths.³⁸ In contrast, DTIMS, TWIMS, and TIMS methodologies can yield CCS values through direct measurement or calculation derived from calibration curves between drift time and CCS values of calibrants.³⁹ Furthermore, in contrast to the drift time observed in DTIMS, TWIMS, and TIMS, as well as the compensation voltage utilized in DMS, CCS as a molecular identifier remains unaffected by experimental conditions and facilitates cross-platform comparisons as well as untargeted analysis.⁴⁰ Therefore, in the current study, CCS values of 14 cannabinoids were experimentally derived (**SI, Table S3** and **Figure S5**), for their proton, sodium, and Ag(I) adducts. To the best of our knowledge, this is the first time that experimental CCS (eCCS) values of Ag(I) adducts of cannabinoid isomers are reported. They showed a relatively higher variation than CCS values of proton and sodium adducts (**Table 6.1**), which facilitates the distinction between them. Comparison of the eCCS values of protonated Δ^9 -THC (**3**) and CBD (**4**) in this study with those obtained in other studies (see **SI, Table S4** for other different IMS) showed relative deviations (RD) of only -0.2% to -2.1% , demonstrating the accuracy of eCCS values measured by cIMS.

We also compared the eCCS values of protonated and sodiated species with predicted CCS (pCCS) values obtained by the machine learning-based online tool AllCCS. (**SI, Table S4**). For protonated species, the prediction errors ($\frac{pCCS - eCCS}{eCCS} \times 100\%$) were all within $\pm 2.1\%$, showing good prediction accuracy. Twelve out of 13 sodiated species of cannabinoids had a prediction error of $\leq 5\%$. However, for sodiated 9β -hydroxyhexahydrocannabinol (**8**), the pCCS was overestimated by 6.5% . While the AllCCS platform shows fairly good CCS prediction power for most protonated and sodiated cannabinoids, this platform does not include argentated species, which are more distinctive for cannabinoids based on our derived eCCS values. On the contrary, Duez et al.²⁹ obtained theoretical CCS (tCCS) values of

Ag(I)-complexed alkylamines based on density functional theory (DFT) computational methods. Thus, we applied this methodology to cannabinoids for the first time. The tCCS values agree quite nicely with the experimental values, with an overall error of 2.6% for these 14 cannabinoids (**Table 6.1**). However, there is quite some variation within this set, with errors ranging from -4% for $\Delta(4)$ 8-iso-THC (**6**) to +6% (for THC (**3**) and THCA (**10**)). For seven out of the 14 cannabinoids an absolute calculation error within 2% was obtained,⁴¹ and the average calculation error of 2.6% is smaller than observed by other DFT-based studies, e.g., ISiCLE, with an average error of 3.2%.⁴² However, this study also points to clear limits of this approach, especially for isomers with small differences in structures. For example, the relative difference of eCCS between Δ 8-THC (**2**) and Δ 8-iso-THC (**5**) is 0.7%, which means that with a calculation error of 2.6%, it is not possible to distinguish between these isomers. The DFT calculation faces an intrinsic limitation due to the subjective empirical selection of possible conformations. Ideally, an unbiased set of conformations as obtained from, e.g., molecular dynamics should be used, even though it can be computationally very expensive.³⁹ Then, for each of these, the CCS would be calculated and weighted with their Boltzmann factor. In this way, subjective biases can be mitigated, and thus, the accuracy of the results might be enhanced. On the contrary, a more stringent treatment of buffer gas (N₂) could be incorporated in future version of the Collidoscope prediction software to mitigate errors associated with trajectory integration.³⁰ In the future, the ability to calculate and predict CCS values of cannabinoid-Ag(I) might also benefit from the development of libraries to facilitate untargeted cannabinoid investigations if the prediction error can be strongly reduced. For now, as with gold standard separation on HPLC or GC, reference standards remain indispensable for unambiguous identification.

Table 6.1. Experimentally derived traveling wave collision cross section values in nitrogen ($^{TW}CCS_{N_2}$, Å²) of THC isomers as protonated species, sodiated species, and Ag(I) species measured by cIMS under 7-pass separation settings.

Compounds	MW	eCCS*			tCCS	Calculation error
		[M+H] ⁺	[M+Na] ⁺	[M+Ag] ⁺	[M+Ag] ⁺	
Δ3-THC (1)	314.2	188.4±0.01	197.9±0.03	192.9±0.03	186.1	−3.5%
Δ8-THC (2)	314.2	187.8±0.05	196.4±0.04	190.9±0.02	194.7	2.0%
Δ9-THC (3)	314.2	187.8±0.03	194.8±0.01	183.9±0.01	195.3	6.2%
CBD (4)	314.2	187.8±0.01	188.5±0.02	181.8±0.01	180.3	−0.8%
Δ8-iso-THC (5)	314.2	186.5±0.03	195.7±0.01	189.5±0.01	186.4	−1.7%
Δ(4)8-iso-THC (6)	314.2	186.6±0.04	195.8±0.01	187.1±0.01	179.2	−4.2%
9α-hydroxyhexahydrocannabinol (7)	332.2	191.2±0.02	201.7±0.02	195.6±0.01	195.1	−0.3%
9β-hydroxyhexahydrocannabinol (8)	332.2	191.6±0.2	193.0±0.01	185.9±0.01	193.9	4.3%
8-hydroxy-iso-THC (9)	332.2	187.9±0.01	200.8±0.02	184.6±0.02	190.2	3.0%
THCA (10)	358.2	194.0±0.2	212.2±0.01	190.9±0.01	202.6	6.1%
CBDA (11)	358.2	193.6±0.03	206.7±0.01	188.6±0.01	192.7	2.2%
Δ8-THCV (12)	286.2	174.9±0.01	188.0±0.02	187.9±0.01	186.4	−0.8%
Δ8-iso-THCV (13)	286.2	173.5±0.01	186.4±0.02	183.8±0.01	181.5	−1.3%
Δ9-THCV (14)	286.2	174.7±0.01	185.9±0.01	184.9±0.01	183.6	−0.7%

* $^{TW}CCS_{N_2} \pm SD$ (Å²), $n = 3$.

Sequential Premobility and Postmobility Fragmentation for Further Investigation of Stereoisomers of 9α-Hydroxyhexahydrocannabinol and 9β-Hydroxyhexahydrocannabinol. It has been observed in our previous study that the distinction of cannabinoid isomers mainly relied on Ag(I)-alkene complexation.^{4,12,13} Interestingly, the three hydrated THC isomers (compound 7–9), with no olefinic double bonds, still exhibited different eCCS and MS fragments in the presence of

Ag(I). This showed that Ag(I) can also contribute to the distinction of cannabinoids without olefinic double bonds, which could not be achieved with protonated species. Our early research also revealed that polar groups like hydroxyls weakly interact with Ag(I).³¹ We therefore investigated whether the interaction of Ag(I) and hydroxyls contributed to the distinction and how they interacted.

First, as mentioned above, the presence of Ag(I) uniquely prevented H₂O loss of the three hydrated THC isomers, thus providing evidence of Ag(I)-hydroxyl interactions. When applying various transfer fragmentation energies to fragment these Ag(I) adducts (**SI, Figure S12**), they exhibited different stabilities in the order of $[8\text{-hydroxy-iso-THC} + \text{Ag}]^+ > [9\alpha\text{-hydroxyhexahydrocannabinol} + \text{Ag}]^+ > [9\beta\text{-hydroxyhexahydrocannabinol} + \text{Ag}]^+$, showing different interactions between Ag(I) and hydroxyls with different spatial orientation. In order to study the dehydrated species, we selected Ag(I) adducts at m/z 439 and performed premobility fragmentation to force the H₂O loss. Except for signals of $[M + \text{Ag}]^+$ at m/z 439/441, there were now also signals of $[M + \text{Ag} - \text{H}_2\text{O}]^+$ at m/z 421/423 for all three hydrated THC isomers (**SI, Figure S11c**). Afterward, multiple-pass separation, CCS measurements, and postmobility fragmentation were conducted. As shown in **Figure S13 (SI, Figure S13)** and summarized in **Table S5 (SI, Table S5)**, $[9\alpha\text{-hydroxyhexahydrocannabinol} + \text{Ag}]^+$ had a CCS value of 195.6. After H₂O loss, it formed two dehydrated Ag(I) adducts with CCS values of 182.0 and 190.6. $[9\beta\text{-hydroxyhexahydrocannabinol} + \text{Ag}]^+$ showed a much smaller CCS value of 185.9 and formed three dehydrated Ag(I) adducts during premobility fragmentation, with CCS values of 181.9, 183.9, and 190.6. Despite the large difference in eCCS (195.6 vs 185.9) of $9\alpha\text{-hydroxyhexahydrocannabinol}$ and $9\beta\text{-hydroxyhexahydrocannabinol}$ Ag(I) species, after H₂O (hydroxyl) loss, the eCCS values (and thus the corresponding 3D structure) became almost identical, providing more evidence of the interaction between Ag(I) and hydroxyls. $[8\text{-hydroxy-iso-THC} + \text{Ag}]^+$ with the eCCS of 184.6 formed only one dehydrated product (eCCS = 179.7). By comparing eCCS and postmobility fragmentation of dehydrated species (**SI, Table S5** and **Figure S13**) with reference standards, it was found that one of the dehydrated species

formed from 9 α -hydroxyhexahydrocannabinol and 9 β -hydroxyhexahydrocannabinol might be Δ 8-THC, while others remained unassigned. In short, it is likely that the interaction of Ag(I) and hydroxyls can also contribute to the distinction of cannabinoids without olefinic double bonds by different 3D conformers, stability, and dehydration. Similarly, Ollivier et al.⁴³ found that the formation of lithium adducts would affect the mobility and dehydration of oligosaccharides and used this for the distinction of α -linked and β -linked glucans. Besides, in this study, we observed a large difference in eCCS between [9 α -hydroxyhexahydrocannabinol + Na]⁺ and [9 β -hydroxyhexahydrocannabinol + Na]⁺ (201.7 vs 193.0). Likewise, stereoisomers epicatechin and catechin, with different spatial orientations of only one hydroxyl moiety, could be separated by cIMS in the form of sodium adducts.²¹ These findings indicate that not only Ag(I) but also other metal ions, e.g., Li⁺ and Na⁺, interacted differently with hydroxyls depending on their stereochemistry, further substantiating the claim that such interactions can be used to facilitate the distinction of stereoisomers.

Analysis of Cannabis Extracts, Acid-Catalyzed CBD Mixtures, and Commercial Δ 8-THC Edibles. *Identification Workflow for Cannabinoids.* Combining the aforementioned information, a workflow (**Figure 6.4**) for the identification of cannabinoids in complex samples was developed. Samples were mixed with a methanolic AgNO₃ solution and subjected to cIMS via direct infusion for full-scan in positive ionization mode followed by multipass separation (1–7 passes) of selected ions (cannabinoid-Ag(I) species) to obtain the maximum number of peaks in a single pass. During this stage, the eCCS of each detected peak was calculated. Afterward, transfer fragmentation was performed at 30 V, at which pronounced diagnostic fragments were obtained for all investigated cannabinoids (the range of 20–40 V was tested, **SI, Figure S12**). Finally, the identification procedure was used to check (i) precursor ions with Ag(I) isotope pattern (distinct [M + ¹⁰⁷Ag]⁺ and [M + ¹⁰⁹Ag]⁺ doublet with a ratio of approximately 1);⁴⁴ (ii) eCCS of Ag(I) adducts (compared with reference standards); and (iii) MS/MS

fragmentation (compared with reference standards). For the eCCS comparison with reference standards, the maximum RD was set at $\pm 1\%$, considering the good intraday, interday, and interpass repeatability ($RSD \leq 0.3\%$, **SI, Table S6**), despite $\pm 2\%$ being more commonly tolerated.⁴¹ This procedure applied a three-step check for the targeted analysis of the 14 cannabinoids investigated in this study. Detected signals that could not pass all steps of the check would be assigned as belonging to other compounds and in need of further investigations.

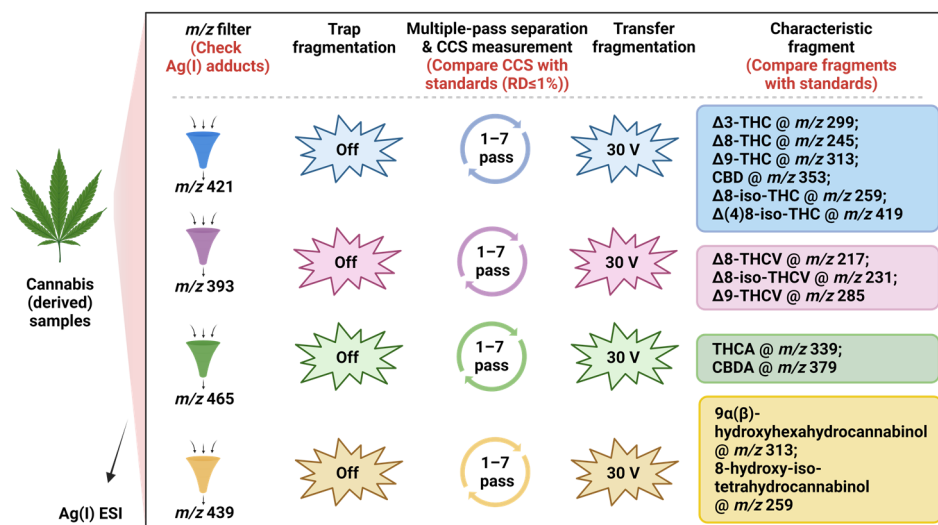


Figure 6.4. Qualitative identification workflow for cannabinoid isomers in a complex matrix.

Qualitative Analysis of Cannabinoids in Samples. With the developed identification procedure, the distribution of 14 cannabinoids (four different MW) was investigated in Cannabis extracts, Δ8-THC gummies, and eight acid-treated CBD mixtures (**SI, Table S1** and **Figure S14**). The extracted ion chromatograms acquired with and without mobility separation demonstrate the necessity of ion mobility separation to resolve cannabinoids with the same molecular weight (**SI, Figures S14-1** to **S14-5**) when using direct infusion analysis. Besides, by checking Ag(I) isotope patterns, compounds that could not form Ag(I) adducts were easily excluded. The eCCS RD of detected cannabinoids in samples from specific standards were within $\pm 0.7\%$ (**SI, Table S7**), much smaller than the reported CCS

reproducibility of $\pm 2\%$ in literature.⁴¹ Subsequent comparison of characteristic fragments further improved the identification confidence. The screening results showed THCA (**10**), CBDA (**11**), Δ^9 -THC (**3**), CBD (**4**), and Δ^9 -THCV (**14**) were abundant cannabinoids in Cannabis extracts. Δ^3 -THC (**1**), Δ^8 -THC (**2**), Δ^9 -THC (**3**), $\Delta(4)8$ -iso-THC (**6**), 9α -hydroxyhexahydrocannabinol (**7**), and 9β -hydroxyhexahydrocannabinol (**8**) were found in Δ^8 -THC gummies. The largest number of cannabinoids that are isomers of THC/CBD that were detected in a single acid-treated CBD mixture was five. The identification results obtained by cIMS matched well with those obtained by UHPLC-UV/MS and GC-FID/MS (SI, **Figure S15**),⁴ with the analysis time shortened from tens of minutes to milliseconds (actual separation), or taking into account the actual machine use, within 3 min. It is noteworthy that the UHPLC-UV/MS method was unable to analyze acid-treated CBD mixtures with many cannabinoid isomers, and the GC-FID/MS method could not analyze acidic cannabinoids in Cannabis extracts due to thermal decomposition. However, with the cIMS method, the quite different samples could all be analyzed. Therefore, the developed cIMS method exhibited a unique combination of high accuracy, efficiency, and versatility for the qualitative analysis of cannabinoid samples.

Quantitative Analysis of Cannabinoids in Samples. To explore the quantitative ability of the developed method, eight acid-treated CBD mixtures containing more isomeric cannabinoids than other samples investigated in this study were analyzed, and the major cannabinoids Δ^8 -THC (**2**), Δ^9 -THC (**3**), and CBD (**4**) were quantified as a proof of concept (**Figure 6.5A**, and SI, **Figure S14**). Calibration curves (SI, **Figure S16**) showed excellent linearity for Δ^8 -THC (**2**) in the range of 1–250 $\text{ng}\cdot\text{mL}^{-1}$ ($R^2 = 0.9999$), Δ^9 -THC (**3**) in the range of 0.1–25 $\text{ng}\cdot\text{mL}^{-1}$ ($R^2 = 0.9987$), and CBD (**4**) in the range of 0.04–10 $\text{ng}\cdot\text{mL}^{-1}$ ($R^2 = 0.9986$). Following that, the absolute weight percentages (w/w%, after solvent evaporation) of the three cannabinoids in the mixtures were compared to results obtained by GC-FID (SI, **Table S8**).⁴ Plotting the results obtained by the two methods (**Figure 6.5B–6.5D**) showed linear correlation ($R^2 > 0.985$), but the cIMS method generally overestimated all three

cannabinoids compared to the GC-FID method. Large deviations were observed for $\Delta 8$ -THC (**2**) in R#8 (RD of 121%), $\Delta 9$ -THC (**3**) in R#4 (RD of 164%), and CBD (**4**) in R#6 (RD of -71%), yet these deviations can be attributed to the low cannabinoid concentrations nearing the LOD of the GC-FID method. The systematic overestimation of the cIMS method could be attributed to matrix effects caused by competitive ionization, insufficient mobility separation, and the occurrence of diagnostic quantification fragments in other compounds. Particularly, for samples with multiple cannabinoid isomers, e.g., acid-treated CBD mixtures, a smaller number of separation passes was used to prevent wrap-around effects and thus resulted in overlapping peaks of isomers and thus to obvious overestimations. To improve the quantification performance, slicing of targeted peaks for more passes of separation might be a solution despite the sacrifice in time and operational simplicity. Moreover, data processing for subtracting signals from unresolved cannabinoids could be explored to further increase the quantification accuracy despite the complexity. Finally, the absence of an internal standard in the quantification of absolute cannabinoid content via MS fragments is another source of systematic errors.⁴⁵ Therefore, using internal standards or determination of the ratio between two compounds with similar ionization efficiency might be a promising solution.^{21,46} With this in mind, we compared the ratio of $\Delta 9$ -THC/ $\Delta 8$ -THC obtained by the cIMS method and the GC-FID method for the purposes of (i) evaluating the relative quantification capability of the developed cIMS method; (ii) checking whether the protocols of converting CBD (**4**) to $\Delta 8$ -THC (**2**) mainly produced $\Delta 8$ -THC (**2**); and (iii) checking whether illegal $\Delta 9$ -THC (**3**) would be produced during $\Delta 8$ -THC (**2**) production. As summarized in **Table S9 (SI, Table S9)** and shown in **Figure 6.5E**, there was an excellent correlation ($R^2 = 0.999$) of measured $\Delta 9$ -THC/ $\Delta 8$ -THC ratios between the cIMS method and GC-FID method in all samples, except for R#8. There, the low concentrations of $\Delta 8$ -THC and $\Delta 9$ -THC, as shown in **Figure 6.5B,C**, resulted in a large difference ($\Delta 9$ -THC/ $\Delta 8$ -THC = 3.6 and = 2.2 by GC-FID and cIMS, respectively). For other samples, both methods showed near-identical $\Delta 9$ -THC/ $\Delta 8$ -THC ratios (slope = 1.05), demonstrating the capability of relative

quantification. The $\Delta 9$ -THC/ $\Delta 8$ -THC ratios also revealed that seven out of eight $\Delta 8$ -THC production methods yielded $\Delta 9$ -THC, and half of these methods produced more $\Delta 9$ -THC than $\Delta 8$ -THC (R#1, R#2, R#6, and R#8 with $\Delta 9$ -THC/ $\Delta 8$ -THC ratio >1). If such mixtures are infused in $\Delta 8$ -THC edibles, not surprisingly, these edibles would be problematic from forensic and health perspectives in terms of $\Delta 9$ -THC, apart from being likely problematic regarding the presence of other compounds as well. Strikingly, $\Delta 9$ -THC (**3**) was detected in both of the investigated commercial $\Delta 8$ -THC gummies (**SI, Figure S14**). In short, the developed cIMS method could be used for reliable relative quantification and has the potential for the direct analysis of $\Delta 9$ -THC in commercial $\Delta 8$ -THC samples.

Comparing the cIMS method with the gold standard GC-FID method, the cIMS method shows substantial advantages in terms of analysis time (~ 150 ms vs ~ 33 min) and sensitivity. LODs achieved with the cIMS method for $\Delta 8$ -THC (**2**), $\Delta 9$ -THC (**3**), and CBD (**4**) were 15, 75, and 1652 times lower than those achieved with the GC-FID method (**SI, Table S10**). Even though the relative quantification performance was comparable to that of the GC-FID method, the absolute quantification ability remains to be improved. Further comparison with the very recent work using DMS¹⁴ can be done in terms of obtained LODs, which are 2–4 orders of magnitude lower in the current study with cIMS-qTOF-MS (0.008 – 0.2 ng·ml⁻¹ in this study vs 10 – 20 ng·ml⁻¹). The DMS-based method was used for the quantitative analysis of one $\Delta 8$ -THC oil and one hemp oil, and the detected cannabinoid concentrations were compared to the commercially declared amounts. Even though the isomeric composition is relatively simple, with a maximum of three isomers, the RD between detected and claimed amounts varied from -2.1% to -82.5% across different cannabinoids. However, no validation with a chromatographic method was performed, which makes it challenging to pinpoint whether these deviations stem from method inaccuracies or incorrect product labeling.

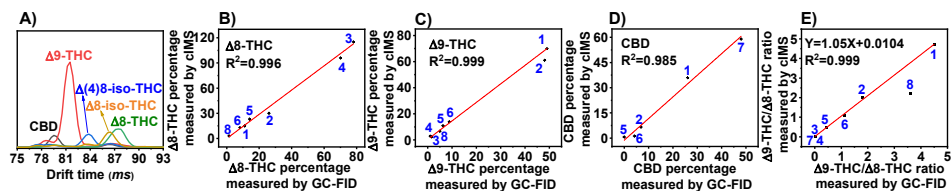


Figure 6.5. A) Extracted mobiligram of the characteristic fragments in R#6 (EIC m/z 353 for CBD; EIC m/z 313 for Δ9-THC; EIC m/z 419 for Δ(4)8-iso-THC($\times 5$); EIC m/z 259 for Δ8-iso-THC; EIC m/z 245 for Δ8-THC) after 4-pass separation; comparison of B) absolute Δ8-THC percentage, C) absolute Δ9-THC percentage, D) absolute CBD percentage, and E) the ratio of Δ9-THC/Δ8-THC in acid-treated CBD samples measured by the developed cIMS method and GC-FID method.

Conclusions

An ultrafast, ultrasensitive, and highly selective method using cIMS-qTOF-MS was developed for the analysis of Cannabis and Cannabis-derived samples. This method enabled the reliable identification of 14 cannabinoids with four different molecular weights, including acidic cannabinoids, neutral cannabinoids, and diastereoisomeric cannabinoids. This method can be expanded for more cannabinoids when reference standards are available. The analysis took milliseconds, and the full measurement of a sample took roughly 3 min. Up to six isomeric cannabinoids in one sample could be separated, which was enough to resolve even the most complex cannabinoid mixture encountered in this study. The identification of these cannabinoids in complex samples was achieved by combining 3 molecular identifiers: Ag(I) isotope pattern and m/z , CCS values, and characteristic MS fragments. Moreover, experimental and theoretical CCS values of the cannabinoid-Ag(I) species were obtained for the first time. The eCCS values were very distinctive for the 14 cannabinoids, while the tCCS values, despite displaying only an average calculation error of 2.6%, yield species-to-species errors that are still too large for practical application, likely due to the small 3D structural differences of these cannabinoid isomers. Not only cannabinoids with C=C bonds but also cannabinoids without olefinic double bonds (three hydrated THC isomers) could be distinguished with the developed method by forming Ag^+ or Na^+ adducts. Most likely, different spatial orientations of hydroxyl groups result in different interactions

with the metal ions. Through the examination of a diverse range of samples, including Cannabis extracts, commercial Δ^8 -THC edibles, and acid-treated CBD mixtures, the developed method demonstrated the ability to reliably identify and sensitively quantify cannabinoid isomers in complex matrixes in milliseconds rather than tens of minutes taken by the current gold standard UHPLC-UV/MS and GC-FID/MS methods. Besides, minimal solvent consumption is another merit. However, manual operation and high cost of the equipment as well as data interpretation need to be considered too, but to some extent, this is also true for chromatographic methods.

Supporting Information

The supporting information is available free of charge at <https://pubs.acs.org/doi/10.1021/acs.analchem.3c05879>, and the table of contents is presented below.

Supporting Information Table of Contents

Table S1	Preparation of acid-treated CBD mixtures	Page S4
Table S2	Cannabinoid composition information of Cannabis and Δ^8 -THC gummies provided by merchants	Page S5
Figure S1	^1H NMR spectra of THCA, Δ^9 -THCV, Δ^8 -THCV, and Δ^8 -iso-THCV standards	Page S6-S10
Figure S2	Reversed-phase UHPLC-UV (215 nm) profiles of Δ^3 -THC, Δ^9 -THCV, THCA, Δ^8 -THCV and Δ^8 -iso-THCV standards	Page S11
Figure S3	GC-FID profile of the mixture of Δ^8 -THCV and Δ^8 -iso-THCV, and EI-MS spectra of Δ^8 -THCV and Δ^8 -iso-THCV	Page S12-S14
Figure S4	Silica-Ag(I) HPLC-DAD (215 nm) profile of the mixture of Δ^8 -THCV and Δ^8 -iso-THCV	Page S15
Table S3	Calibrants used for multipass CCS calibrations	Page S16
Figure S5	Calibration curves for drift time and CCS values	Page S16
Figure S6	Mobiligrams of the mixture of Δ^8 -THC, Δ^9 -THC, Δ^3 -THC, CBD, Δ^8 -iso-THC and $\Delta(4)^8$ -iso-THC in protonated, sodiated, and Ag(I) species for different numbers of passes	Page S17
Figure S7	Characteristic fragments of investigated cannabinoids	Page

	in the presence of Ag(I)	S18-S21
Figure S8	Mobiligram of the mixture of 8-hydroxy-iso-tetrahydrocannabinol, 9 α -hydroxyhexahydrocannabinol, and 9 β -hydroxyhexahydrocannabinol in the form of Ag(I) species	Page S22
Figure S9	Reversed-phase UHPLC-ESI-Orbitrap mass spectra of hydrated THC isomers	Page S23
Figure S10	EI mass spectra of hydrated THC isomers after GC separation	Page S24
Figure S11	Mass spectra of protonated hydrated THC isomers, Ag(I) species of hydrated THC isomers, and premobility fragmentation of hydrated THC isomers in the presence of Ag(I)	Page S25-S27
Table S4	Comparison of predicted CCS values by AllCCS, CCS values from references and experimental CCS values measured by cIMS of THC isomers as protonated species and sodiated species	Page S28
Figure S12	Postmobility fragmentation of Ag(I) species of investigated cannabinoids after a 7-pass separation under different transfer energies	Page S29-S41
Figure S13	Pre- and postmobility fragmentation of hydrated THC isomers in the presence of Ag(I)	Page S42-S44
Table S5	CCS of 9 α -hydroxyhexahydrocannabinol, 9 β -hydroxyhexahydrocannabinol, and 8-hydroxy-iso-THC as well as their dehydrated species in the presence of Ag(I)	Page S45
Table S6	Intraday, interday, and interpass relative standard deviation of [Δ 8-THC + Ag] ⁺ CCS	Page S46
Figure S14	Mobiligram and mass spectra of cannabinoids in samples	Page S47-S103
Table S7	CCS values of detected cannabinoids in acid-treated CBD mixtures	Page S104
Figure S15	Reversed-phase UHPLC-UV (215 nm) profiles of samples C#1, C#2, and C#3 as well as GC-FID profiles of samples G#1 and G#2	Page S105-S106
Figure S16	Calibration curves between the extracted ion chromatogram peak area of characteristic fragments and concentrations of Δ 8-THC, Δ 9-THC, and CBD	Page S107
Table S8	Absolute weight percentages of Δ 8-THC, Δ 9-THC, and CBD in acid-treated CBD mixtures by cIMS and GC-FID	Page S107
Table S9	Ratio of Δ 9-THC/ Δ 8-THC in acid-treated CBD	Page S108

	mixtures analyzed by cIMS and GC-FID	
Table S10	Comparison of LODs between the cIMS method and GC-FID method	Page S109
References		Page S110

Acknowledgments

The authors acknowledge financial support from the Natural Science Foundation of China (22276050, 22276049) and the China Scholarship Council 2020 International Cooperation Training Program for Innovative Talent. The authors thank Prof. Daniele Passarella (Dipartimento di Chimica, Università degli Studi di Milano, Italy) for kindly providing $\Delta(4)$ -8-iso-THC. The authors appreciate the useful discussions with Prof. Pascal Gerbaux and Dr. Quentin Duez (Center of Innovation and Research in Materials and Polymers (CIRMAP), University of Mons-UMONS, Belgium) about CCS calculations. The authors also thank Carlo Roberto de Bruin (Laboratory of Food Chemistry, Wageningen University, The Netherlands) and Alex Muck (Waters Corporation, Stamford Avenue, Altrincham Road, Wilmslow, UK) for technical support.

References

- (1) Felletti, S.; De Luca, C.; Buratti, A.; Bozza, D.; Cerrato, A.; Capriotti, A. L.; Laganà, A.; Cavazzini, A.; Catani, M. Potency testing of cannabinoids by liquid and supercritical fluid chromatography: where we are, what we need. *Journal of Chromatography A* **2021**, *1651*, 462304.
- (2) Golombek, P.; Müller, M.; Barthlott, I.; Sproll, C.; Lachenmeier, D. W. Conversion of cannabidiol (CBD) into psychotropic cannabinoids including tetrahydrocannabinol (THC): a controversy in the scientific literature. *Toxics* **2020**, *8*, 41.
- (3) Marzullo, P.; Foschi, F.; Coppini, D. A.; Fanchini, F.; Magnani, L.; Rusconi, S.; Luzzani, M.; Passarella, D. Cannabidiol as the substrate in acid-catalyzed intramolecular cyclization. *Journal of Natural Products* **2020**, *83*, 2894-2901.
- (4) Huang, S.; van Beek, T. A.; Claassen, F. W.; Janssen, H.-G.; Ma, M.; Chen, B.; Zuilhof, H.; Salentijn, G. I. Comprehensive cannabinoid profiling of acid-treated CBD samples and Δ^8 -THC-infused edibles. *Food Chemistry* **2024**, *440*, 138187.
- (5) LoParco, C. R.; Rossheim, M. E.; Walters, S. T.; Zhou, Z.; Olsson, S.; Sussman, S. Y. Delta-8 tetrahydrocannabinol: a scoping review and commentary. *Addiction* **2023**, *118*, 1011-1028.
- (6) Meehan-Atrash, J.; Rahman, I. Novel Δ^8 -tetrahydrocannabinol vaporizers contain unlabeled adulterants, unintended byproducts of chemical synthesis, and heavy metals. *Chemical Research in Toxicology* **2022**, *35*, 73-76.
- (7) Draper, S. L.; McCarney, E. R. Benchtop nuclear magnetic resonance spectroscopy in forensic chemistry. *Magnetic Resonance in Chemistry* **2023**, *61*, 106-129.
- (8) Tose, L. V.; Santos, N. A.; Rodrigues, R. R. T.; Murgu, M.; Gomes, A. F.; Vasconcelos, G. A.; Souza, P. C. T.; Vaz, B. G.; Romão, W. Isomeric separation of cannabinoids by UPLC combined with ionic mobility mass spectrometry (TWIM-MS)—Part I. *International Journal of Mass Spectrometry* **2017**, *418*, 112-121.
- (9) Kiselak, T. D.; Koerber, R.; Verbeck, G. F. Synthetic route sourcing of illicit at home cannabidiol (CBD) isomerization to psychoactive cannabinoids using ion mobility-coupled-LC-MS/MS. *Forensic Science International* **2020**, *308*, 110173.
- (10) Zietek, B. M.; Mengerink, Y.; Jordens, J.; Somsen, G. W.; Kool, J.; Honing, M. Adduct-ion formation in trapped ion mobility spectrometry as a potential tool for studying molecular structures and conformations. *International Journal for Ion Mobility Spectrometry* **2018**, *21*, 19-32.
- (11) Hädener, M.; Kamrath, M. Z.; Weinmann, W.; Groessl, M. High-resolution ion mobility spectrometry for rapid Cannabis potency testing. *Analytical Chemistry* **2018**, *90*, 8764-8768.
- (12) Huang, S.; Claassen, F. W.; van Beek, T. A.; Chen, B.; Zeng, J.; Zuilhof, H.; Salentijn, G. I. J. Rapid distinction and semiquantitative analysis of THC and CBD by silver-impregnated paper spray mass spectrometry. *Analytical Chemistry* **2021**, *93*, 3794-3802.
- (13) Huang, S.; Qiu, R.; Fang, Z.; Min, K.; van Beek, T. A.; Ma, M.; Chen, B.; Zuilhof, H.; Salentijn, G. I. J. Semiquantitative screening of THC analogues by silica gel TLC with an Ag(I) retention zone and chromogenic smartphone detection. *Analytical Chemistry* **2022**, *94*, 13710-13718.
- (14) Ieritano, C.; Thomas, P.; Hopkins, W. S. Argentination: a silver bullet for cannabinoid separation by differential mobility spectrometry. *Analytical Chemistry* **2023**, *95*, 8668-8678.
- (15) Franklin, E.; Wilcox, M. Gradient HPLC-UV method for cannabinoid profiling. *Chromatography Today* **2019**, 34-37.
- (16) Geci, M.; Scialdone, M.; Tishler, J. The dark side of cannabidiol: the unanticipated social and clinical implications of synthetic Δ^8 -THC. *Cannabis and Cannabinoid Research* **2022**, *8*, 270-282.
- (17) Radwan, M. M.; Wanas, A. S.; Gul, W.; Ibrahim, E. A.; ElSohly, M. A. Isolation and characterization of impurities in commercially marketed Δ^8 -THC products. *Journal of Natural Products* **2023**, *86*, 822-829.
- (18) Giles, K.; Ujma, J.; Wildgoose, J.; Pringle, S.; Richardson, K.; Langridge, D.; Green, M. A cyclic ion mobility-mass spectrometry system. *Analytical Chemistry* **2019**, *91*, 8564-8573.

- (19) Colson, E.; Decroo, C.; Cooper-Shepherd, D.; Caulier, G.; Henoumont, C.; Laurent, S.; De Winter, J.; Flammang, P.; Palmer, M.; Claereboudt, J.; *et al.* Discrimination of regioisomeric and stereoisomeric saponins from aesculus hippocastanum seeds by ion mobility mass spectrometry. *Journal of the American Society for Mass Spectrometry* **2019**, *30*, 2228-2237.
- (20) Ropartz, D.; Fanuel, M.; Ujma, J.; Palmer, M.; Giles, K.; Rogniaux, H. Structure determination of large isomeric oligosaccharides of natural origin through multipass and multistage cyclic traveling-wave ion mobility mass spectrometry. *Analytical Chemistry* **2019**, *91*, 12030-12037.
- (21) de Bruin, C. R.; Hennebelle, M.; Vincken, J.-P.; de Bruijn, W. J. C. Separation of flavonoid isomers by cyclic ion mobility mass spectrometry. *Analytica Chimica Acta* **2023**, *1244*, 340774.
- (22) Ruotolo, B. T.; Benesch, J. L. P.; Sandercock, A. M.; Hyung, S.-J.; Robinson, C. V. Ion mobility-mass spectrometry analysis of large protein complexes. *Nature Protocols* **2008**, *3*, 1139-1152.
- (23) Thalassinos, K.; Grabenauer, M.; Slade, S. E.; Hilton, G. R.; Bowers, M. T.; Scrivens, J. H. Characterization of phosphorylated peptides using traveling wave-based and drift cell ion mobility mass spectrometry. *Analytical Chemistry* **2009**, *81*, 248-254.
- (24) Bush, M. F.; Hall, Z.; Giles, K.; Hoyes, J.; Robinson, C. V.; Ruotolo, B. T. Collision cross sections of proteins and their complexes: a calibration framework and database for gas-phase structural biology. *Analytical Chemistry* **2010**, *82*, 9557-9565.
- (25) Campuzano, I.; Bush, M. F.; Robinson, C. V.; Beaumont, C.; Richardson, K.; Kim, H.; Kim, H. I. Structural characterization of drug-like compounds by ion mobility mass spectrometry: comparison of theoretical and experimentally derived nitrogen collision cross sections. *Analytical Chemistry* **2012**, *84*, 1026-1033.
- (26) McCullagh, M.; Goscinnny, S.; Palmer, M.; Ujma, J. Investigations into pesticide charge site isomers using conventional IM and cIM systems. *Talanta* **2021**, *234*, 122604.
- (27) Zhou, Z.; Shen, X.; Tu, J.; Zhu, Z.-J. Large-scale prediction of collision cross-section values for metabolites in ion mobility-mass spectrometry. *Analytical Chemistry* **2016**, *88*, 11084-11091.
- (28) Zhou, Z.; Luo, M.; Chen, X.; Yin, Y.; Xiong, X.; Wang, R.; Zhu, Z.-J. Ion mobility collision cross-section atlas for known and unknown metabolite annotation in untargeted metabolomics. *Nature Communications* **2020**, *11*, 4334.
- (29) Duez, Q.; van Huizen, N. A.; Lemaure, V.; De Winter, J.; Cornil, J.; Burgers, P. C.; Gerbaux, P. Silver ion induced folding of alkylamines observed by ion mobility experiments. *International Journal of Mass Spectrometry* **2019**, *435*, 34-41.
- (30) Ewing, S. A.; Donor, M. T.; Wilson, J. W.; Prell, J. S. Collidoscope: an improved tool for computing collisional cross-sections with the trajectory method. *Journal of the American Society for Mass Spectrometry* **2017**, *28*, 587-596.
- (31) van Beek, T. A.; Subrtova, D. Factors involved in the high pressure liquid chromatographic separation of alkenes by means of argentation chromatography on ion exchangers: overview of theory and new practical developments. *Phytochemical Analysis* **1995**, *6*, 1-19.
- (32) Kaneti, J.; de Smet, L. C. P. M.; Boom, R.; Zuilhof, H.; Sudhölter, E. J. R. Computational probes into the basis of silver ion chromatography. II. silver(I)-olefin complexes. *The Journal of Physical Chemistry A* **2002**, *106*, 11197-11204.
- (33) Damyanova, B.; Momtchilova, S.; Bakalova, S.; Zuilhof, H.; Christie, W. W.; Kaneti, J. Computational probes into the conceptual basis of silver ion chromatography: I. silver (I) ion complexes of unsaturated fatty acids and esters. *Journal of Molecular Structure: THEOCHEM* **2002**, *589-590*, 239-249.
- (34) Walsh, K. B.; McKinney, A. E.; Holmes, A. E. Minor cannabinoids: biosynthesis, molecular pharmacology and potential therapeutic uses. *Frontiers in Pharmacology* **2021**, *12*, 777804.
- (35) Bloemendal, V. R. L. J.; Sondag, D.; Elferink, H.; Boltje, T. J.; van Hest, J. C. M.; Rutjes, F. P. J. T. A revised modular approach to (-)-trans- Δ^8 -THC and derivatives through late-stage Suzuki-Miyaura cross-coupling reactions. *European Journal of Organic Chemistry* **2019**, *2019*, 2289-2296.
- (36) Citti, C.; Russo, F.; Sgrò, S.; Gallo, A.; Zanutto, A.; Forni, F.; Vandelli, M. A.; Laganà, A.; Montone, C. M.; Gigli, G.; *et al.* Pitfalls in the analysis of phytocannabinoids in Cannabis inflorescence. *Analytical and Bioanalytical Chemistry* **2020**, *412*, 4009-4022.

- (37) Pukala, T. Importance of collision cross section measurements by ion mobility mass spectrometry in structural biology. *Rapid Communications in Mass Spectrometry* **2019**, *33*, 72-82.
- (38) Dodds, J. N.; Baker, E. S. Ion mobility spectrometry: fundamental concepts, instrumentation, applications, and the road ahead. *Journal of the American Society for Mass Spectrometry* **2019**, *30*, 2185-2195.
- (39) Christofi, E.; Barran, P. Ion mobility mass spectrometry (IM-MS) for structural biology: insights gained by measuring mass, charge, and collision cross section. *Chemical Reviews* **2023**, *123*, 2902-2949.
- (40) Belova, L.; Celma, A.; Van Haesendonck, G.; Lemière, F.; Sancho, J. V.; Covaci, A.; van Nuijs, A. L. N.; Bijlsma, L. Revealing the differences in collision cross section values of small organic molecules acquired by different instrumental designs and prediction models. *Analytica Chimica Acta* **2022**, *1229*, 340361.
- (41) Plante, P.-L.; Francovic-Fontaine, É.; May, J. C.; McLean, J. A.; Baker, E. S.; Laviolette, F.; Marchand, M.; Corbeil, J. Predicting ion mobility collision cross-sections using a deep neural network: DeepCCS. *Analytical Chemistry* **2019**, *91*, 5191-5199.
- (42) Colby, S. M.; Thomas, D. G.; Nuñez, J. R.; Baxter, D. J.; Glaesemann, K. R.; Brown, J. M.; Pirrung, M. A.; Govind, N.; Teeguarden, J. G.; Metz, T. O.; *et al.* ISiCLE: a quantum chemistry pipeline for establishing in silico collision cross section libraries. *Analytical Chemistry* **2019**, *91*, 4346-4356.
- (43) Ollivier, S.; Ropartz, D.; Fanuel, M.; Rogniaux, H. Fingerprinting of underivatized monosaccharide stereoisomers using high-resolution ion mobility spectrometry and its implications for carbohydrate sequencing. *Analytical Chemistry* **2023**, *95*, 10087-10095.
- (44) Meier, F.; Garrard, K. P.; Muddiman, D. C. Silver dopants for targeted and untargeted direct analysis of unsaturated lipids via infrared matrix-assisted laser desorption electrospray ionization (IR-MALDESI). *Rapid Communications in Mass Spectrometry* **2014**, *28*, 2461-2470.
- (45) Wang, M.; Wang, C.; Han, X. Selection of internal standards for accurate quantification of complex lipid species in biological extracts by electrospray ionization mass spectrometry—what, how and why? *Mass Spectrometry Reviews* **2017**, *36*, 693-714.
- (46) Liang, Z.; Wang, H.; Wu, F.; Wang, L.; Li, C.; Ding, C.-F. Drug adulteration analysis based on complexation with cyclodextrin and metal ions using ion mobility spectrometry. *Journal of Pharmaceutical Analysis* **2023**, *13*, 287-295.

Rapid Analysis of Δ^8 -Tetrahydrocannabinol, Δ^9 -Tetrahydrocannabinol, and Cannabidiol in Δ^8 -Tetrahydrocannabinol Edibles by Ag(I) Paper Spray Mass Spectrometry after Simple Extraction

Huang, S.; van Beek, T. A.; Beij, E.; Ma, M.; Chen, B.; Zuilhof, H.; Salentijn, G. IJ.

Manuscript submitted to Food Chemistry.



Abstract

Δ 8-THC products have an unclear legal and safety status, yet are quite popular. This creates urgency in understanding their cannabinoid composition, especially regarding the major cannabinoids Δ 8-tetrahydrocannabinol (THC), Δ 9-THC, and cannabidiol (CBD). Here, a simple and fast method was developed for different Δ 8-THC products, combining easy extraction and Ag(I)-impregnated paper spray mass spectrometric analysis. Distinction of Δ 8-THC, Δ 9-THC, and CBD, which is challenging by protonated ESI-MS, was achieved within 1 min (MS² fragments at m/z 353/355 were unique for CBD, while the MS³ fragments at m/z 245 and m/z 217 were specific for Δ 8-THC and Δ 9-THC respectively). A single-step extraction/dilution with methanol (MeOH) resulted in over 85% extraction recovery of Δ 8-THC, Δ 9-THC, and CBD from Δ 8-THC edibles. Acceptable matrix effects were measured for Δ 8-THC (from $-7.1 \pm 1.4\%$ to $17 \pm 2.9\%$), Δ 9-THC (from $2.2 \pm 0.3\%$ to $17 \pm 1.8\%$) and the Δ 9-THC: Δ 8-THC ratio ($7.4 \pm 1.0\%$ to $15 \pm 1.5\%$) in both brownie and vape oil samples with only one exception for 0.1% Δ 9-THC in vape oil ($34 \pm 2.2\%$). The quantification of Δ 9-THC: Δ 8-THC ratios in acid-treated CBD mixtures, predominantly composed of Δ 8-THC, Δ 9-THC, and CBD, using the AgPS-MS method, showed similar results to those obtained with the benchmark GC-FID method (with deviations 0 to -11%). Next, the analysis of five commercial Δ 8-THC products for Δ 8-THC content by the AgPS-MS method was compared to the gold standard GC-FID method, with deviations ranging from -14% to 12% . The developed method revealed that four out of the five commercial products contained illegal levels of Δ 9-THC ($> 0.3\%$), consistent with the GC-FID results. The presence of other isomers Δ 8-iso-THC, Δ (4)8-iso-THC, and Δ 3-THC can be flagged by characteristic MS² and MS³ signals, indicating the need for further confirmation. Overall, the method is an attractive approach for large-scale and quick screening of Δ 8-THC samples.

Introduction

$\Delta 8$ -THC products have experienced a rapid and significant rise in popularity in recent years.¹ One of the major reasons is that The U.S. Agriculture Improvement Act of 2018 (2018 Farm Bill) defined the legal limit of $\Delta 9$ -THC as 0.3% (w/w%),² and CBD as legal. Thus, the easy conversion of cheap CBD to $\Delta 8$ -THC³ created a legal loophole. As a structural isomer of $\Delta 9$ -THC, $\Delta 8$ -THC differs only in the position of the olefinic double bond. In terms of psychoactivity, $\Delta 8$ -THC possesses roughly half of the potency of $\Delta 9$ -THC.^{4,5} $\Delta 8$ -THC, as a constituent of many different types of products, especially edibles, is marketed as a “legal high”.^{1,6} However, many issues have been identified with $\Delta 8$ -THC edibles. For example, from a forensic perspective, illegal levels of $\Delta 9$ -THC ($> 0.3\%$) are frequently found in commercial $\Delta 8$ -THC edibles,^{7,8} while from a food safety aspect, intoxication cases induced by consuming $\Delta 8$ -THC edibles are on the rise.⁹ These issues can be partly explained by the production process of $\Delta 8$ -THC, in which inevitably byproducts such as $\Delta 9$ -THC and other THC isomers are formed, which are difficult to remove before incorporation into food matrixes.^{1,10} Moreover, the lack of regulations, limited information about some of these isomers and wrong/unclear labeling of $\Delta 8$ -THC and CBD content can easily result in overdose consumption and, thus rising hospitalization.¹¹ Therefore, it is crucial to know the isomeric cannabinoid compositions of $\Delta 8$ -THC edibles.

Analysis and distinction of cannabinoid isomers, e.g., $\Delta 8$ -THC, $\Delta 9$ -THC, and CBD, are challenging. Normally, high-resolution chromatographic separation is needed because of the structural similarities.^{3,12,13} NMR can be used as an alternative, but compounds with lower concentrations are easily overlooked.¹⁴⁻¹⁶ Combining speed and sensitivity, ion mobility spectrometry (IMS) has been employed to resolve isomeric cannabinoids. However, the resolution between $\Delta 8$ -THC and $\Delta 9$ -THC is still an issue,^{17,18} unless silver ions are introduced into the IMS.¹⁹ The use of the unique adduct-formation behavior of cannabinoids with silver ions amplifies structural differences and enhances isomer separation in IMS.^{20,21} In recent work, we demonstrated that Ag(I) enables the distinction of isomeric cannabinoids in both

chromatographic and mass spectrometric analyses due to their different affinities for Ag(I).^{3,22,23} While this IMS approach is very powerful, it is also expensive and requires dedicated, state-of-the-art equipment that is not readily available in most labs.

Thus, fast, sensitive, easy, and cheap methods for routine analysis of Δ 8-THC products are still needed. Ambient ionization mass spectrometry (AIMS), which is characterized by high speed, acceptable sensitivity, and ease of use (with no or limited sample pretreatment), stands out as an option.²⁴ Falconer et al.²⁵ applied direct analysis in real-time mass spectrometry (DART-MS) for rapid screening and characterization of approximately 500 vaping liquid samples related to lung injury outbreaks. Within \sim 1.5 min, multiple analytes, including Δ 9-THC and CBD, could be analyzed qualitatively. However, the distinction of cannabinoid isomers (e.g., Δ 8-THC, Δ 9-THC, CBC, and CBD) failed. Similarly, Chambers et al.²⁶ qualitatively analyzed cannabinoid-infused products, personal-care products, and hemp materials in their native forms by DART-high-resolution mass spectrometry (HRMS), yet here again, the ability to distinguish isomers was insufficient. In our previous work, we achieved the first successful differentiation of cannabinoid isomers using Ag(I) impregnated paper spray mass spectrometry (AgPS-MS). This technique enabled us to distinguish between Δ 9-THC and CBD and to semiquantify their ratio in commercial CBD oils.²² However, to the best of our knowledge, there have been no reports about the distinction of Δ 8-THC and Δ 9-THC by AIMS, which is of course essential for the analysis of Δ 8-THC products.

In the current study, we therefore investigated the possibility of using the AgPS-MS method as a fast, easy, and cheap strategy for the distinction between Δ 8-THC and Δ 9-THC and rapid screening of Δ 8-THC products. Δ 8-THC and Δ 9-THC are structurally more similar, having only different positions of a single olefinic double bond instead of having different numbers of olefinic bonds (which is the case for Δ 9-THC and CBD). As a result, Δ 8-THC and Δ 9-THC are expected to have similar affinities for Ag(I). Therefore, multi-stage fragmentation may be necessary to produce more diagnostic fragments. Moreover, considering the huge variety of Δ 8-THC products, a generic, yet simple extraction method that could be used for

different types of matrixes would be preferable in combination with fast instrumental analysis. Lastly, to further reduce the technical expertise required for this analytical method, 3D-printed accessories to simplify paper spray mass spectrometric operations would enable broader applicability in forensic and food safety screening. Therefore in this paper, we aimed to develop a simple and robust procedure to analyze Δ^8 -THC containing samples by the combination of simple extraction, an easy-to-make 3D-printed paper spray device and AgPS-MS analysis.

Materials and Methods

Chemicals and Reagents. Silver nitrate (AgNO_3 , analytical grade) was obtained from Fisher Scientific (Loughborough, Leicestershire). Methanol (MeOH , HPLC-grade) was purchased from VWR Chemicals (Gliwice, Poland). Chloroform (CHCl_3 , $\geq 99\%$) was bought from Sigma-Aldrich (St. Louis, MO, USA). Chromatography paper was purchased from Hangzhou Special Paper Co., Ltd. (Hangzhou, China). Crystalline CBD (declared purity 99%) was obtained from CBDolie.nl. Δ^8 -THC (purity $> 98\%$), Δ^9 -THC (purity $> 98\%$), Δ^9 -THCV (purity $> 90\%$), Δ^8 -iso-THC (purity $> 98\%$), and Δ^3 -THC (named as $\Delta^6\text{a},10\text{a}$ -THC in the general introduction, purity $> 90\%$) were isolated and identified as in our previous studies, and their purities were determined by NMR and HPLC-UV peak integrations at 215 nm.^{3,21} Δ^4 -8-iso-THC was provided by Prof. Danielle Passarella (Dipartimento di Chimica, Università degli Studi di Milano, Milano, Italy). Δ^8 -THC infused brownies, rice crackers, Cannabis leaves, and vape oils were purchased online (**Supporting Information (SI), Table S1**). Normal brownies and vape oils without cannabinoids were obtained in local shops (Wageningen, the Netherlands). Different acid-treated CBD mixtures were obtained in our previous study (**SI, Table S2**).³

Design and Fabrication of 3D-Printed Paper Spray Device/3D-Printing Settings. A 3D-printed paper spray device was designed and produced to stabilize the paper tip, facilitate the sample and solvent application, and position it in front of

the MS. All components of the paper spray device (**SI, Figure S1**) were designed and assembled using computer-aided design (CAD) software SolidWorks 2021 (Dassault Systèmes SolidWorks Corporation, Waltham, USA), and exported in a 3D manufacturing format (.3MF). The sample well slide was fabricated using a high-resolution stereolithography (SLA) printer (Form 3, FormLabs, Somerville, MA, USA). The print file was generated using Preform version 3.33.0 (FormLabs) at a layer resolution of 100 μ m and printed using FormLabs clear resin (V4). Other paper spray accessories, including an arm for anchoring the whole device to the MS, a slide holder, a paper cartridge holder, a slide button for sliding sample wells, and paper cartridge parts, were printed using the Original Prusa i3 MK3S+ (Prusa, Prague, Czech Republic) fused deposition modeling (FDM) printer. These parts were converted into G-Code for 3D printing with PrusaSlicer 2.7.1 (Prusa), using the 0.10 mm “Detail” preset and the following parameters: nozzle diameter 0.4 mm, nozzle temperature 210 °C, bed temperature 60 °C, and organic supports on the build plate only. All FDM parts were printed using biobased filament (Polylite PLA PRO, Polymaker, Utrecht, The Netherlands).

Preparation of Paper Tips, Ag(I)-Impregnated Paper Tips and Ag(I)-Impregnated Paper Tips for 3D-Printed Cartridge. Clean paper tips and Ag(I)-impregnated tips were prepared as described in our previous study.²² Briefly, isosceles triangle paper tips with a height of 10 mm and a base of 5 mm were obtained by cutting chromatography paper with a homemade paper cutter. The paper tips were thoroughly washed by immersing them in MeOH in a sonication bath for half an hour and dried in a vacuum oven overnight. These paper tips are referred to as *clean*. Ag(I)-impregnated tips were prepared from *clean* paper tips following the same procedure, except that a 0.10 mol·L⁻¹ AgNO₃ MeOH solution instead of MeOH was used for immersing paper tips. Ag(I)-impregnated paper tips for the 3D-printed cartridge were placed in the fixed position of the 3D-printed cartridge, after which the cartridge cover was closed for subsequent attachment to the cartridge holder (**SI, Figure S2**).

Linear Ion Trap Mass Spectrometer. A Thermo Velos Pro linear ion trap mass spectrometer (Thermo Fisher Scientific, San Jose, CA, USA) was used in positive mode with a spray voltage of 4 kV, S-lens RF level 68.6%, and capillary temperature of 250 °C, unless specified otherwise. All full-scan measurements were performed with a m/z 100–2000 scan range. Two MS scanning events, including MS^2 and MS^3 , were set to get both acquisitions in one single analysis (**SI, Table S3**). MS transitions of cannabinoids investigated in this study are shown in **Table S4 (SI, Table S4)**. For Δ^9 -THC: Δ^8 -THC ratio measurements, the selected reaction monitoring (SRM) mode was used with the precursor ions m/z 422 ± 2 for MS^2 fragmentation and m/z 313 ± 1 for MS^3 fragmentation.

Paper Spray Setup. *Conventional Paper Spray.* The standard paper spray experiments were conducted as outlined in our previous study.²² Briefly, the paper tip was held by an alligator clip on a modified desorption electrospray ionization (DESI) ion source (Prosolia, USA) with a rotational and x-y-z positioner. This setup was directly connected to the high voltage (HV) supply of the instrument. The front of the paper tip was carefully positioned 4–6 mm from the MS inlet. A voltage of 4 kV was applied after a 15 μ L sample solution was put on the paper tip for spray generation unless otherwise indicated.

3D-Printed Cartridge Paper Spray. A 3D-printed cartridge was used for paper spray experiments. The setup involved pre-assembling a (i) paper spray cartridge holder to a (ii) rotator and (iii) slide holder positioned in front of the MS inlet, which could be done easily by two screws. Samples were deposited in wells of the sample well slide. Then, one-time-use paper spray cartridges could be positioned with the rotator to contact the samples, allowing them to become wetted, after which spray could be generated. Switching between samples was accomplished by sliding the sample well slide and replacing the paper cartridge (**SI Video**).

GC-FID/MS. GC-FID/MS analysis was achieved using the method developed in our previous work.^{3,21} Briefly, a DB-5MS UI capillary column (Agilent J&W GC

column, USA) was connected to an Agilent 5975C VL MSD GC-FID/MS system (Agilent, Amstelveen, the Netherlands). The initial column temperature was set to 200 °C and increased by 1 °C·min⁻¹ to 222.5 °C. Then, the temperature was raised at 5 °C·min⁻¹ to 250 °C and held for 5 min, totaling 33 min of analysis. A 1 µL of sample was injected with a 1:10 split ratio at an injection temperature of 200 °C. Helium was the carrier gas at a constant flow with a linear velocity of 26 cm·s⁻¹. The mass spectrometer was operated in 70 eV electron ionization (EI) mode, scanning from m/z 35 to 500 at 4 spectra·s⁻¹. Measurements were delayed by 3 min after injection to protect the mass spectrometer filament.

Sample Extraction and Extraction Efficiency. *Sample Extraction.* 10.0 ± 1.0 mg of Δ 8-THC infused brownies or rice crackers were accurately weighed (M5, Mettler Instrumente AG, Zurich, Switzerland) in 1.5 mL Eppendorf safe-lock tubes (Eppendorf Nederland B.V., Nijmegen, Netherlands) followed by adding 1.00 mL of MeOH to each tube with a micropipette (Eppendorf research plus, 100–1000 µL, Nijmegen, Netherlands). For Δ 8-THC infused Cannabis leaves, 10.0 ± 1.0 mg was weighed in 15 ml polypropylene screw cap centrifuge tubes (Sarstedt, Nümbrecht, Germany), and 10.0 mL of MeOH was added with a pipette (Eppendorf research plus, 1–10 mL, Nijmegen, Netherlands). These tubes were put into a tube box (or tube rack for 15 mL tubes) and manually shaken for 10 min to extract cannabinoids unless otherwise specified. Obtained solutions were filtered over 0.2 µm PTFE membrane syringe filters (Ø 13 mm, Pall Corporation, Port Washington, NY, USA) and then used for subsequent analysis. Three consecutive MeOH extractions were performed by removing the supernatant after 10-min manual shaking and adding 1.00 mL of fresh MeOH. For tubes containing Cannabis leaves, 10.0 mL instead of 1.00 mL of fresh MeOH was added. The fourth extraction followed a standard procedure described in literature.^{27,28} Specifically, 1.00 mL (or 10.0 mL for Cannabis leaves) of MeOH:CHCl₃ (v:v = 9:1) was added to the sample, followed by vigorous vortexing (Fisherbrand, WhirliMixer, Loughborough, UK) for 1 min. After that, the mixture was centrifuged (Eppendorf 5424R centrifuge, Eppendorf AG, Hamburg, Germany)

at 14000 relative centrifugal force (rcf) for 15 min, and the supernatant was used for subsequent analysis. For $\Delta 8$ -THC infused vape oils, an easy dilution-and-analysis strategy was used, namely 10.0 ± 1.0 mg of vape oils was weighed and diluted by MeOH to $1.00 \text{ mg} \cdot \text{mL}^{-1}$ and then subjected to analysis.

Extraction Efficiency. The extraction efficiency of each extraction was evaluated by the GC-FID method and expressed as: extraction efficiency (%) = $A_{\text{single}}/A_{\text{total}} \times 100$, where A_{single} means the characteristic GC-FID peak area of the single extraction, and A_{total} means the summed-up peak areas from all four extractions, assuming 100% extraction recovery.

Matrix Effects. 100.0 ± 0.3 mg of a normal brownie was extracted by adding 10.0 mL of MeOH and hand-shaking for 10 min and filtered as described above, resulting in the “normal brownie extract”. 100.0 ± 0.3 mg of a normal vape oil was diluted by 10.0 mL of MeOH, resulting in the “normal vape extract.” These extracts were spiked with cannabinoids and referred to as sample type II. The MeOH standard solution containing corresponding concentrations of cannabinoids was referred to as sample type I. Sample types I and II were prepared ($n = 3$) containing 0.1%, 0.3%, and 1% of $\Delta 8$ -THC, $\Delta 9$ -THC, and CBD, as well as 0.5% of $\Delta 9$ -THCV (IS) (w/w%) (**SI, Table S5**). These samples were analyzed by the described AgPS-MS and GC-FID methods.

Matrix Effect for Each Cannabinoid with the AgPS-MS² and AgPS-MS³ Methods. The matrix effect for each cannabinoid with both the AgPS-MS² and AgPS-MS³ methods was calculated as: matrix effect (%) = $((A_{\text{II}}/A_{\text{I}}) - 1) \times 100$. First, the extracted ion chromatogram (EIC) of each cannabinoid was normalized to the total ion chromatogram (TIC) (EIC/TIC) to correct for spray instability. A_{II} and A_{I} were the normalized characteristic EIC areas of each cannabinoid (m/z 245 for $\Delta 8$ -THC in the MS² spectrum, m/z 313 for $\Delta 9$ -THC in the MS² spectrum, and m/z 353 for CBD in the MS² spectrum; m/z 217 for $\Delta 9$ -THC in the MS³ spectrum, m/z 245 for $\Delta 8$ -THC in the MS³ spectrum) in sample type II and sample type I, respectively.

Matrix Effect for the $\Delta 9$ -THC: $\Delta 8$ -THC Ratio with the AgPS-MS² and AgPS-MS³

Methods. The matrix effect for the Δ 9-THC: Δ 8-THC ratio with the AgPS-MS² and AgPS-MS³ methods were expressed as: $(R_{\text{matrix}} - R_{\text{solvent}})/R_{\text{solvent}} \times 100$, where R_{matrix} represents the characteristic peak area ratio of Δ 9-THC: Δ 8-THC (m/z 313: m/z 245 in MS² spectrum and m/z 217: m/z 245 in MS³ spectrum) in the matrix, and R_{solvent} represents the characteristic peak area ratio of Δ 9-THC: Δ 8-THC (m/z 313: m/z 245 in MS² spectrum and m/z 217: m/z 245 in MS³ spectrum) in the solvent.

Matrix Effect for Each Cannabinoid with the GC-FID Method. The matrix effect for each cannabinoid with the GC-FID method was calculated as: matrix effect (%) = $((A_{\text{II}}/A_{\text{I}}) - 1) \times 100$. A_{II} and A_{I} were the characteristic GC-FID areas of each cannabinoid.

Calibration Curve Construction and Evaluation of LOD. Stock solutions of Δ 8-THC at 1.00 mg·mL⁻¹, Δ 9-THC at 1.00 mg·mL⁻¹, CBD at 1.00 mg·mL⁻¹, and internal standard (IS) Δ 9-THCV at 5.00 mg·mL⁻¹ were prepared in MeOH.

Δ 9-THC: Δ 8-THC Ratio Calibration Curve. Δ 8-THC and Δ 9-THC stock solutions were used to prepare calibration solutions with various Δ 9-THC: Δ 8-THC ratios (0.00100, 0.00200, 0.00500, 0.0100, 0.0200, 0.0500, 0.100, 0.200, 0.500, and 1.00; $n = 3$ per ratio), maintaining the Δ 8-THC concentration at a constant 50.0 $\mu\text{g}\cdot\text{mL}^{-1}$. To achieve this, specific volumes of methanolic stock solutions were mixed and diluted with MeOH to a final volume of 2.00 mL. These samples were then analyzed with the AgPS-MS method in selected reaction monitoring (SRM) mode with precursor ions at m/z 422 \pm 2 for MS² fragmentation and MS² fragments at m/z 313 \pm 2 for MS³ fragmentation. The characteristic MS² and MS³ extracted ion chromatogram (EIC) area ratios of Δ 9-THC: Δ 8-THC were plotted against the concentration ratios of Δ 9-THC: Δ 8-THC to construct calibration curves for AgPS-MS² and AgPS-MS³. A correction was made by subtracting the signal of m/z 313 from Δ 8-THC in MS² spectra to obtain a net MS² signal intensity of Δ 9-THC. Similarly, the signal of m/z 245 from Δ 9-THC in MS³ spectra was subtracted to obtain a net MS³ signal intensity of Δ 8-THC. The characteristic MS² EIC area ratios of Δ 9-THC: Δ 8-THC were obtained after subtracting the MS² background value of

$0.53 \times \text{EIC} (m/z 245)$ from $\Delta 8$ -THC and expressed as $(A_{\text{EIC}(m/z 313)} - (0.53 \times A_{\text{EIC}(m/z 245)})) / A_{\text{EIC}(m/z 245)}$. Similarly, the characteristic MS^3 EIC area ratios of $\Delta 9$ -THC: $\Delta 8$ -THC were obtained after subtracting the MS^3 background value of $0.074 \times \text{EIC} (m/z 217)$ for $\Delta 8$ -THC and expressed as $A_{\text{EIC}(m/z 217)} / (A_{\text{EIC}(m/z 245)} - (0.074 \times A_{\text{EIC}(m/z 217)}))$.

$\Delta 8$ -THC, $\Delta 9$ -THC, and CBD Concentration Calibration Curve. Three-standard solutions of 200, 100, 50.0, 10.0, 5.00, and 1.00 $\mu\text{g}\cdot\text{mL}^{-1}$, each containing 50.0 $\mu\text{g}\cdot\text{mL}^{-1}$ of the internal standard, were prepared by mixing stock solutions of $\Delta 8$ -THC, $\Delta 9$ -THC, and CBD and serially diluting them with MeOH. These solutions were analyzed using the AgPS-MS and GC-FID methods. Characteristic peak areas were normalized by the area of the internal standard and the obtained ratios were plotted against the concentrations to construct calibration curves for quantification. The limit of detection (LOD) of $\Delta 8$ -THC, $\Delta 9$ -THC, and CBD by the AgPS-MS method was estimated by: $\text{LOD} = 3 \times \text{SD}$ of the lowest concentration of the calibration curve/slope of the calibration curve.²⁹

Sample Analysis. *$\Delta 9$ -THC: $\Delta 8$ -THC Ratio Analysis of Acid-treated CBD Mixtures.* Acid-treated CBD mixtures were prepared in MeOH at 100 $\mu\text{g}\cdot\text{mL}^{-1}$ and analyzed by the AgPS-MS method and the GC-FID method.

Screening Analysis of $\Delta 8$ -THC Products. $\Delta 8$ -THC products were extracted or diluted as described above. The internal standard was added to the sample extracts prior to AgPS-MS analysis to achieve the same final internal standard concentration as used in the calibration curves. Concentrations of $\Delta 8$ -THC, $\Delta 9$ -THC, and CBD were calculated with the constructed calibration curves, and their absolute percentages were expressed as below, considering any dilution factors applied:

$$\text{Weight percentage (\%)} = \frac{C \times V}{W} \times 100,$$

with: C = calculated concentration in extract ($\mu\text{g}\cdot\text{mL}^{-1}$); V = volume of extract (mL); W = total sample weight (μg).

Standard Addition of $\Delta 8$ -THC Products. A 1.00 $\text{mg}\cdot\text{mL}^{-1}$ $\Delta 8$ -THC vape oil extract was diluted with MeOH to 0.250 $\text{mg}\cdot\text{mL}^{-1}$. A 10.0 $\text{mg}\cdot\text{mL}^{-1}$ $\Delta 8$ -THC

brownie extract was blow-dried and reconstituted in MeOH to 20.0 mg·mL⁻¹. The resulting “ Δ 8-THC edible extracts” were spiked with various volumes of Δ 8-THC and Δ 9-THC stock solutions, along with a fixed volume of Δ 9-THCV (IS) stock solution to make solutions containing 200, 150, 100, 50.0, and 0 μ g·mL⁻¹ of Δ 8-THC and 40.0, 30.0, 20.0, 10.0, and 0 μ g·mL⁻¹ of Δ 9-THC, in addition to what was already present in the samples. Each solution also contained 50.0 μ g·mL⁻¹ of the internal standard. Ratios of the characteristic EIC of Δ 8-THC (m/z 245 in the MS³ spectrum) and Δ 9-THC (m/z 217 in the MS³ spectrum) to the internal standard (m/z 189 in the MS³ spectrum) were calculated and plotted against the added concentrations of Δ 8-THC and Δ 9-THC to construct calibration curves. The X-intercept of each calibration curve was determined and used to identify the concentration of Δ 8-THC and Δ 9-THC in the non-spiked Δ 8-THC edible extracts. The absolute percentages of Δ 8-THC and Δ 9-THC were calculated as previously described, accounting for any dilution factors applied.

Results and Discussion

Ag(I)-Impregnated Paper Spray Mass Spectrometric Distinction of Δ 8-THC and Δ 9-THC. Distinguishing isomeric cannabinoids using AIMS is challenging. In 2021, we demonstrated for the first time that by using a AgPS-MS² method, cannabinoid isomers (Δ 9-THC and CBD) with identical mass spectra and MS/MS product ion spectra of protonated precursor ions³⁰ show completely different product ion spectra when selecting silver adducts as precursor ions.²² Similarly, using this AgPS-MS² method, Δ 8-THC, and Δ 9-THC produce distinct MS² spectra with a base peak at m/z 313 for Δ 9-THC and m/z 245 for Δ 8-THC (**Figure 7.1A** and **7.1B**).^{3,21} However, in the MS² spectrum of Δ 8-THC (**Figure 7.1A**), there is also a significant (~50%) peak at m/z 313. This equals the mass of the characteristic MS² fragment of Δ 9-THC. While this is not an issue in combination with a chromatographic separation³ or IMS separation,²¹ it presents a challenge in paper spray analysis, where there is no physical separation of molecules or ions prior to the MS analysis.

To rule out the possibility of conversion from $\Delta 8$ -THC to $\Delta 9$ -THC and thus leading to the observed signal of m/z 313 in the MS² spectrum of $\Delta 8$ -THC, the peak area ratio of m/z 313 to m/z 245 was measured for pure $\Delta 8$ -THC under various conditions, including different CID energies, capillary temperatures, and spray voltages. This is based on the assumption that if any degradation were to occur, it would likely happen during the spray process, influenced by one or more of the factors mentioned above. The ratio remained constant within the range of 0.46–0.56 regardless of the parameter changes. When MS parameters are constant, the ratio of m/z 313: m/z 245 is 0.53 ± 0.01 across a wide concentration range of 0.5–1000 $\mu\text{g}\cdot\text{mL}^{-1}$ (**SI, Figure S3**). This suggests that the fragment at m/z 313 in the MS² spectrum of $\Delta 8$ -THC is a genuine fragment of $\Delta 8$ -THC and not due to *in situ* conversion to $\Delta 9$ -THC, as such conversion would likely cause a change in the ratio of m/z 313: m/z 245 with parameter adjustments.

Considering the above, the m/z 313 signal in the $\Delta 8$ -THC spectrum can be subtracted as the background value in the MS data from samples. Quantitative analysis of the $\Delta 9$ -THC to $\Delta 8$ -THC ratio in samples can be achieved by first subtracting the background value of $0.53 \times \text{EIC} (m/z 245)$ in pure $\Delta 8$ -THC and then determining the EIC area ratio of m/z 313: m/z 245 in the MS² spectra. A similar strategy was shown to be effective for analyzing $\Delta 9$ -THC:CBD ratios in commercial CBD oils in our previous study.²²

For $\Delta 8$ -THC products, it is important to obtain content information for both $\Delta 8$ -THC and $\Delta 9$ -THC as both possess psychoactive properties. When $\Delta 8$ -THC and $\Delta 9$ -THC coexist, m/z 245 in the MS² spectrum can be used to quantify $\Delta 8$ -THC. To quantify $\Delta 9$ -THC, the m/z 313 signal first requires subtracting a high background value ($0.53 \times \text{EIC} (m/z 245)$) produced by $\Delta 8$ -THC during the MS² stage. This high background value potentially hinders direct and sensitive $\Delta 9$ -THC analysis. To further improve the selectivity, MS³ fragmentation was performed by fragmenting the m/z 313 fragments from the MS² stage. The MS³ spectrum of $\Delta 8$ -THC is dominated by a fragment at m/z 245 (**Figures 7.1C**), and the MS³ spectrum of $\Delta 9$ -THC is dominated by a fragment at m/z 217 (**Figure 7.1D**). Even though there is a

minor peak at m/z 245 in the MS³ spectrum of Δ 9-THC, the signal intensity is only around 7% of the base peak (m/z 217). The EIC peak area ratio of m/z 245 to m/z 217 in the MS³ spectra of pure Δ 9-THC was consistently 0.074 ± 0.0038 , regardless of different CID energies and isolation windows (SI, Table S6 and Figure S4). When using the AgPS-MS³ method, the MS³ fragment at m/z 217 can be used to characterize Δ 9-THC, and the MS³ fragment at m/z 245 can be used to characterize Δ 8-THC after subtracting the background value of $0.074 \times \text{EIC} (m/z 217)$.

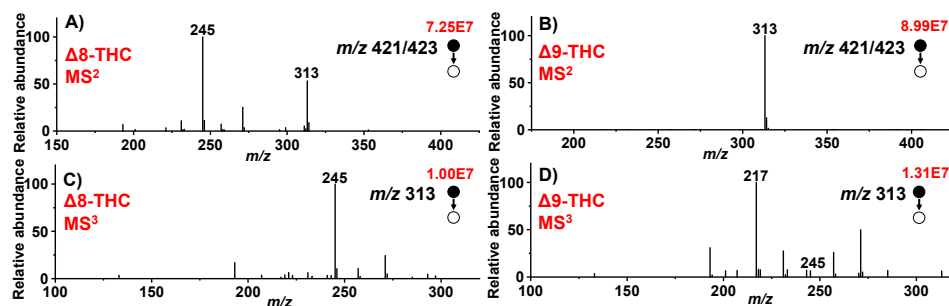


Figure 7.1. AgPS-MS² spectra of A) Δ 8-THC and B) Δ 9-THC (m/z 422 \pm 2 as precursor ions) as well as AgPS-MS³ spectra of C) Δ 8-THC and D) Δ 9-THC (product ions from the MS² fragment at m/z 313 \pm 2).

Extraction Efficiency. The broad scope of Δ 8-THC products poses great challenges for sample extraction and pretreatment due to the diversity of the matrixes and their physicochemical properties.²⁶ Generally, extraction procedures are needed according to the different forms of products, e.g., solid-phase extraction, ultrasound-assisted extraction, and Soxhlet extraction.^{27,28,31} These sample pretreatment operations require expertise, resources, and time, which limits large scale screening of different forms of Δ 8-THC products. Since the objective of the current work is to develop an easy and fast method for screening of different types of Δ 8-THC products, a simple and straightforward sample extraction step, which is suitable for both solid and liquid products, is deemed preferable prior to the rapid analysis by AgPS-MS. In our previous work, extraction by MeOH vortexing was demonstrated as an efficient strategy for extracting Δ 9-THC and CBD from CBD oils in a short time, with minimal matrix effects.²² Moreover, MeOH was demonstrated to be the

optimum solvent for extracting cannabinoids from Cannabis plant materials and food matrixes.^{32,33} Therefore, MeOH was selected as the extraction solvent to extract $\Delta 8$ -THC, $\Delta 9$ -THC, and CBD from $\Delta 8$ -THC brownies, rice crackers, Cannabis leaves, and vape oils; handshaking instead of vortexing was used for reducing dependency on instruments.

To evaluate the recovery of a single extraction by such a simple method, firstly, four repeated extractions of the solid samples were conducted, aiming to achieve exhaustive extraction of $\Delta 8$ -THC, $\Delta 9$ -THC, and CBD. Three consecutive extractions in MeOH were performed, followed by a fourth extraction using a commonly applied extraction method involving vortexing and centrifuging that was assumed would recover the remaining cannabinoids almost completely (recoveries of 79.9%–114.3% have been reported).^{27,28} Here, this fourth extraction yielded almost no additional $\Delta 8$ -THC, $\Delta 9$ -THC, and CBD, supporting that assumption. Secondly, the combined recoveries from the four extractions were considered quantitative and the recoveries of the individual extraction steps were normalized against this total recovery (100%). As a result (**Figure 7.2**), a single extraction by handshaking already resulted in recoveries of $94.4 \pm 2.9\%$ for $\Delta 8$ -THC and $97.7 \pm 2.1\%$ for $\Delta 9$ -THC in $\Delta 8$ -THC brownies; $87.9 \pm 16\%$ for $\Delta 8$ -THC and $85.7 \pm 17\%$ for $\Delta 9$ -THC in $\Delta 8$ -THC rice crackers; $96.7 \pm 0.6\%$ for $\Delta 8$ -THC, $95.8 \pm 1.3\%$ for $\Delta 9$ -THC and $96.0 \pm 0.2\%$ for CBD in $\Delta 8$ -THC-coated Cannabis leaves. For liquid products, namely vape oils in this study, MeOH was used for dilution, and the resulting clear mixtures obtained were directly used for subsequent analysis. Therefore, a recovery of 100% was assumed for these liquid products.

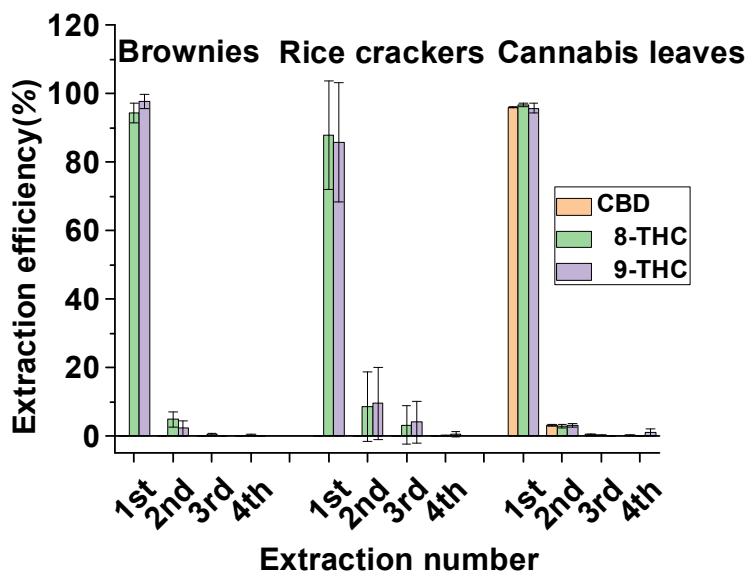


Figure 7.2. Extraction efficiency for Δ 8-THC, Δ 9-THC, and CBD from solid Δ 8-THC products as a function of the number of extractions.

Matrix Effects. To evaluate the matrix effects in the detection of Δ 8-THC, Δ 9-THC, and CBD in combination with this extraction method, normal brownies and vape oils without cannabinoids were used as representative matrixes for solid and liquid products, respectively (Table 1, SI, Table S7). Three different spiking weight percentages, 0.1%, 0.3%, and 1% (low, medium, and high) for Δ 8-THC, Δ 9-THC, and CBD were assessed. Using the AgPS-MS² method, matrix effects were generally more pronounced, ranging from $-40 \pm 1.1\%$ to $-19 \pm 2.0\%$ for Δ 8-THC, $-35 \pm 0.7\%$ to $-4.5 \pm 0.5\%$ for Δ 9-THC, and $7.3 \pm 1.7\%$ to $17 \pm 2.4\%$ for Δ 9-THC: Δ 8-THC ratio. In contrast, the AgPS-MS³ method showed significantly reduced matrix effects for Δ 8-THC, with acceptable values ranging from $-7.1 \pm 1.4\%$ to $17 \pm 2.9\%$ across two different matrixes at three concentration levels.³⁴ Similarly, matrix effects for Δ 9-THC (signal enhancement from $2.2 \pm 0.3\%$ to $17 \pm 1.8\%$) were acceptable except in the vape oil matrix at a spiking percentage of 0.1%, where a matrix effect of $34 \pm 2.2\%$ was observed. For the ratio of Δ 9-THC: Δ 8-THC, satisfactory matrix (-25% – 25% ³⁴) were observed in all these situations ($7.4 \pm 1.0\%$ to $15 \pm 1.5\%$). The overall

reduced matrix effects of the AgPS-MS³ method indicate better selectivity for Δ 8-THC and Δ 9-THC due to the additional fragmentation step. Moreover, since Δ 8-THC and Δ 9-THC are structural isomers, differing only in the position of the C=C bond, they were similarly affected by the matrixes and thus the ratio Δ 9-THC: Δ 8-THC was less affected (all within $\pm 25\%$)³⁴ by matrix effects in both the AgPS-MS² ($7.3 \pm 1.7\%$ to $17 \pm 2.4\%$) and AgPS-MS³ ($7.4 \pm 1.0\%$ to $15 \pm 1.5\%$) methods compared with the individual compounds. Besides, the matrix effects for Δ 9-THCV ($-60 \pm 1.2\%$ to $-33 \pm 0.6\%$ in the AgPS-MS² and $-39 \pm 2.1\%$ to $-12 \pm 1.0\%$ in the AgPS-MS³) were quite different (more suppressed) from Δ 8-THC and Δ 9-THC, indicating that more suitable internal standards e.g., deuterated internal standards are desired to improve the analysis performance.³⁵ For CBD, which was only identified by the AgPS-MS² method, there were pronounced signal enhancements of over 25% ³⁴ with only one exception of the brownie matrix at a spiking percentage of 1% (matrix effect of $16 \pm 3.6\%$). On the other hand, due to the chromatographic separation procedure (33 min), a GC-FID based method developed previously³ showed minor matrix effects ($-1.6 \pm 0.0\%$ to $7.2 \pm 0.1\%$) for all the three cannabinoids in the two matrixes at three spiking weight percentages.³⁴ Therefore, such a simple sample pretreatment method, if combined with the GC-FID method, would have very limited matrix effects on the analysis of the three isomeric cannabinoids. If combined with the much faster AgPS-MS method (tens of seconds vs. 33 min), matrix effects for Δ 8-THC and Δ 9-THC were generally acceptable (-25% – 25%).³⁴ However, the matrix effects were more pronounced and significant for CBD, exceeding the tolerant limit.³⁴ Since CBD is legal and non-psychoactive, its measurement in this study is primarily to determine whether it is present in high abundance and thus could interfere with the Δ 8-THC and Δ 9-THC determinations. Therefore, minimizing the matrix effect for CBD is not as crucial as it is for Δ 8-THC and Δ 9-THC in Δ 8-THC samples (as opposed to CBD-based products, such as CBD oils). In short, such a simple extraction could result in satisfactory recoveries ($85.7 \pm 17\%$ to $97.7 \pm 2.1\%$) of Δ 8-THC, Δ 9-THC, and CBD,^{27,28,31} and acceptable matrix effects ($7.4 \pm 1.0\%$ to $15 \pm 1.5\%$) for Δ 9-THC: Δ 8-THC ratios when combined with

fast and direct paper spray analysis.³⁴

Table 7.1. Matrix effect of AgPS-MS³ and GC-FID methods.

Spiking matrix and concentration (w/w%)	AgPS-MS				GC-FID		
	Δ 8-THC	Δ 9-THC	CBD*	Δ 9-THC: Δ 8-THC	Δ 8-THC	Δ 9-THC	CBD
Blank vape (0.1%)	17 \pm 2.9%	34 \pm 2.2%	49 \pm 2.6%	14 \pm 3.4%	-1.6 \pm 0.02%	-0.9 \pm 0.02%	0.85 \pm 0.01%
Blank vape (0.3%)	1.9 \pm 0.1%	17 \pm 1.8%	36 \pm 1.7%	15 \pm 1.5%	2.2 \pm 0.02%	0.8 \pm 0.005%	3.3 \pm 0.03%
Blank vape (1%)	-7.0 \pm 0.9%	3.8 \pm 0.5%	24 \pm 0.2%	12 \pm 0.5%	0.8 \pm 0.002%	0.1 \pm 0.0005%	2.1 \pm 0.007%
Blank brownie (0.1%)	1.5 \pm 0.1%	12 \pm 1.9%	49 \pm 1.2%	10 \pm 1.8%	-1.6 \pm 0.02%	0.06 \pm 0.002%	4.2 \pm 0.05%
Blank brownie (0.3%)	1.3 \pm 0.1%	8.9 \pm 0.7%	30 \pm 1.4%	7.4 \pm 1.0%	3.2 \pm 0.02%	7.2 \pm 0.06%	5.9 \pm 0.03%
Blank brownie (1%)	-7.1 \pm 1.4%	2.2 \pm 0.3%	16 \pm 3.6%	9.9 \pm 1.9%	-1.4 \pm 0.003%	-0.8 \pm 0.003%	0.7 \pm 0.004%

* CBD was measured by the AgPS-MS² method; \pm SD ($n = 3$).

Calibration Curve and LOD. Δ 8-THC is normally produced from CBD accompanied by side products (such as Δ 9-THC) as well as residual CBD, and all these compounds can end up in commercial Δ 8-THC products.³ Based on our previous work, the AgPS-MS² method can be used to resolve Δ 9-THC and CBD, with characteristic fragments at m/z 313 for Δ 9-THC and m/z 353/355 for CBD.²² Here, the quantification performance of Δ 8-THC, Δ 9-THC, and CBD by the AgPS-MS² and AgPS-MS³ methods was evaluated. It is worth mentioning that with the MS settings of two scan events, both MS² and MS³ acquisitions can be obtained in one spray experiment, and thus, the quantification of Δ 8-THC, Δ 9-THC, and CBD can be achieved in a single analysis.

Calibration Curve of Δ 9-THC: Δ 8-THC Ratio. To investigate the relative quantification potential of the developed method, calibration curves of Δ 9-THC: Δ 8-THC ratio with the AgPS-MS² method and the AgPS-MS³ method were established in MeOH (**SI, Figure S5**). Concentration dependency was found for both the AgPS-MS² method ($R^2 = 0.9854$) and the AgPS-MS³ method ($R^2 = 0.9764$) within the Δ 9-

THC: Δ 8-THC ratio range of 1.00×10^{-3} to 1.00. This demonstrates that the developed method can be effectively used to determine the ratio of these two isomers in the absence of other cannabinoids, and is suitable for relatively simple samples.

Calibration Curve of Δ 8-THC, Δ 9-THC, and CBD and their LODs. To explore the potential for absolute quantification, Δ 9-THCV was used as an internal standard (IS) and added to samples just prior to the analysis. Δ 9-THCV, as a phytocannabinoid, is structurally similar to Δ 8-THC and Δ 9-THC but not likely to exist in synthetic Δ 8-THC products.³⁶ The linear range for Δ 8-THC, Δ 9-THC, and CBD is 1.00–200 $\mu\text{g}\cdot\text{mL}^{-1}$ ($R^2 = 0.9973$ for Δ 8-THC, $R^2 = 0.9994$ for Δ 9-THC, and $R^2 = 0.9852$ for CBD) with an LOD of 0.1 $\mu\text{g}\cdot\text{mL}^{-1}$ for Δ 8-THC and Δ 9-THC and 0.2 $\mu\text{g}\cdot\text{mL}^{-1}$ for CBD when using the AgPS-MS² method. The AgPS-MS³ method had the same linear range of 1.00–200 $\mu\text{g}\cdot\text{mL}^{-1}$ for Δ 8-THC and Δ 9-THC ($R^2 = 0.9977$ for Δ 8-THC and $R^2 = 0.9959$ for Δ 9-THC) but gave a slightly higher LOD of 0.3 $\mu\text{g}\cdot\text{mL}^{-1}$ for Δ 8-THC and Δ 9-THC (**SI, Figure S6, S7**). Despite the slight compromise in sensitivity from MS² to MS³, the enhanced selectivity through two rounds of selecting the targeted signal and fragmenting is expected to decrease matrix interference as discussed above. Moreover, in the MS³ spectrum, m/z 217 only exists in the spectrum of Δ 9-THC, while m/z 245 is mainly originating from Δ 8-THC with a minor contribution from Δ 9-THC. This makes the analysis and identification of Δ 8-THC and Δ 9-THC more straightforward — again, in the absence of other isomers that might produce the same fragments. For CBD, the characteristic (most intense) fragment occurs at m/z 353/355 in the MS² spectrum, with a minor fragment at m/z 313 (around 2.8% of the base peak).²² Further fragmenting m/z 313 signal of CBD resulted in the MS³ spectrum with m/z 217 as the base peak accompanied by a minor peak at m/z 245 (around 5% of the base peak), which equals the mass of the characteristic fragments of Δ 9-THC and Δ 8-THC, respectively. Therefore, the contribution of m/z 217 and m/z 245 in the MS³ stage of CBD would interfere with the quantification of Δ 8-THC and Δ 9-THC, especially when large amounts of CBD exist. Moreover, since CBD (containing two C=C bonds) has stronger affinities for

Ag(I) compared with Δ 8-THC and Δ 9-THC (containing only one C=C bond), a substantial CBD content would likely affect quantitative performance via argentation competition. Consequently, CBD levels should be monitored as well.

Analysis of Acid-Treated CBD Mixtures. As mentioned, producing Δ 8-THC from CBD regularly results in Δ 9-THC and other THC isomers.¹⁰ In our previous study,³ we applied different conversion methods, including methods that could be used in a home kitchen, to produce Δ 8-THC from CBD, aiming to understand the possible cannabinoid profile in Δ 8-THC infused edibles. Chromatographic methods (with run times of 30–40 min) were needed to distinguish and quantify isomeric cannabinoids in different acid-treated CBD mixtures. Considering that such acid-treated CBD protocols are commonly used to produce Δ 8-THC for infusion into food matrixes, fast and easy methods for screening for Δ 8-THC and Δ 9-THC content would allow for faster optimization of the production process and thereby ensuring that Δ 9-THC does not end up in Δ 8-THC products. Therefore, the ratios of Δ 9-THC: Δ 8-THC in seven acid-treated CBD mixtures were measured by the AgPS-MS method and results were compared with those obtained by the GC-FID method in our previous study (**SI, Figure S8, S9, Table S8**).³ For samples #1 and 2, there were minor deviations (0 to −11%) between the results obtained by the two methods probably because Δ 8-THC and Δ 9-THC are much more abundant than other THC isomers. For sample #7, no peak at m/z 245 and dominant signals at m/z 353/355 were observed in the MS² spectrum, indicating no Δ 8-THC and abundant CBD, which matches the result obtained by GC-FID. For samples #3, 4, 5, and 6, in which Δ 8-iso-THC and Δ (4)-8-iso-THC were present in higher amounts than either Δ 8-THC (sample #6) or Δ 9-THC (samples #3, #4 and #5), varying deviations were observed for the AgPS-MS² (−36% to 200%) and AgPS-MS³ methods (−36% to 69%). An overall better result was achieved by the AgPS-MS³ method than the AgPS-MS² method, indicating that an additional fragmentation step effectively reduces interferences from other THC isomers. Besides, the results show that the Ag-PS² and AgPS-MS³ methods are suitable to determine the ratios of Δ 9-THC: Δ 8-

THC in samples containing minor other THC isomers.

It is clear that samples that contain high amounts of other isomers are problematic. First, it complicates the accurate analysis of $\Delta 8$ -THC and $\Delta 9$ -THC content. Second, from a consumer perspective, these isomers are concerning because they are not well-studied and may have negative health effects. In order to provide a strategy to flag these samples for further analysis, purified cannabinoid isomers with MW = 314 from our previous work²¹ were investigated by the AgPS-MS method and the spectra were compared with $\Delta 8$ -THC and $\Delta 9$ -THC (**SI, Figure S10, S11**). $\Delta 8$ -iso-THC produced MS² fragments at m/z 313 (20% of the base peak) and MS³ fragments at m/z 217 and m/z 245 (both 40% of the base peak) that would certainly interfere with the $\Delta 8$ -THC and $\Delta 9$ -THC quantification. However, the pronounced MS² fragment at m/z 299 and MS³ fragment at m/z 243 of $\Delta 8$ -iso-THC, which are barely visible in $\Delta 8$ -THC and $\Delta 9$ -THC can be used to flag its presence. Similarly, $\Delta(4)8$ -iso-THC produced MS² fragments at m/z 313 (35% of the base peak) and MS³ fragments at m/z 217 and m/z 245 (both 25% of the base peak), interfering with the analysis of $\Delta 8$ -THC and $\Delta 9$ -THC. At the same time, a strong MS² signal at m/z 299 and an MS³ signal at m/z 223, which were very minor or absent in $\Delta 8$ -THC and $\Delta 9$ -THC allows discrimination of $\Delta(4)8$ -iso-THC from both $\Delta 8$ -THC and $\Delta 9$ -THC. $\Delta 3$ -THC produced MS² fragments at m/z 313 (55% of the base peak) and MS³ fragments at m/z 217 (55% of the base peak) and m/z 245 (20% of the base peak) — as well as a specific and discriminatory MS² fragment at m/z 299 and MS³ fragment at m/z 243, compared to $\Delta 8$ -THC and $\Delta 9$ -THC. In summary, the existence of such isomeric cannabinoids would contribute to different extents in overestimating $\Delta 8$ -THC and $\Delta 9$ -THC and thus result in the deviation of $\Delta 9$ -THC: $\Delta 8$ -THC ratios from those measured by the GC-FID method. At the same time, the presence of diagnostic fragments (m/z 299 in MS² spectra and m/z 223 or m/z 243 in MS³ spectra) for their presence can be used to observe whether this potential problem really occurs, and — only in that case — flag samples for more detailed follow-up analysis in the lab.

Analysis of Commercial Δ 8-THC Products. *Fast screening analysis.* To broaden the application of the developed method for analyzing commercial Δ 8-THC products, it would be advantageous if it could rapidly determine the following: i) whether the detected Δ 8-THC content matches the declared Δ 8-THC content on the label; ii) whether the products contain other THC/CBD isomers and iii) whether the products contain a high content of Δ 9-THC. Therefore, separate quantification of Δ 8-THC and Δ 9-THC was performed by using an internal standard. Additionally, CBD was quantified to prevent excessive CBD in the products from causing false indications of Δ 8-THC and Δ 9-THC levels. Finally, samples were monitored for the presence of MS² signals at m/z 299 and MS³ signals at m/z 223 to flag samples suspected of containing substantial amounts of, and thus interference from, other cannabinoid isomers. Since the used internal standard Δ 9-THCV produced MS³ signals at m/z 243 (**SI, Figure S12**), m/z 243 cannot be used for flagging in this situation. A more appropriate internal standard, such as heavy-isotope labeled standard, would solve this issue. Moreover, it would suffer less from (differential) matrix effects, as indicated above.

From their MS² spectra (**SI, Figure S13**), it is quite obvious that Δ 8-THC rice crackers contained much more Δ 9-THC than Δ 8-THC. The dominant signal at m/z 313 and the almost invisible signal at m/z 245 highlight this difference, a quite disturbing result in itself. When focusing on the analytical chemistry again, this discrepancy suggests that the AgPS-MS² method was expected to give a more accurate quantification of Δ 8-THC. Alternatively, the signal at m/z 245 produced by Δ 9-THC in the MS³ stage could be subtracted (namely a background value of $0.074 \times \text{EIC} (m/z 217)$) when using the AgPS-MS³ method, as discussed in the analysis of acid-treated CBD mixtures. Signals at m/z 353/355 indicated the presence of CBD in Δ 8-THC Cannabis leaves and Δ 10-THC vape oil, and thus overestimation of Δ 8-THC and Δ 9-THC. The quantification results were compared with those obtained by GC-FID and summarized in **Table 7.2** and **Table S9 (SI, Table S9)**. For Δ 8-THC, there was a good correspondence between the results obtained by the AgPS-MS³ method and the GC-FID method with minor deviations of 0–12% in four out of the

five Δ^8 -THC products. In the rice crackers, indeed the AgPS-MS² method gave a more accurate quantification with a much smaller deviation (409% by AgPS-MS³ and -14% by AgPS-MS²) from the results of GC-FID. When the subtraction strategy was applied to the AgPS-MS³ method, the deviation could be reduced from 409% to -45% ($0.56 \pm 0.08\%$ vs. $0.061 \pm 0.01\%$ of Δ^8 -THC before and after subtraction). When comparing with the claimed contents, except for two Δ^8 -THC products without Δ^8 -THC information, the other three Δ^8 -THC products overclaimed their Δ^8 -THC content, as reported before.⁸ For Δ^9 -THC, an overall overestimation (deviation from 65% to 427%) compared to the results obtained by GC-FID was encountered for the AgPS-MS method with the exception of Δ^8 -THC rice crackers (acceptable deviation of 13%). The overestimations can be partly explained by the abundant presence of CBD, as detected in Δ^8 -THC Cannabis leaves and Δ^{10} -THC vape oil. Monitoring for relevant markers (MS² signals at m/z 299 and MS³ signals at m/z 223) revealed that besides CBD, these products likely contained other isomers: Δ^8 -iso-THC, $\Delta(4)$ -iso-THC, and Δ^3 -THC (**SI, Figure S13, S14**). The isomeric cannabinoid compositions were then analyzed by the GC-FID method (**SI, Table S10, Figure S15, S16**). Except for the rice crackers, the total amounts of CBD, Δ^8 -iso-THC, $\Delta(4)$ -iso-THC, and Δ^3 -THC in other products were much higher than those of Δ^9 -THC, leading to the overestimation of Δ^9 -THC. These THC isomers, without having more knowledge about pharmacological effects,³⁷ should be given attention. However, methodologically, resolving these isomeric cannabinoids remains challenging even with time-consuming chromatographic methods.^{3,12,13} It is noteworthy that in the Δ^{10} -THC vape oil, which claimed to contain 70–75% Δ^8 -THC and 15–20% Δ^{10} -THC (**SI, Table S1**), no Δ^{10} -THC was detected by NMR. Instead, the main cannabinoids identified by NMR after isolation by preparative HPLC-MS were Δ^8 -THC and Δ^3 -THC.²¹ GC-FID/MS analysis revealed major peaks corresponding to Δ^8 -THC and Δ^3 -THC, along with minor peaks identified as Δ^8 -iso-THC, $\Delta(4)$ -iso-THC, Δ^9 -THC, and CBD, with no significant signal for Δ^{10} -THC (**SI, Figure S16**). In any case, this highlights the need for analytical methods capable of detecting and distinguishing cannabinoid isomers with minor structural

differences, such as C=C bond position. Due to the unavailability of a Δ 10-THC standard, no AgPS-MS spectra could be acquired for Δ 10-THC. However, it is expected that its MS² and MS³ spectra will allow for a differentiation, as Δ 10-THC differs in the position of the C=C bond compared to other THC isomers investigated in this study, all of which exhibit different MS² and MS³ spectra (**SI, Figures S10 and S11**).

The developed AgPS-MS method enables fast distinction of isomeric cannabinoids and is suitable for estimating Δ 8-THC with acceptable accuracy (deviations of 0–13%). Moreover, the developed method is able to flag problematic products containing either too much Δ 9-THC (e.g., > 0.3%), or other THC/CBD isomers or both. The existence of other isomeric cannabinoids could be flagged by characteristic MS² and MS³ signals, which means that these samples should be further analyzed using confirmatory methods. If such isomers are absent but Δ 9-THC is present, Δ 9-THC can be quantified with acceptable accuracy, as demonstrated in the Δ 8-THC rice crackers sample. However, in most of these products, both issues — presence of Δ 9-THC and other THC/CBD isomers — occur simultaneously, leading to an overestimation of Δ 9-THC. Despite this overestimation, all four products that contained illegal levels of Δ 9-THC (> 0.3%) were correctly identified as such. While it is true that when the Δ 9-THC content is close to the 0.3% legal limit, such overestimation might result in a false positive result, this would show up in the confirmatory analysis. This is then needed in any case due to the detection of other THC/CBD isomers, that would have been flagged by characteristic MS² and MS³ signals.

Table 7.2. Comparison of the absolute percentages of $\Delta 8$ -THC, $\Delta 9$ -THC, and CBD in $\Delta 8$ -THC infused products measured by the AgPS-MS method, GC-FID method, and claimed content.

Sample	$\Delta 8$ -THC (w/w%)			$\Delta 9$ -THC (w/w%)			CBD (w/w%)		
	Ag-PSMS ³	GC-FID	Claimed content	Ag-PSMS ³	GC-FID	Claimed content	Ag-PSMS ²	GC-FID	Claimed content
$\Delta 8$ -THC brownies	0.80 \pm 0.04	0.73 \pm 0.01	1.4	0.070 \pm 0.01	0.025 \pm 0.002	NA	0.01 \pm 0.001	ND	NA
$\Delta 8$ -THC rice crackers	0.095 \pm 0.01*	0.11 \pm 0.002	1.4	1.7 \pm 0.09	1.5 \pm 0.02	NA	0.02 \pm 0.004	ND	NA
$\Delta 8$ -THC Cannabis leaves	10 \pm 1.1	9.9 \pm 0.1	NA	1.5 \pm 0.1	0.91 \pm 0.01	< 0.3	3.4 \pm 0.3	4.4 \pm 0.03	NA
$\Delta 8$ -THC vape oil	62 \pm 5.4	62 \pm 1.2	NA	7.7 \pm 0.6	3.7 \pm 0.07	< 0.3	0.62 \pm 0.13	ND	NA
$\Delta 10$ -THC vape oil	38 \pm 4.3	34 \pm 0.3	70–75	7.9 \pm 0.6	1.5 \pm 0.07	< 0.3	5.1 \pm 0.5	0.69 \pm 0.01	NA

NA, not available; ND, non-detectable, i.e., <LOD; * measured by the AgPS-MS² method.

Standard Addition for Quantification. To explore if better accuracy could be obtained by correcting for matrix effects, the standard addition of $\Delta 8$ -THC and $\Delta 9$ -THC into $\Delta 8$ -THC brownie and $\Delta 8$ -THC vape oil extracts was performed (SI, **Figure S17**). The results are summarized in **Table 7.3**. Similar to fast screening results, quantification of the dominant cannabinoid $\Delta 8$ -THC by the AgPS-MS method exhibited acceptable deviation (–25%–25%) from that obtained by the GC-FID method (–16% for $\Delta 8$ -THC brownies and –6.1% for $\Delta 8$ -THC vape oil), showing minor interferences from matrixes and other isomers. For $\Delta 9$ -THC, higher accuracy was achieved compared to the fast screening method. However, significant interferences from abundant isomeric cannabinoids resulted in deviations of 76% for $\Delta 8$ -THC brownies and 56% for $\Delta 8$ -THC vape oil. Additionally, this method is much more labor-intensive. While standard addition allows for better accuracy, interference from other isomers still causes substantial deviations, making the effort

unjustified. Therefore, we did not apply this method to all samples.

Table 7.3. Absolute percentages of Δ 8-THC, Δ 9-THC, and CBD in Δ 8-THC infused products measured by the standard addition method.

Sample	Δ 8-THC (w/w%)			Δ 9-THC (w/w%)		
	Ag-PSMS ³	GC-FID	Deviation	Ag-PSMS ³	GC-FID	Deviation
Δ 8-THC brownies	0.61 ± 0.014	0.73 ± 0.07	-16%	0.051 ± 0.006	0.029 ± 0.004	76%
Δ 8-THC vape oil	62 ± 3.8	66 ± 3.4	-6.1%	6.4 ± 0.46	4.1 ± 0.26	56%

Prototype 3D-Printed Device for AgPS-MS. In conventional PS-MS, a paper tip is positioned with its tip directed toward the MS orifice, with a metal clip; then 15–20 μ L of sample/spray solution is dropped on the paper tip, followed by application of a high voltage to commence spray. Despite PS-MS being easy and fast in use, manually positioning the paper tip in front of the MS inlet somewhat limits its user-friendliness and throughput.²⁴ Moreover, conventional paper spray is characterized by quite an unstable spray and no separation, due to, amongst other factors, the single deposition of solvent for spray generation. In previous research,³⁸ 3D-printing has been demonstrated to allow design and production of paper spray devices to improve such aspects. Therefore, a 3D-printed device, consisting of a one-time-use paper cartridge, sample well slide, cartridge holder, and slide holder (**Figure 7.3A**) was designed. The slide holder and paper cartridge holder were first fixed in front of the MS inlet, so that the cartridge holder only needs to be turned vertically when loading paper cartridges or loading samples (**Figure 7.3B**). Subsequently, the sample well slide with multiple sample wells was put in the slide holder, and the slide button (**Figure 7.3A**) was used to switch between samples, by moving the slide. Spray was produced when the paper tip was in contact with samples and wetted the paper. A video of the operation of the device can be found in the SI. By using this device, (i) there was no need for manual positioning of the paper tip, which enhances operational simplicity; (ii) cross-contamination introduced by the metal clip was avoided; (iii) preliminary, low-resolution paper-

chromatographic separation of Δ^9 -THC and CBD was achieved (**Figures 7.3C and 7.3D**), as the sample with all compounds is introduced in a repeatable manner at the back of the paper tip. Since CBD has more hydroxyl groups that can interact with the very polar paper, maximum intensity was observed later than for the THC molecules. Despite the separation being low resolution, it might be further optimized, e.g., based on silver-affinity as demonstrated on TLC plates,²³ or a continuous solvent supply design.³⁸ Differences in elution profiles can be leveraged to improve the distinction between isomers, in combination with their MS^2/MS^3 profiles. The total cost of the 3D-printed device was only 1.28 euros with 0.09 euros as the costs for each one-time-use cartridge, which is overall thus quite cost-effective (**SI, Table S11**).

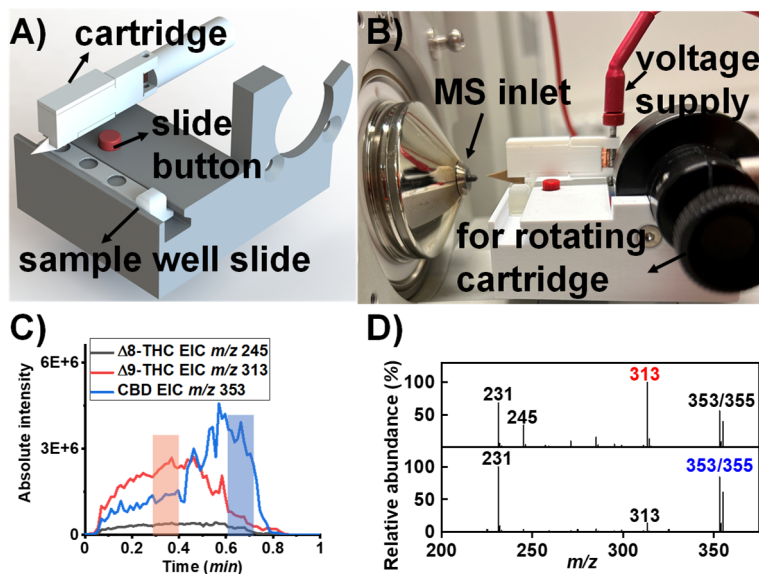


Figure 7.3. A) 3D-printed device; B) 3D-printed device mounted to MS; C) MS^2 EIC chromatogram of Δ^8 -THC (m/z 245), Δ^9 -THC (m/z 313), and CBD (m/z 353); D) averaged MS^2 spectra of measurements over 0.1 min (red shade area and blue shade area) for the mixture of Δ^8 -THC, Δ^9 -THC, and CBD. Note: A more pronounced characteristic signal of Δ^9 -THC at m/z 313 was found at an earlier elution time (0.3 min), and a more pronounced characteristic signal of CBD at m/z 353/355 was found after a longer elution time (0.6 min).

Conclusions

In conclusion, a fast and easy method to distinguish between Δ 8-THC and Δ 9-THC for screening of Δ 8-THC products was developed. This method combines a simple MeOH extraction and a fast AgPS-MS analysis. It enabled the semiquantification of Δ 9-THC: Δ 8-THC ratios and the individual content of Δ 8-THC and Δ 9-THC in various matrixes. Different acid-treated CBD mixtures and commercial Δ 8-THC products were analyzed and benchmarked against the GC-FID method that serves as current benchmark. For samples mainly containing Δ 8-THC, Δ 9-THC, and CBD, the quantification of Δ 9-THC: Δ 8-THC was comparable to that of GC-FID. The analysis of commercial Δ 8-THC products showed that the developed AgPS-MS method enabled reliable quantification of Δ 8-THC, and in fact revealed that four out of five commercial products contained illegal levels of Δ 9-THC ($> 0.3\%$), which was confirmed by GC-FID. Besides, the presence of other isomers like Δ 8-iso-THC, $\Delta(4)$ 8-iso-THC, and Δ 3-THC could also be identified. The implementation of a 3D-printed device for the paper spray improved operational simplicity and provides the potential for high-throughput analysis. Further optimization of 3D-printed paper cartridges could improve the paper-chromatographic separation and thus decrease the interferences from co-eluting isomers. The developed method is highly promising for user-friendly and large-scale screening analysis of Δ 8-THC products for badly needed forensic and food regulation purposes.

Supporting Information

The supporting information is available free of charge at https://drive.google.com/drive/folders/1zvzKLhuQaIQk9moQp1yB36Ug81MVQo_pJ?usp=sharing, and the table of contents is presented below.

Supporting Information Table of Contents

Table S1	Product information of commercial Δ 8-THC edibles	Page S3
Table S2	Percentage (w/w%) of Δ 8-THC, Δ 9-THC, CBD, Δ 8-iso-THC, and $\Delta(4)$ 8-iso-THC in acid-treated CBD	Page S4

	mixtures analyzed by GC-FID	
Figure S1	Top view and side view of the 3D-printed device for paper spray experiment	Page S5
Figure S2	3D designs of the 3D-printed paper spray cartridge	Page S5
Table S3	MS settings of different scanning events	Page S6
Table S4	MS transitions of cannabinoids investigated in the study	Page S6
Table S5	The preparation of sample sets I and II	Page S6
Figure S3	The EIC area ratio of m/z 313: m/z 245 in Δ 8-THC AgPS-MS ² spectrum as a function of different CID energies, capillary temperature, spray voltage, and Δ 8-THC concentrations	Page S7
Table S6	MS settings for investigating the fragmentation of Δ 9-THC	Page S8
Figure S4	The MS ³ EIC peak area ratio of m/z 245: m/z 217 for Δ 9-THC under different MS settings	Page S8
Table S7	Matrix effects on Δ 8-THC, Δ 9-THC, Δ 9-THCV, CBD, and Δ 9-THC: Δ 8-THC by AgPS-MS ² and AgPS-MS ³ method	Page S9
Figure S5	Calibration curves of Δ 9-THC: Δ 8-THC ratio by the AgPS-MS ² method and the AgPS-MS ³ method	Page S10
Figure S6	Calibration curves of Δ 8-THC, Δ 9-THC, and CBD by the AgPS-MS ² method and the AgPS-MS ³ method	Page S10
Figure S7	AgPS-MS ² spectrum and AgPS-MS ³ spectrum of 1 $\mu\text{g}\cdot\text{mL}^{-1}$ of Δ 8-THC, Δ 9-THC, and CBD	Page S11
Figure S8	AgPS-MS ² spectra of acid-treated CBD reaction mixtures	Page S12
Figure S9	AgPS-MS ³ spectra of acid-treated CBD reaction mixtures	Page S13
Table S8	Δ 9-THC: Δ 8-THC ratio in acid-treated CBD mixtures measured by GC-FID method and AgPS-MS method	Page S14
Figure S10	AgPS-MS ² spectrum of Δ 8-THC, Δ 9-THC, CBD, Δ 8-iso-THC, Δ (4)8-iso-THC, and Δ 3-THC	Page S15
Figure S11	AgPS-MS ³ spectrum of Δ 8-THC, Δ 9-THC, CBD, Δ 8-iso-THC, Δ (4)8-iso-THC, and Δ 3-THC	Page S16
Figure S12	AgPS-MS ² and AgPS-MS ³ spectra of commercial Δ 9-THCV	Page S17
Figure S13	AgPS-MS ² spectra of commercial Δ 8-THC products	Page S18
Figure S14	AgPS-MS ³ spectra of commercial Δ 8-THC products	Page S19
Table S9	Percentages of Δ 8-THC, Δ 9-THC, and CBD in commercial Δ 8-THC products measured by the AgPS-	Page S20

	MS method and GC-FID method	
Table S10	Isomeric cannabinoid compositions analyzed by the GC-FID method	Page S21
Figure S15	Calibration curves of Δ 8-THC, Δ 9-THC, and CBD by the GC-FID method	Page S21
Figure S16	GC-FID chromatograms of Δ 8-THC brownie, Δ 8-THC rice cracker, Δ 8-THC Cannabis leaves, Δ 8-THC vape oil, and Δ 10-THC brownie	Page S22
Figure S17	Standard addition calibration curves	Page S23
Table S11	3D-printing material, time, and cost list	Page S24
References		Page S25

Acknowledgments

The authors acknowledge financial support from the Natural Science Foundation of China (22276050, 22276049), and the China Scholarship Council 2020 International Cooperation Training Program for Innovative Talent. We thank prof. Daniele Passarella (Dipartimento di Chimica, Università degli Studi di Milano, Italy) for generously providing Δ 8-iso-THC and Δ (4)8-iso-THC. We also thank Canan Aksoy from the Organic Chemistry Group at Wageningen University for technical support in 3D printing.

References

- (1) Peng, H.; Shahidi, F. Cannabis and Cannabis edibles: a review. *Journal of Agricultural and Food Chemistry* **2021**, *69*, 1751-1774.
- (2) Congress, U. S. *Agriculture improvement act of 2018*; **2018**. <https://www.congress.gov/115/plaws/publ334/PLAW-115publ334.pdf> (accessed 2024 May 27).
- (3) Huang, S.; van Beek, T. A.; Claassen, F. W.; Janssen, H.-G.; Ma, M.; Chen, B.; Zuilhof, H.; Salentijn, G. I. Comprehensive cannabinoid profiling of acid-treated CBD samples and Δ^8 -THC-infused edibles. *Food Chemistry* **2024**, *440*, 138187.
- (4) Casajuana Kögel, C.; López-Pelayo, H.; Balcells-Olivero, M. M.; Colom, J.; Gual, A. Psychoactive constituents of Cannabis and their clinical implications: a systematic review. *Adicciones* **2018**, *30*, 140-151.
- (5) Hollister, L. E.; Gillespie, H. Delta-8-and delta-9-tetrahydrocannabinol; comparison in man by oral and intravenous administration. *Clinical Pharmacology and Therapeutics* **1973**, *14*, 353-357.
- (6) Babalonis, S.; Raup-Konsavage, W. M.; Akpunonu, P. D.; Balla, A.; Vrana, K. E. Δ^8 -THC: legal status, widespread availability, and safety concerns. *Cannabis and Cannabinoid Research* **2021**, *6*, 362-365.
- (7) Council, U. S. C. *The unregulated distribution and sale of consumer products marketed as delta-8 THC*; **2021**. <https://irp.cdn-website.com/6531d7ca/files/uploaded/USCC%20Delta-8%20Kit.pdf> (accessed 2024 May 27).
- (8) Gleb, O. *New leafreport research reveals more than 50% of delta-8 THC hemp-derived products tested had illegal levels of delta-9 THC*; **2022**. <https://www.leafreport.com/education/delta-8-thc-products-market-report-11339> (accessed 2024 May 27).
- (9) Simon, T. A.; Simon, J. H.; Heaning, E. G.; Gomez-Caminero, A.; Marcu, J. P. Delta-8, a Cannabis-derived tetrahydrocannabinol isomer: evaluating case report data in the food and drug administration adverse event reporting system (FAERS) database. *Drug, Healthcare and Patient Safety* **2023**, *15*, 25-38.
- (10) Golombek, P.; Müller, M.; Barthlott, I.; Sproll, C.; Lachenmeier, D. W. Conversion of cannabidiol (CBD) into psychotropic cannabinoids including tetrahydrocannabinol (THC): a controversy in the scientific literature. *Toxics* **2020**, *8*, 41.
- (11) Kaczor, E. E.; Greene, K.; Babu, K. M.; Berthold, E. C.; Sharma, A.; Carreiro, S. P. Commercial delta-8 THC products: an analysis of content and labeling. *The Journal of Medical Toxicology* **2024**, *20*, 31-38.
- (12) Chan-Hosokawa, A.; Nguyen, L.; Lattanzio, N.; Adams, W. R. Emergence of delta-8 tetrahydrocannabinol in DUID investigation casework: method development, validation and application. *Journal of Analytical Toxicology* **2022**, *46*, 1-9.
- (13) Reber, J. D.; Karschner, E. L.; Seither, J. Z.; Knittel, J. L.; Dozier, K. V.; Walterscheid, J. P. An enhanced LC-MS-MS technique for distinguishing Δ^8 - and Δ^9 -tetrahydrocannabinol isomers in blood and urine specimens. *Journal of Analytical Toxicology* **2022**, *46*, 343-349.
- (14) Marzullo, P.; Foschi, F.; Coppini, D. A.; Fanchini, F.; Magnani, L.; Rusconi, S.; Luzzani, M.; Passarella, D. Cannabidiol as the substrate in acid-catalyzed intramolecular cyclization. *Journal of Natural Products* **2020**, *83*, 2894-2901.
- (15) Meehan-Atrash, J.; Rahman, I. Novel Δ^8 -tetrahydrocannabinol vaporizers contain unlabeled adulterants, unintended byproducts of chemical synthesis, and heavy metals. *Chemical Research in Toxicology* **2021**, *35*, 73-76.
- (16) Draper, S. L.; McCarney, E. R. Benchtop nuclear magnetic resonance spectroscopy in forensic chemistry. *Magnetic Resonance in Chemistry* **2023**, *61*, 106-129.
- (17) Tose, L. V.; Santos, N. A.; Rodrigues, R. R.; Murgu, M.; Gomes, A. F.; Vasconcelos, G. A.; Souza, P. C.; Vaz, B. G.; Romão, W. Isomeric separation of cannabinoids by UPLC combined with ionic mobility mass spectrometry (TWIM-MS)—Part I. *International Journal of Mass Spectrometry* **2017**, *418*, 112-121.

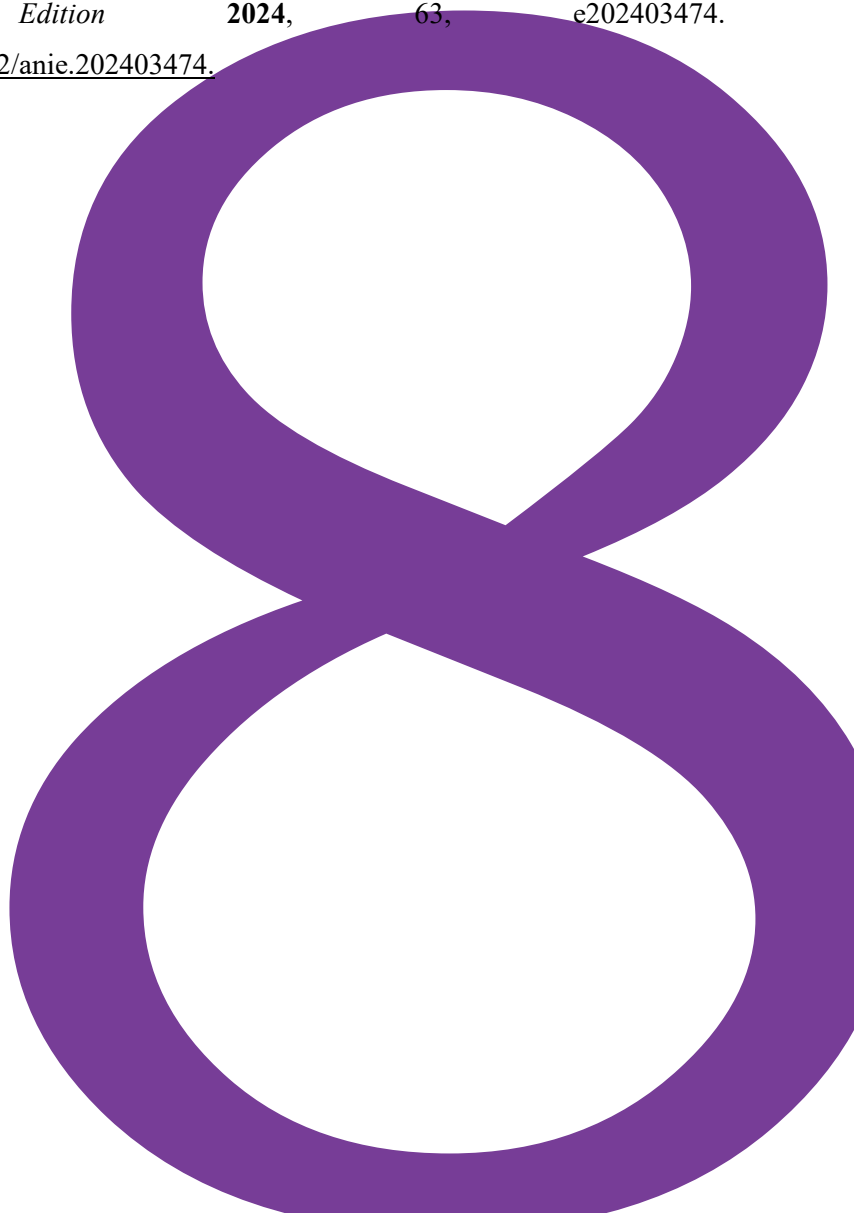
- (18) Kiselak, T. D.; Koerber, R.; Verbeck, G. F. Synthetic route sourcing of illicit at home cannabidiol (CBD) isomerization to psychoactive cannabinoids using ion mobility-coupled-LC-MS/MS. *Forensic Science International* **2020**, *308*, 110173.
- (19) Ieritano, C.; Thomas, P.; Hopkins, W. S. Argentinization: a silver bullet for cannabinoid separation by differential mobility spectrometry. *Analytical Chemistry* **2023**, *95*, 8668-8678.
- (20) Zietek, B. M.; Mengerink, Y.; Jordens, J.; Somsen, G. W.; Kool, J.; Honing, M. Adduct-ion formation in trapped ion mobility spectrometry as a potential tool for studying molecular structures and conformations. *International Journal of Mass Spectrometry* **2018**, *21*, 19-32.
- (21) Huang, S.; Righetti, L.; Claassen, F. W.; Krishna, A.; Ma, M.; van Beek, T. A.; Chen, B.; Zuilhof, H.; Salentijn, G. I. J. Ultrafast, selective, and highly sensitive nonchromatographic analysis of fourteen cannabinoids in Cannabis extracts, Δ 8-tetrahydrocannabinol synthetic mixtures, and edibles by cyclic ion mobility spectrometry-mass spectrometry. *Analytical Chemistry* **2024**, *96*, 10170-10181.
- (22) Huang, S.; Claassen, F. W.; van Beek, T. A.; Chen, B.; Zeng, J.; Zuilhof, H.; Salentijn, G. I. Rapid distinction and semiquantitative analysis of THC and CBD by silver-impregnated paper spray mass spectrometry. *Analytical Chemistry* **2021**, *93*, 3794-3802.
- (23) Huang, S.; Qiu, R.; Fang, Z.; Min, K.; Van Beek, T. A.; Ma, M.; Chen, B.; Zuilhof, H.; Salentijn, G. I. Semiquantitative screening of THC analogues by silica gel TLC with an Ag(I) retention zone and chromogenic smartphone detection. *Analytical Chemistry* **2022**, *94*, 13710-13718.
- (24) Brown, H. M.; McDaniel, T. J.; Fedick, P. W.; Mulligan, C. C. The current role of mass spectrometry in forensics and future prospects. *Analytical Methods* **2020**, *12*, 3974-3997.
- (25) Falconer, T. M.; Morales-Garcia, F. Rapid screening of vaping liquids by DART-MS. *Journal of AOAC International* **2023**, *106*, 436-444.
- (26) Chambers, M. I.; Musah, R. A. DART-HRMS as a triage approach for the rapid analysis of cannabinoid-infused edible matrices, personal-care products and *Cannabis sativa* hemp plant material. *Forensic Chemistry* **2022**, *27*, 100382.
- (27) Di Marco Pisciotano, I.; Guadagnuolo, G.; Soprano, V.; De Crescenzo, M.; Gallo, P. A rapid method to determine nine natural cannabinoids in beverages and food derived from *Cannabis sativa* by liquid chromatography coupled to tandem mass spectrometry on a QTRAP 4000. *Rapid Communications in Mass Spectrometry* **2018**, *32*, 1728-1736.
- (28) Di Marco Pisciotano, I.; Guadagnuolo, G.; Soprano, V.; Esposito, M.; Gallo, P. A survey of Δ 9-THC and relevant cannabinoids in products from the Italian market: a study by LC-MS/MS of food, beverages and feed. *Food Chemistry* **2021**, *346*, 128898.
- (29) Little, T. *Method validation essentials, limit of blank, limit of detection, and limit of quantitation*; 28; **2015**. Retrieved from BioPharm International. <https://www.biopharminternational.com/view/method-validation-essentials-limit-blank-limit-detection-and-limit-quantitation> (accessed 2024 July 27).
- (30) Wishart, D. S.; Hiebert-Giesbrecht, M.; Inchehborouni, G.; Cao, X.; Guo, A. C.; LeVatte, M. A.; Torres-Calzada, C.; Gautam, V.; Johnson, M.; Liigand, J.; *et al.* Chemical composition of commercial Cannabis. *Journal of Agricultural and Food Chemistry* **2024**, *72*, 14099-14113.
- (31) Christodoulou, M. C.; Christou, A.; Stavrou, I. J.; Kapnissi-Christodoulou, C. P. Evaluation of different extraction procedures for the quantification of seven cannabinoids in Cannabis-based edibles by the use of LC-MS. *Journal of Food Composition and Analysis* **2023**, *115*, 104915.
- (32) Brighenti, V.; Pellati, F.; Steinbach, M.; Maran, D.; Benvenuti, S. Development of a new extraction technique and HPLC method for the analysis of non-psychoactive cannabinoids in fibre-type *Cannabis sativa* L.(hemp). *Journal of Pharmaceutical and Biomedical Analysis* **2017**, *143*, 228-236.
- (33) Escrivá, Ú.; Andrés-Costa, M. J.; Andreu, V.; Picó, Y. Analysis of cannabinoids by liquid chromatography-mass spectrometry in milk, liver and hemp seed to ensure food safety. *Food Chemistry* **2017**, *228*, 177-185.
- (34) SWGTOX. Scientific working group for forensic toxicology (SWGTOX) standard practices for method validation in forensic toxicology. *Journal of Analytical Toxicology* **2013**, *37*, 452-474.

- (35) Stokvis, E.; Rosing, H.; Beijnen, J. H. Stable isotopically labeled internal standards in quantitative bioanalysis using liquid chromatography/mass spectrometry: necessity or not? *Rapid Communications in Mass Spectrometry* **2005**, *19*, 401-407.
- (36) Walsh, K. B.; McKinney, A. E.; Holmes, A. E. Minor cannabinoids: biosynthesis, molecular pharmacology and potential therapeutic uses. *Frontiers in Pharmacology* **2021**, *12*, 777804.
- (37) Michael Geci, M. S. The dark side of cannabidiol: the unanticipated social and clinical implications of synthetic Δ^8 -THC. *Cannabis and Cannabinoid Research* **2023**, *8*, 270-282.
- (38) Salentijn, G. I.; Permentier, H. P.; Verpoorte, E. 3D-printed paper spray ionization cartridge with fast wetting and continuous solvent supply features. *Analytical Chemistry* **2014**, *86*, 11657-11665.

Rim-based Binding of Perfluorinated Acids to Pillararenes Purifies Water

This chapter was published as:

Gao, T. N.; Huang, S.; Nooijen, R.; Zhu, Y.; Kociok-Köhn, G.; Stuerzer, T.; Li, G.; Bitter, J. H.; Salentijn, G. IJ.; Chen, B.; Miloserdov, F. M.; Zuilhof, H. Rim-based binding of perfluorinated acids to pillararenes purifies water. *Angewandte Chemie International Edition* **2024**, *63*, e202403474. <https://doi.org/10.1002/anie.202403474>.



Abstract

Per- and polyfluoroalkyl substances (PFAS) pose a rapidly increasing global problem as their widespread use and high stability lead worldwide to water contamination, with significant detrimental health effects.¹⁻⁹ Supramolecular chemistry has been invoked to develop materials geared toward the specific capture of PFAS from water,¹⁰⁻¹⁷ to reduce the concentration below advisory safety limits (e.g., 70 ng/L for the sum of perfluorooctane sulfonic acid, PFOS and perfluorooctanoic acid, PFOA). Scale-up and use in natural waters with high PFAS concentrations has hitherto posed a problem. Here we report a new type of host-guest interaction between deca-ammonium-functionalized pillar[5]arenes (DAF-P5s) and perfluoroalkyl acids. DAF-P5 complexes show an unprecedented 1:10 stoichiometry, as confirmed by isothermal calorimetry and X-ray crystallographic studies, and high binding constants (up to 10^6 M^{-1}) to various polyfluoroalkyl acids. In addition, non-fluorinated acids do not hamper this process significantly. Immobilization of DAF-P5s allows a simple single-time filtration of PFAS-contaminated water to reduce the PFOS/PFOA concentration 10^6 times to 15–50 ng/L level. The effective and fast (< 5 min) orthogonal binding to organic molecules without involvement of fluorinated supramolecular hosts, high breakthrough capacity (90 mg/g), and robust performance (> 10 regeneration cycles without decrease in performance) set a new benchmark in PFAS-absorbing materials.

Introduction

Per- and polyfluoroalkyl substances (PFAS) are broadly used chemicals for a wide range of consumer and industrial applications, such as in stain-repellent sprays, non-stick pans, firefighting foams and food paper coatings. However, the extremely high stability of these materials also turns out to be one of their drawbacks, e.g., leading to increasing water pollution. Dangerous contamination levels of soils and surface waters with PFAS have already reached many parts of the world, frequently exceeding the US Environmental Protection Agency (EPA)'s advisory limit for perfluorooctane sulfonic acid (PFOS) and perfluorooctanoic acid (PFOA) (70 ng/L) by several orders of magnitude.^{3,4,6,7} Toxicity research has demonstrated that this will cause developmental toxicity, immune function disorder, immunotoxicity, and a range of chronic diseases.^{1,2,5,8,9} The ideal material for PFAS removal combines the following features: 1) a high affinity for PFAS; 2) high capacity; 3) fast absorption and desorption kinetics; 4) high specificity, as water also contains many other natural acids at much higher concentrations; 5) easy and robust regeneration; 6) scalable and eco-friendly synthesis. Efforts to develop PFAS-absorbing materials focused e.g., on high surface-area materials, like activated carbon, covalent organic frameworks (COFs), metal-organic frameworks (MOFs) and porous aromatic frameworks, or on advanced organic materials with tailor-made macrocycle-based cavities, such as cyclodextrin- or calixarene-based polymers and networks.^{15,18-22} Activated carbon, zeolite, COFs, MOFs and porous aromatic frameworks represent porous materials that use defined channel structures and tailored binding sites to absorb PFAS. Porous materials show a high affinity and capacity toward PFAS, but the specificity toward PFAS is low, as these materials suffer from competitive binding with other organic co-contaminants or natural organic matter, which is detrimental for practical applications (**Figure 8.1**).²³⁻²⁵ In addition, the rates of PFAS absorption for this class of materials are relatively slow, typically taking 2–20 h to reach equilibrium. On the other side, supramolecular host-guest interactions can add to or replace such pore-based interactions, using the specific fluorophilic properties of PFAS or their negative charge.²⁶ Fluorophilicity refers to the specific aggregation of fluorinated

compounds with themselves or with other fluorinated compounds.²⁷ This property has been used in supramolecular host-guest complexes to bind e.g., PFOA to a fluorinated β -cyclodextrin polymer with high affinity ($K = 7 \times 10^4 \text{ M}^{-1}$), which was ca. 100 times higher than for similar non-perfluorinated cyclodextrins.¹⁰⁻¹³ Such polymer can effectively remove PFAS, but the absorption rates are also slow (1–2 days to reach equilibrium). Furthermore, the production of such highly fluorinated polymers would again involve poly- and per-fluorinated materials, which is not sustainable. Alternatively, charge-based interactions were invoked in the 1:1 complex formation of calix[5]arenes bearing five guanidinium groups with PFAS binding constants up to $4.8 \times 10^6 \text{ M}^{-1}$; efficient PFAS sensing was obtained, but water clean-up only reached $\mu\text{g/L}$ levels.¹⁴ This category of materials shows a high specificity toward PFAS, but suffers from a low capacity. Among all the reported host-guest complexes with PFOA/PFOS, there is maximally one guest per host molecule, and reports that directly take natural river water or tap water are scarce. Until now, there are no materials that would feature all six properties required for efficient PFAS removal. Herein, we report an approach invoking fluorine-free pillararenes that overcomes all these reported limitations.

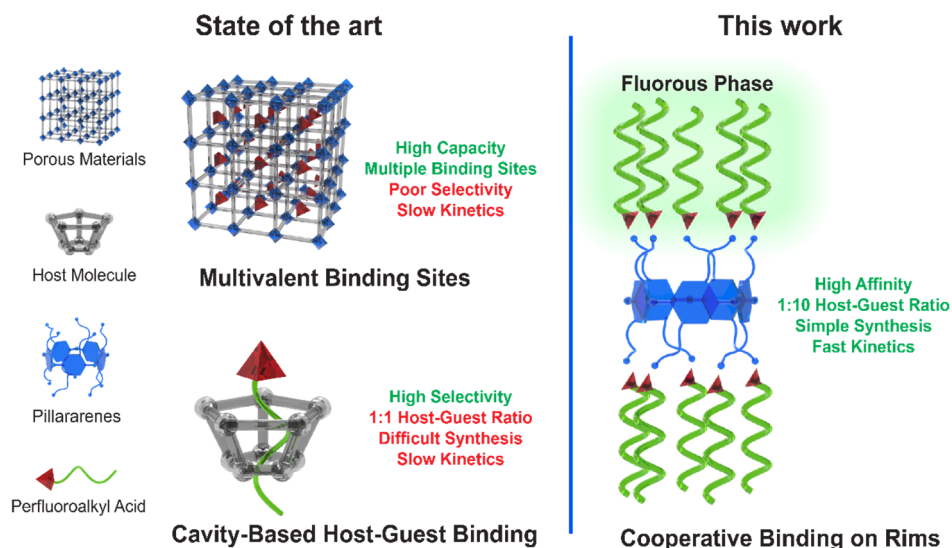


Figure 8.1. Materials for capture of polyfluoroalkyl acids: (left) state of the art, (right) current work.

Materials and Methods

See **Supporting Information (SI)**.

Results and Discussion

Pillararenes,^{28–33} and especially pillar[5]arenes, are characterized by a powerful three-facet combination of features: a pillar-like structure with well-defined cavity size (4.7 Å),²⁹ easy functionalization with very wide range of functionalities,^{34–38} and routes that allow multigram synthesis.^{39,40} Herein we report a new host-guest interaction between fluorine-free, deca-ammonium-functionalized pillar[5]arenes (DAF-P5s) and polyfluoroalkyl acids with an unprecedented 1:10 host-guest ratio and high binding constants in water up to 10^6 M^{-1} (**Figure 8.1**). We also demonstrate the ability to use this novel mode of interactions to develop robust and high-performing PFAS absorbents that allow for the one-step clean-up of natural, heavily polluted waters to current EPA-acceptable levels within 5 min.

To study the binding of perfluorinated acids to pillararene-based hosts, we synthesized a series of deca-ammonium and deca-trimethylammonium substituted P5s with C_2 and C_4 alkyl chains (**1–3**, **Figure 8.2**) according to literature procedures.^{41,42} Due to the ^1H NMR silent feature of PFAS, the binding constants were determined by isothermal titration calorimetry (ITC). The first striking observation was an extremely high ca. 1:10 pillararene-PFAS binding stoichiometry, suggesting that host-guest interactions occur on the rim rather than in the cavity of the pillararenes. For a range of perfluoroalkyl acids guests (**a–d**), including PFOS (**a**) and PFOA (**b**), with 11 to 17 fluorine atoms and varying negatively charged end groups (carboxylate, sulfonate, phosphonate; see **Figure 8.2** and **Table 8.1**), pillararene hosts **1–3** show an excellent affinity, with a 1:10 stoichiometry and binding constants in the 10^4 – 10^6 M^{-1} range, up to $5 \times 10^6 \text{ M}^{-1}$. Blank titrations of **1** and water, and **b** with water confirmed that the ITC signal originates from the binding between pillararenes and PFAS instead of PFAS micelle formation (**SI, Figures S42–43**).

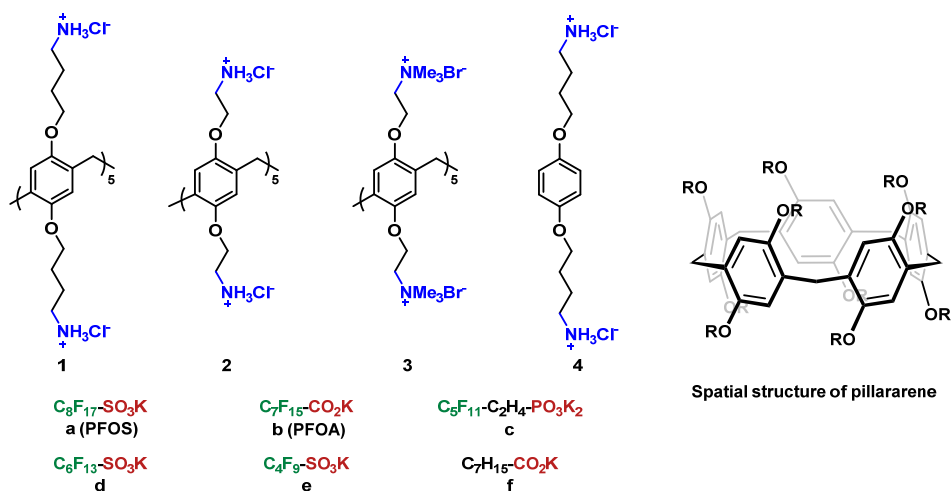


Figure 8.2. Structures of investigated DAF-P5s **1-3** with positively charged rims, monomer **4**, polyfluorinated anions **a-e** and anion of octanoic acid **f**.

The consistently high stoichiometry ratio was further confirmed by isolation of adducts **1a** and **1b** and their characterization by quantitative ¹H and ¹⁹F NMR with an internal standard (**SI**, **Figures S16–19**).

Table 8.1. Results of ITC titration of pillararenes **1-3** with guests **a-f**. Top value is a host-guest binding ratio; bottom value is a binding constant M⁻¹.^[a]

	1	2	3
a	1:10 ± 1 (1.3 ± 0.1) × 10 ⁶	1:10 ± 1 (5.1 ± 0.4) × 10 ⁶	1:13 ± 1 (3.4 ± 0.7) × 10 ⁶
b	1:10 ± 1 (1.7 ± 0.5) × 10 ⁵	1:10 ± 1 (1.9 ± 0.5) × 10 ⁵	1:11 ± 1 (5.52 ± 0.9) × 10 ⁵
c	1:10 ± 1 (6.6 ± 0.2) × 10 ⁵	1:12 ± 1 (1.9 ± 0.4) × 10 ⁵	n.d. ^[b] n.d. ^[b]
d	1:8 ± 1 (1.2 ± 0.1) × 10 ⁵	1:12 ± 2 (1.4 ± 0.1) × 10 ⁵	1:10 ± 1 (3.9 ± 0.9) × 10 ⁶
e	n.d. ^[b]	n.d. ^[b]	n.d. ^[b]
f	1:1 (1.4 ± 0.1) × 10 ⁴	n.d. ^[b] n.d. ^[b]	1:1 (2.7 ± 0.1) × 10 ⁴

[a] All values are average of triplicate experiments, see **SI** for the full details; [b] n.d. = not detected.

To get a better understanding of the structure and host-guest arrangement we performed crystallization and single-crystal X-Ray diffraction studies. We were able to grow a crystal of **1b** suitable for X-Ray analysis by slow evaporation of solvent from a methanol-water solution. The structure of the complex confirms that the binding happens exclusively on the rim, as no PFOA molecule was found in the host cavity. The crystal structure contains 19 molecules of PFOA per 2 molecules of **1**, confirming the overall ca. 1:10 stoichiometry observed in ITC and NMR experiments. Out of 19 perfluorinated chains, 18 are oriented along the pillararene axis, creating a well-distinct fluororous phase above and below the pillararene ring. Only one residual chain is oriented perpendicular to the pillararene axis and interacts with the perfluorinated phase of a neighboring pillararene group (**Figure 8.3**). In addition, multiple hydrogen bonding interactions between carboxylates, ammonium groups, methanol and water molecules were observed. These solid-phase data are thus in line with the solution-phase studies.

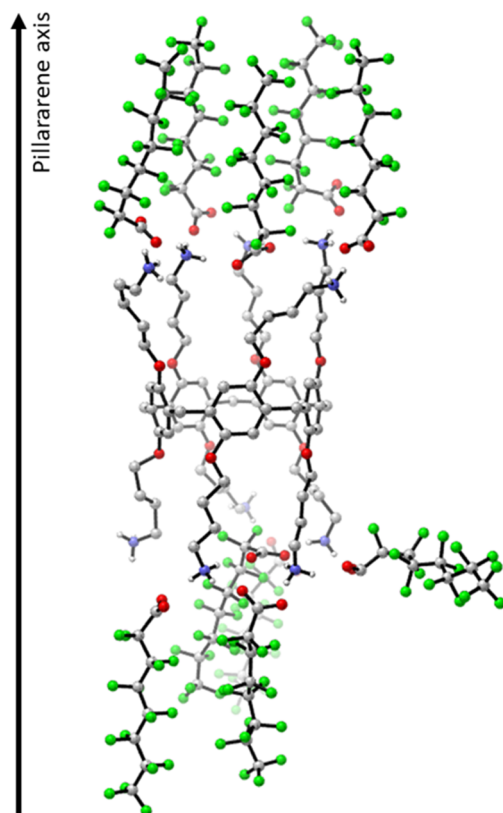


Figure 8.3. X-ray crystal structure of adduct **1b**, all C-H bonds; MeOH, H₂O solvent molecules; and disordered alkyl chains were omitted for clarity.

For a better understanding of the high binding constant, wB97M-V/QZVP calculations were performed (**detailed information in SI**), as this level of density functional theory has recently been established to calculate the fluororous-phase interactions with a high accuracy.⁴³ To this aim, the top five fluororous chains were placed together as we found them in the crystal structure (so without the presence of the P5). Next, the charged carboxylate groups were replaced by H atoms to eliminate the charge effects without changing the position of any of the other atoms in the fluorinated chains. The energy of this fluororous chain cluster was then compared with the energy of five separated fluororous chains, and this yielded that this fluororous-phase cluster provides 24 kcal/mol “fluororous-phase” stabilization compared to the separated chains. It is worth mentioning that even this significant energy is an

underestimation of the fluorophilic effect, because in e.g., DAF-P5-resin materials with a high density of pillararenes there will be fluororous-phase clusters that can also interact with other clusters. In addition, full optimization of a truncated structure (removal of the 5 PFOA molecules from one rim of the crystal structure and reduction of the alkoxyamines to H atoms on that same rim, for computational efficiency, on the hypothesis that both rims are interacting with PFOA independently from one another) showed that this mutual fluorophilic stabilization was maintained when the structure optimized without restraints. These computational data thus support a complexation mechanism that combines electrostatic interactions between the carboxylate moieties and the relatively densely packed amine moieties (either protonated in neutral water or permanently charged by quaternization) with the formation of the local fluororous phase, yielding the high affinity toward PFAS guests arranged on the rim.

This hypothesis was further confirmed by analysis of the difference in binding in various hosts **1–3** and guests **a–e**. The first important observation is that shortening the CF₂ chain from eight to six and then to four carbon atoms in perfluoroalkyl sulfonic acids (**a** vs **d** vs **e**) results first in a 10–50 fold decrease in the binding constant (**a** vs **d**) for both **1** and **2**, and then for **e** no interactions are even detectable anymore by ITC (i.e., binding constant < 10³ M⁻¹). This trend is in line with a decrease of fluorophilic interactions occurring due to the shorter length of the fluorinated chain. Perfluoroalkyl acids with longer CF₂ chains (e.g., perfluorodecanoic acid) were not measured due to their poor solubility in water. In addition to sulfonic acid PFOS (**a**) and carboxylic acid PFOA (**b**), the corresponding phosphoric acid (**c**) also forms 1:10 complexes with pillararenes with K values of 1.9–6.6 × 10⁵ M⁻¹. This highlights that the nature of the anion does not significantly affect the resulting pillararene-PFAS assembly. Similarly, the nature of the ammonium cation group on the pillararene was not significant for the 1:10 adduct formation, as R-NH₃⁺ (**1**, **2**) and R-NMe₃⁺ (**3**) both showed a similar level of interaction. This latter example particularly suggests that hydrogen bonding interactions between P5 and PFAS are not crucial for the 1:10 adduct formation. In

short: the rim-guest interaction is determined by fluorophilic and generic electrostatic attractions.

Control experiments with monomer **4** (**Figure 8.2**, **SI**, **Table S4**) showed no binding for both PFOS (**a**) and PFOA (**b**), supporting the necessity of multiple interactions to achieve appreciable binding. Similarly, no interactions were observed (with ITC) for polyethylenimine $[(\text{CH}_2\text{-CH}_2\text{-NH-})_n]$ in contact with either **a** or **b**. This showcases the importance of the pillararene structure for the host-guest interaction, pointing to multivalency effects as e.g., observed in macrocycle-protein based studies.⁴⁴ In addition, we observed that non-fluorinated alkyl anions display the well-known 1:1 in-cavity host-guest chemistry with these pillararene compounds. For example, ITC measurements revealed for octanoic acid **f** a typical 1:1 binding with pillararenes **1–3** ($K = 1.4\text{--}2.7 \times 10^4 \text{ M}^{-1}$), in line with previous literature.^{45–47}

The high 1:10 host-guest ratio opens up intriguing possibilities for the development of efficient practical absorbents for PFAS, as PFAS pollution is an urgent environmental problem. Our reasoning was that these positively charged DAF-P5s would strongly bind to multiple units of PFAS, potentially enabling the cleanup of PFAS-polluted water through filtration using DAF-P5-loaded materials. Another advantage of our system is the straightforward synthesis of DAF-P5s **3**, which takes only 3 steps with a 33 % overall unoptimized yield from readily available, commercial materials. It can be easily performed on a multigram scale,⁴⁶ and likely allows further scale up.

To demonstrate a proof-of-principle application, DAF-P5s were covalently bound to a commercial resin, TentaGel S (see **SI** for details). The DAF-P5-functionalized resin featured a 10 wt% loading of DAF-P5s, determined through weight change and XPS measurements. Subsequently, 100 mg of DAF-P5-resin was packed into a standard 1 mL solid phase extraction (SPE) cartridge. The SPE cartridge was connected to a peristaltic pump, and 1100 mL of PFOS solution (10 mg/L, i.e., corresponding to a heavily polluted water) was flushed through at a 1 mL/min flow rate. The residual PFOS concentration was determined by UPLC-MS. For the first 900 mL of purified water the residual concentration of PFOS was of

only 19–42 ng/L, i.e., significantly lower than the EPA-advised limit of 70 ng/L (**Figure 8.4a**). Phrased differently, the one-time pass reduced the PFOS concentration from 10^6 ng/L to 19–42 ng/L. It is worth mentioning that in the very first fraction collected within the first 5 min, the residual concentration was already reduced to 49 ng/L, while upon further flushing with water up to 30 min an even better performance was reached. This is a big advantage in comparison with benchmark materials, such as activated carbon, which need at least hours to reach equilibrium.^{48,49} The initial 5–30 min delay in optimal performance is also in line with the cooperative fluorophilic absorption mechanism we proposed. For comparison, analogous experiments with activated carbon resulted in residual PFOS concentration of 230–515 μ g/L, i.e., four orders of magnitude higher than with the DAF-P5-functionalized resin (**SI, Figure S4**).

The DAF-P5-functionalized resin also demonstrated a high capacity and robust performance. The PFOS breakthrough capacity of DAF-P5-resin is 90 mg/g calculated from the breakthrough volume. By calculating the ratio between P5-loading and PFOS-absorption, we realized the P5-PFOS ratio in the saturation state is ca. 1:4.3. This P5-PFOS ratio suggests that the DAF-P5s are immobilized vertically on the surface of the resin, with one rim bound to resin, while the other rim is used to absorb PFOS, resulting a \sim 1:5 ratio. The resin could be easily regenerated to 80 % of its initial capacity by washing with 0.1 g/L NaCl in neutral MeOH. From the second regeneration onward, the capacity remained stable for at least 10 cycles, importantly with maintaining the residual PFOS concentration continues to be below 50 ng/L. Similarly, DAF-P5-resin also shows excellent absorbing performance to PFOA. The residual concentration is 35–48 ng/L, and the PFOA capacity of DAF-P5-resin is 80 mg/g (**Figure 8.4b**), which is two times higher compared with the top benchmark materials (40 mg/g for PAF).²² Notably, this is the capacity for a 10 wt% loading of DAF-P5, which thus still has 90 wt% of non-absorbing resin support; recalculating on the active P5 absorbent, the capacity reaches 800 mg/g.

One of the biggest challenges in the remediation of water from PFAS is the

insufficient efficiency of absorbent in the presence of potentially competing, natural organic co-contaminants, such as carboxylic acids. Common organic molecules are known to interact with the cavity of pillararenes,^{30,46} but it was not known to which degree this would interfere with the binding of PFAS to the rim. To demonstrate this property, we ran a competitive experiment, absorbing PFOA (1 µg/L) in the presence of a 10000-fold excess of its non-fluorinated counterpart, octanoic acid (OA, 10 mg/L). The residual concentration of OA increased dramatically after purifying 150 mL of solution, while the PFOA residual concentration stayed in range of 1–5 ng/L, order of magnitude lower than the safety advisory limit (**Figure 8.4c**).

For further proof of the effectiveness of our absorbent, we conducted experiments using environmental samples collected from various locations in China. Specifically, we obtained water samples from the Yitong River in Changchun, the Jin River in Chengdu, and tap water from Changchun, Chengdu, and Shanghai. In our experiments, we introduced 0.025wt % of the DAF-P5-resin to each of these samples. After subjecting them to 5 minutes of sonication, we removed the absorbent from the samples through filtration, and measured the [PFOS + PFOA] concentrations (**Figure 8.4d**). Clearly, the DAF-P5 resin effectively removes the PFOA and PFOS from water, yielding a residual concentration of the total of [PFOS + PFOA] that is lower than 10 ng/L in all cases. The DAF-P5-resin is not affected by natural organic co-contaminants, allowing it to maintain its efficiency for complex environmental samples.

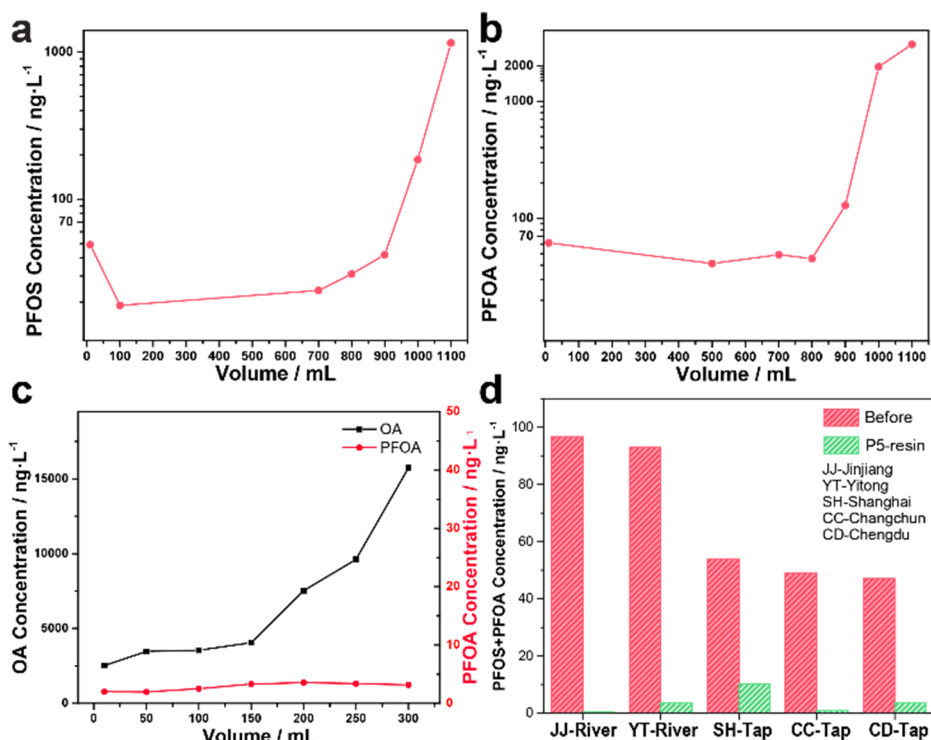


Figure 8.4. a. Residual concentration of PFOS after flushing heavily polluted water (10 mg/L PFOS) through a DAF-P5-functionalized resin. b. Residual concentration of PFOA after flushing heavily polluted water (10 mg/L PFOA) through a DAF-P5-functionalized resin. c. Residual concentration of PFOA and octanoic acid (OA) in mixture solution (original concentrations: PFOA = 1 $\mu\text{g/L}$; octanoic acid = 10 mg/L). d. Purification of environmental samples after 5 minutes treatment.

Conclusions

In conclusion, we report a new type of supramolecular binding between perfluoroalkyl acids to fluorine-free macrocyclic pillararene hosts, with an unprecedented 1:10 binding stoichiometry and high binding constants (up to $5 \times 10^6 \text{ M}^{-1}$). Crucial for these rim-based (rather than cavity-based) complexes is the combination of electrostatic host-guest attractions with strong fluorophilic interactions between PFAS molecules. This allows for the efficient removal of PFAS from water, in a fashion orthogonal to the in-cavity complexation of common organic molecules. DAF-P5-functionalized resin effectively reduces PFOA and PFOS concentrations also in natural river waters and tap water to safe levels via simple

filtration. The easily scalable synthesis of DAF-P5-functionalized materials together with the demonstrated high capacity and robust performance are expected to strongly contribute to the remediation of PFAS-polluted water.

Supporting Information

The supporting information is available free of charge at <https://onlinelibrary.wiley.com/doi/10.1002/anie.202403474>, and the table of contents is presented below.

Supporting Information Table of Contents

General information	Page 3
Synthesis of DAF-P5s	Page 4
Isolation of host-guest complexes	Page 6
Interpretation of ITC result	Page 7
Crystallographic details	Page 8
Computational study of fluorophilic interaction	Page 10
PFAS absorption experiments	Page 26
NMR data	Page 30
ITC data	Page 37
References	Page 51

Acknowledgments

Financial support from graduate school VLAG of Wageningen University (graduate fellowship of T.G.), China Scholarship Council (graduate fellowship to S.H.), the National Science Foundation of China (grants 21871208 and 22011530163, to H.Z.) and the Technology Development Project of Jiaying University is greatly acknowledged. We also thank Barend van Lagen (Wageningen University) for many helpful discussions.

References

- (1) Barry, V.; Winquist, A.; Steenland, K. Perfluorooctanoic acid (PFOA) exposures and incident cancers among adults living near a chemical plant. *Environmental Health Perspectives* **2013**, *121*, 1313-1318.
- (2) Conder, J. M.; Hoke, R. A.; Wolf, W. d.; Russell, M. H.; Buck, R. C. Are PFCA's bioaccumulative? A critical review and comparison with regulatory criteria and persistent lipophilic compounds. *Environmental Science & Technology* **2008**, *42*, 995-1003.
- (3) Cousins, I. T.; Vestergren, R.; Wang, Z.; Scheringer, M.; McLachlan, M. S. The precautionary principle and chemicals management: the example of perfluoroalkyl acids in groundwater. *Environment International* **2016**, *94*, 331-340.
- (4) Hu, X. C.; Andrews, D. Q.; Lindstrom, A. B.; Bruton, T. A.; Schaidler, L. A.; Grandjean, P.; Lohmann, R.; Carignan, C. C.; Blum, A.; Balan, S. A. Detection of poly-and perfluoroalkyl substances (PFASs) in US drinking water linked to industrial sites, military fire training areas, and wastewater treatment plants. *Environmental Science & Technology Letters* **2016**, *3*, 344-350.
- (5) Lau, C.; Butenhoff, J. L.; Rogers, J. M. The developmental toxicity of perfluoroalkyl acids and their derivatives. *Toxicology and Applied Pharmacology* **2004**, *198*, 231-241.
- (6) Loos, R.; Locoro, G.; Comero, S.; Contini, S.; Schwesig, D.; Werres, F.; Balsaa, P.; Gans, O.; Weiss, S.; Blaha, L. Pan-European survey on the occurrence of selected polar organic persistent pollutants in ground water. *Water Research* **2010**, *44*, 4115-4126.
- (7) Sun, M.; Arevalo, E.; Strynar, M.; Lindstrom, A.; Richardson, M.; Kearns, B.; Pickett, A.; Smith, C.; Knappe, D. R. Legacy and emerging perfluoroalkyl substances are important drinking water contaminants in the Cape Fear River Watershed of North Carolina. *Environmental Science & Technology Letters* **2016**, *3*, 415-419.
- (8) Sunderland, E. M.; Hu, X. C.; Dassuncao, C.; Tokranov, A. K.; Wagner, C. C.; Allen, J. G. A review of the pathways of human exposure to poly-and perfluoroalkyl substances (PFASs) and present understanding of health effects. *Journal of Exposure Science & Environmental Epidemiology* **2019**, *29*, 131-147.
- (9) Zeng, Z.; Song, B.; Xiao, R.; Zeng, G.; Gong, J.; Chen, M.; Xu, P.; Zhang, P.; Shen, M.; Yi, H. Assessing the human health risks of perfluorooctane sulfonate by in vivo and in vitro studies. *Environment International* **2019**, *126*, 598-610.
- (10) Karoyo, A. H.; Borisov, A. S.; Wilson, L. D.; Hazendonk, P. Formation of host-guest complexes of β -cyclodextrin and perfluorooctanoic acid. *The Journal of Physical Chemistry B* **2011**, *115*, 9511-9527.
- (11) Kucharzyk, K. H.; Darlington, R.; Benotti, M.; Deeb, R.; Hawley, E. Novel treatment technologies for PFAS compounds: a critical review. *Journal of Environmental Management* **2017**, *204*, 757-764.
- (12) Rahman, M. F.; Peldszus, S.; Anderson, W. B. Behaviour and fate of perfluoroalkyl and polyfluoroalkyl substances (PFASs) in drinking water treatment: a review. *Water Research* **2014**, *50*, 318-340.
- (13) Yang, A.; Ching, C.; Easler, M.; Helbling, D. E.; Dichtel, W. R. Cyclodextrin polymers with nitrogen-containing tripodal crosslinkers for efficient PFAS adsorption. *ACS Materials Letters* **2020**, *2*, 1240-1245.
- (14) Zheng, Z.; Yu, H.; Geng, W.-C.; Hu, X.-Y.; Wang, Y.-Y.; Li, Z.; Wang, Y.; Guo, D.-S. Guanidinocalix [5] arene for sensitive fluorescence detection and magnetic removal of perfluorinated pollutants. *Nature Communications* **2019**, *10*, 5762.
- (15) Abubakar, S.; Skorjanc, T.; Shetty, D.; Trabolsi, A. Porous polycalix [n] arenes as environmental pollutant removers. *ACS Applied Materials & Interfaces* **2021**, *13*, 14802-14815.
- (16) Weiss-Errico, M. J.; O'Shea, K. E. Enhanced host-guest complexation of short chain perfluoroalkyl substances with positively charged β -cyclodextrin derivatives. *Journal of Inclusion Phenomena and Macrocyclic Chemistry* **2019**, *95*, 111-117.
- (17) Xiao, L.; Ling, Y.; Alsbaiee, A.; Li, C.; Helbling, D. E.; Dichtel, W. R. β -Cyclodextrin polymer network sequesters perfluorooctanoic acid at environmentally relevant concentrations. *Journal of the American Chemical Society* **2017**, *139*, 7689-7692.

- (18) Ji, W.; Xiao, L.; Ling, Y.; Ching, C.; Matsumoto, M.; Bisbey, R. P.; Helbling, D. E.; Dichtel, W. R. Removal of GenX and perfluorinated alkyl substances from water by amine-functionalized covalent organic frameworks. *Journal of the American Chemical Society* **2018**, *140*, 12677-12681.
- (19) Ateia, M.; Arifuzzaman, M.; Pellizzeri, S.; Attia, M. F.; Tharayil, N.; Anker, J. N.; Karanfil, T. Cationic polymer for selective removal of GenX and short-chain PFAS from surface waters and wastewaters at ng/L levels. *Water Research* **2019**, *163*, 114874.
- (20) Gagliano, E.; Sgroi, M.; Falciglia, P. P.; Vagliasindi, F. G.; Roccaro, P. Removal of poly-and perfluoroalkyl substances (PFAS) from water by adsorption: Role of PFAS chain length, effect of organic matter and challenges in adsorbent regeneration. *Water Research* **2020**, *171*, 115381.
- (21) Huang, J.; Shi, Y.; Xu, J.; Zheng, J.; Zhu, F.; Liu, X.; Ouyang, G. Hollow covalent organic framework with "shell-confined" environment for the effective removal of anionic per- and polyfluoroalkyl substances. *Advanced Functional Materials* **2022**, *32*, 2203171.
- (22) Liu, X.; Zhu, C.; Yin, J.; Li, J.; Zhang, Z.; Li, J.; Shui, F.; You, Z.; Shi, Z.; Li, B. Installation of synergistic binding sites onto porous organic polymers for efficient removal of perfluorooctanoic acid. *Nature Communications* **2022**, *13*, 2132.
- (23) Ochoa-Herrera, V.; Sierra-Alvarez, R. Removal of perfluorinated surfactants by sorption onto granular activated carbon, zeolite and sludge. *Chemosphere* **2008**, *72*, 1588-1593.
- (24) Yu, J.; Lv, L.; Lan, P.; Zhang, S.; Pan, B.; Zhang, W. Effect of effluent organic matter on the adsorption of perfluorinated compounds onto activated carbon. *Journal of Hazardous Materials* **2012**, *225*, 99-106.
- (25) Zhang, D.; Zhang, W.; Liang, Y. Adsorption of perfluoroalkyl and polyfluoroalkyl substances (PFASs) from aqueous solution-A review. *Science of the Total Environment* **2019**, *694*, 133606.
- (26) Hoang, K. C.; Mecozzi, S. Aqueous solubilization of highly fluorinated molecules by semifluorinated surfactants. *Langmuir* **2004**, *20*, 7347-7350.
- (27) Gröschel, A. H.; Müller, A. H. Self-assembly concepts for multicompartment nanostructures. *Nanoscale* **2015**, *7*, 11841-11876.
- (28) Ogoshi, T.; Hashizume, M.; Yamagishi, T.-a.; Nakamoto, Y. Synthesis, conformational and host-guest properties of water-soluble pillar [5] arene. *Chemical Communications* **2010**, *46*, 3708-3710.
- (29) Ogoshi, T.; Kanai, S.; Fujinami, S.; Yamagishi, T.-a.; Nakamoto, Y. para-Bridged symmetrical pillar [5] arenes: their Lewis acid catalyzed synthesis and host-guest property. *Journal of the American Chemical Society* **2008**, *130*, 5022-5023.
- (30) Ogoshi, T.; Yamagishi, T.-a.; Nakamoto, Y. Pillar-shaped macrocyclic hosts pillar [n] arenes: new key players for supramolecular chemistry. *Chemical Reviews* **2016**, *116*, 7937-8002.
- (31) Song, N.; Kakuta, T.; Yamagishi, T.-a.; Yang, Y.-W.; Ogoshi, T. Molecular-scale porous materials based on pillar [n] arenes. *Chem* **2018**, *4*, 2029-2053.
- (32) Xue, M.; Yang, Y.; Chi, X.; Zhang, Z.; Huang, F. Pillararenes, a new class of macrocycles for supramolecular chemistry. *Accounts of Chemical Research* **2012**, *45*, 1294-1308.
- (33) Zuilhof, H.; Sue, A. C.-H.; Escorihuela, J. On the stability and formation of pillar [n] arenes: a DFT study. *The Journal of Organic Chemistry* **2021**, *86*, 14956-14963.
- (34) Demay-Drouhard, P.; Du, K.; Samanta, K.; Wan, X.; Yang, W.; Srinivasan, R.; Sue, A. C.-H.; Zuilhof, H. Functionalization at will of rim-differentiated pillar [5] arenes. *Organic Letters* **2019**, *21*, 3976-3980.
- (35) Strutt, N. L.; Zhang, H.; Schneebeli, S. T.; Stoddart, J. F. Functionalizing pillar [n] arenes. *Accounts of Chemical Research* **2014**, *47*, 2631-2642.
- (36) Guo, M.; Wang, X.; Zhan, C.; Demay-Drouhard, P.; Li, W.; Du, K.; Olson, M. A.; Zuilhof, H.; Sue, A. C.-H. Rim-differentiated C 5-symmetric tiara-pillar [5] arenes. *Journal of the American Chemical Society* **2018**, *140*, 74-77.
- (37) Wan, X.; Li, S.; Tian, Y.; Xu, J.; Shen, L.-C.; Zuilhof, H.; Zhang, M.; Sue, A. C.-H. Twisted pentagonal prisms: AgnL2 metal-organic pillars. *Chem* **2022**, *8*, 2136-2147.

- (38) Yang, W.; Samanta, K.; Wan, X.; Thikekar, T. U.; Chao, Y.; Li, S.; Du, K.; Xu, J.; Gao, Y.; Zuilhof, H. Tiara [5] arenes: synthesis, solid-state conformational studies, host–guest properties, and application as nonporous adaptive crystals. *Angewandte Chemie International Edition* **2020**, *59*, 3994–3999.
- (39) Mirzaei, S.; Wang, D.; Lindeman, S. V.; Sem, C. M.; Rathore, R. Highly selective synthesis of pillar [n] arene (n = 5, 6). *Organic Letters* **2018**, *20*, 6583–6586.
- (40) Ogoshi, T.; Aoki, T.; Kitajima, K.; Fujinami, S.; Yamagishi, T.-a.; Nakamoto, Y. Facile, rapid, and high-yield synthesis of pillar [5] arene from commercially available reagents and its X-ray crystal structure. *The Journal of Organic Chemistry* **2011**, *76*, 328–331.
- (41) Fang, Y.; Yuan, X.; Wu, L.; Peng, Z.; Feng, W.; Liu, N.; Xu, D.; Li, S.; Sengupta, A.; Mohapatra, P. K. Ditopic CMPO-pillar [5] arenes as unique receptors for efficient separation of americium (III) and europium (III). *Chemical Communications* **2015**, *51*, 4263–4266.
- (42) Silveira, E. V.; Nascimento, V.; Wanderlind, E. H.; Affeldt, R. F.; Micke, G. A.; Garcia-Rio, L.; Nome, F. Inhibitory and cooperative effects regulated by pH in host–guest complexation between cationic Pillar [5] arene and reactive 2-carboxyphthalanilic acid. *The Journal of Organic Chemistry* **2019**, *84*, 9684–9692.
- (43) Pollice, R.; Chen, P. Origin of the immiscibility of alkanes and perfluoroalkanes. *Journal of the American Chemical Society* **2019**, *141*, 3489–3506.
- (44) Sisui, C.; Baron, A. J.; Branderhorst, H. M.; Connell, S. D.; Weijers, C. A.; de Vries, R.; Hayes, E. D.; Pukin, A. V.; Gilbert, M.; Pieters, R. J. The influence of ligand valency on aggregation mechanisms for inhibiting bacterial toxins. *ChemBioChem* **2009**, *10*, 329–337.
- (45) Hu, X.-B.; Chen, L.; Si, W.; Yu, Y.; Hou, J.-L. Pillar [5] arene decaamine: synthesis, encapsulation of very long linear diacids and formation of ion pair-stopped [2] rotaxanes. *Chemical Communications* **2011**, *47*, 4694–4696.
- (46) Wu, G.-y.; Shi, B.-b.; Lin, Q.; Li, H.; Zhang, Y.-m.; Yao, H.; Wei, T.-b. A cationic water-soluble pillar[5]arene: synthesis and host–guest complexation with long linear acids. *RSC Advances* **2015**, *5*, 4958–4963.
- (47) Zhang, D.; Cheng, J.; Wei, L.; Song, W.; Wang, L.; Tang, H.; Cao, D. Host–guest complexation of monoanionic and dianionic guests with a polycationic pillararene host: Same two-step mechanism but striking difference in rate upon inclusion. *The Journal of Physical Chemistry Letters* **2020**, *11*, 2021–2026.
- (48) Senevirathna, S.; Tanaka, S.; Fujii, S.; Kunacheva, C.; Harada, H.; Shivakoti, B. R.; Okamoto, R. A comparative study of adsorption of perfluorooctane sulfonate (PFOS) onto granular activated carbon, ion-exchange polymers and non-ion-exchange polymers. *Chemosphere* **2010**, *80*, 647–651.
- (49) Fagbayigbo, B. O.; Opeolu, B. O.; Fatoki, O. S.; Akenga, T. A.; Olatunji, O. S. Removal of PFOA and PFOS from aqueous solutions using activated carbon produced from *Vitis vinifera* leaf litter. *Environmental Science and Pollution Research* **2017**, *24*, 13107–13120.

General Discussion



9.1 Solutions Provided in this Thesis to Overcome Challenges of Analyzing Cannabis and Cannabis products

As the globalization of the Cannabis market accelerates, a wide array of Cannabis products continues to emerge, presenting numerous challenges in the analysis of Cannabis and Cannabis products. From the perspective of analytical method development, this thesis has focused on cannabinoids and different chromatographic and mass spectrometric methods have been developed using the Ag(I)-alkene complexation mechanism. Apart from that, as a class of nearly ubiquitous "forever chemicals" with significant health concerns, PFAS may also be present as contaminants in Cannabis and Cannabis products (as well as in a much wider context).¹ Based on principles of host-guest chemistry and fluorine affinity, materials with high selectivity and efficiency for binding and removing PFAS contaminants were developed. Detailed challenges and solutions that have been documented in this thesis are summarized in **Table 9.1**.

Table 9.1. Challenges of analyzing Cannabis and Cannabis products and solutions provided in this thesis.

Overall objective		
Analytical differentiation and detection of cannabinoids and PFAS for the classification of Cannabis plants and quality/safety control of Cannabis products		
Challenges addressed	Underlying principle of methodology	Developed method(s), validation, and highlights
Chapter 3		
1. Inability of state-of-the-art to distinguish Δ^9 -THC and CBD without chromatography.	1. Ag(I)-alkene complexation enhances ionization efficiency of Δ^9 -THC and CBD by two orders of magnitude.	Ag(I)-impregnated paper spray tandem MS; benchmarked against RP-UHPLC-UV.
2. A growing CBD product market requires fast and high-throughput screening for trace amounts of Δ^9 -THC for compliance with the law.	2. Differential affinity of Δ^9 -THC and CBD with Ag(I) ions leads to different mass spectrometric fragmentation pathways and enables the distinction between Δ^9 -THC and CBD.	Reliable quantification of the Δ^9 -THC/CBD ratio in commercial CBD oils within seconds (good correspondence with the benchmark, $R^2 > 0.98$) and low-solvent consumption (15 μ L).

Chapter 4

1. Frequent false positive results in Cannabis analysis by fast colorimetric test without separation.

2. Inability to separate THC analogues and CBD analogues by silica TLC plates.

3. Low-cost and high-throughput analytical methods for on-site Cannabis classification are needed (hemp vs. marijuana).

1. Partially modified Ag(I)-TLC plate achieved digital chromatographic separation between THC analogues and CBD analogues based on different Ag(I) affinities toward cannabinoids with different numbers of C=C bonds.

2. Smartphone-based color analysis relies on the relationship between color intensity and concentration of THC analogues following colorimetric development.

Silica gel TLC with an Ag(I) retention zone and chromogenic smartphone detection; benchmarked against RP-HPLC-UV/MS.

Classification of hemp and marijuana with minimal solvent consumption (a few mL) in ~10 min and reliable semiquantification of THC analogues – also in presence of high CBD levels (good correspondence with the benchmark $R^2 = 0.97$).

Chapter 5

1. Insufficient separation of isomers Δ^8 -THC, Δ^9 -THC, CBD, Δ^8 -iso-THC, Δ^8 (4)-iso-THC by reversed-phase UHPLC.

2. Inability to distinguish those five isomers by conventional MS/HRMS.

3. Unclear cannabinoid composition in increasingly popular acid-treated CBD samples and Δ^8 -THC-infused edibles.

1. Silica-Ag(I) HPLC-DAD/MS achieved baseline separation of five THC isomers based on normal-phase separation combined with an argentation mechanism.

2. Unique MS² spectra of Ag(I) adducts of Δ^8 -THC, Δ^9 -THC, CBD, Δ^8 -iso-THC, and Δ^8 (4)-iso-THC were obtained based on differential Ag(I) affinities toward cannabinoids with different position of C=C bond.

3. The five isomers were separated by GC using a two-step gradient temperature program and all isomers showed different EI spectra.

Silica-Ag(I)-HPLC-DAD/MS & GC-FID/MS; cross-validated.

Sufficient separation, distinct ESI-MS spectra & EI-MS spectra of five isomers; two orthogonal methods provide reliable (good correspondence between the two developed methods $R^2 > 0.99$) and comprehensive cannabinoid profiling (various amounts of Δ^8 -THC (0–89%), illegal levels of Δ^9 -THC of up to nearly 50%, and the presence of other THC isomers and hydrated THC isomers) of acid-treated CBD samples and Δ^8 -THC-infused edibles.

<p>Chapter 6</p> <p>1. Lengthy separation of multiple cannabinoid isomers ($\Delta 8$-THC, $\Delta 9$-THC, CBD, $\Delta 8$-iso-THC, $\Delta(4)8$-iso-THC, 9α-hydroxyhexahydrocannabinol, 9β-hydroxyhexahydrocannabinol, 8-hydroxy-iso-THC, THCA, CBDA, $\Delta 8$-THCV, $\Delta 8$-iso-THCV, $\Delta 9$-THCV) by HPLC and GC.</p> <p>2. Limited resolution toward cannabinoid isomers by RP-UHPLC, inability to analyze acidic cannabinoids without derivatization by GC.</p> <p>3. Similar or often identical CCS values of protonated cannabinoid isomers in ion mobility spectrometry.</p>	<p>1. Differential Ag(I) affinities of cannabinoids with different numbers and positions of C=C bonds result in different 3D conformation and MS performance of Ag(I) adducts and thus distinct mobiligrams, CCS, and MS² spectra for structural isomers.</p> <p>2. Differential Ag(I) affinities toward cannabinoids without C=C bonds but different orientations of OH groups result in different 3D conformation, stabilities, and MS performance of Ag(I) adducts and thus distinct mobiligrams, CCS, and MS² spectra for diastereoisomers.</p>	<p>Ag(I)-cyclic IMS-MS; benchmarked against RP-UHPLC-UV/HRMS and GC-FID/MS.</p> <p>Ultrafast (milliseconds); highly sensitive (0.008–0.2 ng·ml⁻¹); ability to analyze both acidic and neutral cannabinoids without derivatization; distinction of diastereoisomers; reliable (good correspondence with the GC-FID/MS method $R^2 > 0.98$).</p>
<p>Chapter 7</p> <p>1. Inability to distinguish $\Delta 8$-THC and $\Delta 9$-THC by conventional ESI-MS.</p> <p>2. Increasingly popular $\Delta 8$-THC products need fast and routine screening methods.</p>	<p>1. A 3D-printed cartridge assisted in the alignment of the paper tip toward the MS inlet and enabled easy paper spray analysis and high-throughput potential.</p> <p>2. MS³ fragments of Ag(I) adducts allowed distinction of $\Delta 8$-THC and $\Delta 9$-THC based on differential Ag(I) affinities</p>	<p>3D-printed cartridge and Ag(I) paper spray MS³; benchmarked against GC-FID/MS.</p> <p>Fast (seconds); low-solvent consumption (15–20 μL); user-friendly; reliable (good correspondence with the benchmark $R^2 > 0.98$).</p>
<p>Chapter 8</p> <p>1. Poor selectivity, slow kinetics, and difficult synthesis of current PFAS-absorbing materials.</p>	<p>1. Synthesis of poly- and per-fluorinated-free pillararenes (DAF-P5) for highly sensitive and selectively binding PFAS via the pillararene rim-guest interaction determined by</p>	<p>Using DAF-P5-resin (columns) based on the highly sensitive and selective rim-based binding of PFAS to pillararenes; sensitive UHPLC-HRMS</p>

2. Unsustainability of poly- and per-fluorinated involved PFAS-absorbing materials.	fluorophilic and generic electrostatic attractions.	method for PFAS detection in water (LOD 1 ng·L ⁻¹).
3. Heavy and widespread contamination of PFAS in water but low Health Advisory Level (70 ng/L).	2. Covalent modification of DAF-P5 on resin for repeated use.	Much better PFAS removal performance than commercial activated carbon; high affinity (1:10 host-guest ratio); simple synthesis; fast kinetics (< 5 min); recyclability.
4. Expected contamination of PFAS in Cannabis and cannabinoid products via irrigation and production processes.	3. Preparation of DAF-P5-resin columns enables automatic large-scale water purification.	

9.2 Remaining Challenges in Each Chapter and Possible Solutions

9.2.1 Paper Chromatographic Separation Combined with Paper Spray MS for More Selectivity toward Cannabinoid Analysis

Paper spray MS is one of the most commonly used AIMS methods (see **Chapters 1 and 2**). Its advantages include affordability, availability, and the potential for chemical modification of paper tips.² As demonstrated in **Chapters 3 and 7**, easy modification of paper tips by physically absorbing AgNO₃ could improve sensitivity and selectivity toward cannabinoid analysis (for distinction of Δ9-THC from CBD and Δ8-THC, respectively). Sensitivity was achieved by the formation of cannabinoid-Ag(I) adducts to increase ionization efficiency. Selectivity was achieved through different MS fragmentation patterns induced by varying Ag(I) affinities toward cannabinoids with different positions and numbers of olefinic double bonds. Specifically, dominant MS² fragments at *m/z* 313 for Δ9-THC and *m/z* 353/355 for CBD can be used to distinguish between the two isomers. Similarly, dominant MS³ fragments at *m/z* 217 for Δ9-THC and *m/z* 245 for Δ8-THC serve as markers for differentiating these isomers. However, these characteristic signals are not unique to a single cannabinoid. For example, CBD also produces weak MS² fragments at *m/z* 313, which account for around 0.3% of the base peak signal (*m/z* 353/355). When the cannabinoid composition of a sample is relatively simple (e.g., containing only Δ9-THC and CBD), this can be addressed by subtracting the minor interfering signal (e.g., the minor contribution of CBD to the MS² signal at *m/z* 313

(**Chapter 3**). The situation becomes more complex when other cannabinoid isomers are involved, as they can also produce the same MS² signals. For example, Δ 8-THC produces a significant MS² signal at m/z 313, accounting for around 50% of the base peak. Although selectivity improves from MS² to MS³ fragmentation, other isomers that might coexist with Δ 8-THC (such as Δ 8-iso-THC, Δ (4)8-iso-THC, Δ 3-THC, etc.) still contribute (weakly) to MS³ signals at m/z 217 and m/z 245, complicating the analysis of Δ 8-THC and Δ 9-THC (**Chapter 7**). In addition, the coexistence of multiple cannabinoid isomers results in argention and ionization competition, which can lead to ion suppression or enhancement. Together, these factors compromise the sensitivity and accuracy of sample analysis and can make cannabinoid identification in complex samples indirect and ambiguous. **Chapter 6** introduces ion mobility separation before MS fragmentation, greatly improving the identification and semiquantification of cannabinoids despite the presence of multiple isomers. Therefore, separation (even with relatively low resolution) before MS analysis might improve the performance of paper spray analysis of cannabinoid isomers.

Thus, to further improve the selectivity of the developed method, paper chromatographic separation of cannabinoids before paper spray analysis could be a promising strategy. In **Chapter 7**, preliminary low-resolution separation of Δ 9-THC and CBD was achieved by using a 3D-printed cartridge for Ag(I) impregnated paper spray. Such low-resolution separation can facilitate identification of cannabinoids based on differential retention and is promising to be further improved e.g., by a continuous solvent supply design. The achieved separation was likely based on the fact that CBD (two hydroxyl groups) can interact more with the very polar paper compared with THC (one hydroxyl group). Considering the very different Ag(I) affinity of THC and CBD as demonstrated by computational calculation and Ag(I) strong cation exchange (SCX) column separation (**Chapters 3 and 7**), Ag(I)-SCX paper separation was preliminarily explored. SCX paper tips were prepared by chemical modification.^{3, 4} Specifically, the hydroxyl groups on the chromatographic paper tips were first activated under alkaline conditions. After washing and drying,

epoxy and sulfonic acid groups were introduced sequentially. The paper tips were then neutralized, washed, and dried to obtain SCX paper tips. The SCX paper tips were subsequently immersed in 1% NH_4OAc aqueous solution and 5% AgNO_3 solution, then dried to produce Ag(I) -SCX paper tips. Δ^9 -THC and CBD were applied to the bottom of paper tips, and MeOH was used as the eluent. The separation performance was visually assessed using a colorimetric test with the FBBB method (see **Chapter 4**). Compared to blank paper, which shows almost no difference in retention between Δ^9 -THC and CBD, Ag(I) -SCX paper could selectively retain CBD at the sample loading spot (**Figure 9.1**). In contrast, most Δ^9 -THC moves with the MeOH eluent despite a small portion still being retained in the sample loading spot. This method showed promise for selectively analyzing THC when it coexists with CBD, potentially eliminating the need for MS fragmentation to distinguish between them. Alternatively, if optimization allows CBD to be eluted much later than Δ^8 -THC or Δ^9 -THC, MS fragmentation will still be needed, but ionization competition among co-eluted cannabinoids could be reduced. From microscope images (150x magnification), it can be observed that the fiber structure of the Ag(I) -SCX paper tip has changed. Compared to the unmodified paper, the paper pores have become larger, which may have compromised its separation performance and thus should be considered during the optimization of chemical modification. On the other hand, Ag(I) -modified TLC plates, as developed in **Chapter 4**, could be tested for this purpose. This strategy could be promising for several reasons: i) aluminum-backed TLC plates can be easily cut into triangular shapes and produce electrospray from the sharp tip, similar to paper spray MS;⁵ ii) compared with chromatography paper, silica TLC plates, with their finer silica particles and structure, are expected to provide enhanced resolution for cannabinoids; iii) the mixed separation method (normal-phase combined with argentation) as demonstrated in **Chapter 5** could contribute to better separation of cannabinoid isomers prior to paper spray.

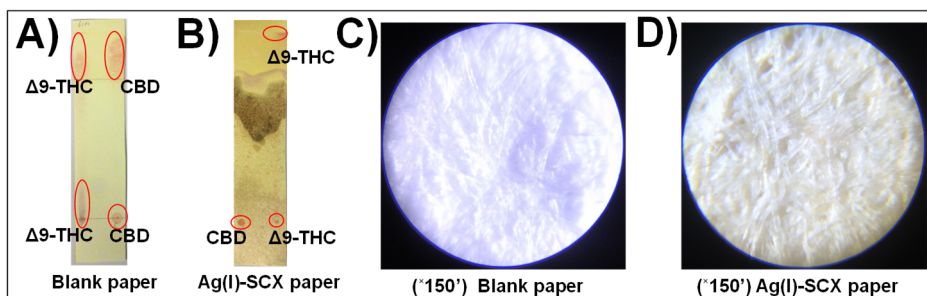


Figure 9.1. Low-resolution paper chromatographic separation of Δ^9 -THC and CBD by A) blank paper, B) Ag(I)-SCX paper; and microscope images of C) blank paper, and D) Ag(I)-SCX paper. The black color in the middle of (B) Ag(I)-SCX paper is an artifact from the manual spraying process.

9.2.2 Selective Paper Microfluidic Device with Colorimetric Test for Convenient and Fast On-Site Screening of THC

Colorimetric tests are quite attractive for on-site screening due to the advantages of being cheap and easy-to-execute, but low selectivity easily results in false positive results. In **Chapter 4** Ag(I)-TLC plates were developed to separate THC analogues and CBD analogues before colorimetric development and smartphone analysis to improve accuracy. Smartphone analysis, despite its semiquantification capability, requires strict control of photo acquisition conditions and specialized knowledge for color analysis. It could be done in a simpler way by using visual inspection for qualitative purposes instead of smartphone analysis. Additionally, TLC separation still requires some expertise or training, specific tools, and multiple solvents.

A simple separation strategy was thus preliminarily explored, using a thick (~ 0.3 cm thickness) paper microfluidic device with different modifications on each side: one hydrophobic side and one hydrophilic side. Specifically, filter papers were immersed in an octadecyltrichlorosilane solution to make them hydrophobic. Subsequently, one side of the hydrophobic paper was treated with plasma to make it hydrophilic. This process resulted in a paper microfluidic device with one hydrophilic side and one hydrophobic side. The hydrophilic side can be modified with an aqueous AgNO_3 solution to create an Ag(I)-loaded surface. The hydrophobic side, which is used for detection/color readout, prevents the penetration of the

aqueous AgNO_3 solution, thus avoiding background color from Ag(I) . When samples in MeOH solutions are applied from the hydrophilic side, the MeOH and its dissolved cannabinoids can penetrate the entire paper tip due to gravitational and capillary pressure to the hydrophobic side, as MeOH will still be able to wet the hydrophobically modified material. Then, a color reagent is applied and visual interpretation of the color can be performed on the hydrophobic side. Preliminary tests were conducted with $\Delta 9$ -THC and CBD standard solutions loaded on the Ag(I) modified side (**Figure 9.2**). $\Delta 9$ -THC, which interacts less with Ag(I) than CBD, was easily carried by MeOH to the hydrophobic side, while CBD with higher Ag(I) affinity was (more) retained on the hydrophilic/ Ag(I) side. Subsequent color development by FBBB under alkaline conditions (**Chapter 4**) on the hydrophobic side provided a visual observation of THC without much color interference induced by AgNO_3 . Therefore, such an approach is promising for further development for on-site screening of suspect Cannabis samples with reduced false-positive results as it will be simpler to perform and cheaper than the TLC-based approach.

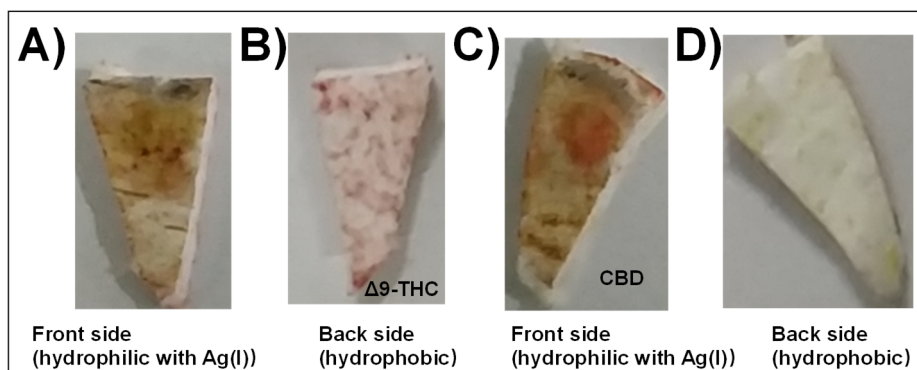


Figure 9.2. A) Front side and B) back side of the paper microfluidic device after loading $\Delta 9$ -THC and color development by FBBB; C) front side and D) back side of the paper microfluidic device after loading CBD and color development by FBBB.

9.2.3 High-Throughput DESI-Ion Trap MS for Effective Investigation of Acid-Catalyzed CBD Intramolecular Cyclization

With the legalization of CBD worldwide, much attention has been paid to the acid-catalyzed CBD conversion to produce THC.⁶ Such an acid-catalyzed CBD intramolecular cyclization process generally produces multiple THC isomers with different or unclear pharmacological activity and legal status. Therefore, it is important to understand the acid-treated CBD conversion process for medicinal and forensic purposes. In **Chapter 5**, eight different protocols were investigated to convert CBD to THC with different acid-treatment in bulk solution. The reaction time varied from 6–43 h, and multiple isomers were identified from the final products by chromatographic-based methods. As described in **Chapter 5**, different acids, solvents, and reaction times led to different cannabinoid isomer compositions in reaction products. To get a more comprehensive overview of how these different conditions affect product formation specifically, more systematic experiments with detailed investigation of each reaction condition are needed and thus a high-throughput reaction screening method would be beneficial.

Reactive DESI,^{7,8} which involves chemical reactions during the desorption ionization process, shows significant promise. It has the advantages of: i) accelerated reactions in microdroplets due to partial solvation of reactants, ordered orientation of reactant molecules, fast solvent evaporation, fast diffusion and mixing, and extreme pH formed in the interface of microdroplets; ii) small sample volumes (μL); iii) low sample concentrations (nmol/spot); iv) online screening of large numbers of reaction conditions. It would be useful to construct a platform as shown in **Figure 9.3** to investigate the acid-catalyzed CBD conversions including online monitoring of reaction intermediates, high-throughput screening and identification of reaction products, and distinction of isomers formed in such a process by introducing Ag(I) ions participating in multi-stage fragmentation in the ion trap. Specifically, CBD plus AgNO_3 solution is sprayed to form primary droplets and impact an inert surface on which different reagents are deposited. After this, secondary droplets are formed and move to the MS. Reactions happen during the transferring process to the MS

inlet and an ion trap is used for distinction of THC isomers through multi-stage fragmentations (**Chapters 3, 5 and 7**). Ag(I) ions would not play a role in the CBD conversion based on our previous investigation of CBD with Ag(I)-impregnated paper spray mass spectrometry method under various conditions (**Chapter 3**). In summary, the conversion of CBD in confined volumes is expected to be accelerated and intermediate and product isomers are expected to be rapidly distinguished by introducing Ag(I) ions followed by multi-stage fragmentations.

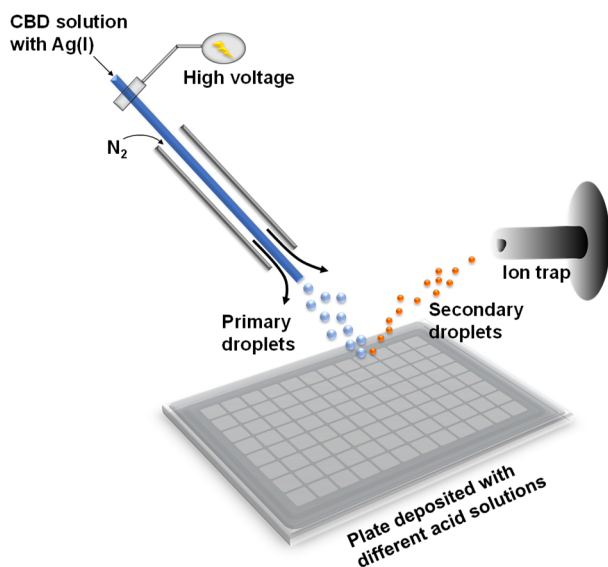


Figure 9.3. Reactive desorption electrospray ionization (DESI) for investigation of acid-catalyzed CBD intramolecular cyclization.⁹

9.2.4 DESI Cyclic-IMS for High-Throughput Analysis of Cannabis Samples and UHPLC-Cyclic IMS for More Selective Analysis of Cannabinoids

Ag(I)-cyclic IMS revolutionized cannabinoid isomer analysis as demonstrated in **Chapter 6**. However, challenges remain, including the fact that loop injection and flow injection slow down the analysis process due to the need for sample preparation and equipment flushing between samples. In **Chapter 6**, different samples underwent various extraction procedures, as described in **Table 9.2**. The sample extracts were then mixed with the methanolic $AgNO_3$ solution, followed by loop/flow injection into the cIMS. The solvent used for sample extraction must be

compatible with MeOH. This can be achieved by either using MeOH-compatible solvents for extraction or by blow-drying the sample extracts and reconstituting them with MeOH-compatible solvents. Additionally, thorough flushing of the injector between samples is necessary to avoid cross-contamination. Despite the millisecond-separation merits, such constraints decrease the analytical throughput.

To improve the analytical throughput, DESI, one of the most widely used AIMS techniques as introduced in **Chapters 1** and **2**, is a promising candidate. It offers several advantages, including no/minimal sample pretreatment, a high degree of automation, reduced cross-contamination, and compatibility with various sample forms.¹⁰ The commercial DESI-cyclic IMS interface offers an alternative to loop injection-cyclic IMS for high-throughput Cannabis sample analysis. In principle, multiple samples, regardless of their form, could be placed on a flat surface without sample pretreatment. DESI directs electrospray droplets, which can incorporate Ag(I) ions, onto the sample surface and then form secondary droplets. Upon desolvation of the secondary droplets, gaseous ions are formed, which are then detected by the mass spectrometer. This approach circumvents the need for sample preparation, ensuring that only gaseous ions (e.g., Ag(I)-cannabinoid adducts) enter the cyclic IMS equipment, thereby preventing potential contamination from AgNO₃ solutions.

To first explore whether Ag(I)-cannabinoid adducts produced during the DESI ionization process could be detected by cIMS, CBD standard solution was mixed with AgNO₃ MeOH and spotted on the glass slide. MeOH was used as the spray solvent, and direct DESI mass spectra were acquired (**Figure 9.4**). The Ag(I) adducts at m/z 421/423, and characteristic fragments of CBD at m/z 353/355 were clearly seen, demonstrating the possibility of analyzing cannabinoids by DESI-MS. Ion mobility separation of cannabinoid isomers could thus be expected when switching on the ion mobility function and multiple samples could be analyzed on the same glass slide to increase throughput. Further investigation could explore using AgNO₃ in MeOH solution as a spray solvent rather than mixing AgNO₃ with samples for more convenience, even though that would introduce more AgNO₃ into the instrument. Additionally, *in situ* analysis could be attempted for samples such as hair

for retrospective forensic purposes. Using ion mobility separation or MS with fragmentation can easily distinguish hair samples containing Δ^8 -THC, Δ^9 -THC, or CBD. Distinction of Δ^8 -THC and Δ^9 -THC in biological matrixes is assumed to be challenging with current techniques.¹¹

Another challenge is the insufficient separation of multiple coexisting isomers which jeopardizes accurate quantification. In **Chapter 6**, ion mobility separation of six THC/CBD isomers was achieved within milliseconds. However, many of them were not baseline separated, such as Δ^8 -iso-THC and Δ^8 -THC, and Δ^8 -iso-THC and Δ^3 -THC. The inadequate ion mobility separation, occurring after ESI ionization, compromised the quantification of individual cannabinoids due to competitive ionization of coeluted analytes and overlapping diagnostic quantification fragments. Although it is possible to enhance ion mobility resolution of these cannabinoid isomers by increasing the number of separation passes and separating different isomers in distinct passes, ionization competition cannot be mitigated. This is because there is no physical separation of molecules and ions before ionization.

For more accurate quantification, an additional dimension of separation before ESI ionization would be ideal, creating a “separation-ionization-separation-distinct MS² fragmentation” process. UHPLC, commercially coupled with cyclic IMS, is a promising candidate for this purpose. As demonstrated in **Chapter 5**, Ag(I) can be introduced into the MS either through an argentation column or by post-column mixing with Ag(I) solutions. This approach is expected to provide very high resolution for complex cannabinoid isomers by leveraging chromatographic separation, mobility separation, and MS distinction, leading to more precise qualitative and quantitative analysis.

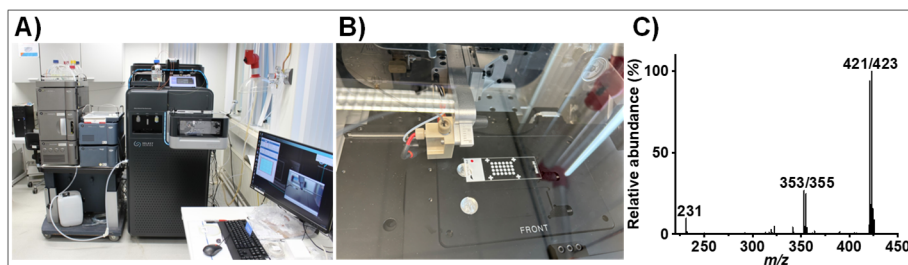


Figure 9.4. Photos of (A) DESI-cyclic IMS-MS setup, (B) measurement of multiple samples on one glass slide, and (C) mass spectrum of CBD with m/z 421/423 as precursor ions and trap energy of 20V.

9.2.5 Deca-Ammonium-Functionalized Pillar[5]arenes (DAF-P5s) used in Cannabis Sample Pretreatment to Selectively Concentrate PFAS for Sensitive Detection

Per- and poly-fluoroalkyl substances (PFASs) are highly fluorinated aliphatic compounds with numerous precursors.¹² The wide application in daily life, high stability and persistence, bio-accumulation, and potential bio-toxicity make their analysis in environment and food urgent.^{13,14} Due to their distinctive physicochemical properties, PFASs often occur at trace levels in different matrixes, demanding sensitive and selective analytical methods.¹⁵ Therefore, it poses challenges for both sample pretreatment and instrumental analysis. On the other hand, it is reasonable to assume that Cannabis and Cannabis products can become contaminated with PFAS through irrigation and production processes. As Cannabis edibles and other consumables grow in popularity, analyzing PFAS levels will likely become an important part of quality control for these products. Therefore, effective enrichment methods are needed to detect PFAS in complex matrixes.

As described in **Chapter 8**, DAF-P5 pillararenes have high affinity and selectivity to PFAS. The binding between PFAS and DAF-P5 is driven by electrostatic host-guest attractions and strong fluorophilic interactions with PFAS molecules in aqueous solutions. Such binding can be easily disrupted using a NaCl solution in MeOH ($0.1 \text{ g} \cdot \text{L}^{-1}$), which was employed for regenerating DAF-P5-resin columns. Inspired by this, DAF-P5-resin might be used to selectively concentrate

PFAS from aqueous fractions of Cannabis sample extracts (e.g., via LLE) by absorption and elution in different solvents, thereby achieving lower limits of detection (LOD). Given the high binding affinity, selectivity, and regeneration performance of DAF-P5-resin, its use in Cannabis sample pretreatment for PFAS analysis could be highly beneficial.

9.3 Future Development of Cannabis and Cannabinoid Analysis

Beyond the challenges mentioned above, an outlook of future developments in the analysis of Cannabis/cannabinoids is presented below.

9.3.1 Sample Preparation

Despite the speed and ease of many developed instrumental analysis methods, sample preparation, which is an important but often overlooked part of chemical analysis, is normally the most time-consuming and labor-intensive and becomes the bottleneck of fast sample analysis.¹⁶ For Cannabis and cannabinoid analysis, different considerations need to be taken into account according to specific sample types. An overview of the studied extraction approaches and their evaluation¹⁷ regarding to effectiveness (mainly about recovery and matrix effects), safety (mainly about chemicals), cost (mainly about devices), simplicity (mainly about operations), and greenness (mainly about solvents and energy) is presented in **Table 9.2**.

Table 9.2. Sample preparation in different chapters.

Chapter	Sample	Sample Preparation	Duration	Recovery	Matrix Effects	*Evaluation
3	CBD oil	CBD oil was diluted with sunflower oil to 0.2% (w/w %) based on declared content; 2.00 mL MeOH was added to 50.0 mg diluted oil for extraction under magnetic stirring.	~2 min	87.3 ± 1.2% for Δ9-THC; 92.3 ± 1.4% for CBD.	-2.2 ± 0.4% for Δ9-THC; -2.0 ± 0.3% for CBD.	Effectiveness: ★★★★★; safety: ★★★; cost: ★★★; simplicity: ★★★; greenness: ★★★★★.

4	Cannabis plant materials	Cannabis plant materials were ground and homogenized; 300 μ L MeOH was added to 100.0 mg sample for extraction under vortexing; extracted samples were syringe filtered.	~3 min	NE	NE	Effectiveness: NE; safety: ★★★; cost: ★★★★★; simplicity: ★★; greenness: ★★★
5	Δ 8-THC gummies	200.00 mL MTBE/water 1/1 (v/v) solution was added to 1.00 g gummy for extraction under ice bath ultrasonication; the MTBE layer was syringe filtered after phase separation.	~50 min	100 \pm 17 % to 101 \pm 16 %	-2.6 % to 14 % for GC-FID/MS; -9.6% to 11 % for silica-Ag(I) HPLC-DAD.	Effectiveness: ★★★★★; safety: ★★; cost: ★★★; simplicity: ★; greenness: ★.
6	Cannabis plant material, Δ 8-THC gummies	600–700 μ L MeOH was added to 6.0–7.0 mg Cannabis plant materials for extraction under ultrasonication; extracted samples were syringe filtered. 1.00 mL MTBE/water (v/v = 1:1) was added to 10.0 mg gummy for extraction under hand shaking; MTBE layer was syringe filtered after phase separation.	~10 min for Cannabis plant materials; ~25 min for gummies.	NE	NE	Effectiveness: NE; safety: ★★★; cost: ★★★; simplicity: ★; greenness: ★★★.

7	Δ8-THC	1.00 mL MeOH	~10 min	94.4±2.9% for Δ8-THC and to	-7.1±1.4%	Effectiveness:
	brownie,	was added to 10.0	for Δ8-THC	97.7±2.1% for Δ9-THC in Δ8-THC brownie;	17±2.9%	★;
	Δ8-THC	mg Δ8-THC	THC	87.9±16% for Δ8-THC and to	2.2±0.3%	safety:
	rice	brownie and rice	brownie,	85.7±17% for Δ9-THC in Δ8-THC for Δ9-	34±2.2%	★★★★★;
	cracker,	cracker and 10.0	Δ8-THC	96.7±0.6% for Δ8-THC, 95.8±1.3% to	7.4±1.0%	cost:
	Δ8-THC	mL MeOH was	rice	for Δ9-THC and	15±1.5%	★;
	Cannabis	added to 10.0 mg	cracker,	96.0±0.2% for	for Δ9-	simplicity:
	leaves,	Δ8-THC Cannabis	Δ8-THC	CBD in Δ8-THC	THC : Δ8-	★★★★★;
	vape oils	leaves for	Cannabis	coated Cannabis	THC ratio.	greenness:
		extraction under	leaves;	leaves. 100% for		★★.
		hand shaking;	seconds for	vape oils.		
		extracted samples	vape oils.			
		were syringe				
		filtered. 10.0 mg				
		vape oil was				
		diluted 10 times				
		with MeOH.				

NE: no evaluation; *Evaluation: ★★★★★ means the maximum extent, ★ means the minimum extent, and the degrees represented by the other numbers of stars (2–4) follow accordingly.

(i) Cannabis plant

Cannabis plant analysis is mainly done for the purposes of classification or monitoring the growth process. Therefore, in-field analysis is preferred, and accordingly, sample preparation methods with minimal solvent consumption and equipment-dependence are desired. As described in **Chapter 2**, optical spectroscopic methods are most frequently used for Cannabis plant analysis. Especially with (near)-infrared ((N)IR) spectroscopy and Raman spectroscopy (RS) methods, typically *in situ* analysis without any sample pretreatment or simply grinding of Cannabis plant material is used. For other analytical methods, grinding, homogenization, solid-liquid extraction, and filtration are generally needed before analysis. In **Chapter 4**, despite the fact that only a small amount of harmful organic solvent and relatively cheap equipment (grinder and vortex) were used for the sample preparation step, it is still not ideal for in-field application (**Table 9.2**). Future efforts can be made considering the following two aspects: incorporating portable 3D-printed sample processing modules to replace the grinder and vortexer and utilizing

green solvents to replace harmful organic solvents. Our group developed modular 3D-printed sampling tools for on-site grinding and extraction of wheat kernels, which could also be promising to be used for processing Cannabis plant materials.¹⁸ The use of green solvents could minimize the harmfulness to the environment and operators in the field. Among green solvents, EtOH stands out to be a promising candidate not only due to its non-toxicity to the environment and humans but also because of its polarity compatibility with both acidic and neutral cannabinoids to ensure sufficient recovery.¹⁹⁻²¹ However, the more significant co-extraction of polar pigments by EtOH than other less polar solvents, e.g., CHCl₃ and hexane, should be considered, and thus simple pre-separation before detection as described in **Chapter 4**, is desired to reduce interferences from the matrix. In terms of less polar solvents, cooking oils might be interesting alternatives to these organic solvents. Bills et al.²² applied sesame seed oil to preconcentrate Δ9-THC and synthetic cannabinoids in biological fluids on paper due to their similar polarity. In **Chapter 3**, sunflower oil was also used as a replacement for organic solvents to dilute commercial CBD oils before extraction to reduce the consumption of organic solvents. The applications of cooking oil extraction in Cannabis plant materials is worth exploring. Romano et al.²³ compared EtOH, naphtha, petroleum ether, and olive oil for their extraction performance of cannabinoids and terpenes from Cannabis plant materials and demonstrated that olive oil is the best choice since it is non-toxic, cheap, and gave high recovery of cannabinoids and terpenes.

(ii) Cannabis products

While Cannabis plant samples are highly complex, Cannabis products are more diverse in terms of matrix, cannabinoid profile, and associated analytical challenges. Such products come in different shapes and forms and have various ingredients, such as oil, sugar, gelatin, fat, and colorings, demanding specialized sample pretreatment methods for each of them.²⁴ In **Chapters 3, 5, 6, and 7**, different extraction methods were used for various Cannabis products (**Table 9.2** and **Figure 9.5**). **Chapters 3, 6 and 7** aimed to develop fast screening methods, and thus, fast and simple sample pretreatment strategies were used. Despite generally good recoveries, various

degrees of matrix effects were encountered in those non-chromatographic methods due to coeluting substances changing the ESI ionization efficiency of target analytes (signal enhancement or suppression).²⁵ Consequently, efforts were made to correct for matrix effects. In **Chapter 3**, a matrix-based calibration curve was used, while in **Chapter 7**, a standard-addition strategy was employed. Besides, in all three developed non-chromatographic methods (two paper spray MS methods in **Chapters 3** and **7**, and one cyclic IMS method in **Chapter 6**), relative quantification of cannabinoids was shown to provide higher accuracy than absolute quantification. This is likely because the cannabinoids investigated are structural isomers that experience similar matrix effects, leading to limited impacts on their ratios and relative percentages, which is sufficient for screening purposes. In **Chapter 5**, a more sophisticated and time-consuming process was used to deal with an intact piece of gummy, which mainly consists of sugar and gelatin and is sticky and dense. Combined with sufficient chromatographic separations, together, the developed methods ensured more accurate and precise quantification of cannabinoids in gummies for confirmatory purposes. For future development, the green sample preparation concept should be taken into account to contribute to a greener analytical methodology.²⁶ The ideal situation would be to eliminate the need for sample pretreatment, which demands significant advancements in instrumental analysis. Currently, ((N)IR), RS, and DART-MS have applications in this area, as described in **Chapter 2**. Generally, ((N)IR) and RS methods rely heavily on chemometric models, necessitating specific models for different analytes and sample forms, complicating the analysis process. Conversely, DART-MS, which does not require chemometric models, offers a more direct and accurate analysis but struggles to distinguish cannabinoid isomers and analyze acidic cannabinoids due to their thermal instability. Additionally, without sample pretreatment, all these methods have difficulties achieving a low LOD for specific cannabinoids.

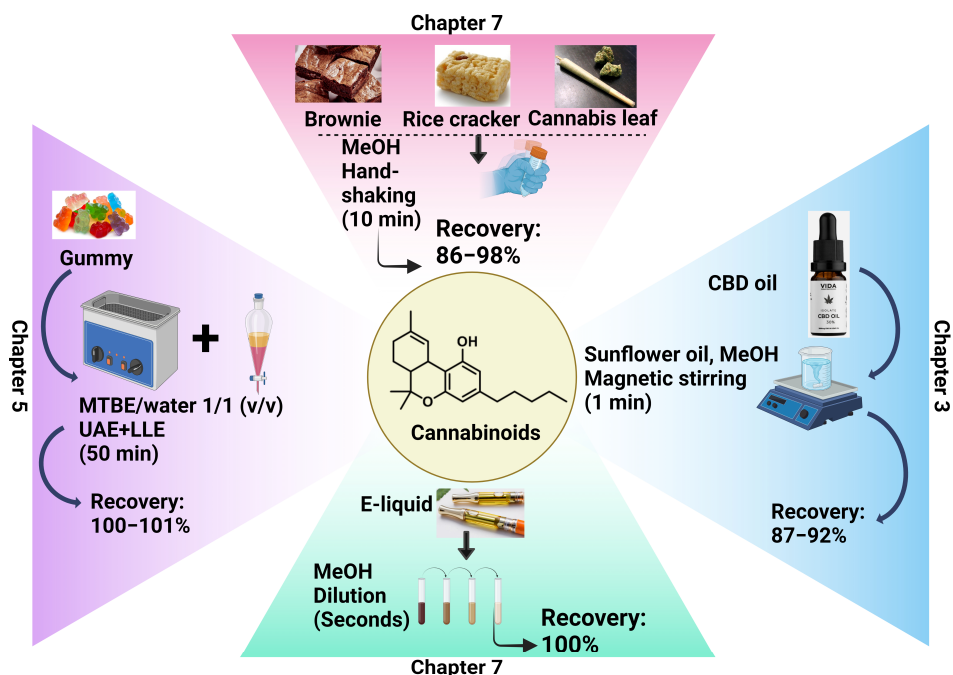


Figure 9.5. Extraction of Cannabis products in this thesis (abbreviations: methyl *tert*-butyl ether (MTBE); ultrasound-assisted extraction (UAE); liquid-liquid extraction (LLE)).

9.3.2 Absolute Quantification

In this thesis, relative quantification was achieved by the developed non-chromatographic methods. Specifically, in **Chapter 3** and **Chapter 7**, the ratios of $\Delta 9$ -THC:CBD and $\Delta 9$ -THC: $\Delta 8$ -THC were measured by paper spray tandem MS. In **Chapter 6**, the ratio of $\Delta 9$ -THC: $\Delta 8$ -THC was measured by cyclic-IMS tandem MS. The found ratios were in good correspondence with those obtained by gold standard chromatographic methods since they are structural isomers with similar matrix effects (**Table 9.2**). This is a quick and cheap solution for screening purposes. Absolute quantification of individual cannabinoids ($\Delta 8$ -THC and $\Delta 9$ -THC) was also explored in **Chapter 7** by two strategies: i) using a structural analogue ($\Delta 9$ -THCV) as an internal standard and ii) applying a standard addition method. The structural analogue $\Delta 9$ -THCV (with a propyl side chain) despite its small structural difference from $\Delta 9$ -THC (with a pentyl side chain) was found to have quite different matrix effects from the targeted analytes and thus introduced large quantification errors.

This is aligned with the conclusion of Khamis et al.²⁷ that structural analogues should be avoided if isotopically labelled internal standards are available. Currently, deuterated internal standards have wide applications in cannabinoid quantification, but the different lipophilicity from their analytes and hydrogen-deuterium exchange during the ionization process compromises the quantification performance. ¹³C-labeled internal standards with identical physicochemical properties to their ¹²C counterparts do not suffer from these constraints.^{27,28} Standard addition is another more labor-intensive option to achieve absolute quantification with the advantages of not needing analyte-free matrixes and internal standards.²⁹ However, it did not work out in **Chapter 7**, probably due to severe interference from multiple coeluting cannabinoid isomers. In the future, absolute quantification of cannabinoids by non-chromatographic methods is promising and should preferably make use of ¹³C-labeled internal standards.

9.3.3 Standardized Reference Methods for Cross-Validation of New Methods

Method validation is “the confirmation, by examination and the provision of objective evidence, that the requirements for a specific intended use are fulfilled”.³⁰ Even though many laboratories are making efforts to develop new methods to meet new requirements of cannabinoid analysis, less attention is paid to method validation, especially for newly developed methods. One of the criteria for validating screening methods is the comparison with classical methods to demonstrate the equivalence of results obtained by newly developed methods and accepted classical methods.³¹ Although HPLC and GC-based methods are commonly regarded as reference methods, there are no globally standardized methodologies for the analysis of cannabinoids in Cannabis and Cannabis products, probably because there is no generic method to fit diverse samples.³² In this thesis, various reference methods were used to fit different purposes (**Table 9.1**). RP-HPLC-based methods can analyze both acidic and neutral cannabinoids without the need for derivatization. The coupling of MS/HRMS aids in identifying specific cannabinoids in complex matrixes. However, the limited resolution is insufficient for separating multiple

isomers. GC-based methods can overcome this issue, but the thermal degradation of acidic cannabinoids must be considered. The use of different reference methods complicates the standardized comparison and evaluation of new methods. For future development, standardized methodologies for analyzing Cannabis and Cannabis products are needed to facilitate the validation of new methods and cross-lab comparisons. Ideally, these methodologies should be capable of analyzing at least the commonly studied acidic cannabinoids, neutral cannabinoids, and cannabinoid isomers with minimal sample preparation steps.

In conclusion, analytical methods based on selective molecular interactions were developed for the analysis of Cannabis and related samples. These methods, including TLC-based method, AIMS-based method, GC-based method, (U)HPLC-based method, IMS-based method, are promising to meet diverse application needs for the analysis of Cannabis and Cannabis products in different scenarios. Challenges in resolving cannabinoid isomers and improving analytical speed and throughput were addressed. Future efforts can be devoted to further improving selectivity for cannabinoid isomers, developing greener and more efficient sample pretreatment methods, and standardizing cross-validation for new methods. With joint efforts, the safe use of Cannabis and Cannabis-derived products is foreseeable.

References

- (1) Committee. *Packaging*; rev. HF 100-93rd **2023**. Retrieved from State of Minnesota House of Representatives.
https://www.revisor.mn.gov/bills/text.php?number=HF100&version=0&session=ls93&session_year=2023&session_number=0 (accessed 2024 June 19).
- (2) McBride, E. M.; Mach, P. M.; Dhummakupt, E. S.; Dowling, S.; Carmany, D. O.; Demond, P. S.; Rizzo, G.; Manicke, N. E.; Glaros, T. Paper spray ionization: applications and perspectives. *TrAC Trends in Analytical Chemistry* **2019**, *118*, 722-730.
- (3) Song, J.; Jin, Y.; Fu, G.; He, A.; Fu, W. A facile approach toward surface sulfonation of natural cotton fibers through epoxy reaction. *Journal of Applied Polymer Science* **2012**, *124*, 1744-1750.
- (4) Eldin, M. S. M.; Elmageed, M. H. A.; Omer, A. M.; Tamer, T. M.; Yossuf, M. E.; Khalifa, R. E. Novel proton exchange membranes based on sulfonated cellulose acetate for fuel cell applications: preparation and characterization. *International Journal of Electrochemical Science* **2016**, *11*, 10150-10171.
- (5) Hsu, F.-L.; Chen, C.-H.; Yuan, C.-H.; Shiea, J. Interfaces to connect thin-layer chromatography with electrospray ionization mass spectrometry. *Analytical Chemistry* **2003**, *75*, 2493-2498.
- (6) Golombek, P.; Müller, M.; Barthlott, I.; Sproll, C.; Lachenmeier, D. W. Conversion of cannabidiol (CBD) into psychotropic cannabinoids including tetrahydrocannabinol (THC): a controversy in the scientific literature. *Toxics* **2020**, *8*, 41.
- (7) Girod, M.; Moyano, E.; Campbell, D. I.; Cooks, R. G. Accelerated bimolecular reactions in microdroplets studied by desorption electrospray ionization mass spectrometry. *Chemical Science* **2011**, *2*, 501-510.
- (8) Cooks, R. G.; Feng, Y.; Huang, K. H.; Morato, N. M.; Qiu, L. Re-imagining drug discovery using mass spectrometry. *Israel Journal of Chemistry* **2023**, *63*, e202300034.
- (9) Meher, A. K.; Chen, Y.-C. Electrospray modifications for advancing mass spectrometric analysis. *Mass Spectrometry* **2017**, *6*, S0057-S0057.
- (10) Takats, Z.; Wiseman, J. M.; Gologan, B.; Cooks, R. G. Mass spectrometry sampling under ambient conditions with desorption electrospray ionization. *Science* **2004**, *306*, 471-473.
- (11) Antunes, M.; Barroso, M.; Gallardo, E. Analysis of cannabinoids in biological specimens: an update. *International Journal of Environmental Research and Public Health* **2023**, *20*, 2312.
- (12) Ullah, S.; Alsberg, T.; Berger, U. Simultaneous determination of perfluoroalkyl phosphonates, carboxylates, and sulfonates in drinking water. *Journal of Chromatography A* **2011**, *1218*, 6388-6395.
- (13) Al Amin, M.; Sobhani, Z.; Liu, Y.; Dharmaraja, R.; Chadalavada, S.; Naidu, R.; Chalker, J. M.; Fang, C. Recent advances in the analysis of per- and polyfluoroalkyl substances (PFAS)—a review. *Environmental Technology & Innovation* **2020**, *19*, 100879.
- (14) Iannone, A.; Carriera, F.; Passarella, S.; Fratianni, A.; Avino, P. There's something in what we eat: an overview on the extraction techniques and chromatographic analysis for PFAS identification in agri-food products. *Foods* **2024**, *13*, 1085.
- (15) Androulakis, A.; Alygizakis, N.; Bizani, E.; Thomaidis, N. S. Current progress in the environmental analysis of poly- and perfluoroalkyl substances (PFAS). *Environmental Science: Advances* **2022**, *1*, 705-724.
- (16) Xia, L.; Yang, J.; Su, R.; Zhou, W.; Zhang, Y.; Zhong, Y.; Huang, S.; Chen, Y.; Li, G. Recent progress in fast sample preparation techniques. *Analytical Chemistry* **2020**, *92*, 34-48.
- (17) Chen, Y.; Guo, Z.; Wang, X.; Qiu, C. Sample preparation. *Journal of Chromatography A* **2008**, *1184*, 191-219.
- (18) Bosman, A. J.; Freitag, S.; Ross, G. M. S.; Sulyok, M.; Krska, R.; Ruggeri, F. S.; Salentijn, G. I. J. Interconnectable 3D-printed sample processing modules for portable mycotoxin screening of intact wheat. *Analytica Chimica Acta* **2024**, *1285*, 342000.
- (19) Stefkov, G.; Cvetkovikj, Karanfilova, I.; Stoilkovska Gjorgievska, V.; Trajkovska, A.; Geskovski, N.; Karapandzova, M.; Kulevanova, S. Analytical techniques for phytocannabinoid profiling

- of Cannabis and Cannabis-based products—a comprehensive review. *Molecules* **2022**, *27*, 975.
- (20) Fernández, S.; Carreras, T.; Castro, R.; Perelmuter, K.; Giorgi, V.; Vila, A.; Rosales, A.; Pazos, M.; Moyna, G.; Carrera, I.; *et al.* A comparative study of supercritical fluid and ethanol extracts of Cannabis inflorescences: chemical profile and biological activity. *The Journal of Supercritical Fluids* **2022**, *179*, 105385.
- (21) Compagnin, G.; De Luca, C.; Nosengo, C.; Catani, M.; Cavazzini, A.; Greco, G.; Krauke, Y.; Felletti, S. Sustainable cannabinoids purification through twin-column recycling chromatography and green solvents. *Analytical and Bioanalytical Chemistry* **2024**, *416*, 4091-4099.
- (22) Bills, B.; Manicke, N. Using sesame seed oil to preserve and preconcentrate cannabinoids for paper spray mass spectrometry. *Journal of the American Society for Mass Spectrometry* **2020**, *31*, 675-684.
- (23) Romano, L. L.; Hazekamp, A. Cannabis oil: chemical evaluation of an upcoming Cannabis-based medicine. *Cannabinoids* **2013**, *1*, 1-11.
- (24) Yang, S.; Sun, M. Recent advanced methods for extracting and analyzing cannabinoids from Cannabis-infused edibles and detecting hemp-derived contaminants in food (2013–2023): a comprehensive review. *Journal of Agricultural and Food Chemistry* **2024**, *72*, 13476-13499.
- (25) Zhou, W.; Yang, S.; Wang, P. G. Matrix effects and application of matrix effect factor. *Bioanalysis* **2017**, *9*, 1839-1844.
- (26) López-Lorente, Á. I.; Pena-Pereira, F.; Pedersen-Bjergaard, S.; Zuin, V. G.; Ozkan, S. A.; Psillakis, E. The ten principles of green sample preparation. *TrAC Trends in Analytical Chemistry* **2022**, *148*, 116530.
- (27) Khamis, M. M.; Adamko, D. J.; El-Aneed, A. Strategies and challenges in method development and validation for the absolute quantification of endogenous biomarker metabolites using liquid chromatography-tandem mass spectrometry. *Mass Spectrometry Reviews* **2021**, *40*, 31-52.
- (28) Berg, T.; Strand, D. H. ^{13}C labelled internal standards—a solution to minimize ion suppression effects in liquid chromatography–tandem mass spectrometry analyses of drugs in biological samples? *Journal of Chromatography A* **2011**, *1218*, 9366-9374.
- (29) Hasegawa, K.; Minakata, K.; Suzuki, M.; Suzuki, O. The standard addition method and its validation in forensic toxicology. *Forensic Toxicology* **2021**, *39*, 311-333.
- (30) Standard, I. 78-2: *Chemistry—layouts for standards—part 2: methods of chemical analysis*; **1999**. Retrieved from ISO. <https://www.iso.org/standard/3726.html> (accessed 2024 July 30).
- (31) Gonzalez, C.; Spinelli, S.; Gille, J.; Touraud, E.; Prichard, E. Validation procedure for existing and emerging screening methods. *TrAC Trends in Analytical Chemistry* **2007**, *26*, 315-322.
- (32) Deidda, R.; Dispas, A.; De Bleye, C.; Hubert, P.; Ziemons, É. Critical review on recent trends in cannabinoid determination on Cannabis herbal samples: from chromatographic to vibrational spectroscopic techniques. *Analytica Chimica Acta* **2022**, *1209*, 339184.

Summary



This thesis describes the development of high-resolution analytical methods based on selective molecular interactions for the safe use of Cannabis and Cannabis-derived products. In **Chapter 1**, the Cannabis plant, its main active compounds (cannabinoids), and derived products, along with their safety concerns, are introduced. Afterward, a brief overview of the state-of-the-art in Cannabis and cannabinoid analysis is provided, covering GC and HPLC-based methods, colorimetric spot tests, ambient ionization mass spectrometry (AIMS) methods, and ion mobility spectrometry (IMS) methods. Finally, an outline of the thesis, including the scope and aims of the research, is presented.

In **Chapter 2**, an overview of methods for analyzing Cannabis and Cannabis products over the past decade is presented, with a primary focus on fast analysis. Methods including colorimetric tests, electrochemical, optical spectroscopic, immunochemical, nuclear magnetic resonance (NMR), IMS, and AIMS methods are summarized. Key performance parameters such as portability, analysis time, qualitative/quantitative capability, advantages, and disadvantages are evaluated. Finally, potential application scenarios for these methods are outlined.

The amount of psychoactive $\Delta 9$ -THC in commercial CBD products must be strictly controlled for quality assurance and forensic purposes. **Chapter 3** describes the distinction between $\Delta 9$ -THC and CBD by a fast and simple Ag(I)-impregnated paper spray mass spectrometric method, relying on different Ag(I) affinities, leading in turn to different MS^2 fragments. This marks the first time that resolution of isomeric cannabinoids by AIMS is achieved. The method enables reliable quantitative analysis of $\Delta 9$ -THC:CBD ratios in commercial CBD oils within tens of seconds, providing potential for quality control of CBD products.

As Cannabis cultivation rapidly expands worldwide, there is an urgent need for fast, low-cost, and high-throughput analytical methods to classify Cannabis, e.g., hemp and marijuana. Typically, the target analytes for classifying hemp and marijuana are (potentially) psychoactive cannabinoids, such as $\Delta 9$ -THC, and non-psychoactive cannabinoids with therapeutic benefits, such as CBD. An Ag(I)-TLC method using variable Ag(I) complexation, for Cannabis classification is described

in **Chapter 4**. This method applies smartphone-based color analysis for semiquantification of THC analogues (THCA, Δ^9 -THC, and CBN) after completely separating them chromatographically from CBD analogues (CBDA, CBD, and CBG) on modified Ag(I)-TLC plates. The method allows for the differentiation between hemp and marijuana within 10 minutes, requiring only a few milliliters of solvent, and demonstrates the potential for in-field Cannabis classification.

Δ^8 -THC — prepared from CBD by treatment with acid — is gaining popularity as an alternative to Δ^9 -THC in cannabinoid-infused edibles. The production of Δ^8 -THC results in byproducts, including Δ^9 -THC and other isomers with limited toxicological information. **Chapter 5** details the development of silica-Ag(I) HPLC-DAD/MS and GC-FID/MS methods for analyzing Δ^8 -THC-related products, with a focus on THC isomers such as Δ^8 -THC, Δ^9 -THC, CBD, Δ^8 -iso-THC, and $\Delta^4(8)$ -iso-THC. The GC-FID/MS method is quicker and more robust, while the silica-Ag(I) HPLC-DAD/MS method offers an orthogonal approach and distinct ESI spectra for THC isomers. Both methods allow comprehensive determination of cannabinoid profiles in “ Δ^8 -THC” samples from lab-based and kitchen-based syntheses starting from CBD, as well as in commercial Δ^8 -THC edibles. This demonstrates their potential for more accurate and selective qualitative and quantitative analysis of Δ^8 -THC products compared to commonly used RP-HPLC methods.

The expanding Cannabis market and the intricate composition of its products necessitate the development of advanced analytical methodologies for comprehensive, sensitive, selective, and unambiguous yet fast determination of cannabinoids to facilitate forensic and medical applications. Special focus is required on cannabinoid isomers, which, despite structural similarities, have varied pharmacology and legality. **Chapter 6** describes a method to analyze cannabinoid isomers in diverse samples within milliseconds by leveraging the unique adduct-forming behavior of silver ions in advanced cyclic ion mobility spectrometry coupled with time of flight mass spectrometry. This method enables the reliable identification of fourteen cannabinoid isomers with four different MWs, including thermolabile

acidic cannabinoids, neutral cannabinoids, and diastereomeric cannabinoids. A combined workflow for the 3-step identification of cannabinoid isomers in Cannabis and Cannabis-derived samples is established (molecular weight and isotope pattern of Ag(I) adducts, $^{TW}CCS_{N_2}$, and MS/MS fragments with comparison to reference standards). Finally, $\Delta 8$ -THC, $\Delta 9$ -THC, and CBD in samples are relatively quantified to show the potential to reliably identify and sensitively quantify cannabinoid isomers in complex matrixes.

Despite the comprehensive analysis of $\Delta 8$ -THC products by chromatography-based methods described in **Chapter 5**, fast analytical methods for large-scale screening analysis of these ever-popular products remain needed. In **Chapter 7**, studies are described on the development of a fast and easy method to distinguish between $\Delta 8$ -THC and $\Delta 9$ -THC for screening purposes. This method combines a straightforward MeOH extraction with rapid Ag(I)-impregnated paper spray mass spectrometry analysis based on distinct MS³ fragmentation patterns of isomeric cannabinoids. The developed approach enables reliable quantification of $\Delta 8$ -THC in various commercial $\Delta 8$ -THC products and detects the presence of $\Delta 9$ -THC and other isomers like $\Delta 8$ -iso-THC, $\Delta(4)8$ -iso-THC, and $\Delta 3$ -THC. The use of a 3D-printed device for the paper spray improves operational simplicity and shows potential for user-friendly, large-scale screening of $\Delta 8$ -THC products.

PFAS pose a rapidly increasing global problem due to their widespread use and high stability, leading to water contamination with significant health impacts. Cannabis products can become contaminated with PFAS when plants are exposed to high PFAS levels, raising concerns about the safety of cannabis and its derivatives. To address this issue, methods for effectively removing PFAS from the growing environment (water) of Cannabis and sensitive analytical techniques to analyze PFAS are described in **Chapter 8**. High PFAS removal efficiency is achieved through a new type of supramolecular binding between PFAS and fluorine-free macrocyclic pillararene hosts modified resin. This resin enables a 10^6 -fold reduction of PFAS in contaminated water via a simple single filtration within 5 min and allows for over 10 regeneration cycles without performance loss.

The research presented in this thesis significantly advances the development of high-resolution analytical methods based on selective molecular interactions, aimed at ensuring the safe use of Cannabis and Cannabis-derived products. In **Chapter 9**, the solutions proposed in this thesis to overcome the challenges of analyzing Cannabis and its products are discussed and evaluated. Remaining challenges in each chapter are discussed, along with potential solutions and future prospects in this field.

Acknowledgments



Acknowledgments

More than twenty years ago, when I woke up early and worked late to do farm chores before and after school, when my family had to sell more than half of our annual harvest just to pay the school fees for my sister and me, and when, despite all our hard work, we still couldn't have enough to eat or wear, my mother would always tell us, "Knowledge changes destiny." This sentence has been deeply etched into my bones throughout my academic journey, constantly appearing in my mind. The pursuit of knowledge is not an easy road, but I've been incredibly fortunate to meet many great mentors and friends who have guided and supported me to where I am today. If I were to list all their names, my acknowledgments would probably be longer than my thesis itself. To everyone who has helped me, whether your name appears here or not, you are always in my heart. Thank you, from the bottom of my heart.

My thesis committee

Thank you for your valuable time and effort in reading my thesis and for your insightful feedback and suggestions. I truly appreciate your hard work!

My SUPERvisor team

My promoter, **Han Zuilhof**, thank you for giving me the opportunity to pursue my PhD. Without this opportunity, it would have been difficult for me to see and experience the world beyond China. From the time I took the IELTS to the end of my PhD journey, you have always given me sincere encouragement. I often felt inadequate, like I wasn't doing enough, but over these years, you helped me rebuild my confidence, both in research and in life, and I believe this will have a profound impact on my future. In research, you set a clear direction for me and corrected my course when I strayed. You worked late into the night and on weekends to help me with computational chemistry simulations, pushing the progress of my project. Although you are always busy, you never forgot to check in on my well-being. Thank you for inviting me to your home for meals; thank you for ensuring I had a warm

and comfortable work environment when the office heating stopped working; thank you for treating me to coffee remotely when I was in Zurich; and thank you for visiting my son every time you went to Changsha. There are so many other things I'm grateful for. Years from now, I may forget the cold winters of Wageningen, but I will never forget these warm moments. Thank you for bringing so much warmth and kindness to my past years in Wageningen. I genuinely enjoyed working at ORC — maybe that's why I often stayed from 7 a.m. until 10 p.m.

My promoter, **Bo Chen**, you are the most selfless teacher I've ever met. You always go above and beyond to help and support your students, never hesitating to sacrifice your own interests without asking for anything in return. I am incredibly lucky to be one of your students. When I was a complete novice in research and knew nothing about mass spectrometry, you welcomed me into your lab and guided me patiently, teaching me every detail step by step. You overcame countless obstacles to secure a PhD opportunity for me at Wageningen University, even using your own salary to support me. What seemed like an impossible path, you cleared for me with your determination, and you have led me all the way to where I am today. I often worry about how I can ever repay you, but you always laugh and say that seeing your students grow and succeed makes you happier than anything else. While you are lenient in life, you are extremely strict in research — I can't even remember how many times I cried after being criticized for my work. It was painful, but each time it helped me refocus on the essence of the problem and the fundamental principles of my research, allowing me to overcome challenges. Your dedication to your students and your pursuit of excellence in research will always serve as a model for me. I hope you'll smoke less and eat meals on time.

My co-promoter, **Gert Salentijn**, you have played a dual role in my supervisor team as both a mentor and a big brother. I deeply admire your passion for research and your dedication to your students. Even during weekends and holidays, you made time to meet with me online when I needed guidance. Whenever I sent you a manuscript, you would provide detailed feedback within a week. Your WhatsApp was always open for my questions, no matter the time. We also had many meaningful

non-academic conversations, where you gave me advice, encouragement, and warmth during moments of confusion and doubt. You were like a guiding light during what felt like the darkest times. Thank you for inviting me to spend Christmas at your home. I also appreciate you introducing Tara to me, the adorable little angel who brought me so much joy and healing. As your first PhD student in the strictest sense, I know you invested a lot of time and effort in me, and for that, I am truly grateful.

My co-promoter, **Teris van Beek**, you always say you're not my supervisor, but reflecting on my entire PhD journey, I cannot count how many online and offline meetings we have had or how many emails you have sent me guiding my research progress. You spent countless hours teaching me how to analyze NMR spectra and conduct GC-MS experiments. You took me to the coffee shop to buy experimental samples. You reviewed my manuscripts with such seriousness and attention to detail, examining every word, sentence, and punctuation mark. No matter what challenges I faced, you were always there, putting yourself in my shoes to help me overcome my difficulties. Most of my impressions of the Netherlands outside of Wageningen come from you — my first trips to Leiden, Haarlem, Giethoorn, Palace Het Loo, and many more places were with you. Thank you for organizing those thoughtful trips that pulled me out of the lab to experience the beauty and culture of the Netherlands. And thank you for welcoming me to your home for delicious dinners prepared by your wife, for letting me pick fruits in your orchard, and for playing with your cats — all these experiences gave me the warmth of family. Even though you say you're not my supervisor, I feel proud and blessed to be your student.

I often marvel at how I must have used up all the luck I'd accumulated in my first 30 years to have such an amazing supervisor team. Whether in academic guidance or caring for students, you — my SUPERvisors, set the gold standard, serving as a model I will strive to follow for the rest of my life.

My paranympths

Canan Aksoy and **Minnie Leong**, thank you for taking care of the many details

for my defense. Canan, I'm so glad to have you as a close sister at ORC. We've cried and laughed together and shared everything. I've witnessed your important life moments, from moving and renovating to getting married and having a child. Your warmth and kindness have deeply touched me, and I'm so lucky to have you. Minnie, thank you for guiding and helping me grow. I truly enjoy the time we spend learning and discussing together. I appreciate your thoughtful advice during our hikes. Thank you so much for all the delicious meals you prepared for me with such care. Your warm greetings mean a lot to me. Being around you always makes me feel safe, not just because of your height but because of your personality and charm. You shine brightly in any crowd.

My HNNU teachers

Ming Ma, thank you for advocating for my opportunity to pursue a PhD abroad and for helping me overcome countless obstacles. I appreciate your phone calls for guidance and encouragement. When I was feeling lost, you patiently helped me analyze various situations and clarify my thoughts. Whenever I face difficulties, you are always willing to lend your full support. Without your assistance, I wouldn't have come this far. **Zhengfa Fang**, thank you for your guidance and help over the years. **Fengjiang Yu**, thank you for your efforts in creating the conditions that allowed me to study abroad.

Paper Team members

I thoroughly enjoyed every one of our group meetings — they were always productive and relaxed. **Anouk Bosman**, when we attended RAFA together, I appreciated how you respected my habit of taking a nap without disturbing me — you're so considerate! **Peiheng Wang**, thank you for sending samples to Zurich. **Ids Lemmink**, though sometimes I found it overwhelming with all your questions and issues, you often made me laugh, and I'm really glad to have you around. **Qiaofeng Li**, I regret we didn't meet earlier — we have so many things to talk about! **Ziyang Wu**, thank you for consistently bringing me snacks every day. **Ruobing Liu**, thanks

for the keychain — I carry it with me daily.

My students

Thank you, **Sjors Rasker** and **Jeffrey van der Hoeven**. Supervising your master theses has made me realize the challenges and difficulties of being a good supervisor.

My ORC colleagues

Laura Righetti, it felt like we were old friends from the moment we met. Although you haven't been at ORC for long, it seems we've already shared so many experiences together. Whether it's discussing projects, conducting experiments, enjoying various instant noodles, chatting while lounging on the small bed, or exploring Zurich, every moment has been special. Thank you so much for your companionship. **Frank Claassen**, you are an incredibly patient and experienced troubleshooter in the lab, and Frank is always right! Thank you for helping me resolve all kinds of technical problems in my experiments, for lending me your pipettes for four years, for helping me find housing, and for buying me a heater. There are countless other moments when you've helped me overcome challenges that I can't list here. Life would have been much harder without you. **Hans-Gerd Janssen**, thank you for your guidance on my research project and for generously providing multiple silver-silica columns. I truly enjoy your humorous and engaging presentations! **Michel Nielen**, thank you for taking the time to discuss mass spectrometry fragmentation pathways with me — your bright smile is incredibly friendly. **Maurice Franssen**, thank you for your care for my student's project, for our discussions on enzyme hydrolysis. I also appreciate your quiet dedication in taking care of the ORC dishwasher. **Fedor Miloserdov**, thank you for many discussions on organic chemistry mechanisms. **Louis de Smet**, thank you for your great kindness to help me book the defense date. **Barend van Lagen**, my Dutch teacher, your sudden passing was hard to accept, and I've been very sad for a long time. We were the early birds at ORC, starting our day with cheerful morning talks

by the coffee machine. You patiently trained me in Dutch, and now I can handle daily greetings, but it's a pity no one will check on my progress anymore. **Hans Beijleveld**, thank you for your technical help with HPLC and GC. You're also a very brave firefighter, which I deeply admire. **Sidharam Pujari**, you are truly a kind and helpful person — whenever I asked for your help, you never refused. Thank you for inviting me to spend Christmas at your home. **Judith Firet**, as fellow early sisters at ORC, we shared many happy morning talks. Thank you for bringing warmth and laughter into my life. **Henny Li**, thank you for sharing your quirky videos with me and for always including me in WEDAY games, even though I'm really not good at sports. Playing with you was a joy, and I truly miss you after you left. **Dieuwertje Streefkerk**, it's been a pleasure working in the same lab with you. Thank you for maintaining such high standards of cleanliness and order, allowing me to conduct my experiments in what I believe to be the most spotless lab. I also greatly appreciate your help in sending samples to Zurich. **Tjerk Sminia**, I enjoyed our discussions about organic chemistry mechanisms. **Hendra Willemen**, your warm greetings at the coffee corner always brightened my day. **Elly Geurtsen, Aleida Ruisch, Eveline van Dijk**, thank you so much for your invaluable help with all the administrative tasks.

Qiang Shi, every time we discuss organic chemistry, we end up talking for hours. You've taught me so much during those conversations. I still remember how you jokingly suggested at the beginning of my PhD that I should quit because it was too difficult. But the resilient me didn't give up, haha! Throughout these years of studying, while everyone else encouraged me to persevere, you were the only one telling me to consider quitting. I'll never forget that! **Dongdong Liang**, thank you for your tremendous support during the early days of my PhD, both in life and in my studies. You really helped me get through the challenging adjustment period. **Muthusamy Subramaniam**, thank you for teaching me how to conduct organic chemistry experiments, and I'll always cherish the fun times we spent eating together and chatting. I hope everything is going well for you in the UK. **Yanzhang Luo**, thank you for helping me with the 600 MHz and 700 MHz NMR measurements and

for your invaluable advice on both my studies and future career. **Guanna Li** and **Akash Krishna**, thank you for your guidance and assistance in computational chemistry. Guanna, I absolutely love your vibrant personality, and I still haven't had the chance to give you the chocolate I brought from Switzerland! Akash, I fondly remember the brief yet delightful time we were office mates.

My sunshine, **Natassa Lional**. It's hard for me to imagine my PhD journey without you. You're like a happy little fairy, always finding ways to make me laugh. Our conversations were filled with laughter, and your delicious cooking brought me so much comfort. Although we haven't gone out often, every outing with you has been a delightful escape. I'm a bit sad that graduation will mean we'll part ways, but I truly wish for your everlasting happiness. **Ariadni Geballa-Koukoulou**, you are one of the kindest and most optimistic people I've ever met. The time we spent together with your boyfriend in Prague was unforgettable. If you had stayed longer at ORC, I'm sure we would have shared even more wonderful memories. Thank you so much for designing my perfect thesis cover and for your very warm encouragement.

Yu Han, we spent over three years together in Wageningen and at ORC. We helped each other through many tough times. We moved several times together using a tricycle. You are genuinely a kind-hearted person, and I wish you success and happiness in your studies and life ahead. **Tunan Gao**, it was a great pleasure working with you, and I've always admired your ability to balance work and life. Best of luck with your defense and finding a job you love. **Yifei Zhou**, I truly enjoyed the time we spent together in the same office and lab. Our many engaging conversations, both academic and personal, have become cherished memories for me. I am also incredibly grateful for your kindness in biking a long distance in the summer heat to bring me a heavy mattress when I first arrived in the Netherlands. **Zhen Yang**, it's funny how, despite being on different floors, we saw each other so frequently because we both preferred staying at the lab. I admire your straightforwardness and calmness. Your sharp insights never fail to impress me. Thank you for the calligraphy you gave me. **Xuecong Li**, you're such a warm and fun person. Even though I often teased you about your corny jokes, I'm truly grateful for how you

were always willing to help and answer my questions. I got used to your occasional “inspections” of our office, and I look forward to you visiting Zurich one day to inspect my work again! **Chuanbao Zheng**, thank you so much for your help when I applied for the VLAG scholarship and for inviting me to celebrate the Lunar New Year with your friends. I wish you success in both your studies and love life. **Mingcong Liu**, I’m very glad you joined ORC. It’s a pity I was away from the Netherlands most of the time after you arrived. We only had hotpot together once! I hope your four years here will be happy and fulfilling.

Julia Mestres Martinez, I love how you greet me with “good night” every time we meet. I apologize for giving you the impression that I just sleep all day without doing anything. **Jayaruwan Gamaethiralalage**, I still remember sitting next to you on my very first day in the Netherlands. You were always so patient in answering all my questions and gave me lots of encouragement and formatting advice while I was writing my thesis. I’m sorry I missed your defense, but I’m truly happy for you. Wishing you all the best in both your family life and career! **Stijn Paulusma**, thank you for your generous offer to let me stay at your place when I couldn’t find accommodation. **Irene Shajan**, I love your radiant smile, and your homemade Indian food was incredible! **Jasper van de Sande**, thank you for teaching me how to use the freeze dryer. **Eman Abdelraheem**, thank you for your encouraging words during experiments. **Clementina Vitali**, **Simon van Hurne**, **Yuri Damen**, **Daniele Chinello**, **Julian Engelhardt**, **Thijmen van Voorthuizen**, **Giacomo Nisini**, **Brian van 't Veer**, **Leonie Straub**, I enjoyed our conversations, which made my time at ORC colorful and fulfilling.

To those who have already left ORC — **Alyssa van den Boom**, **Annemieke van Dam**, **Sevil Sahin**, **Michel de Haan** — I often think of you and appreciate the kindness and help you gave me. **Laura Carbonell Rozas**, though our time together was short, it was truly delightful. I hope you return to Wageningen soon.

My WFSR friends

Erik Beij, thank you for your tremendous help with 3D design and printing.

Your efficiency and dedication made working with you a pleasure. **Ilaria Di Marco Pisciotano**, I'm glad you're back at WFSR, and I've enjoyed our discussions. **Ane Arrizabalaga Larranaga**, chatting and drinking with you has always been fun.

My Wageningen friends

Ed van Ouwerkerk and **Margreet van Ouwerkerk**, my Dutch grandparents, thank you for providing me with a home in the Netherlands and for giving me so much unconditional love. You've helped me become a better person. Please stay healthy forever! **Bert Verbeeke** and **Jeanine Verbeeke**, thank you for offering my family a place to stay for the night. Thank you for creating such a warm place for so many students! **EJ (Evert Jan) Bakker**, **Maike Wigboldus**, **Lu Zhou**, **Phil Arend**, **Christina van der Bijl-Faasse**, thank you for teaching me so many valuable lessons. I miss our hikes and trips together. **Chen Zhang**, **Yingying Liu**, **Yanbing Wang**, **Junxin Gao**, **Sen Xie**, **Roger Hao**, **Gina Ho**, **Lisheng Jiang**, **Yangyang Shi**, thank you for your companionship and the joyful discussions we've shared. **Weixuan Peng**, you are such a dependable friend. Thank you for comforting me when I was feeling down and for always being there for me.

Marijke Zuilhof, you've always felt more like an older sister to me. You remember my love for chocolate, cake, and ice cream, and would always stock up on them to make me feel welcome. When you discovered a great restaurant, you'd invite me along, and if you found beautiful lavender, you'd drive me to see it. You even knew I hated the cold and bought me cozy gloves. After your trip to Israel, you brought me back so many thoughtful gifts. I'll never forget how you would cycle through the rain to make sure I got home safely. Talking with you is always so easy and uplifting, and I find myself wanting to share so many things with you. You've truly spoiled me like a little sister. **Yan Zuilhof**, you have such a great sense of humor and kindness. Eating and chatting with you is always filled with laughter. Your artwork, animations, and drumming are amazing. Thank you for the gifts you brought me from China.

Yixin Hu, you once told me that I would always have a home in Wageningen,

and you've truly lived up to that promise. During this past year, as I moved from place to place, your house has been a safe haven for me and my luggage. Your incredible Hunan cuisine has been a comforting treat for this wanderer. **Zulin Mei** and **Xiulu Sun**, thank you for your companionship, encouragement, and all your help with my thesis formatting. Wishing you both a bright future ahead.

Zenobi Group

Renato Zenobi, I am deeply grateful for your care and support during my four-and-a-half-month exchange. Thank you so much for welcoming me into your warm and loving group. **Ri Wu, Yuye Zhou, Yuanzhi Xia, Congrui Tan, Chengcheng Xu, Kim Greis, Lukas Benzenberg, Julian Harrison, Philipp Bittner**, many thanks for your great help and kindness.

My longtime friends

Shiming Liu, Zixuan Zhu, Ben Han, Kai Zhang, Ruiqi Gao, Ping Guo, thank you for our solid friendship over the years. Many people have come and gone, but you have always been there. Whenever I think of you, I am filled with warmth and happiness.

My Family

刘亚枝, 秦琴, 胡成杰, 黄成, 你们是我亲自挑选的兄弟姐妹。感谢你们始终无条件地支持我, 满足我所有的请求。感谢你们跨越时差, 用长途电话陪伴我度过那些孤独的夜晚。更感谢你们在我出国的这些年里, 悉心照顾我的父母和干爹干妈。

我的**外公外婆**, 谢谢你们把我拉扯大, 子欲养而亲不待, 但你们永远在我的记忆和梦里。谢谢我的**舅舅杨凯**, 你是我的启蒙老师。谢谢我的**二姨, 三姨, 四姨**, 我的**表妹周方, 沈雅琪、沈雅馨**, **表弟周元、杨轶卓**, 我的**堂哥黄欢**, 你们的爱让我茁壮成长。

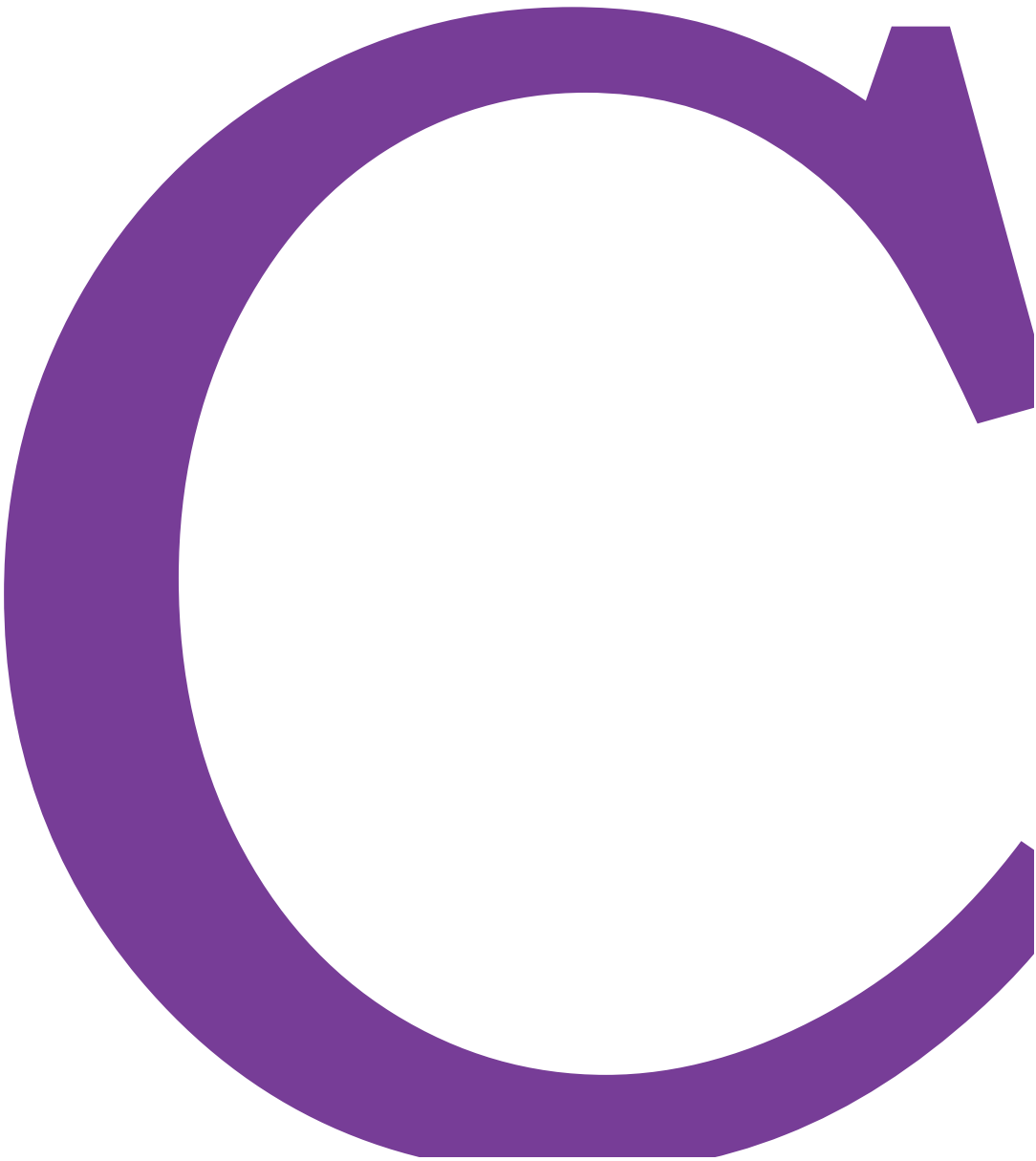
我的**父母**, 谢谢你们生我养我, 用尽全部的力气供我和妹妹上学。在那

个女子读书无用论盛行的年代和农村，你们不顾世俗的反对，砸锅卖铁供我们读书，告诉我们知识改变命运。谢谢你们给我生了世界上最好的**妹妹**——**黄柳**，三十多年来，我们相互扶持，相亲相爱，一起经历过寒冷、饥饿和无助，也一起沐浴阳光、爱和希望，我们会越来越好的。谢谢我的**干爹**和**干妈们**，谢谢你们视我为亲生闺女，给予我无条件的爱。

谢谢我的**老公**，**贺佐勇**。我们相识13年，结婚8年，一半的时间都是分隔两地。谢谢你这么多年来对我的支持和包容，对家庭的奉献。你总是鼓励支持我追求我的梦想，自己一人扛起属于我们两个人的家庭重任。谢谢你与我风雨同舟，替我遮风挡雨。愿我如星君如月，夜夜流光相皎洁。

最后，感谢我的**儿子贺槐序**选择了我当妈妈。每每想起当你的妈妈不需要任何的资质和考核，就觉得有愧于你。缺席你成长的重要时光也是我无法弥补的深深遗憾。但是妈妈想要用自己的努力和行动给你树立榜样，有梦想就大胆去追求。道阻且长，行则将至；行而不辍，未来可期。

Curriculum Vitae



About the Author

Si Huang was born on September 29, 1990, in Xiaogan, Hubei, China. In 2013, she earned dual bachelor's degrees in Food Science and Engineering from Huazhong Agricultural University and in English from Huazhong University of Science and Technology. She then completed a master's degree in Applied Chemistry at South China



Normal University in 2016, under the guidance of Prof. Dr. Weiguang Zhang and Prof. Dr. Jun Fan. After completing her master's, Si worked as a lecturer in Analytical Chemistry at Hunan Normal University. In 2019, she began her PhD studies at the Laboratory of Organic Chemistry, Wageningen University, supervised by Prof. Dr. Han Zuilhof, Prof. Dr. Bo Chen, Dr. Gert Salentijn, and Dr. Teris van Beek. Her research focused on developing analytical methods using chromatographic and mass spectrometric techniques, with particular emphasis on cannabinoids. This thesis presents the work she conducted during her PhD.

In 2024, she joined the Organic Chemistry Laboratory at ETH Zurich as a visiting researcher. She is currently working there as a postdoctoral researcher.

List of Publications

- [1] Si Huang; Teris A. van Beek; Erik Beij; Ming Ma; Bo Chen; Han Zuilhof; Gert IJ. Salentijn, Rapid Analysis of Δ 8-Tetrahydrocannabinol, Δ 9-Tetrahydrocannabinol, and Cannabidiol in Δ 8-Tetrahydrocannabinol Edibles by Ag(I) Paper Spray Mass Spectrometry after Simple Extraction, ***submitted to Food Chemistry***. (Chapter 7 in this Thesis)
- [2] Si Huang; Laura Righetti; Frank W. Claassen; Akash Krishna; Ming Ma; Teris A. van Beek; Bo Chen; Han Zuilhof; Gert IJ. Salentijn, Ultrafast, Selective, and Highly Sensitive Nonchromatographic Analysis of Fourteen Cannabinoids in Cannabis Extracts, Δ 8-Tetrahydrocannabinol Synthetic Mixtures, and Edibles by Cyclic Ion Mobility Spectrometry–Mass Spectrometry, ***Analytical Chemistry***, **2024**, 96: 10170–10181. (Chapter 6 in this Thesis)
- [3] Si Huang; Teris A. van Beek; Frank W. Claassen; Hans-Gerd Janssen; Ming Ma; Bo Chen; Han Zuilhof; Gert IJ. Salentijn, Comprehensive Cannabinoid Profiling of Acid-Treated CBD Samples and Δ 8-THC-Infused Edibles, ***Food Chemistry***, **2024**, 440: 138187. (Chapter 5 in this Thesis)
- [4] Tu-Nan Gao; Si Huang; Rick Nooijen; Yumei Zhu; Gabriele Kociok-Köhn; Tobias Stuerzer; Guanna Li; Johannes H. Bitter; Gert IJ. Salentijn; Bo Chen; Fedor M. Miloserdov; Han Zuilhof, Rim-Based Binding of Perfluorinated Acids to Pillararenes Purifies Water, ***Angewandte Chemie International Edition***, **2024**, 63: e202403474. (Chapter 8 in this Thesis)
- [5] Mincong Liu; Si Huang; Linli Tan; Jiaxin Pan; Shuting Xie; Han Zuilhof; Bo Chen; Ming Ma, A Simple and Low-Energy Strategy for the Separation of Water and Acetonitrile, ***Journal of Separation Science***, **2023**, 46, 2300426.
- [6] Si Huang; Ruiying Qiu; Zhengfa Fang; Ke Min; Teris A. van Beek; Ming Ma; Bo Chen; Han Zuilhof; Gert IJ. Salentijn, Semiquantitative Screening of THC Analogues by Silica Gel TLC with an Ag(I) Retention Zone and Chromogenic Smartphone Detection, ***Analytical Chemistry***, **2022**, 94: 13710-13718.

(Chapter 4 in this Thesis)

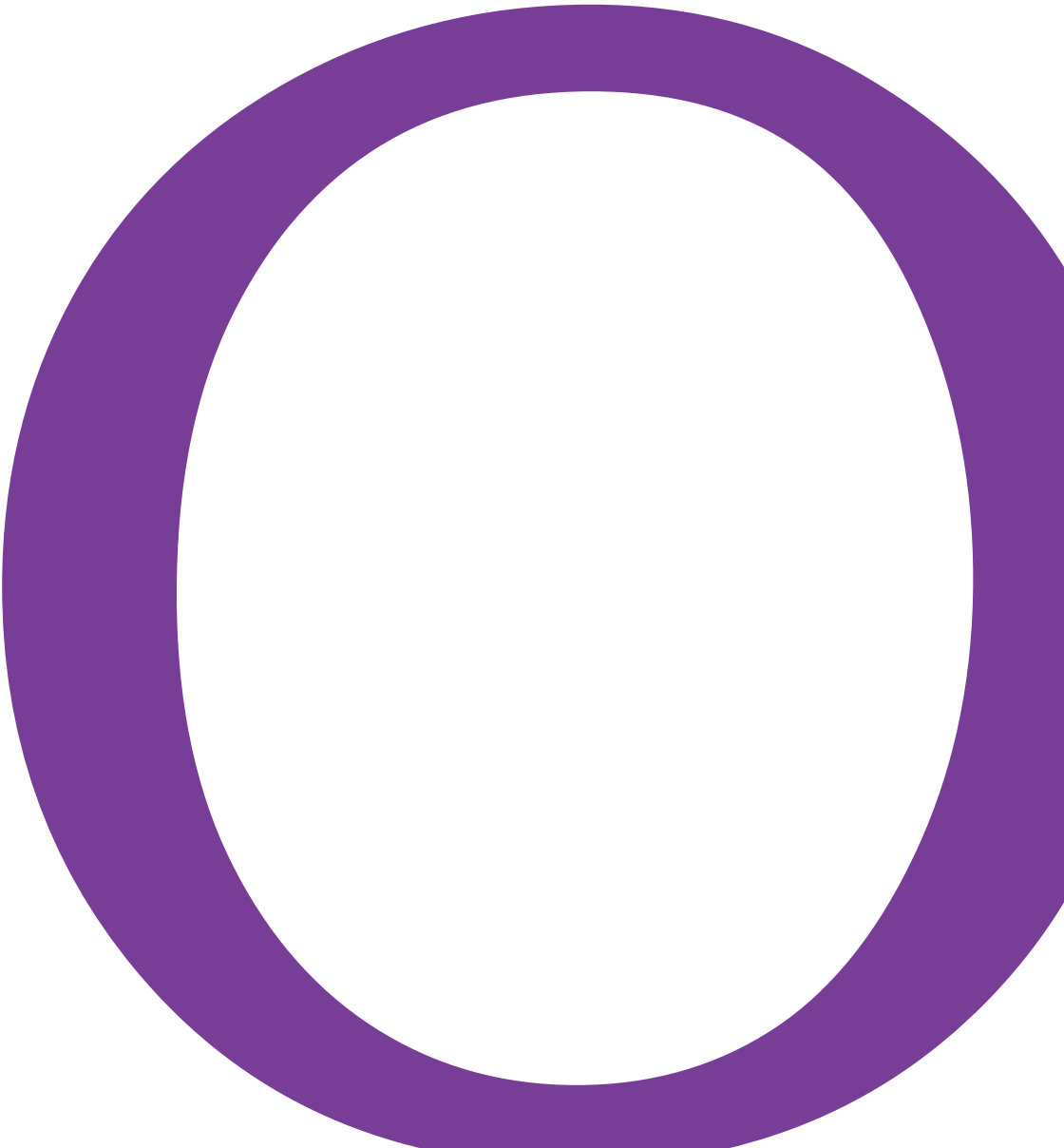
- [7] Si Huang; Frank W Claassen; Teris A. van Beek; Bo Chen; Jianguo Zeng; Han Zuilhof; Gert IJ. Salentijn, Rapid Distinction and Semiquantitative Analysis of THC and CBD by Silver-Impregnated Paper Spray Mass Spectrometry, *Analytical Chemistry*, **2021**, 93: 3794- 3802. (Chapter 3 in this Thesis)
- [8] Ping Guo; Ke Min; Wei Luo; Si Huang; Zihui Yang; Ming Ma; Shubin Liu; Zhengfa Fang; Bo Chen; Han Zuilhof, Ionization of Glycans from Alkali Metal Salt-impregnated Paper, *Talanta*, **2021**, 234, 122674.
- [9] Si Huang; Si-Yuan Cheng; Shu-Yuan Zhang; Yi-Lun Yan; Song-Liang Cai; Xin-Le Li; Sheng-Run Zheng; Jun Fan; Wei-Guang Zhang, Protein Amorphous silica composites for chromatographic purification of immunoglobulin G., *New Journal of Chemistry*, **2020**, 44: 7884-7890.
- [10] Ke Min; Ping Guo; Dongying Chen; Si Huang; Wei Luo; Ming Ma; Bo Chen; Shouzhao Yao; Han Zuilhof, Direct and Quantitative in-situ Analysis of Third-hand Smoke in and on Various Matrices by Ambient Desorption Corona Beam Ionization Mass Spectrometry, *Talanta*, **2020**, 219, 121330.
- [11] Deping Hu; Yuandong Li; Hui Zhao; Yang Zhao; Si Huang; Juan Li; Zhenjie Li; Yuanxing Duan; Yingzhuang Chen; Jianjun Xia, Online High-pH Reversed-phase Liquid Chromatography × Low-pH Reversed-phase Liquid Chromatography-Tandem Electrospray Ionization Mass Spectrometry Combined with Pulse Eution Gradient in the First Dimension for the Analysis of Alkaloids in *Macleaya Cordata* (willd.) R. Br, *Journal of Separation Science*, **2020**, 43: 1423– 1430.
- [12] Rong Yang; Yang Y. Hu; Si Huang; Zheng F. Fang; Ming Ma; and Bo Chen, Separation and Analysis of Ginsenoside Rg1: An Experiment for the Separation and Analysis of Natural Products, *Journal of Chemical Education*, **2020**, 97, 778–785.
- [13] Wangming Tan; Ye Chen; Xiyue Xiong; Si Huang; Zhengfa Fang; Yingzhuang Chen; Ming Ma; Bo Chen, Synthesis of a Poly(sulfobetaine-co-polyhedral oligomeric silsesquioxane) Hybrid Monolith via an in-situ Ring

- Opening Quaternization for Use in Hydrophilic Interaction Capillary Liquid Chromatography, *Microchim Acta*, **2020**, 187, 109.
- [14] Xiang Guo; Qianqian Cao; Yawen Liu; Tao He; Jingwen Liu; Si Huang; Hao Tang; Ming Ma, Organic Electrochemical Transistor for in Situ Detection of H₂O₂ Released from Adherent Cells and Its Application in Evaluating the In Vitro Cytotoxicity of Nanomaterial, *Analytical Chemistry*, **2019**, 92: 908-915.
- [15] Feng Chang; Yunfang Yue; Zihui Yang; Si Huang; Zhihua Liu; Kunmiao Wang; Yan Peng; Yingzhuang Chen; Ming Ma; Bo Chen, The Fabrication of Poly (polyethylene glycol diacrylate) Monolithic Porous Layer Open Tubular (mono-PLOT) Columns and Applications in Hydrophilic Interaction Chromatography and Capillary Gas Chromatography for Small Molecules, *Electrophoresis*, **2019**, 40: 521-529.
- [16] Zhangyan Ma; Tengting Wu; Peipei Li; Meiling Liu; Si Huang; Haitao Li; Youyu Zhang; Shouzhao Yao, A Dual (Colorimetric and Fluorometric) Detection Scheme for Glutathione and Silver (I) Based on the Oxidase Mimicking Activity of MnO₂ Nanosheets, *Microchim Acta*, **2019**, 186, 498.
- [17] Yingzhuang Chen; Yajun Wu; Xiaoming Liu; Bowen Li; Deping Hu; Si Huang; Ming Ma; Bo Chen, Pulsed Elution Modulation for On-line Comprehensive Two-dimensional Liquid Chromatography Coupling Reversed Phase Liquid Chromatography and Hydrophilic Interaction Chromatography, *Journal of Chromatography A*, **2019**, 1583: 98-107.
- [18] Xiaowei He; Yan He; Si Huang; Zhengfa Fang; Jingjing Liu; MingMa; Bo Chen, Fluoro-functionalized Paper-based Solid-phase Extraction for Analysis of Perfluorinated Compounds by High-performance Liquid Chromatography Coupled with Electrospray Ionization–Tandem Mass Spectrometry, *Journal of Chromatography A*, **2019**, 1601: 79-85.
- [19] Wei Zhou; Zihui Yang; Si Huang; Zhengfa Fang; Bo Chen; Ming Ma, Rapid Quantitative Analysis of Ginkgo Flavonoids Using Paper Spray Mass Spectrometry, *Journal of Pharmaceutical and Biomedical Analysis*, **2019**,

171, 158-163.

- [20] Shaoqian Liu, Zhengfa Fang, Zhanghong Yang, Heda Dong, Si Huang*, Improvement of Stability Constant Determination of Sulfosalicylic Acid-Copper (II) Complex, *University Chemistry*, **2018**, 33, 59-62

Overview of Completed Training Activities



Overview of Completed Training Activities

Discipline Specific Activities	Organizer	Place	Year
Advanced Organic Chemistry	ORC	Wageningen	2021
The 22nd National Symposium and Exhibition on Chromatography of China (poster)	CCS	Shanghai	2019
9th International Symposium on Recent Advances in Food Analysis	UCT, WUR	Prague	2019
Ultra-Sensitive Mass Spectrometric Analysis of Trace Biological Samples Symposium	SIOC, CAS	Shanghai	2020
The 32nd CCS Congress (poster)	CCS	Zhuhai	2021
The 13th National Conference on Biomedical Chromatography and Related Technologies (outstanding poster)	CCS	Yanji	2021
FAST Symposium 2021	COAST	Amersfoort	2021
CHAINS Symposium 2021	KNCV	Online	2021
10th International Symposium on Recent Advances in Food Analysis	UCT, WUR	Prague	2022
15th International Metabolomics Workshop (oral)	LEI	Leiden	2023
Early Career Scientists Event 2023 (poster)	ILSI Europe	Wageningen	2023
IUPAC World Chemistry Congress 2023 (poster)	KNCV, NWO	The Hague	2023
NOW Teknowlogy 2023 (poster)	NWO	Utrecht	2023

General Courses	Organizer	Place	Year
VLAG PhD week	VLAG	Baarlo	2019
The Essentials of Scientific Writing & Presenting	WGS	Wageningen	2022
Intensive Writing Week	WGS	Wageningen	2022
Presenting with Impact	WGS	Wageningen	2023
Adobe Illustrator Scientific artwork & Infographics	WUR Library	Online	2023
Writing Propositions for your PhD	WGS	Wageningen	2023
Career Assessment	WGS	Wageningen	2023

Other Activities	Organizer	Place	Year
Preparation of PhD research proposal	VLAG	Wageningen	2022
Weekly group meetings Colloquia (oral)	ORC	Wageningen	2019-2023
Seminar Series Colloquia (oral)	ORC	Wageningen	2019-2023
Thesis (MSc) Supervision	ORC	Wageningen	2021-2023
PhD Study Tour	ORC	Belgium, Germany, Switzerland	2023
Seminar presentation (oral)	WFSR	Wageningen	2023
Seminar presentation (oral)	Ulm University	Ulm	2023
Seminar presentation (oral)	ETHZ	Zurich	2023

The research described in this thesis was financially supported by Natural Science Foundation of China (22276049, 22276050), and the China Scholarship Council 2020 International Cooperation Training Program for Innovative Talent.

Financial support from Wageningen University for printing this thesis is gratefully acknowledged.

Cover design was made by Ariadni Geballa-Koukoula using Adobe Illustrator and Freepik.

Printed by proefschriftenprinten.nl.